UNIVERSITÄT ZU LÜBECK

From the Institute of Nutritional Medicine
of the University of Lübeck
Director: Prof. Dr. Christian Sina

Antibody and B cell development after vaccination against COVID-19

Dissertation
for Fulfillment of
Requirements
for the Doctoral Degree
of the University of Lübeck

from the Department of Natural Sciences

Submitted by

Jana Sophia Buhre

from Stadthagen

Lübeck 2024

First referee: Prof. Dr. Marc Ehlers

Second referee: Prof. Dr. Lars Redecke

Date of oral examination: 27.09.2024

Approved for printing. Lübeck, 03.04.2025

List of Content

A. Summary

During the COVID-19 pandemic, new mRNA- and adenovirus-based vaccine formats encoding the viral spike protein (S) were developed. These newly developed vaccine formats have helped to successfully combat the pandemic. However, there is a high rate of breakthrough infections, which is why the vaccine-induced immune responses should be investigated in detail. Both vaccine formats induce antibodies that have neutralizing functions via their Fab-part. The effect of IgG antibodies also depends on Fc-mediated effector functions, which are influenced by the IgG subclass and its Fc *N*-glycosylation pattern.

At the beginning of this work, it was known that both vaccines induce IgG1 and IgG3 antibodies initially and especially after two vaccinations, but information on long-term antibody responses was lacking. The aim of this work was therefore to longitudinally describe and characterize the vaccine-induced IgG subclasses, their Fc *N*-glycosylation and their Fc-mediated effector functions.

It was shown that the mRNA vaccines produced significantly higher IgG1 and IgG3 antibody levels in the short term compared to adenovirus-based vaccination, but that these levels equalized in the long term. In contrast to this equalization, late-emerging IgG4 antibodies were only observed in people who received two mRNA vaccinations. It is generally assumed that IgG4, in contrast to IgG1 and IgG3, has a more inhibitory function. In functional assays, anti-S IgG1 was confirmed as a strongly activating subclass. In contrast, IgG4 antibodies, which increased with every vaccination, showed activating but also inhibitory immunomodulatory effects. These need to be further investigated in the future in order to better assess their role in the long-term vaccination response.

In addition, a dynamic development of glycosylation was observed: Highly galactosylated and sialylated IgG antibodies appeared shortly after each vaccination, while significantly lower galactosylated and sialylated IgG antibodies were found in the long term. This wave pattern was described for all IgG subclasses and indicates that differently glycosylated antibodies exert different effector functions, which could mean a new general understanding of early and late antibody responses after vaccination. In contrast to this dynamic, the new vaccines were only able to induce afucosylated antibodies temporarily and only after the first vaccination.

By investigating a cohort of patients with inflammatory diseases who received tumor necrosis factor (TNF) inhibitors during vaccination, the influence of TNF on the longitudinal antibody response and thus also on B-cell differentiation could be described. The patients showed lower IgG levels, altered antibody glycosylation patterns and reduced Fc-mediated effector functions both in the short and long term after repeated vaccination. Anti-TNF therapy not only reduced the long-lived IgG response, but also the short-lived IgG response resulting from the re-activation of memory cells. Accordingly, an increased risk of breakthrough infection was observed in patients treated with anti-TNF. These results suggest that patients receiving anti-TNF therapy may benefit little from a booster vaccination.

A. Zusammenfassung

Während der COVID-19 Pandemie wurden neue mRNA und Adenovirus-basierte Vakzine entwickelt, die das virale Spike (S) Protein kodieren. Diese neu entwickelten Impffstoffe haben dazu beigetragen, die Pandemie erfolgreich zu bekämpfen. Allerdings gibt es eine hohe Quote an Durchbruchinfektionen, weshalb die durch die Vakzine induzierten Immunantworten tiefgreifend untersucht werden sollten. Beide Vakzinformate induzieren Antikörper, die über ihren Fab-Teil neutralisierende Funktionen haben. Die Wirkung von IgG Antikörpern ist außerdem abhängig von Fc-vermittelten Effektor-Funktionen, die von der IgG Subklasse und deren Fc *N*-Glykosylierungsmuster beeinflusst werden.

Zu Beginn dieser Arbeit war bekannt, dass beide Impfstoffe initial und nach zwei Impfungen insbesondere anti-S IgG1 und IgG3-Antikörper induzieren, aber es fehlten Informationen über kurz- und langfristige Antikörperantworten. Das Ziel dieser Arbeit war daher die longitudinale Beschreibung und Charakterisierung der impfstoffinduzierten IgG Subklassen, ihrer Fc *N*-Glykosylierung und ihrer Fc-vermittelten Effektor-Funktionen.

Es konnte gezeigt werden, dass die mRNA-Impfstoffe im Vergleich zur Adenovirus-basierten Impfung kurzfristig deutlich höhere IgG1 und IgG3-Antikörperlevel generierten, die sich jedoch langfristig anglichen. Im Gegensatz zu dieser Angleichung wurden spät auftretende IgG4 Antikörper nur bei Personen beobachtet, die zwei mRNA-Impfungen erhalten hatten. Es wird allgemein angenommen, dass IgG4 im Gegensatz zu IgG1 und IgG3 eine eher inhibitorische Funktion hat. In funktionalen Immun-Assays wurde anti-S IgG1 als eine stark aktivierende Subklasse bestätigt. Im Gegensatz dazu zeigten die IgG4-Antikörper, die mit jeder Impfung stiegen, aktivierende, aber auch inhibitorische immunmodulatorische Effekte. Diese müssen in Zukunft weiter untersucht werden, um ihre Rolle in der langfristigen Impfantwort besser beurteilen zu können.

Darüber hinaus wurde eine dynamische Entwicklung der IgG Fc-Glykosylierung beobachtet: Hoch galaktosylierte und sialylierte IgG-Antikörper zeigten sich kurz nach jeder Impfung, wobei langfristig deutlich niedriger galaktosylierte und sialylierte IgG-Antikörper gefunden wurden. Dieses Wellenmuster wurde für alle

IgG Subklassen beschrieben und deutet auf eine unterschiedliche Effektor-Funktion hin, was ein neues generelles Verständnis von frühen und späten Antikörperantworten nach Impfung bedeuten könnte. Im Gegensatz zu dieser Dynamik konnten die neuen Impfstoffe nur nach einer Impfung und nur temporär afukosylierte Antikörper induzieren.

Durch die Untersuchung einer Kohorte von Patienten mit inflammatorischen Erkrankungen, die während der Impfungen Tumor-Nekrose-Faktor (TNF)-Inhibitoren erhielten, konnte der Einfluss von TNF auf die longitudinale Antikörperantwort und damit auch auf die B-Zell-Differenzierung beschrieben werden. Die Patienten hatten sowohl kurz- als auch langfristig nach wiederholter Impfung niedrigere IgG Titer, veränderte Antikörper-Glykosylierungsmuster und reduzierte Fc-vermittelte Effektor-Funktionen. Die anti-TNF Therapie reduzierte nicht nur die langlebige IgG Antwort, sondern auch die durch Re-Aktivierung von Gedächtniszellen entstandene kurzlebige IgG Antwort. Dementsprechend wurde bei Patienten, die mit anti-TNF behandelt wurden, ein erhöhtes Risiko für eine Durchbruchinfektion beobachtet. Diese Ergebnisse deuten darauf hin, dass Patienten unter anti-TNF Therapie nur wenig durch Booster Vakzinierungen profitieren könnten.

1. Introduction

1.1 Vaccination

Undoubtedly, our environment is full of various bacteria, viruses, parasites, and fungi, some of which are pathogenic. To combat against the latter ones, our body relies on immunity. In general, immunity against pathogens can be acquired through two main strategies: passive and active. Passive immunity involves transferring antitoxins or antibodies from one individual to another, providing temporary protection. The most common example of passive immunity is the immunity that infants receive from their mothers during pregnancy. The antibodies are transferred to the infant across the placenta and provide protection against pathogens during the first few months of life. However, this protection is temporary and degrades over time (Firth et al., 2005).

In contrast to passive immunity, active immunity offers protection through the body's own immune system. One way to achieve active immunity is to become infected with pathogens so that the immunologic memory protects against re-infection for many years or even for life. Nevertheless, some pathogens trigger such a severe initial disease that the infected individual can die. Other pathogens, such as Malaria, do not induce a protective immune response, resulting in frequent reinfections (Doolan et al., 2009). Another example is the human immunodeficiency virus (HIV), which is difficult for our immune system to fight and leads to chronic infections (Pantaleo & Fauci, 1996).

Vaccination is another way of preventing infections and gaining active immunity. It is one of medicine's greatest achievements and, alongside access to clean drinking water, has saved the most lives (Soni et al., 2020).

Smallpox was once a major threat to human health. For centuries, hundreds of millions of people died from this disease, and it was frequently epidemic. In 1796, Edward Jenner was considered the inventor of modern vaccinations. He recognized parallels between the more severe smallpox disease and the much milder cowpox disease and used virulent material from a woman with cowpox to vaccinate a boy. Weeks later, the boy showed immunity to true smallpox. Jenner used the Latin word for *vacca*, meaning cow, to describe his actions and invented the nowadays well-established term of vaccination (Riedel, 2005).

Since then, the concept of vaccination has been continuously developed and has saved many lives. The World Health Organization (WHO) declared in 1980 that smallpox has been successfully eradicated, and vaccinations against other diseases such as measles or diphtheria are frequently used and have led to a significant reduction in prevalence (Broder et al., 2006; Modlin et al., 1977; World Health Organization, 1980).

Nevertheless, there remain diseases such as HIV and Norovirus infection for which there are still no effective vaccines. However, research into the development of new vaccination strategies and formulations is ongoing (McMichael, 2006; Tan, 2021). Vaccination has come to the fore again, particularly in recent years. This has been triggered by the coronavirus disease 2019 (COVID-19) pandemic and the vaccines that have been rapidly developed against the virus represent new forms of vaccines and demonstrate the ongoing process of developing new vaccination strategies (Kaur & Gupta, 2020).

The principle of vaccination is not only used in connection with pathogens. Much work is being done on the strategy for vaccination against tumors (Saenz-Badillos et al., 2001). Efforts to vaccinate against cancer are not new, and developed formats include, amongst others, messenger RNA (mRNA)-based vaccines. These formats, as well as adenovirus-based strategies, were quickly applied to develop vaccines against COVID-19 during the pandemic (Fang et al., 2022; Kreiter et al., 2011).

Another application of active immunization is antigen-specific immune therapies (AIT) in the context of allergies, which rely on the introduction of the antigen in a non-pathogenic manner (Epp et al., 2018; Larché et al., 2006). A similar strategy is being pursued in the context of autoimmune diseases, where research is focusing on the development of autoantigen-specific immunizations to redirect autoantigen-driven immune responses to less inflammatory reactions (Anderson & Jabri, 2013; Bartsch et al., 2018; Oefner et al., 2012).

Paradoxically, vaccination against pathogens is intended to activate the immune system, while vaccination against allergies or autoimmune diseases aims to dampen the immune system. The two strategies obviously pursue opposing goals, which must be taken into account when developing both types of vaccines.

1.1.1 Vaccination strategies

Vaccinations are based on the introduction of (whole or partial) pathogens into the immune system. In contrast to natural infections, this happens in a regulated manner. The following requirements apply for the approval of a new vaccine: Efficacy, safety, and quality (Rashid et al., 2009). This minimizes possible negative consequences (safety), but the immune response triggered by the vaccination still provides reliable immunity comparable to a natural infection (efficacy, quality). This protective immunity can lead to herd immunity if the vaccination is administered extensively to many people, thereby extending the vaccine-induced protection to people who cannot be vaccinated themselves (e.g. due to medical constitutions), have only limited vaccination success or do not want to be vaccinated (Rashid et al., 2012).

Different types of vaccination strategies can be distinguished and will be described in the following sections.

1.1.1.1 Vaccines containing live-attenuated or inactivated pathogens

Live-attenuated vaccines are based on the introduction of living pathogens that are less pathogenic than the naturally occurring wild type form but have the same immunogenicity.

One example of a live-attenuated vaccine approach is Edward Jenner’s use of the cowpox virus in humans. For some diseases, naturally occurring weaker strains of the pathogens are available, but often these counterparts do not exist (Ada, 2005). The nowadays commonly used vaccine against measles is an example of a live-attenuated virus vaccination, which was generated in the laboratory. Back in the 1950s and 1960s, measles caused many children to die, and John Franklin Enders started to cultivate isolated viruses from an infected child. By cultivating the virus under sub-optimal conditions, such as a wrong temperature or pH, John Enders developed an attenuated strain. When administered to children, it triggered a weaker immune response than to the natural infection, but afterwards the children showed good protection against the natural virus (Katz et al., 1962). By today, live-attenuated variants can be generated much more efficiently and targeted by genetic engineering (Ada, 2005; Plotkin, 2010). Although live-attenuated pathogens provide good results in terms of protective immunity, they can cause serious side effects and are regularly the subject of safety concerns. In contrast to live-attenuated vaccines, inactivated vaccines provide more safety as compared to live-attenuated forms, but also have lower efficacy and must be administered several times to gain a certain level of long-term immunity (Ada, 2005).

1.1.1.2 Adjuvant-based vaccines

Not every disease can be prevented by vaccination with live-attenuated or inactivated pathogens. For some diseases, live-attenuated strains are not available or there are safety concerns (Coffman et al., 2010; Z.-B. Wang & Xu, 2020). However, the realization that only specific parts of the pathogen are sufficient to induce specific immunity has led to the generation of various vaccination strategies. Surface proteins, carbohydrates, or polysaccharides, which are naturally exposed at the external surface of pathogens, were shown to be the major targets of vaccination-induced protection. Therefore, the isolation of such surface molecules led to the development of subunit vaccinations (Ada, 2005).

Protein-based vaccinations have shown promising results by inducing T-cell dependent (TD) immune responses. Compared to polysaccharide-based vaccines, they tend to have better safety and efficacy outcomes (Pasquale et al., 2015). Polysaccharide-based vaccines show a T-cell independent (TI) immune response and therefore there are attempts to couple them to carrier to proteins (Bröker et al., 2017). Nevertheless, to compensate for the comparatively low immunogenicity of subunit vaccinations, adjuvants (from the Latin word *adjuvare*, which means to help) are used to increase the immunogenicity (Coffman et al., 2010).

Aluminum salts were the first adjuvants to be approved and used. In the 1920s, the physician Alexander Glenny found that toxoid preparations enriched with aluminum salts led to better vaccination outcomes than the toxoid alone (Glenny et al., 1926). Nowadays, aluminum salts serve as adjuvants in various vaccines, for example against diphtheria, pertussis, tetanus, polio, hepatitis, and pneumococcus (Kool et al., 2012). Even though the mechanism of action of aluminium salts is not yet completely understood, a strong T helper (T_H)2 and a weaker T_H1 immune response can be observed (Coffman et al., 2010).

In the 1940s, Jules Freund used paraffin oil as an adjuvant (incomplete Freund's adjuvant, IFA, paraffin oil) plus inactivated *Mycobacterium tuberculosi*s ((Mtb), resulting in complete Freund's adjuvant, CFA)) combined with an aqueous protein solution as vaccine inducing very strong T_H1 and T_H17-responses (Freund et al., 1937). Even though CFA is not approved for usage in humans, another oil-based adjuvant Montanide, or squalene-based formulas like MF59 (Addavax) followed and are regularly used in different vaccines against the flu, cancer, Malaria or HIV (Petrovsky & Aguilar, 2004). Furthermore, the use of adjuvant combinations that activate multiple immune responses is under development and is a promising approach (Coffman et al., 2010; Levast et al., 2014).

It is generally recognized that adjuvants are of great importance for an adequate immune response and the success of a vaccination. However, it is not yet clear what type of immune response a vaccine should elicit to induce tolerance, as in the case of AIT (Jensen-Jarolim et al., 2021), or a combative immune response, as in the case of vaccination against pathogens (Pulendran et al., 2021).

1.1.1.3 Vaccination strategies during COVID-19

Since the end of 2019, we have been facing a global threat to health and the economy caused by massive rates of pneumonia due to COVID-19 a result of infection with Severe acute respiratory syndrome coronavirus type 2 (SARS-CoV-2). The virus of unknown origin spread from China and triggered an initial wave in infection within a few weeks – worldwide (Ciotti et al., 2020). Varying degrees of disease severity such as mild symptoms, acute respiratory distress syndrome (ARDS), multiple organ failure or death were reported (Teijaro & Farber, 2021). Many countries faced high morbidity and mortality, and COVID-19 became a pandemic disease for which there were no suitable treatments or therapeutic interventions (Chakraborty et al., 2021). Simultaneously, various companies reacted quickly and developed new vaccines against COVID-19, which were used for the first time at the end of 2020. Two vaccinations one to three months apart very likely helped in the acute phase of the pandemic. The vaccines reduced severe cases and the need for hospitalization (Mohammed et al., 2022; Stoliaroff-Pepin et al., 2023).

The first licensed vaccines were newly developed vaccine formats based on mRNA or adenovirus-based vector deoxyribonucleic acid (DNA) encoding for the spike (S) surface protein of the virus. The concept of using mRNA or DNA to encode pathogen-specific molecules is not new. There are different approaches to deliver the sequence either naked, through lipid nanoparticles (LNPs), polymer-based vectors or viral vectors (Chakraborty et al., 2021). The mRNAs are encapsulated with LNPs, which protect the mRNA from degradation. The approach to use viral vectors is based on adenoviruses, which cannot replicate in humans. After the introduction of mRNA or viral vectors, protein translation is induced (Figure 1).

A special feature of such mRNA or vector-based vaccines is that they do not require an additional adjuvant, as they are already capable of inducing co-stimulatory signals. In addition to the antigen-encoding parts, the sequence itself also contains components that are recognized by the immune system as pathogen-associated molecular patterns (PAMPs) via Toll-like receptors (TLRs) and trigger the production of mainly Th1-cytokines. The mRNA is recognized by TLR3 and TLR7, while the double stranded (ds)DNA of the viral vector binds to TLR9. This further enhances the immunogenicity of these new vaccine formats (Castrodeza-Sanz et al., 2023; Teijaro & Farber, 2021). However, the sequences have been modified to interact less with PAMPs. Excessive activation of the innate immune system by PAMPs can have a detrimental effect on vaccination success by blocking mRNA translation (Linares-Fernández et al., 2020).

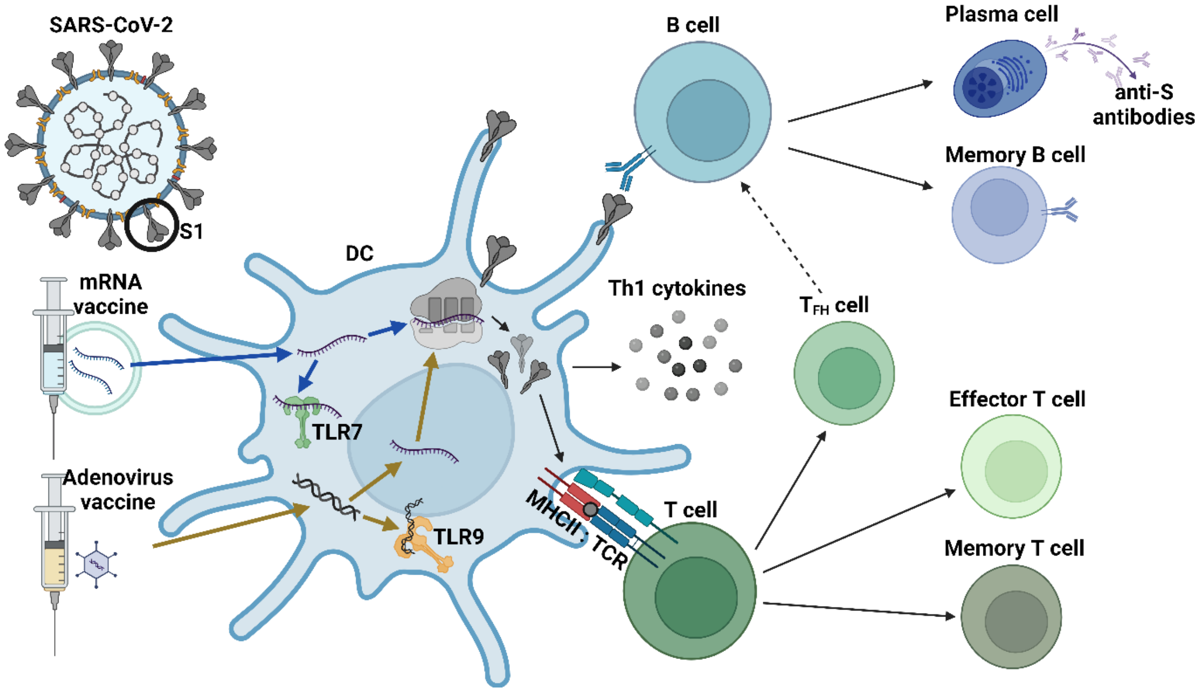

Figure 1: The mode of action of the newly developed vaccine formats against COVID-19. The mRNA vaccines encode for the SARS-CoV-2 spike (S) protein encapsulated in lipid nanoparticles, while the adenovirus vaccine contains the viral vector encoding for the S protein. Upon vaccination, the mRNA/viral vector enters all host cells, including dendritic cells (DC) and ribosomes facilitate the translation from mRNA to S protein. Additionally, the mRNA vaccine triggers RNA sensors, e.g. Toll-like receptor 7 (TLR7), while the double-stranded DNA from the adenovirus vector gets recognized by the TLR9. The intrinsic adjuvant potential of the vaccines leads to the production of Th1 cytokines, which subsequently activate further antigen-presenting cells, e.g. DCs. Activated DCs present the antigen to primed B cells or processed antigens in the context of MHCII to T cells, and B cells differentiate, under the help of T follicular helper (T_{FH}) cells to either plasma or memory B cells. Simultaneously, T cells differentiate into either T_{FH} cells, effector, or memory T cells. MHCII = major histocompatibility complex II, TCR = T cell receptor. This illustration was created with BioRender.com according to Teijaro & Farber, 2021 and adapted.

The first mRNA vaccine Comirnaty (BNT162b2) against COVID-19 was jointly developed by BioNTech and Pfizer (Oliver et al., 2020). To date, the vaccine has been adapted several times for different age groups and the new Omicron variant. A second mRNA vaccine from Moderna was approved shortly after the one from BioNTech, which contains mRNA packaged into LNPs. Both mRNA vaccines achieved up to 95% efficacy against COVID-19 infections in phase III clinical trials (Baden et al., 2021; Polack et al., 2020). Afterward, vaccines with DNA administered in non-replicating recombinant adenovirus-based systems followed.

The vaccines were from AstraZeneca and Janssen-Cilag. The efficacy of adenovirus-based vaccines was found to be lower at around 70% (Shay et al., 2021; Voysey et al., 2021).

Next to these new vaccine strategies, both protein-based and inactivated virus-containing vaccines have been introduced and licensed in Germany (Table 1). In contrast to the mRNA and adenovirus-based vaccines, the protein vaccines contain adjuvants. To date, almost 65 million people in Germany have received at least one vaccination against COVID-19 (source: https://impfdashboard.de/, retrieved: 04/2024).

Table 1: List of approved vaccinations in Germany.
The vaccines from BioNTech/Pfizer and Moderna have been approved in different concentrations for follow-up vaccinations and different variants of the virus. Paul-Ehrlich-Institute (Source: https://www.pei.de/DE/arzneimittel/impfstoffe/covid-19/covid-19-node.html, retrieved: 04/2024).

Name	Vaccine format	Adjuvant	Company	Approval
Comirnaty	mRNA in LNP	-	BioNTech/Pfizer	21.12.2020
Spikevax	mRNA in LNP	-	Moderna	06.01.2021
Vaxzevria	DNA in Vector	-	AstraZeneca	29.01.2021
Jcovden	DNA in Vector	-	Janssen-Cilag	11.03.2021
Nuvaxovid	Protein	Saponin	Novavax	20.12.2021
VidPrevtyn	Protein	AS03 (Squalen, DL-α-Tocopherol and Polysorbate 80)	Sanofi Pasteur	10.11.2022
Bimervax	Protein	Oil-in-water	HIPRA	30.03.2023
Valneva	Inactivated	Alum, CpG 1080	Valneva	24.06.2022

1.1.2 Vaccination-induced immune responses

Every human being is born with a certain type of protection that contributes to our health in the first months and years of our lives by responding to threats, called the innate immune response. This response acts as a first line of defence against invading pathogens and depends on the ability to recognize highly conserved patterns that are not present in an uninfected body, PAMPs or so-called danger-associated molecular patterns (DAMPs) via pattern-recognition receptors (PRRs) such as TLRs (Murphy et al., 2012). PRRs are located on the membranes of innate immune cells, such as dendritic cells (DCs), neutrophils or macrophages. When PAMPs interact with these receptors, they trigger the immune response that leads to the destruction of pathogens by phagocytosis and the release of effector molecules (Murphy et al., 2012). Therefore, these cells are also the first to be activated in response to vaccination.

The main players in the second response of our immune system, adaptive immunity, are T and B lymphocytes. These cells have developed highly diverse and specific antigen receptors and facilitate the development of immunological memory and further protective immunity (Ahmed & Gray, 1996; Plotkin, 2005). Antigen-presenting cells (APCs), like DCs, are considered the link between the innate and adaptive immune response. They accomplish this by engulfing and processing antigens and presenting them as peptides in the context of major histocompatibility complex (MHC)II to $CD4^+$ T helper cells. Additionally, infected host cells present foreign peptides via MHCI to $CD8^+$ cytotoxic T cells, which have cytotoxic potential and can lyse infected cells (Iwasaki & Medzhitov, 2010; Murphy et al., 2012).

The importance of the antigen-specific and secreted B cell receptors (BCRs) became clear when the two physicians Emil von Behring and Shibasaburo Kitasato discovered that adaptive immunity can be transferred from one individual to another. They performed experiments in which they transferred serum from animals previously infected with diphtheria to naïve animals, which then showed protection against the disease. This passive immunization led to the conclusion that the reason for the protective effects was to be found in the cell-free parts of the blood, and they called it the antitoxin (van Behring & Kitasato, 1890). This corresponding factor was later identified as antibodies.

1.2 B cells

B cells, or B lymphocytes, are an important component of the adaptive immune system. These cells, which belong to the white blood cells, make up around 10% of all peripheric mononuclear blood cells (PBMCs). Their crucial role in maintaining health is beyond question (Kleiveland, 2015). The relevance of B cells becomes particularly clear when looking at diseases caused by B cell deficiency, which have devastating consequences for health (Pieper et al., 2013). The importance of B cells for a functioning immune system is based on their ability to produce antibodies as plasma cells and to contribute to an immunological memory as memory B cells (Pieper et al., 2013).

B cells derive from hematopoietic stem cells in the bone marrow and develop over several stages until they become mature, naïve B cells. B cells develop into immature B cells in the bone marrow and then mature further in secondary lymphoid tissues (Melchers, 2015). Once mature, they can be activated by antigen stimulation in T cell dependent (TD) or independent (TI) manner. During their development, multiple checkpoints regulate the proper function of B cells and minimize the risk of them developing into autoreactive B cells. In the secondary lymphoid organs, mature B cells reside in roughly spherical follicles and are held in place by follicular dendritic cells (Victora & Nussenzweig, 2022). After activation, B cells can develop into extrafollicular plasma cells and extrafollicular memory B cells in a TD or TI manner, or they can migrate to germinal centers (GCs) to develop TD into GC-derived plasma cells and memory B cells (Kurosaki et al., 2015; Mesin et al., 2016; Paus et al., 2006). Naïve B cells have the potential to differentiate into any B cell receptor isotype. This is regulated by cytokines and mainly occurs during the initial T:B cell interaction upon antigen stimulation and during the GC reaction (Roco et al., 2019). However, isotype switching can also occur in a TI manner (Snapper et al., 1992).

1.2.1 T cell-independent activation of B cells

Some antigens, especially non-protein antigens, cannot be presented to the TCR via MHCII, so that B cells cannot be co-activated by T cells. Still, non-protein antigens can lead to the TI class switching and the antibody production, which is mainly caused by repetitive antigen motifs of the antigens leading to crosslinking of BCR (TI-type II) (Hess et al., 2013). Alternatively, additional PRRs can be involved (TI-type I) (Mond et al., 1995). However, the vaccination outcome regarding robust antibody titers is poor and the antibodies have specificity, as the affinity maturation of B cells requires the help of T cells and the formation of GCs (Victora & Nussenzweig, 2022). In addition, no enhanced response to the vaccine can be observed after re-vaccination, suggesting that a TI activation of B cells is not sufficient to generate an immunological memory (Jackson, 1999; Mufson et al., 1991).

TD vaccines are needed to achieve a robust vaccination result, including highly specific, robust antibody titers and an immunological memory.

1.2.2 T cell-dependent activation of B cells

In order to achieve a TD activation of B cells, both cell types must first be primed with a protein antigen. APCs take up the antigen and process it into peptides, which can then be presented to naïve CD4+T cells via MHCII and prime them. When certain co-receptors, in particular CD80/86, are present and the T cell receptor (TCR) recognizes the MHCII:antigen complex, the T cells are finally activated. In contrast to T cells, encounters between protein antigens and naïve B cells lead to activation of the latter by BCR clustering without the need of further APCs (Kurosaki et al., 2015). Activated T and B cells upregulate certain chemokine receptors and migrate into lymphoid organs. When primed T cells encounter B cells via MHCII:antigen and TCR recognition at the T:B cell border within B cell follicles, further activation, proliferation, and differentiation of the cells is initiated. B cells can either differentiate into short-lived plasma cells and extrafollicular memory B cells or enter the GC, where they mature by affinity and differentiate into GC-dependent plasma cells and memory B cells (Kurosaki et al., 2015; Mesin et al., 2016).

It could be shown that the fate of mature B cells strongly depends on the BCR affinity to the antigen. Early TD antibody responses already show a certain level of efficacy, mature B cells with comparatively high levels of antigen-specificity become extrafollicular plasma cells, while clones with lower affinity migrate towards the GC for affinity maturation (Paus et al., 2006). After differentiated B cells leave the GCs, they have highly specific BCRs, which again underlines the contribution of TD B cell activation for a robust and effective vaccination response (Bentebibel et al., 2013; Pallikkuth et al., 2012).

1.2.2.1 Germinal Centers

GCs are microanatomical structures formed in B cell follicles of secondary lymphoid organs after antigen stimulation (Mesin et al., 2016; Victora & Nussenzweig, 2022). GCs contribute to an adequate and specific immune response by inducing clonal expansion, affinity maturation, class switching and differentiation. During the GC response, B cells are sorted into different fates depending on the quality of their BCR: Death, proliferation, or export into the memory or plasma cell subset (Victora & Nussenzweig, 2022).

After antigen stimulation and activation, B cells migrate to the T:B border of B cell follicles in secondary lymphoid tissues, where clonal expansion occurs with the help of $CD4^+$ T follicular helper cells (T_{FH}) (Kurosaki et al., 2015; Victora et al., 2010). It takes approximately one week for B cell follicles to develop into proper GCs, which are mainly composed of GC B cells, T_{FH} cells, and DCs (Mesin et al., 2016). They can be divided into two different zones: the light zone (LZ) and the dark zone (DZ) (Victora & Nussenzweig, 2022).

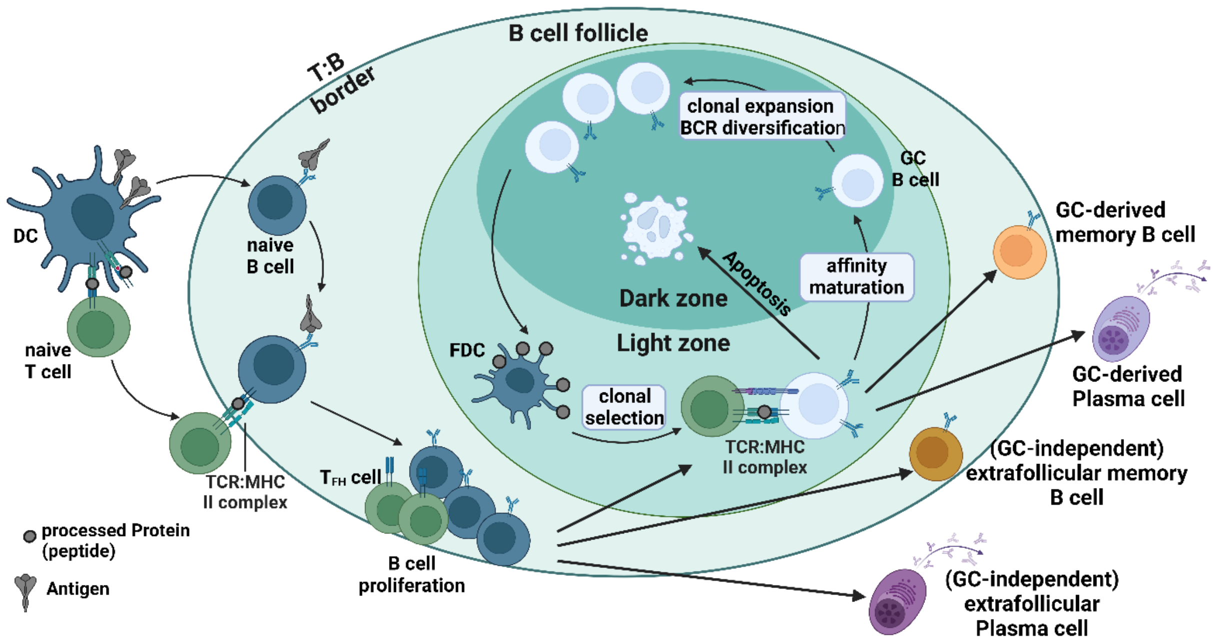

Figure 2: T-cell dependent B cell activation.

After antigen-presentation of Dendritic cells (DCs), these present the processed antigen in the form of a peptide via their MHCII to naïve CD4+ T cells. Meanwhile, naïve B cells are activated by the whole antigen and encounter the activated T cells at the T:B border, causing further B cell proliferation and differentiation of the T cells into T_{FH} cells. The B cells eventually either migrate into the GC or differentiate into GC-independent memory B cells or plasma cells. Within the GC, B cells dynamically cycle between the dark zones (DZs) and light zones (LZs), while affinity maturation and further selection occur through B cell T cell interactions. Before re-entering the DZ for further affinity maturation, the fate of B cells is decided: Apoptosis, differentiation into GC-derived memory B cells, plasma cells, or further affinity maturation within the GC. This illustration was created with BioRender.com according to Kurosaki et al., 2015 and adapted.

In the DZ, the B cells proliferate and undergo somatic hypermutation (SHM), which leads to the generation of a population of B cells that have closely related BCRs but differ slightly in their ability to bind to the same antigen (Victora & Nussenzweig, 2022). Furthermore, next to affinity maturation, class switch recombination (CSR) is an important event that occurs during the GC reaction. The heavy constant region of the immunoglobulin is rearranged, which leads to a switch in the isotype of the BCR. Notably, CSR can also occur outside of GCs, so extrafollicularly derived plasma cells can have BCRs of the isotypes IgG, IgA, or IgE which can be developed in both TD and TI manners (Roco et al., 2019). Molecularly, both affinity maturation and CSR of the BCR are facilitated by SMH. SMH is induced by the enzyme activation-induced cytidine deaminase (AID), which preferentially targets single-stranded DNA of rearranged BCR genes and induces Uracil:Guanine mismatches (Pilzecker & Jacobs, 2019). The point mutations randomly alter the affinity of the antigen-binding sites and are then tested and further selected in the LZ.

The LZ contains a network of DCs with bound antigens in the form of immune complexes on their surface. With the help of cognate CD4+ T_{FH} cells, the freshly mutated BCRs of different clones bind competitively to the antigen. GC B cells with high affinity take up the antigens from the immune complexes and present them as peptides with their MHCII on their surface. T_{FH} cells then promote the survival of these clones through cytokine secretion and the B cells migrate back into the DZ. There, they further increase their specificity. Alternatively, the B cells escape the re-entry into the DZ and differentiate into memory B cells or plasma cells (Mesin et al., 2016; Shlomchik et al., 2019; Victora & Nussenzweig, 2022). Memory B cells can circulate in the bloodstream or colonize secondary lymphoid tissues. Plasma cells, on the other hand, start to produce antibodies, can become long-lived and are be found in certain niches, e.g. in the bone marrow (Manz et al., 1997). GC B cells without bound antigens are negatively selected and undergo apoptosis (Shlomchik et al., 2019). Generally, the migration from DZ to LZ occurs dynamically and repeatedly until GC B cells expressing BCRs with a higher affinity to the antigen are positively selected (Victora et al., 2010). This re-entry of the cycle, which leads to an increased affinity of the BCR to the antigen is referred to as affinity maturation (Mesin et al., 2016). Investigation of the affinity and mutation rates of BCRs of different B cell subsets led to the conclusion that memory B cells develop earlier during the GC reaction and plasma cells develop later (Kräutler et al., 2017; Weisel et al., 2016).

Although the GC reaction is crucial for an adequate and targeted immune response during infection or vaccination, it needs to be limited. The stochastic nature of SHM also harbours the danger of generating auto-reactive B cells that can lead to autoimmune diseases (Ray et al., 1996). Regulating and limiting the GC reaction and thus preventing the generation of too many antigen-specific plasma cells and the development of auto-reactive B cells is facilitated by another T cell subset, Foxp3^{+} regulatory follicular T cells (T_{FR}). Their importance in sustaining a proper and balanced GC response is particularly evident when analyzing individuals with loss-of-function mutations in the Foxp3-gene. In addition to a high number of circulating antibodies, various autoantibody-mediated autoimmune diseases can be observed (Stebegg et al., 2018).

1.3 Antibodies

Plasma cells contribute significantly to humoral immunity as they are able to produce immunoglobulins (Igs), or antibodies, which are secreted forms of their BCRs. Antibodies come in different isotypes (Figure 3), while IgG being the predominant isotype in human blood. About 75% of all antibodies within blood serum belong to this isotype and are described more in detail in the following section.

During B cell development, the natural BCR is of the IgM isotype. IgM is initially expressed and is the first isotype to be secreted when an immune response is initiated. Therefore, IgM levels are often used to diagnose acute infection or exposure to a pathogen (Schroeder & Cavacini, 2010). IgM antibodies account for up to 10% of all Igs and occur naturally as pentamers or hexamers. Due to their multimerization, they possess 10 to 12 antigen binding sites. Although they have a lower binding affinity, these multiple binding sites result in a high binding avidity and make IgM strong complement activators (Keyt et al., 2020).

The rarity of IgD in secreted form is due to a short half-life. It is expressed when B cells leave the bone marrow and migrate into secondary lymphoid tissues, but is absent at later stages of development (Schroeder & Cavacini, 2010). However, recent studies suggest that IgD may actively contribute to protective humoral responses (Flemming, 2018).

IgA, the predominant isotype in mucosal tissues and the most frequently produced subclass in humans, accounts for up to 15% of all Igs (Steffen et al., 2020). It occurs in two subclasses, IgA1 and IgA2. IgA2 in particular is considered the IgA subclass with the higher activating potential. Elevated IgA2 levels have been linked to increased disease severity in autoimmune diseases (Steffen et al., 2020). Further, dimeric IgA1 and IgA2 coupled by a J-chain and labelled with a secretory chain are actively transported to the mucosa and are important for protecting mucosal surfaces from pathogens, regulating microbial composition and maintaining intestinal homeostasis (Pietrzak et al., 2020).

Finally, IgE, the least abundant isotype, accounts for only 0.01% of all antibodies in serum, but is nevertheless considered a strong immune activator due to its high affinity for cell receptors on effector cells. IgE is strongly associated with allergic diseases, hypersensitivity, and parasitic infection responses (Schroeder & Cavacini, 2010).

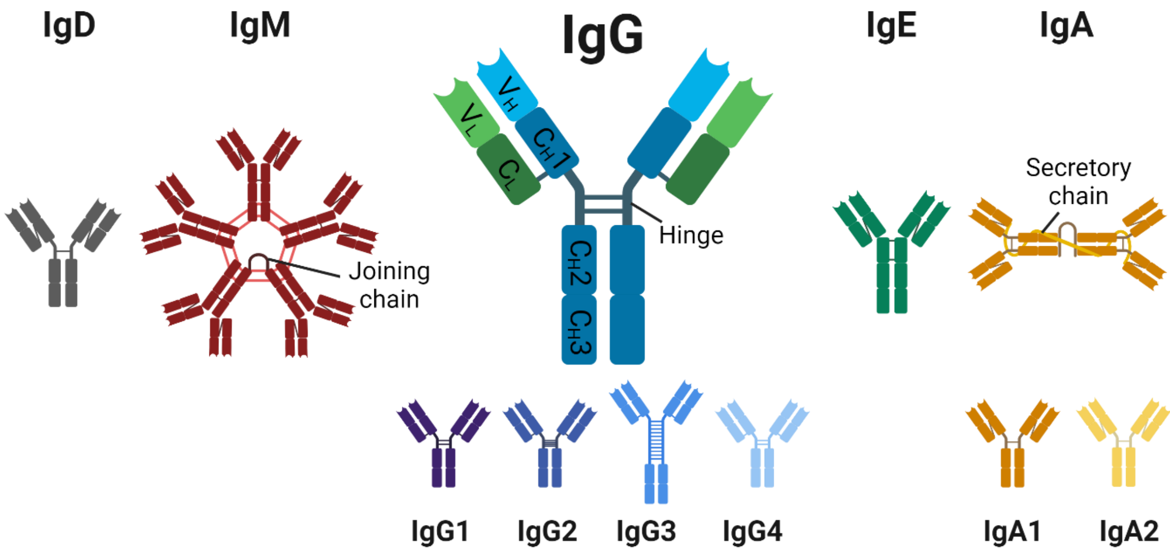

Figure 3: Schematic representation of all human Ig isotypes and the respective subclasses.

The isotypes and their subclasses differ in the flexible Hinge region, which connects the upper to the lower part, and in their Fc-parts that are important for interaction with Fc receptors and C1q. For all antibodies, two identical heavy and light chains are connected to each other by disulfide bridges and form the Y-shaped structure. IgM mainly exists as J-chain coupled pentamers or as J-chain independent hexamers (not shown). The IgG1-4 subclass heavy chains have three constant regions C_H1-3 and one variable region V_H, while the light chain consists of one constant region C_L and one variable region V_L. IgA, which is mostly dimeric, additionally bears a J-chain and a secretory chain, which is added during the active transport through epithelial cells to the mucus. This illustration was created with BioRender.com.

1.3.1 Structure and function of IgG subclass antibodies

There are four different IgG subclasses in humans (hu), namely IgG1-4 (with the following abundancies in serum: IgG1>2>3>4), and in mice, namely murine (mu) IgG1, IgG2a/c, IgG2b and IgG3 (De Haan et al., 2017; Lilienthal et al., 2018; K.-T. Shade & Anthony, 2013; Vidarsson et al., 2014). The following functional IgG subclass pairs between hu and mu have been suggested: hu IgG1 with mu IgG2a (or, in the C57BL/6 strain, IgG2c), hu IgG2 with mu IgG3, hu IgG3 with mu IgG2b, and hu IgG4 with mu IgG1 (Lilienthal et al., 2018). As previously mentioned, IgG antibodies are the predominant isotype in serum, and antigen-specific antibodies serve as markers of recent or active infection with a pathogen, and their levels often correlate with the level of protection by neutralization (Plotkin, 2010). The IgG subclasses are more than 90% identical at the amino acid level but differ in several functions. These include their ability to bind antigens, the formation of immune complexes, complement activation, IgG Fc receptors (FcγR) binding, and thus the activation of effector cell (Vidarsson et al., 2014).

IgG antibodies consist of two identical heavy and light chains connected by disulfide bridges forming the characteristic Y-structure (Figure 3). The heavy chain of IgG subclass antibodies consists of four different regions: the variable domain V_H, and the constant domains C_H1, C_H2, and C_H3. The light part consists of two regions: the variable domain V_L and the constant domain C_L. (Porter, 1973; Vidarsson et al., 2014). The upper part of an antibody, the so-called Fragment-antigen-binding (fab-)part, contains the antigen-binding site. Each IgG molecule has two Fab-parts consisting of the chains V_H, C_H3, V_L, and C_L. This part of the IgG molecule contains antigen-specific parts that also enable neutralizing capabilities through antigen. For example, they cover a specific surface structure of the virus during a viral infection and thus block the interaction of this structure with a cell entry receptor in host cells, making entry into the host cells impossible (Vidarsson et al., 2014). The lower part of an IgG molecule consists of the fragment-crystallizable (Fc-)region, which is crucial for the effector functions of antibodies. By binding of the Fc-part to FcγRs, complement molecules or other glycan-binding enzymes, IgG antibodies significantly influence the effector immune response (Alter et al., 2018; Vidarsson et al., 2014). The Fc-mediated activities of IgG antibodies are strongly influenced by the subclass and Fc *N*-glycosylation pattern. These aspects will be further detailed in the following section.

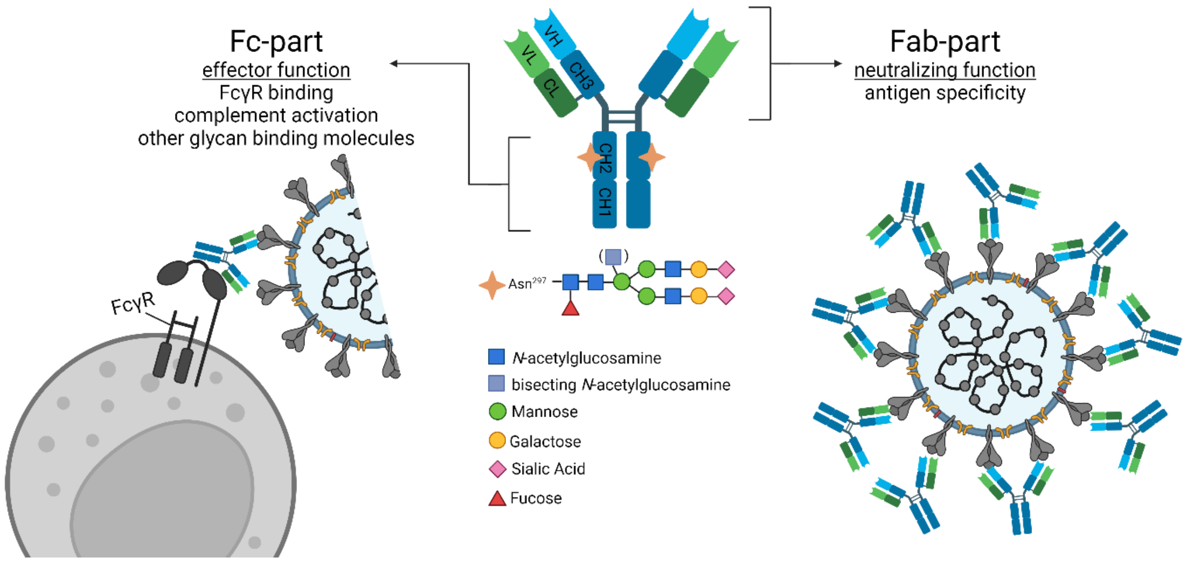

Figure 4: Schematic representation of the IgG molecule, the main functions of the two parts and the Fc glycan structure.
IgG molecules consist of an upper part, the Fab-part, and the lower Fc-part. Regards their functionality, the Fab-part exerts antigen-binding and neutralizing capabilities, while the Fc-part regulates the effector functions, e.g. through FcγR-binding or complement activation. Each IgG heavy chain has an *N*-glycosylation site at the C_H2 domain. The attached *N*-linked biantennary complex-type glycan influences the effector function of each IgG subclass Fc-part. Depending on the B cell stimulation fucose, bisecting *N*-acetylglucosamine, galactose and sialic acid can be added to the glycan core structure, which consists of four *N*-acetylglucosamines and three mannoses. This illustration was created with BioRender.com.

1.3.2 IgG Fc glycosylation

Glycosylation is a highly conserved process that occurs after transcription in the endoplasmic reticulum (ER). Antibodies are also glycoproteins, and unlike the other Ig isotypes, IgG molecules have only one *N*-conserved glycosylation site on each heavy chain of their Fc-part. Asparagine 297 (Asn^{297}, *N*) has complex biantennary glycans attached, which significantly alter the effector functions depending on the composition of the glycan. Precisely, the core structure of the complex glycan consists of two *N*-acetylglucosamines (GlcNAc), followed by three branched mannoses, which then form the basis for the biantennary character of the glycan (Figure 4). A core fucosylation can be attached to the first GlcNAc, and another GlcNAc can be attached to the branched Mannose, leading to bisection. The two terminal mannoses, which represent the two antennae, are terminated by two GlcNAcs, which can be extended by galactose and further sialic acid (Parekh et al., 1985; Pilkington et al., 1995). The enzyme, that facilitates the core fucosylation is alpha1,6-fucosyltransferase 8 (Fut8) (Boruah et al., 2020). Accordingly, many different combinations of attached sugar residues are possible for each IgG subclass, which makes IgG Fc *N*-glycosylation very diverse.

To emphasize the importance of IgG glycosylation patterns, IgG antibodies with removed Fc *N*-glycans show greatly reduced interactions with FcγRs and complement (Tao & Morrison, 1989). Furthermore, different states of the glycan can be associated with different functions and conditions.

Afucosylation of IgG enhances the affinity of IgG antibodies to FcγRs and has been connected to an increased potential in tumor and pathogen clearance. However, other trends are observed in inflammatory diseases (Dekkers et al., 2018; Flevaris & Kontoravdi, 2022; Larsen et al., 2021).

Agalactosylated (G0) IgG antibodies are associated with pro-inflammatory (auto-) immune conditions, while attachment of galactose and terminal sialic acid is linked to less inflammatory or even anti-inflammatory conditions (Ercan et al., 2010; Ohmi et al., 2016). The anti-inflammatory effect of sialylated antibodies has also been demonstrated for other isotypes, namely IgM, IgA, and IgE antibodies (Colucci et al., 2015; Dühring et al., 2023; Steffen et al., 2020), although the latter are still under discussion (Banerjee et al., 2024; Dühring et al., 2023; K.-T. C. Shade et al., 2020).

Interestingly, not only antigen-specific IgG Fc galactosylation and sialylation patterns, but also the corresponding total IgG Fc glycosylation patterns have been linked to certain inflammatory conditions. In patients suffering from rheumatoid arthritis (RA), low levels of total IgG Fc galactosylation and sialylation in serum correspond to disease severity (Parekh et al., 1985). This contribution of the overall level of galactosylation and sialylation to the inflammatory condition also explains the anti-inflammatory effect of high levels of intravenous immunoglobulin (IVIg; high amounts of pooled serum IgG from healthy donors). IVIg contains higher levels of galactosylated and sialylated IgGs, as has been described for total serum

IgG from patients with inflammatory immune diseases, and therefore appears to restore a total IgG Fc glycosylation buffer system by increasing the sialylated subfraction (Anthony et al., 2011; Flevaris & Kontoravdi, 2022; Fokkink et al., 2014; Kaneko et al., 2006; Katz-Agranov et al., 2015; Nimmerjahn & Ravetch, 2008a; Ogata et al., 2013).

In contrast to fucosylation, galactosylation and sialylation, the relevance of IgG Fc bisection is less clear but is with increasing evidence associated with pro-inflammatory conditions (Flevaris & Kontoravdi, 2022).

1.3.3 IgG Fc-mediated effector functions

The Fc-mediated activities of IgG are dependent on two characteristics: the subclass and the Fc *N*-glycosylation pattern. Hu IgG1 and IgG3 as well as mu IgG2a and IgG2b show the highest affinities to classical activating FcγRs on effector immune cells (Bruhns et al., 2009; Buhre et al., 2022; Lilienthal et al., 2018; Y. Wang et al., 2022). Furthermore, they have the highest potential to activate the classical complement pathway, which is facilitated by hexamerization and initial interaction with the six-armed C1q-molecule (Cook et al., 2016; De Jong et al., 2016; Diebolder et al., 2014; Lilienthal et al., 2018; Melis et al., 2015; G. Wang et al., 2016). On the other hand, hu IgG2 and mu IgG3 hardly interact with activating FcγRs or C1q, so their contribution to effector functions is poorly understood (Bruhns et al., 2009; Y. Wang et al., 2022). Hu IgG4 and mu IgG1, in contrast to hu IgG1/IgG3 and mu IgG2a/IgG2b, are the subclasses that are often referred to as inhibitory. Their affinities for activating FcγRs are lower than for the only classical IgG inhibitory receptor FcγRIIb (Bruhns et al., 2009; Y. Wang et al., 2022). Further, they hardly activate C1q and are able to disrupt the hexamer formation of the activating IgG subclasses and thus C1q binding (Melis et al., 2015; Oskam et al., 2023). Additionally, hu IgG4 is the only subclass that performs a dynamic Fab-arm-exchange. This mechanism leads to bispecific IgG4 antibodies that can reduce immune complex formation and hexamerization of the other subclasses (Labrijn et al., 2009; van der Neut Kolfschoten et al., 2007). Human IgG4 has further been described to inhibit the function of antigen-bound IgG1 through Fc-Fc interactions (Lighaam & Rispens, 2016; Rispens et al., 2009). These inhibitory mechanisms can lead to a reduction in the activation potential of the activating subclasses (Lilienthal et al., 2018; Rispens & Huijbers, 2023).

The concept of the activating subclasses hu IgG1/IgG3 and mu IgG2a/IgG2b becomes particularly clear when examining the occurrence of IgG subclasses in inflammatory autoimmune diseases. Shifts from the inhibitory subclass (hu IgG4, mu IgG1) to the activating subclasses have been associated with higher inflammatory autoimmune conditions (Hammers et al., 2011; Lilienthal et al., 2018; Strait et al., 2015; Zuo et al., 2016).

As mentioned above, afucosylated IgG antibodies have an increased affinity for activating FcγRs, namely FcγRIIIa and FcγRIIIb, and are subsequently linked to increased tumor clearance and viral protection (e.g. HIV, Malaria) (Ackerman et al., 2013; Ferrara et al., 2011; Larsen et al., 2021; Nimmerjahn & Ravetch, 2005, 2008b; Shields et al., 2002). Aside from the described protective potential of afucosylated IgG antibodies, these have also been associated with severe forms of dengue fever and COVID-19 (Bournazos et al., 2021; Pongracz et al., 2022).

The association between increased inflammatory conditions and asialylated (and subsequently agalactosylated) IgG molecules could be due to increased affinity for activating FcγRs, increased activation of the complement system via the alternative or lectin pathway (Arnold et al., 2007; Banda et al., 2008; Haddad et al., 2021; Malhotra et al., 1995), and lack of interaction with other glycan-binding receptors (Anthony et al., 2011; Arnold et al., 2007; Bartsch et al., 2018; Buhre et al., 2022; de Jong et al., 2016; Epp et al., 2018; Hess et al., 2013; Kaneko et al., 2006; Lilienthal et al., 2018; Nimmerjahn & Ravetch, 2008b; Oefner et al., 2012; Ohmi et al., 2016; Petry et al., 2021; Pincetic et al., 2014). Consistent with these observations, galactosylated IgG antibodies have been associated with the exertion of inhibitory effector functions through the crosslinking of Dectin-1 with the inhibitory FcγRIIb (Epp et al., 2018; Ito et al., 2014; Karsten et al., 2012). Total IgG sialylation has been described to mediate anti-inflammatory effects via binding of the C-type lectin receptor SignR1 in mice (Anthony et al., 2011).

IgG subclass galactosylation, sialylation and bisection in relation to pathogen control are less clear. Lower levels of galactosylation and fucosylation are linked with better viral control in HIV patients (Ackerman et al., 2013). Similarly, active tuberculosis infections are associated with more pro-inflammatory IgG Fc glycosylation patterns (Lu et al., 2016). In a vaccination study with rhesus macaques, two different adjuvants were compared, and the vaccine with better protection also correlated with lower galactosylated and sialylated IgG antibodies (Vaccari et al., 2016). In contrast, other studies suggest that sialylated IgG1 may interact better with CD23 on B cells within GCs, thereby promoting affinity maturation of BCRs through FcγRIIB upregulation (T. T. Wang et al., 2015). Others claim that galactosylated IgG1 may interact better with C1q and Natural Killer (NK) cells (Boudreau et al., 2022, 2023; Dekkers et al., 2017; Jennewein et al., 2019; Oskam et al., 2023; Quast et al., 2015; Rispens et al., 2009; van Osch et al., 2021; Wei et al., 2021).

Although it was hypothesized that the induction of afucosylated IgG by vaccination should improve the protective potential against pathogens, a clear picture of the role of galactosylation, sialylation and bisecting after vaccination remained unclear.

1.3.4 Regulation of IgG class-switching and Fc glycosylation

Various cytokines acting on B cells play an important role in the induction of IgG class switching: Interferon gamma (IFNγ) has been associated with IgG1 (Toellner et al., 1998), IFNγ and TGFβ together with IgG3 (Murphy et al., 2012) and Interleukin-4 (IL-4) with IgG4 (Snapper et al., 1988). Since IgG1 and IgG3 in particular are the subclasses with high activation potential and consequently protective capabilities, vaccination against pathogens should induce corresponding cytokines to generate IgG1 and IgG3 antibodies.

Glycan structures on newly synthesized proteins, like IgG antibodies, are crucial for protein secretion. As they are involved in proper folding, they act as quality control and mediate transport through the secretory pathways from the ER to the Golgi apparatus and to the plasma membrane (Moremen et al., 2012). IgG Fc glycosylation, which strongly influences IgG Fc-mediated effector functions, is facilitated by specific enzymes. These enzymes hierarchically add specific sugar residues (Moremen et al., 2012). IgG Fc fucosylation is mediated by the enzyme Fut8 and galactosylation is mediated by β-1,4-galactosyltransferase (B4galt1) (Lauc et al., 2013; Wahl et al., 2018). IgG Fc sialylation, which is facilitated by the enzyme α-2,6-sialyltransferase (St6gal1), requires a galactosylated glycan and cytidine monophosphate (CMP)-activated sialic acid as substrate (Meng et al., 2013). When comparing the expression levels of the St6gal1 in IgG-producing plasma cells and the corresponding IgG Fc sialylation levels, strong correlations were observed (Bartsch et al., 2020; Hess et al., 2013; Oefner et al., 2012; Pfeifle et al., 2017). Furthermore, it was shown that the sialylation levels of IgG^+ GC B cells correlate with the glycosylation levels of IgG antibodies. Therefore, it was hypothesized that the programming of the long-term IgG Fc glycosylation takes place during the GC reaction (Bartsch et al., 2020). It was assumed that galactosylation and sialylation are highly co-regulated (Bartsch et al., 2020).

In inflammatory (auto-) immune disorders, (auto)antigen-specific and total IgG Fc glycosylation is altered in the direction of more agalactosylation (and consequently asialylation). This indicates that the regulation of glycosylation is disturbed (Ercan et al., 2010; Scherer et al., 2010). Attenuation of the disease correlates with increased levels of galactosylation and sialylation in total and (auto)antigen-specific IgG antibodies, as has also been described for pregnancy-associated remission (Rook et al., 1991; van de Geijn et al., 2009). In line with these observations, elevated levels of the sex hormone estrogen during pregnancy and its downregulation during menopause correlate positively and negatively with IgG Fc glycosylation levels, respectively (Ercan et al., 2017). Subsequently, an up-regulation of St6gal1 and B4galt1 and a downregulation of disease severity upon treatment with (phyto)estrogens was described (Du et al., 2020; Engdahl et al., 2018; Ercan et al., 2017).

In addition to estrogen, anti-tumor necrosis factor α (TNFα) therapy is a common treatment for inflammatory autoimmune diseases. In RA patients, autoantigen-specific and total IgG galactosylation and sialylation levels increased with anti-TNF therapy, which correlated with a decrease in inflammation (Collins et al., 2013). Next to therapeutic interventions, recent studies have described positive correlations between the body mass index (BMI) and IgG Fc agalactosylation levels (Liu et al., 2018; Nikolac Perkovic et al., 2014). Subsequently, extensive weight loss increases IgG Fc galactosylation (Greto et al., 2021) indicating, that an individual’s metabolic state also regulates IgG Fc glycosylation. Accordingly, total

IgG Fc galactosylation and sialylation levels are used to characterize the biological age of individuals (Yu et al., 2016).

Lately, studies have shown that the type of antigen elicits different IgG Fc glycosylation patterns upon infection or vaccination, which could contribute to protection. In particular, membrane bound antigens have been shown to result in afucosylated IgG antibodies (Larsen et al., 2021).

Furthermore, a recent vaccination study in mice has shown that different adjuvants induce distinct IgG Fc galactosylation and sialylation patterns that are dynamic over time. Especially early IgG antibodies showed higher galactosylation and sialylation levels, while later (probably GC-derived) antibody responses showed lower galactosylation and sialylation levels, with late responses in particular appearing to be adjuvant-dependent (Bartsch et al., 2020). More pro-inflammatory adjuvants seemed to induce lower late IgG galactosylation and sialylation levels, which was shown to be dependent on IFNy and IL-17 dependent (Bartsch et al., 2020).

During the COVID-19 pandemic, new mRNA- and adenovirus-based vaccines were rapidly developed and licensed. However, the induction of anti-S IgG subclasses and their Fc glycosylation pattern for both short-and long-term responses after repeated vaccination were unclear before this project started.

1.4 Aims

Vaccinations are undoubtedly one of medicine’s greatest achievements and have saved many lives. The effectiveness of vaccinations is influenced by various factors such as the type of antigen, the adjuvant, or the vaccination site, but is not yet fully understood. The COVID-19 pandemic has been a severe burden on global health and the economy, but newly developed vaccine formats have prevented many deaths. However, the induction of short- and long-term anti-S IgG subclasses and their Fc glycosylation pattern after repeated vaccination were previously unclear. Therefore, one aim of this thesis was to characterize the longitudinal IgG responses induced by the newly developed vaccine formats and their role in the activation on various innate immune functions.

Furthermore, there are groups of people who require special attention during vaccination due to medical circumstances. An example of such a group is people suffering from inflammatory (auto-) immune diseases that often require constant treatments, which may affect the vaccination outcome. Another aim of this work was to examine the IgG response of a cohort of patients suffering from inflammatory (auto-) immune diseases who received TNF blockers during the period of mRNA vaccination against COVID-19.

2. Material and Methods

2.1 Material

2.1.1 Human cohorts

SARS-CoV-2 naïve and non-hospitalized pre-infected (COVID-19 infection before the first vaccination) subjects were recruited and were divided into groups according to their vaccination schedules (Table 2). Three different vaccine formats were investigated: the mRNA-based vaccines from BioNTech/Pfizer (BNT162b, 30 µg) or from Moderna (mRNA-1273, 100 µg) or the adenovirus-based vaccine from AstraZeneca (ChAdOx1 nCoV-19 or AZD1222, 5x10^10 viral particle with no less than 2.5x10^8 infectious units). As Figure 5 shows, the interval between the first and second vaccination was 21-45 days for the mRNA vaccinations, while for the adenovirus-based vaccination there were 70-84 days between a first and a second vaccination (except for five subjects who received their second dose between day 35 and 61).

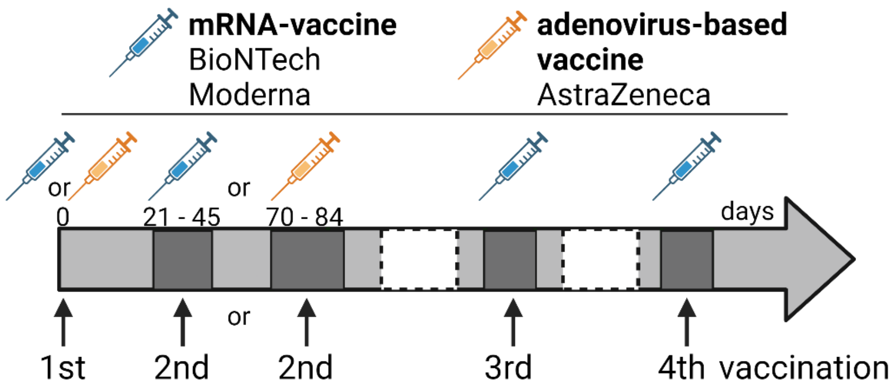

Figure 5: Schematic description of the vaccination scheme.
Vaccination scheme for the mRNA vaccines (BioNTech and Moderna) as well as the adenovirus-based vaccine from AstraZeneca. The mRNA vaccines were administered the second time 21-45 days and AstraZeneca 70-84 days after the first vaccination. Follow-up vaccinations with mRNA vaccines were given in no defined time frame. This illustration was created with BioRender.com.

No specific vaccination schedules were followed for either the third or fourth mRNA vaccination. For this reason, the variance of the time window until the third/fourth vaccination was very large and sometimes could not be reconstructed. For the analysis of the data of the third or fourth vaccination, only the days of sampling until the last vaccination were considered.

As shown in Table 2, the serum samples were collected at different locations: i) at the University of Lübeck (UzL) and the University Medical Center Schleswig-Holstein (UKSH) in Lübeck, Germany (HL), and in collaboration with ii) the Universitätsmedizin Berlin Charité, Germany (BE), iii) the Semmelweis University in Budapest, Hungary (BU) and iv) the UKSH in Kiel, Germany (HK). In addition, full blood and saliva was collected from some individuals in HL.

No selection criteria were set for the cohorts sampled at the UzL or UKSH in Lübeck, Germany, and participants and repetitive sampling were randomized. However, the preferred local vaccination strategy was either two doses of the BioNTech vaccine or a hybrid vaccination with AstraZeneca followed by Moderna. Therefore, the numbers in these two groups were comparatively high. All pre-infected individuals collected in HL received the BioNTech-vaccine and had a mild pre-infection. They were not hospitalized and showed no severe symptoms such as shortness of breath or abnormal chest imaging. The naïve/ pre-infected status of the cohorts from HL was verified by detection of anti-viral nucleocapsid protein (anti-NCP) IgGs up to 270 days after the first (including a second) vaccination. Later, this was no longer defined as an exclusion criterion, as almost all subjects had a breakthrough infection after the second or third vaccination. Therefore, NCP status was no longer considered after 270 days following the first vaccination.

For the investigations of increasing IgG4 levels and their functional activity (see 3.2), samples from the Universitätsmedizin Berlin Charité, Germany were investigated. These samples were recruited as part of the COVIM-Boost study, which took place between 2021 and 2022 the Universitätsmedizin Berlin Charité. These samples were kindly provided by Pinkus Tober-Lau, Prof. Florian Kurth and Prof. Leif Erik Sander. For the same analysis, samples from the Semmelweis University in Budapest, Hungary, were used. These samples were also collected between 2021 and 2022 and were recently published elsewhere (Kiszel et al., 2023). The samples were kindly provided by Dr. Petra Kiszel, Prof. László Cervenak and Prof. Zoltán Prohászka.

For the study with TNF inhibitors (see 3.3), patients with chronic inflammatory immune diseases (rheumatoid arthritis (RA), psoriasis, psoriatic arthritis, systemic lupus erythematosus, spondylarthritis, sarcoidosis, mixed connective tissue diseases) were recruited. These patients were treated with either TNF inhibitors or other DMARDs (disease-modifying anti-rheumatic drugs: anti-α4β7 integrin, anti-BlyS, anti-IL-17, hydroxychloroquine (HCQ), sulfasalazine or steroids) over a period of one to three immunizations. Furthermore, a group of healthy controls was recruited. This cohort has already been described several times (Geisen, Berner, et al., 2021; Geisen et al., 2022; Geisen, Sümbül, et al., 2021) and was sampled at the UKSH in Kiel, Germany. The samples were kindly provided by Dr. Ulf Geisen and Prof. Bimba Hoyer.

All blood and saliva samples were collected after obtaining written informed consent according to the Declaration of Helsinki and a protocol approved by the local ethics boards: Ethics Committee of the University of Lübeck, Germany (No. 20-123), Hungarian Scientific and Research Ethics Committee (ETT-TUKEB; No. IV/4403-2/2020/EKU), Ethics Committee of the Charité - Universitätsmedizin Berlin, Germany (No. EA4/261/21) and Ethics Committee of the Christian-Albrecht University Kiel, Germany (D409/21).

Table 2: Summary of all used cohorts.

Abbreviations: B BioNTech; M Moderna; A AstraZeneca; pre-inf. pre-infected; HL University of Luebeck and University Medical Center Schleswig-Holstein in Luebeck, Germany; BE University Medical Center Berlin-Charité, Germany; BU Semmelweis University Budapest, Hungary; HK University Medical Center Schleswig-Holstein in Kiel, Germany; pre-inf. pre-infected; f female; m male, n.a. not assessed.

Cohort	Vacci-nation	Ori-gin	Section	number of individuals (samples)	individual IDs	Age mean (range)	sex
Vaccination study up to day 270							
B	B+B	HL	3.1	48 (183)	B 1-48	36 (19-66)	26 f, 22 m
M	M+M	HL	3.1	25 (76)	M 1-25	42 (21-61)	21 f, 4 m
A	A+A	HL	3.1	14 (43)	A 1-14	41 (22-62)	7 f, 7 m
AB	A+B	HL	3.1	12 (47)	AB 1-12	30 (23-44)	9 f, 3 m

AM	A+M	HL	3.1	44 (107)	AM 1-44	36 (22-63)	33 f, 11 m
pre-inf. B	B(+B)	HL	3.1	14 (37)	pB 1-14	47 (27-74)	8 f, 6 m
B II	B+B	HL	3.1.5	20	B 1-9, 11-15, 18-20, 27, 29, 32	34 (19-52)	10 f, 10 m
pre-inf. B II	B(+B)	HL	3.1.5	9	pB 1, 2, 4-8, 13, 14	48 (29-74)	5 f, 4 m
M II	M+M	HL	3.2	23 (61)	M 1-17, 19-24	40 (21-60)	19 f, 4 m
Vaccination study third/fourth vaccination							
BU	B+B+B	BU	3.2	23 (32)	BU 1-23	42 (20-82)	15 f, 8 m
BE	B+B+B (+M)	BE	3.2	43 (59)	BE 1-43	49 (28-68)	30 f, 13 m
HL 3rd	B+B+B A+M+B A+M+M A+A+B M+M+B	HL	3.2	14 (15)	B16, 49-53; AM1-4, 32; A2, 3; M26	36 (22-60)	12 f, 2 m
HL before / post 3rd	M+B B+B(+B) A+B+B/M A+A+M A+M(+M) A+M(+B)	HL	3.4	27 (37)	A15; AB3, 4; AM1, 3, 12, 16, 20, 30, 33; B1, 16, 17, 24, 37, 38, 40, 43, 49-53; pB2, 3, 11; pM1	36 (22-63)	18 f, 9 m
Vaccination study with anti-TNF treated patients							
healthy controls	B+B(+B)	HK	3.3	23 (77)	healthy 1-23	43 (22-57)	15 f, 8 m
other DMARDs	B+B(+B)	HK	3.3	12 (38)	oDMARD 1-12	45 (24-61)	6 f, 6 m
anti-TNF	B+B(+B)	HK	3.3	11 (35)	TNFi 1-11	49 (33-83)	9 f, 2 m
Negative controls							
negative controls	-	HL	3.1, 3.2.1	8 (8)	neco 1-8	n.a.	n.a.

2.1.2 Mice

C57BL/6 mice were purchased from the Jackson Laboratories or Janvier Labs. For the *in vivo* experiment 8-12 weeks old female mice were used following the regulatory guidelines and ethical standards of the University of Lübeck. The experiments were approved by the Federal Ministry of Energy, Agriculture, the Environment and Rural Areas Schleswig-Holstein (License number: 39_48-6/18).

2.1.3 Consumables

Table 3: List of the used consumables.

Material	Manufacturer / Vendor
3-way stopcock, Discofix C	Braun (Melsungen, Germany)
8-well tube strips	Kisker Biotech (Steinfurt, Germany)
96-well Polypropylene plate (conical, 450µl/well)	Thermo Fisher (Waltham, MA, USA)
Amicon® Ultra-4 Centrifugal Filter Units	Merck (Darmstadt, Germany)
Costar Assay plates (high binding), 96-well	Corning (Kennebunk, ME, USA)
Cryo-Tubes, 2ml, external thread	Th. Geyer GmbH & Co. KG (Renningen)
Falcon 70µm cell strainer	Corning (Kennebunk, ME, USA)
Falcon tubes (15, 50 mL)	Greiner Bio-one (Kremsmünster, Austria)
Flow Cytometry tube 5 mL	Sarstedt (Sarstedt, Germany)
Grid insert for cryogenic boxes	Th. Geyer GmbH & Co. KG (Renningen)
Injection patches (1.7 x 4 cm)	Gothaplast Verbandpflasterfabrik GmbH (Gotha)
MiniCollect Tube (serum)	Greiner Bio-one (Kremsmünster, Austria)
Needle 26G 0.45x13mm	Braun (Melsungen, Germany)
Needle 26G 0.45x25mm	Braun (Melsungen, Germany)
Needle (Eclipse)	BD Bioscience (San Diego, CA, USA)
Neubauer chamber	Assistant (Sondheim vor der Rhön, Germany)

ORACOL+ Saliva Collection Device	Malvern Medical Developments (Worcester, England)
PCR plate seals ROTILABO®	Carl Roth GmbH & Co. KG (Karlsruhe, Germany)
Pipette tips with and without filter (10, 100, 200, 1000 µL)	Sarstedt (Nümbrecht, Germany)
Reaction tubes (1.5, 2.0 mL)	Sarstedt (Nümbrecht, Germany)
Safety-Multifly-Cannula (21 G x 3/4‘‘, green, 200 mm hose length)	Sarstedt (Nümbrecht, Germany)
Serological pipettes (5, 10, 25, 50 mL)	Sarstedt (Nümbrecht, Germany)
Single-use syringes (1, 2, 5, 10 mL)	Braun (Melsungen, Germany)
Skin disinfectant Softasept N	B. Braun Melsungen AG (Melsungen, Germany)
S-Monovette (K3 EDTA, 7.5ml)	Sarstedt AG & Co. KG (Nümbrecht, Germany)
S-Monovette (Serum, 7.5ml)	Sarstedt AG & Co. KG (Nümbrecht, Germany)
Tourniquet	Holtsch Medizinprodukte (Taunusstein, Germany)
PCR storage rack	Biozym (Oldendorf, Germany)
Pierce™ Centrifuge Columns, 10 mL	Thermo Fisher (Waltham, MA, USA)
Pierce™ Micro-Spin Columns	Thermo Fisher (Waltham, MA, USA)
Pur-Zellin sterile swabs	PAUL HARTMANN GmbH (Wiener Neudorf, Österreich)
Sterillium	PAUL HARTMANN GmbH (Wiener Neudorf, Österreich)

2.1.4 Chemicals

Table 4: List of the used chemicals.

Chemical compound	**Manufacturer / Vendor**
Ammonium chloride (NH_4Cl)	Merck (Darmstadt, Germany)
Calcium chloride ($CaCl_2$)	Sigma-Aldrich (St, Louis, MO, USA)
Chemical Compound	Manufacturer / Vendor
Biocoll® separation solution (Density 1,077 g/mL)	Bio&Sell (Nürnberg, Germany)
BD OptEIA (TMB substrate)	BD Bioscience (San Diego, CA, USA)
BSA (bovine serum albumin)	GE Healthcare (Little Chalfont, UK)
Carbonate-bicarbonate	Sigma-Aldrich (St, Louis, MO, USA)
CMP-sialic acid	Millipore (Billerica, MA, USA)
CnBr activated Sepharose 4B	GE Healthcare (Little Chalfont, UK)
CNBr-activated Sepharose TM 4 Fast Flow	GE Healthcare (Little Chalfont, UK)
Cytofix/Cytoperm	BD Bioscience (San Diego, CA, USA)
Dulbecco´s Phosphate-buffered saline	Thermo Fisher (Waltham, MA, USA)
Ethanol	Carl Roth (Karlsruhe, Germany)
Ethylenediaminetetraacetic acid (EDTA)	Sigma-Aldrich (St, Louis, MO, USA)
FCS (Fetal calf serum)	Thermo Fisher (Waltham, MA, USA)
Fixable viability dye (eFluor780)	Thermo Fisher (Waltham, MA, USA)
Focusing Fluid	Thermo Fisher (Waltham, MA, USA)
Glycine	Merck (Darmstadt, Germany)
HEPES	Life Technologies (Darmstadt, Germany)
Hydrogen chloride (HCl)	Merck (Darmstadt, Germany)
Incomplete Freund's Adjuvant	Sigma-Aldrich (St, Louis, MO, USA)
Ketamin 10 mg/mL	WDT (Garbsen, Germany)
MES	Carl Roth GmbH & Co. KG (Karlsruhe, Germany)

Milk powder	Merck (Darmstadt, Germany)
M. Tuberculosis Des. H37 Ra (non-viable)	BD Bioscience (San Diego, CA, USA)
Reaction buffer B, 5x	Prozyme (Hayward, CA, USA)
Rompun 2% (Xylazine)	Bayer (Lerverkusen, Germany)
Saponin	Sigma-Aldrich (St. Louis, MO, USA)
Sodium acetate (NaOAc)	Sigma-Aldrich (St, Louis, MO, USA)
Sodium azide (NaN_3)	AppliChem (Darmstadt, Germany)
Sodium bicarbonate ($NaHCO_3$)	Merck (Darmstadt, Germany)
Sodium chloride (NaCl)	Merck (Darmstadt, Germany)
Streptavidin (APC-conjugated)	Thermo Fisher (Waltham, MA, USA)
Sulfuric acid (H_2SO_4)	Sigma-Aldrich (St. Louis, MO, USA)
TMB substrate reagent set	BD Biosciences (Heidelberg, Germany)
Tris-HCl	Sigma-Aldrich (St. Louis, MO, USA)
Trisma Base (Tris)	Sigma-Aldrich (St. Louis, MA, USA)
Trypan blue solution	Sigma-Aldrich (St, Louis, MO, USA)
Tween20	Sigma-Aldrich (St. Louis, MO, USA)
UDP-galactose	Millipore (Billerica, MA, USA)

2.1.5 Buffers

Table 5: List of the used buffers.

Buffer	Component	Concentration
ELISA		
Blocking / Sample buffer	Tween20 BSA in PBS	0,05% (w/v) 3% (w/v)
Coating buffer	Carbonate-bicarbonate in ddH_2O	50 mM
Lectin buffer	HEPES $CaCl_2$ NaCl Tween20 in ddH_2O	10 mM 0.1 mM 0.15 mM 0.1%

Milk buffer	Milk powder in PBS	2.5%
Stop solution	H_2SO_4 in ddH_2O	4.2%
Stop solution	H_2SO_4 in ddH_2O	4.2%
Wash buffer	Tween20 in PBS	0.05% (v/v)
Column preparation and antibody purification		
Activation buffer	HCl in ddH_2O	1 mM
Blocking buffer	Tris-HCl in ddH_2O, adjusted to pH 8	0.1 M
Coupling buffer	Sodium bicarbonate ($NaHCO_3$), Sodium chloride (NaCl) in ddH_2O, adjusted to pH 8.3	100 mM 500 mM
Elution buffer	Glycine in ddH_2O, adjusted to pH 2.8	0.1 M
PBS-T	Tween-20 in PBS	0.05%
Quenching buffer	Tris-HCl in ddH_2O, adjusted to pH 8	100 mM
Wash buffer high pH	Tris-HCl Sodium chloride (NaCl) in ddH_2O, adjusted to pH 8.0	100 mM 500 mM
Wash buffer low pH	Sodium acetate ($C_2H_3NaO_2$) Sodium chloride (NaCl) in ddH_2O, adjusted to pH 4.0	100 mM 500 mM
Flow Cytometry		
Red blood cell lysis buffer	EDTA Ammonium chloride (NH_4Cl) Sodium bicarbonate ($NaHCO_3$) in ddH_2O	0.1 mM 155 mM 10 mM
FACS buffer	BSA EDTA in PBS	0.5% (w/v) 0.05% (w/v)
PermWash (Flow Cytometry)	PBS BSA Saponin Sodium azide (NaN_3) in ddH_2O	0.05x 0.1% (w/v) 0.05% (w/v) 0.01% (w/v)

Antibody glycosylation		
MES buffer	MES in ddH20, adjusted to pH 7.2	100 mM

2.1.6 Recombinant proteins

Table 6: List of the used recombinant proteins.

Protein	Manufacturer / Vendor
SARS-CoV-2-S1 (biotinylated)	ACROBiosystems (Newark, DE, USA)
SARS-CoV-2-S1 (his-tag)	ACROBiosystems (Newark, DE, USA)
anti-mouse TNF-α rabbit (monoclonal, clone XT3.11)	BioXCell, (Lebanon, NH, USA)

2.1.7 Antibodies

Table 7: List of the used antibodies.

Specificity	Clone	Isotype	Conjugate	Manufacturer/ Vendor
human IgG	A80-104P	IgG (goat)	HRP	Bethyl Laboratories (Montgomery, TX, USA)
human IgG1	HP-6001	IgG (mouse)	HRP	Southern Biotech (Birmingham, AL, USA)
human IgG2	HP-6014	IgG (mouse)	HRP	
human IgG3	HP-6050	IgG (mouse)	HRP	
human IgG4	HP-6025	IgG (mouse)	HRP	
human IgG4	HP-6025	IgG (mouse)	unconjugated	
human CD138	MI15	IgG1 (mouse)	BV711	Biolegend (SanDiego, CA, USA)
human CD19	HIB19	IgG1 (mouse)	BV510	
human CD27	O323	IgG1 (mouse)	BV785	
human CD38	HIT2	IgG1 (mouse)	BV421	
human IgG-Fc	M1310G05	IgG2a (mouse)	PE	

human IgA	IS11-8E10	IgG1 (mouse)	PE-Vio700	Miltenyi Biotec B.V. & Co. KG (Bergisch Gladbach)
human St6gal1	polyclonal	IgG (goat)	unconjugated	R&D Systems (Minneapolis, MN, USA)
human Fut8	polyclonal	IgG (sheep)	unconjugated	
mouse IgM	polyclonal	IgG (goat)	HRP	Bethyl Lantibodies (Montgomery, TX, USA)
mouse IgG1	polyclonal	IgG (goat)	HRP	
mouse IgG2b	polyclonal	IgG (goat)	HRP	
mouse IgG2c	polyclonal	IgG (goat)	HRP	

2.1.8 Kits

Table 8: List of the used Kits.

Kit	Manufacturer / Vendor
Anti-SARS-CoV-2-S1 IgA-ELISA kit	EUROIMMUN (Lübeck, Germany)
Anti-SARS-CoV-2-S1 IgG-ELISA kit	EUROIMMUN (Lübeck, Germany)
Anti-SARS-CoV-2-NCP IgG-ELISA kit	EUROIMMUN (Lübeck, Germany)
AlexaFluor 488 Antibodies labelling kit	Thermo Fisher (Waltham, MA, USA)

2.1.9 Instruments

Table 9: List of the used instruments.

Instrument	Manufacturer / Vendor
Attune NxT Flow Cytometer	Thermo Fisher (Waltham, MA, USA)
Autoclave VX-75	Systec (Linden, Germany)
Barnstead GenePure Pro (Ultrapure water)	Thermo Fisher (Waltham, MA, USA)
BioGARD Hood	The Baker Company, Inc. (Sanford, ME, USA)
Centrifuge 5424R	Eppendorf (Hamburg, Germany)
Centrifuge Mega Star 3.0R	VWR

Electronic balance	Kern & Sohn (Balingen-Frommern, Germany)
ELISA-Reader Spectra Max iD3	Molecular Devices, LLC. (San Jose, CA, USA)
Incubator AutoFlow NU-5510	NuAire (Plymouth, MN, USA)
Microscope Primovert	Zeiss (Oberkochen, Germany)
NanoDrop-2000C	peqlab Biotechnologie GmbH (Erlangen, Germany)
pH Meter FiveEasy F20	Mettler-Toledo (Columbus, OH, USA)
Pipetboy Accu 2	IntegraBioscience (Zizers, Switzerland)
Pipette (eight- multichannel)	VWR (Radnor, PA, USA)
Pipette (twelve- multichannel)	Eppendorf (Hamburg, Germany)
Pipette (single-channel)	Eppendorf (Hamburg, Germany)
Pipette Multi-channel Eppendorf Xplorer® plus	Eppendorf (Hamburg, Germany)
Platform shaker	Bibby Scientific Limited (Staffordshire, United Kingdom)
Vortex-Genie 2	Scientific Industries (Bohemia, NY, USA)
Vortex ZX3	VELP Scientifica (UsmateVelate, Italy)
Waterbath SW-20C	Julabo (Seelbach, Germany)

2.1.10 Software

Table 10: List of the used software.

Software	Company
Excel	Microsoft (Redmond, WA, USA)
Word	Microsoft (Redmond, WA, USA)
FlowJoe	BD Bioscience (San Diego, CA, USA)
Prism v. 9.0, v 10.0	GraphPad Software (San Diego, CA, USA)
MatLab	The MathWorks Inc., Massachusetts, NE
PLS-Toolbox	Eigenvector Research Inc., Wenatchee, WA
BioRender	BioRender (Toronto, ON, Canada)

2.2 Methods

2.2.1 Sample collection

2.2.1.1 Blood and saliva collection (human)

The blood for the serum analyses was collected in serum monovettes and left upward for coagulation for at least 15 minutes at room temperature (RT). It was then centrifuged at 3000 xg for 10 minutes. The supernatant serum was then aliquoted and stored at 4°C, -20°C, or -80°C, depending on how soon the sample was to be used.

The blood for the cell analyses (PBMCs) was collected in Ethylenediamine tetraacetic acid (EDTA) monovettes. The isolation of the PBMCs (see section 2.2.4.1) was then performed within 3 hours.

Saliva samples were collected using the Saliva Collection system-ORACOL Plus S14 and frozen before use. The device containing the saliva samples was then thawed and centrifuged at 3000 xg for 10 minutes. The aliquots were then stored at -20°C or -80°C, depending on how soon the sample was to be used.

2.2.1.2 Blood collection (mouse)

At the end of each experiment, mice were narcotized with a 200 µL mixture of ketamine/xylazine per mouse. 500 – 800 µL of blood was sampled by heart punctation and mice were sacrificed by cervical dislocation. The blood was collected in serum tubes and centrifuged at 4000 xg for 5 minutes. The supernatant serum was then aliquoted and stored at 4°C, -20°C, or -80°C, depending on how soon the sample was to be used.

2.2.2 ELISA

2.2.2.1 Antigen-specific ELISA

For the detection of S1 (Subunit 1 of the spike protein)-specific antibody isotypes and their subclasses, in-house developed ELISA were used. Serum samples were analyzed with the HL-1 ELISA and saliva samples with the HL-2 ELISA.

Therefore, 33 µl of a 4 µg/mL solution of S1 in coating buffer were coated to 96-well costar assay plates and incubated overnight at 4°C or for at least 1 hour at RT. The antigen solution was then discarded and washed three times with 100 µL of PBS-T. The serum samples were diluted (unless otherwise stated) as follows:

1/1000 for IgG and IgG1 detection, 1/100 for IgG2/IgG3/IgG4 detection. Salivary samples were diluted 1/10. All dilutions were performed in ELISA-buffer using 96-well polypropylene plates, with 33 µL of each sample loaded to a coated well. Binding of the serum antibodies to the antigen was performed for 2 hours at RT on a platform shaker. The serum dilutions were discarded, and wells were washed three times with 100 µl PBS-T. HRP-coupled anti-human IgG, IgG1, IgG2, IgG3, or IgG4 detection antibodies were diluted 1:5.000 (IgG 2, IgG4) or 1:20.000 (IgG, IgG1, IgG3) in ELISA buffer. 33 µL of each dilution was loaded to a coated well and incubated for 40 minutes at RT on a platform shaker. After discarding the detection antibodies, the plates were washed three times with 100 µl of PBS-T and finally detected with 50 µL per well of freshly prepared TMB solution (1:1 mixture). The colour reaction was stopped with 50 µL of 4.2% sulfuric acid and the duration was noted to develop a parallel or subsequent ELISA for the same time. The optical density (OD) at 450 nm was measured.
When antigen-specific ELISA was performed with saliva samples, an additional blocking step was included: After coating, 33 µL of ELISA buffer was added and incubated for at least 1 hour at RT on a platform shaker. After discarding the blocking solution, the wells were washed three times with PBS-T and then loading of the was continued as described above.
OD (450 nm) values are shown or a ratio to reference value was calculated by dividing the sample OD (450 nm) value through the OD (450 nm) value of an internal reference sample from an individual with a historical, non-hospitalized SARS-CoV2 infection (for IgG, IgG1-3) or, as the IgG4 levels of this reference sample were too low to be detected, a sample from an individual with detectable IgG4 levels.

The EUROIMMUN SARS-CoV-2 S1 IgG and IgA and the EUROIMMUN SARS-CoV-2-NCP IgG ELISA were performed according to the manufacturer's instructions.

2.2.2.2 Anti-human IgG1-4 ELISA

The anti-human IgG1-4 ELISA was conducted to verify the purity of the isolated IgG4 antibodies and was performed together with the SNA-ELISA (see section 2.2.2.3).

Isolated and differently glycosylated serum IgG4 antibodies were diluted to different concentrations (0.7 µg and 0.23 µg mL^{-1}) in coating buffer and incubated 50 µL per well in a 96-well plate. Coating was performed for 1 hour at RT on a platform shaker. Next, residual sites were blocked by adding 50 µL blocking buffer per well and incubation for 1 hour RT on a platform shaker. After washing three times with 100 µL of PBS-T, the coated antibodies were detected using 50 µL of a 1:5.000 dilution of anti-human IgG1-4-HRP diluted in milk buffer. Plates were incubated for 2 hours at RT in a platform shaker. After washing three times with 100 µL of PBS-T, the detection was initiated with 50 µL per well of freshly prepared TMB solution (1:1 mixture). The colour reaction was stopped with 50 µL of 4.2% sulfuric acid and the duration was noted. The OD at 450 nm was measured. All samples were analyzed in duplicates.

2.2.2.3 SNA-ELISA

Sambucus nigra (SNA)-lectin has a particularly high affinity to sialic acid (Sauer et al, 2014), and can therefore be used to validate the sialylation level of the isolated and glycoengineered serum IgG4 antibodies.

Isolated and differently glycosylated serum IgG4 antibodies were diluted to different concentrations (0.7 µg and 0.23 µg mL^{-1}) in coating buffer and incubated in 50 µL per well in a 96-well plate. Coating was performed for 1 hour at RT on a platform shaker. Next, residual sites were blocked by adding 50 µL blocking buffer per well and incubation for 1 hour RT on a platform shaker. After washing three times with 100 µL of PBS-T, coated antibodies were detected with 50 µl of SNA-lectin conjugates to HRP diluted in lectin buffer. The plates were incubated for 2 hours at RT in a platform shaker. After washing three times with 100 µL of PBS-T, the detection was initiated with 50 µL of freshly prepared TMB solution (1:1 mixture) per well. The colour reaction was stopped with 50 µL of 4.2% sulfuric acid and the duration was noted. The OD at 450 nm was measured. All samples were analyzed in duplicates.

2.2.3 IgG Fc glycan analysis by LC-MS

The IgG subclass LC-MS analysis was performed as described elsewhere (Buhre et al., 2023; De Haan et al., 2017; Van Coillie et al., 2023). Briefly, the glycopeptide analysis by Liquid Chromatography-Mass Spectrometry (LC-MS) discriminates glycosylation patterns of individual IgG subclasses. Therefore, antibodies were purified from serum using corresponding affinity columns. In this thesis, either human anti-S antibodies, total human IgG antibodies or murine anti-Ova antibodies were purified to analyze the corresponding IgG subclass glycopeptides. The following Fc glycopeptide peaks were discriminated: agalactosylated (G0), galactosylated (G1, G2), sialylated (S), bisected (N), and/or fucosylated (F). For each subclass, the relative fractions were summed.

2.2.3.1 anti-S/total IgG subclass Fc-analysis (human)

Analysis of Fc glycopeptide from serum IgG subclasses was performed as recently described (Van Coillie et al., 2023). In brief, total IgG antibodies were affinity-captured from sera and anti-S antibodies were affinity-captured by using a trimerized spike-protein. The captured antibodies were eluted with 100 M formic acid and dried by vacuum centrifugation. After tryptic cleavage with trypsin IgG subclass glycopeptides were analyzed by LC-MS analysis.

Human IgG1 and IgG4 can be discriminated, while human IgG2 and IgG3 were analyzed together, as their Fc glycopeptide had the same amino acid sequence. Not all subclasses could be identified in all samples; in general, the best signals were observed for IgG1 glycopeptides. In addition to analysing the glycosylation patterns, the sum abundancies of the different IgG subclass glycopeptides were also evaluated.

The LC-MS measurement was conducted by Wenjun Wang, Jan Nouta and Dr. Tamas Poncgracz, who are working at the Center for Proteomics and Metabolomics, under the direction of and in collaboration with Prof. Manfred Wuhrer, Leiden University Medical Center (LUMC), Leiden, the Netherlands and are described in detail elsewhere (De Haan et al., 2017; Selman et al., 2012).

For the analysis of the IgG Fc glycosylation, 12 glycopeptides identified were used in the section 3.1 (missing: G0FN, G1FNS1). For the analysis shown in sections 3.2, 3.3 and 3.4, 14 peptides were identified (see Table S1).

The different glycosylation traits were calculated as with the following formulas:

$$\boldsymbol{Fucosylation\ (F)} = (\mathrm{G0F} + \mathrm{G0FN} + \mathrm{G1F} + \mathrm{G2F} + \mathrm{G1FN} + \mathrm{G2FN} + \mathrm{G1FNS1} + \mathrm{G1FS1} + \mathrm{G2FS1} + \mathrm{G2FNS1} + \mathrm{G2FS2})\ /\ \text{sum of all glycopeptides}$$

$$\boldsymbol{Bisection}\ (\boldsymbol{N}) = (\text{G0FN} + \text{G1FN} + \text{G2FN} + \text{G1FNS1} + \text{G2FNS1}) / \text{ sum of all glycopeptides}$$

$$\boldsymbol{Galactosylation}\ (\boldsymbol{G}) = (0.5 * (\text{G1} + \text{G1F} + \text{G1FN} + \text{G1FNS1} + \text{G1FS1}) + 1 * (\text{G2} + \text{G2F} + \text{G2FN} + \text{G2S1} + \text{G2FS1} + \text{G2FNS1} + \text{G2FS2})) / \text{ sum of all glycopeptides}$$

$$\boldsymbol{Sialylation}\ (\boldsymbol{S}) = (0.5 * (\text{G1FNS1} + \text{G2S1} + \text{G1FS1} + \text{G2FS1} + \text{G2FNS1}) + (1 * \text{G2FS2})) / \text{ sum of all glycopeptides}$$

2.2.3.2 IgG subclass frequency calculation

To further calculate the abundances of the anti-S or total IgG subclasses within a sample, the summed intensities of all analyzed IgG subclass glycopeptides were compared to all summed intensities of all IgG subclass glycopeptide peaks measured via MS. The sum-intensities of anti-S or total IgG1, IgG2/3, plus IgG4 values were summed and set as 100%. Then, the respective percentage of each subclass was determined. In parallel, anti-S1 IgG subclass ELISA were performed with these samples, and both values were plotted against each other as Figure 6 shows as an example for anti-S(1) IgG1.

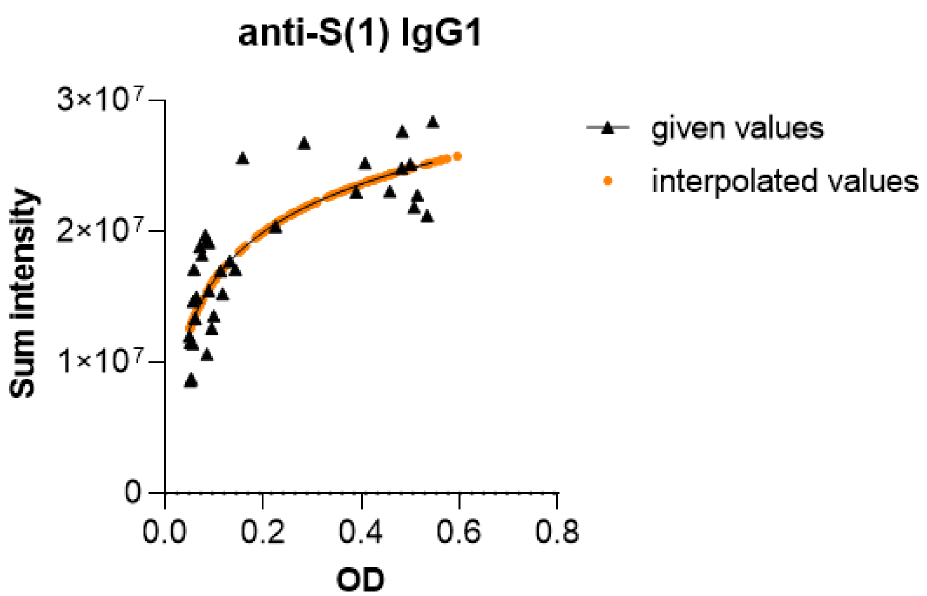

Figure 6: Anti-S(1) IgG1 subclass levels measured by both methods (ELISA and LC-MS). GraphPad was used to create a semi-logarithmic line based on given values, which was used to interpolate the missing LC-MS values. This made it possible to calculate sum-intensity values for samples for which no LC-MS analysis was available.

Since LC-MS glycopeptide data were not available for all samples, especially not for the samples collected or received late, approximate values were calculated. Therefore, standard semi-logarithmic curves were generated for each subclass by plotting OD 450 nm ELISA values against IgG subclass sum-intensities (e.g. for IgG1 in Figure 6). To generate an approximate anti-S IgG2/3 calibration curve, LC-MS based sum-intensity anti-S IgG2/3 data were correlated with summed anti-S1 IgG2/IgG3 ELISA data.

In general, it is important to note that this approach to calculating the percentages is only an approximation. To check whether the calculated values are reliable, they were compared with the calculated values from other publications. Irrgang et al., 2023 reported that the anti-S IgG4 proportion after two mRNA vaccinations (BioNTech) was around 4.8%, shortly after the third vaccination (BioNTech) 13.9%, and long after the third vaccination around 19.3%. The here shown calculated values were higher after the second vaccination, but comparable shortly and long after the third vaccination (see Figure 24). On the other hand, (Kiszel et al., 2023) calculated higher anti-S IgG4 proportions long after the third vaccination, three mRNA vaccinations resulted in about 40% anti-S IgG4 in their calculations, which was higher than in the here presented calculations. One explanation for the early discrepancies could be that the MS method has a detection limit and therefore too low IgG4 values cannot be reliably measured. Low values are therefore missing in the calculations shown here.

2.2.3.3 Ova-specific IgG subclass Fc-analysis (mouse)

The murine anti-Ova IgG subclass LC-MS analysis and data generation were performed as described for the human analysis described above (De Haan et al., 2017). Briefly, the anti-Ova-specific antibodies were purified from serum samples by using an Ova-specific column. After tryptic cleavage, the resulting glycopeptides were analyzed for IgG subclass glycopeptides using LC-MS (see above).

The LC-MS measurement was conducted by Wenjun Wang and Jan Nouta who are working at the Center for Proteomics and Metabolomics, under the direction of and in collaboration with Prof. Manfred Wuhrer, LUMC, Leiden, the Netherlands and are described in detail elsewhere (De Haan et al., 2017; Selman et al., 2012).

Murine IgG1 and IgG3 can be discriminated, while IgG2a/c and IgG2b were analyzed together because their Fc glycopeptide had the same amino acid sequence.

2.2.4 Flow Cytometry

Flow cytometry was performed to characterize the vaccine-induced plasma cells more precisely. PBMCs were therefore isolated and B cells and plasma cells were stained with fluorescent-labelled antibodies, as explained in more detail below.

2.2.4.1 PBMC isolation

Blood samples collected in EDTA tubes were diluted 1:1 with PBS, then very slowly and carefully layered on an equal amount of Biocoll and centrifuged at 800 xg for 25 minutes (without acceleration and brake) at RT. After centrifugation, the supernatant plasma was discarded or aliquoted and PBMCs were isolated. The PBMCs were diluted with PBS to a total volume of 50 mL and counted. 2x10^7 cells were transferred in a new tube and centrifuged at 500 xg for 10 minutes at RT. The supernatant was discarded, and the remaining cells were resuspended and transferred into a 96-well plate for further staining.

2.2.4.2 B cell staining

B cell staining of PBMCs was performed to identify antigen-specific IgG-producing plasma cells ($IgG^{+}S1^{+}CD138^{+}CD19^{int}$) and to further analyze the proportions of the following four subpopulations: $CD27^{high}CD138^{-}$, $CD27^{high}CD138^{+}$, $CD27^{int}CD138^{-}$, $CD27^{int}CD138^{+}$ and their expression levels of Fut8.

2x10^7 cells per well were washed by adding 200 µL FACS-buffer. All washing steps were performed with centrifugation at 600 xg 4°C for 6 minutes.

The supernatant was discarded, and 100 µL of the extracellular staining solution, which was prepared in FACS buffer, was added to each sample, and incubated for 30-40 minutes on ice and in the dark.

Table 11: Staining panel for extracellular B cells and plasma cells from isolated PBMCs.

Marker	Conjugate	Dilution
fixable viability dye	eFluor780	1:1.000
CD19	BV510	1:40
CD138	BV711	1:50
CD27	BV785	1:100
CD38	BV421	1:50
IgG	PE	1:30
IgA	PE-Vio770	1:75

Afterward, cells were washed with 200 µL FACS-buffer and then fixated and permeabilized by adding 100 µL of CytoFix/CytoPerm to the cells for 30-40 minutes at RT in the dark. Cells were then washed twice with 200 µL PermWash and the intracellular staining solution was added to the cells, which were resuspended in the mixture and incubated for 40-60 minutes at RT in the dark.

Table 12: Staining panel for intracellular B cells and plasma cells from isolated PBMCs.

Marker	Conjugate	Dilution
IgG	PE	1:30
IgA	PE-Vio770	1:75
S1	Biotin	1:40
Fut8	AF488	1:50

Cells were washed once with 200 µL PermWash, then a second intracellular staining mixture was added to make detection of the biotinylated S1-Protein possible.

Table 13: Staining panel for the second intracellular B cell and plasma cell staining from isolated PBMCs.

Marker	Conjugate	Dilution
Streptavidin	APC	1:100

After washing twice with 200 µL PermWash, cells were resuspended in 200 µL FACS-buffer and were then filled up to 4 mL with Focusing Fluid. Cells were measured at an approximate flow rate of 200 µL/minute.

The FlowJo software version X 0.7 (BD Biosciences) was used to analyze the Flow Cytometry Standard (FCS) 3.0 files.

The flow cytometric analyses of the TNF-treated patients (see Figure 35) were performed by Dr. Ulf Geisen (Clinic for Rheumatology (director, Prof. Bimba Hoyer), UKSH, Kiel, Germany) as described elsewhere (Geisen et al., 2022).

2.2.5 Column preparation

2.2.5.1 Anti-human IgG4 column

For the depletion and isolation of human serum IgG4, a column that specifically binds IgG4 by an anti-human IgG4 monoclonal antibody (clone: HP-6025) was prepared. The coupling of anti-human IgG4 to sepharose was performed using cyanogen bromide (CNBr)-activated sepharose according to the protocol of Kavran & Leahy, 2014. Briefly, 0.5 g sepharose beads were reconstituted in 10 mL volume activation buffer (1 mM HCl) and incubated for 2 hours at 4°C on a tube rotator. In the meantime, 4 mg anti-human IgG4 in PBS was dialyzed to a coupling buffer using a 10 kDa centrifugal filter. After swelling and activation of the (CNBr)-activated resin, the anti-human IgG4 was added to the sepharose and incubated overnight at 4°C on a tube rotator. To remove unbound protein, the coupled sepharose was washed with coupling buffer and centrifuged at 1000 xg for 5 minutes. The flow-through was collected and the protein concentration was measured at the NanoDrop to calculate the coupling efficacy. To block any free binding sites of the sepharose, blocking was performed using a 0.1 M Tris-HCl (pH 8) solution for 2 hours at RT on a tube rotator. Eventually, the sepharose was washed six times with alternating pH wash buffers (pH 4 and pH 8) and then stored in 20% ethanol in PBS at 4°C until usage.

2.2.5.2 Anti-Ova column

For purification of Ova-specific mouse antibodies a sepharose column was prepared. Therefore, the same protocol as for the anti-IgG4 column was used, however, the Ova-protein was coupled.

2.2.6 Serum IgG4 depletion and purification

2.2.6.1 IgG4 depletion

Serum IgG4 depletion was performed with serum samples of three different groups: long post second (lp2), shortly post third (sp3) and long post third (lp3) vaccination. For this purpose, samples from each group that showed significant amounts of anti-S1 IgG4 were pooled and subsequently purified (see also Table S4).

For the serum IgG4 depletion, the flow by gravity protocol which has been regularly used in our working group (Petry et al., 2021) has been slightly altered. Two micro-spin columns were used and filled with different resins: one with the anti-human IgG4 resin and a second one with blank resin as a control, to have possible column effects in both the depleted and non-depleted sera.

All washing steps were performed by using centrifugation (600 xg, 1 minute at 4°C). After every centrifugation step, the column was examined and checked whether the resin was dry. Otherwise, the centrifugation step was repeated.

Briefly, 50 µL serum was mixed with 100 µL PBS to achieve a 1:3 dilution. The dilution was then given onto each column and incubated for around 40 minutes on a platform-shaker at RT. Afterward, the columns were centrifuged, and the samples were collected in new tubes. 100 µL of PBS was added to the column and centrifuged, the flow-through was collected in the same tube as the sample. This washing step was repeated twice and led to a final flow-through serum dilution of 1:9. The sera were stored at -20°C.

The column was cleaned for another purification by the addition of 500 µL of PBS and centrifugation. To get rid of any bound antibodies to the column, it was eluted by the addition of 500 µL Glycin (0.1 M). After centrifugation, the flow-through was discarded again and the step was repeated. To neutralize the column, it was washed three times with 600 µL of PBS. Afterward, the next depletion was performed, or the column was stored in 20% Ethanol in PBS at 4°C.

To validate the IgG4 depletion success, anti-S1 IgG subclass ELISA (see 2.2.2.2) of the samples was performed.

2.2.6.2 IgG4 purification

For the IgG4 purification and isolation, the IgG4 depletion protocol was slightly altered by adding further washing steps. The purification was performed by using samples of which larger quantities were available, as larger volumes were required. The anti-human IgG4 resin (see 2.2.5.1) was filled into a larger centrifuge column (10 mL).

All washing steps were performed by using centrifugation (1000 xg, 1 minute at 4°C). After every centrifugation step, the column was examined and checked whether the resin was dry. Otherwise, the centrifugation step was repeated.

IgG4 antibodies were purified from serum samples of three different groups: long post second (lp2) vaccination, shortly post third (sp3) vaccination, and long post third (lp3) vaccination. Therefore, 5-6 sera from each group (see Table S4) were chosen and divided into two groups. Each group consisted of 3 pooled samples and stocks of 1 mL were generated (333 µL of each serum). The pooled serum was further diluted with 2 mL PBS. 1 mL of the pooled and diluted samples was added to the column and incubated for 1 hour at RT in the end-over-end shaker.

Afterward, the column was centrifuged, and the flow-through was collected in a new tube. The column was washed two times with 1 mL of PBS and the flow-through was added to the first collected flow-through, which was then frozen for further use. Then, the column was further washed two times with PBS, two times with PBS-T, and again three times with PBS, and the flow-through was discarded.

To elute the bound IgG4 antibodies, the column was rinsed three times with 1 mL glycine (0.1 M) and the flow-through was collected and neutralized in new tubes. The acidic glycine was neutralized with 100 µl of Tris (1M, pH 8.0) to prevent the antibodies from breaking down. (It was confirmed in advance, by measuring the flow-throughs at the Nanodrop, whether the threefold elution was sufficient to rinse most of the antibodies from the column.) The column was then rinsed again with 2 mL of glycine to wash off all antibody residues and the flow-through was discarded. The column was then neutralized by washing it three times with 2 mL PBS and either used directly for the next purification or stored in ethanol until further use.

The antibodies were then immediately buffered to PBS using centrifugation filters and the final concentration was calculated by using the Nanodrop. IgG4 purity was analyzed by ELISA (see 2.2.2.2).

2.2.7 *In vitro* Glycosylation of IgG4

The isolated IgG4 antibodies of all three groups (lp2, sp3, and lp3) were then artificially glycosylated, to achieve different glycoforms: either degalactosylated (degal) or sialylated (sial). Furthermore, part of the native antibodies was kept as native.

2.2.7.1 Desialylation and degalactosylation

The IgG4 desialylation and degalactosylation were performed by incubating the isolated IgG4 antibodies in 5x Reaction buffer with β-1,4-galactosidase and α-2,6-sialidase A (50 mU/ 1 mg protein). The mixture was incubated for 48 hours at 37°C on a shaker at 350 rounds per minute (rpm). The reaction was stopped by dilution in PBS and was stored at 4°C for a maximum of one night before the antibodies were re-buffered into PBS by using centrifugal filters (exclusion size 100 kDa; to separate the antibodies from the smaller enzymes). The deglycosylation-success was verified by SNA-ELISA (see 2.2.2.3).

2.2.7.2 Galactosylation and sialylation

The purified and isolated IgG4 antibodies were incubated with human β-1,4-galactosyltransferase (transferase to antibody ratio = 1:100) together with the substrate UDP-galactose (substrate to antibody ratio = 1.2:1) in 100 mM MES buffer (pH 7.2). 20 mM Manganese (II) chloride was added as a cofactor for the transferase, and the entire preparation was incubated at 37°C, 350 rpm for 24 hours. Secondly, human α-2,6-sialyltransferase (transferase to antibody ratio = 1:10) together with the substrate CMP-sialic acid (substrate to antibody ratio = 1:2) were given into the reaction mixture and incubated for a further 8 hours at 37°C, 350 rpm. The reaction was then stopped by transfer into a falcon tube containing 15 mL MES buffer and stored at 4°C. The antibody was buffered to PBS as soon as possible, which was achieved by using centrifugation filters (exclusion size 100 kDa; to separate the antibodies from the smaller enzymes). The sialylation-success was verified by SNA-ELISA (see 2.2.2.3).

2.2.8 Functional Assays

All functional assays were conducted in cooperation by Mareike Schubert, a Ph.D. student in the laboratory of Dr. Yannic Bartsch at the TwinCore Hannover. Four different assays were performed to analyze several antibody-dependent immune responses, which have been described recently elsewhere (Bartsch et al., 2023): antibody-dependent-neutrophil-phagocytosis (ADNP), antibody-dependent-cell-phagocytosis (ADCP), antibody-dependent-complement-deposition (ADCD) and antibody-dependent-NK cell-activation (ADNKA) by three different readouts (CD107a, IFNy, MIP-1b).

In the functional analyses, the effects of IgG4-depletion or IgG4-enrichment was tested. For this purpose, 1:9 in PBS diluted sera from different time points after vaccination were selected. In addition, purified and glycoengineered IgG4 alone was shipped and tested.

In addition, sera from the anti-TNF study from two different time points were tested. For this purpose, the unmodified serum was shipped and tested as 1:10-dilutions (with PBS).

2.2.9 TriNetX database analysis

The TriNetX-analysis was performed in cooperation by Prof. Ralf Ludwig (Lübeck Institute of Experimental Dermatology (LIED), University of Lübeck and University Medical Center Schleswig-Holstein, Germany).

A population-based retrospective cohort study with propensity score matching was performed according to previously published protocols (Kasperkiewicz et al., 2023; Kridin & Ludwig, 2023). Specifically, data from electronic medical records (EMRs) was retrieved from the TriNetX Global Collaborative Network (with natural language processing), which at the time of analysis included over 127 million EMRs from 106 Health Care Organisations. The following two groups were retrieved: (i) EMRs with a diagnosis of Crohn’s disease (CD), ulcerative colitis (UC), rheumatoid arthritis (RA) or psoriasis (Pso), and two vaccinations with a SARS-CoV-2 mRNA vaccine treated with a TNF inhibitor but not treated with an α4β7 integrin inhibitor or methotrexate (MTX), or, (ii) CD, UC, RA, Pso EMRs with two SARS-CoV-2 mRNA vaccinations treated with an α4β7 integrin inhibitor (vedolizumab) or methotrexate (MTX) but not treated with a TNF inhibitor.

2.2.10 Mouse handling

2.2.10.1 Immunization

To investigate the influence of TNFα-blocking on inflammatory immune responses in mice, mice were immunized with a foreign protein and an inflammatory adjuvant.

C57BL/6 mice were immunized intraperitoneally (i.p.) with 100 µg Ova in 200 µL. Therefore 100 µL of an Ova dissolved in PBS (1 mg/mL) was mixed with 100 µL of the adjuvant. Oil-based adjuvants like eCFA are not soluble in the watery solution, therefore emulsions had to be made.

For preparation of enriched CFA (eCFA), 20 mL of incomplete Freund's adjuvant (IFA) were mixed with 100 mg *Mtb*.H37 RA to a final concentration of 5 mg *Mtb*/mL. Before using eCFA, it was properly vortexed. On the day of injection, the adjuvant was as fresh as possible prepared. 100 µL of adjuvant and 100 µL Ova in PBS solution (1 mg/mL) were filled in individual syringes and connected by a 3-way stopcock. Both phases were then emulsified by rapidly transferring the solutions from one to the other syringe for around 5 minutes. Eventually, 1 mL syringes were filled for injection. Mice were injected on day 0 and sacrificed on day 12.

2.2.10.2 TNFα blocking

The TNFα-blocking experiment was conducted together with Hanna B. Lunding and Janna Quack. The mice were injected every two or three days with 200 µg blocking antibody in PBS (200 µL/ mouse). The first injection started one day before the immunization.

2.2.11 Statistical analysis

Statistical analyses were performed using GraphPad Prism v9.0 and v10.0 and MatLab.

The smoothed mean curves shown in scatter plots were created by polynomial regression. Confidence bands were plotted by using a confidence level of 95%.

p-values <0.05 were considered significant as follows: *, **, ***, ****: p-value < 0.05, 0.01, 0.001, and 0.0001 respectively.

Pearson and Spearman correlations were used to measure the strength of the (linear) relationship between two variables.

Data in bar graphs were presented as mean values ± SD or box-and-whisker (min – max) plots. Differences between two groups were assessed using the Mann-Whitney U test, while differences between more than two groups were assessed using the Kruskal-Wallis test. In paired sample analyses, differences between two groups were assessed using the Wilcoxon test, while differences between more than two groups were assessed using the Friedman test. For the statistical analysis of the mouse experiment, both groups were compared using an unpaired t-test.

In order to compare data obtained in two experiments (as in section 3.2.3), the data were normalized by calculation of z-scores ((value-mean)/standard deviation).

The real-world data (3.3.5) was analyzed by creating Kaplan-Meier curves, which were compared with the log-rank test.

Principal component analyses (PCA) were performed in GraphPad Prism v9.0, while the partial least square-discriminant analyses (PLS-DA) were performed in cooperation with Dr. Franziska Schmelter in our institute in PLS-Toolbox in MatLab. For cross-validation, venetian blinds were used and the area under the receiver operating characteristic curve (AUROC) was calculated.

3. Results

3.1 IgG and B cell responses after two vaccinations with the newly developed mRNA and adenovirus-based vaccines

It has already been described that the mRNA vaccines from BioNTech and Moderna in particular, but also the adenovirus-based vaccine from AstraZeneca, initially induce mainly anti-Spike (S) T_H1-responses after one or two vaccinations. These responses mainly lead to IgG1 and IgG3 levels with strong neutralizing potential (Lixenfeld et al., 2021; Sahin et al., 2020; Swanson et al., 2021). Nevertheless, longitudinal information on these anti-S antibody responses in terms of IgG subclass abundancies and IgG subclass Fc glycosylation patterns was previously unknown.

Here, these different vaccination strategies were investigated up to 270 days after the first vaccination, as shown in Table 2 and Figure 7. In addition, a further vaccination group was included to analyze the influence of infection prior to the first vaccination.

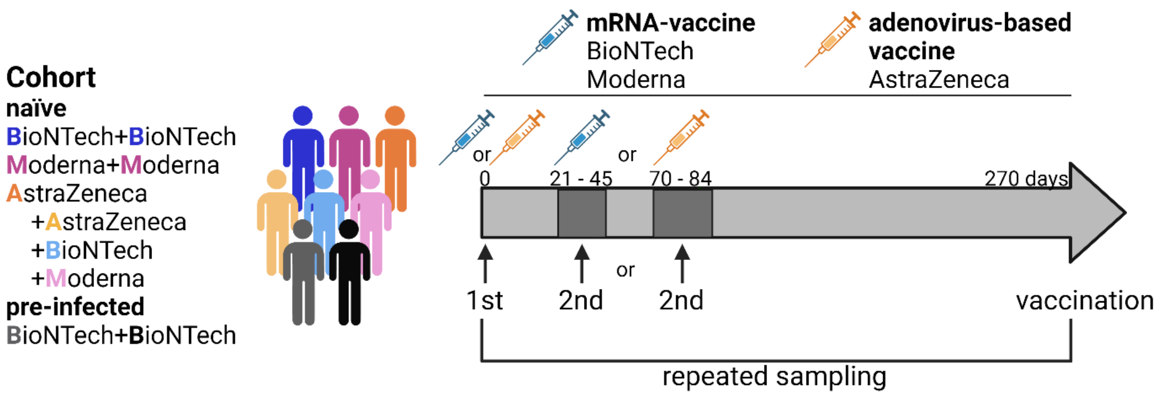

Figure 7: Schematic cohort description of the vaccination groups used in the longitudinal vaccination study.

Naïve as well as pre-infected individuals were recruited, and samples were repeatedly collected up to 270 days after the first vaccination during the period of two immunizations with the mRNA vaccines (BioNTech and Moderna) or the adenovirus-based vaccine (AstraZeneca). The mRNA vaccines were administered the second time 21-45 days after the first shot, while the second AstraZeneca (or in the case of a hybrid-vaccination scheme mRNA) shot was 70-84 days after the first vaccination. This illustration was created with BioRender.com.

To investigate longitudinal IgG subclass antibody responses of the different vaccination groups (Figure 7), anti-S1 serum IgG and IgG1-4 as well as salivary IgG antibody levels were analyzed up to 270 days after the first vaccination using in-house developed ELISA protocols (serum HL-1 protocol; saliva HL-2 protocol) (Figure 8) and the commercially available anti-S1 IgG ELISA from EUROIMMUN (Figure S1). Both anti-S1 IgG ELISA were compared with each other and showed a strong correlation (Figure S1). Therefore, only the anti-S1 IgG HL-1 data and subsequently anti-S1 IgG1-4 data are presented in the following sections. In addition, previous SARS-CoV-2 infection (pre-infected) as well as the absence of SARS-CoV-2 infection (naïve) up to 270 days after the first vaccination were confirmed by the commercially available anti-NCP (nucleocapsid-protein) IgG ELISA from EUROIMMUN (Figure S2).

As shown in Figure 8, the mRNA vaccine in particular induced a strong initial anti-S1 IgG serum response. Among the mRNA vaccines, the formula from Moderna appeared to induce a higher initial anti-S1 IgG antibody level compared to BioNTech's vaccine. A first immunization with AstraZeneca's vaccine induced a weaker anti-S IgG responses compared to the mRNA vaccines. However, a second vaccination with the AstraZeneca vaccine, but especially with a mRNA vaccine, led to a strong increase in the anti-S IgG response. The pre-infected group showed significantly higher anti-S1 IgG levels after the first vaccination than the corresponding naïve group, suggesting a re-activation of pre-existing memory B cells. Although the pre-infected individuals had elevated anti-S1 IgG levels after the first vaccination, the naïve vaccines approached the anti-S1 IgG levels of the pre-infected vaccinees over time.

Interestingly, the same dynamics of anti-S1 IgG antibody level were also observed in salivary samples (Figure 8B).

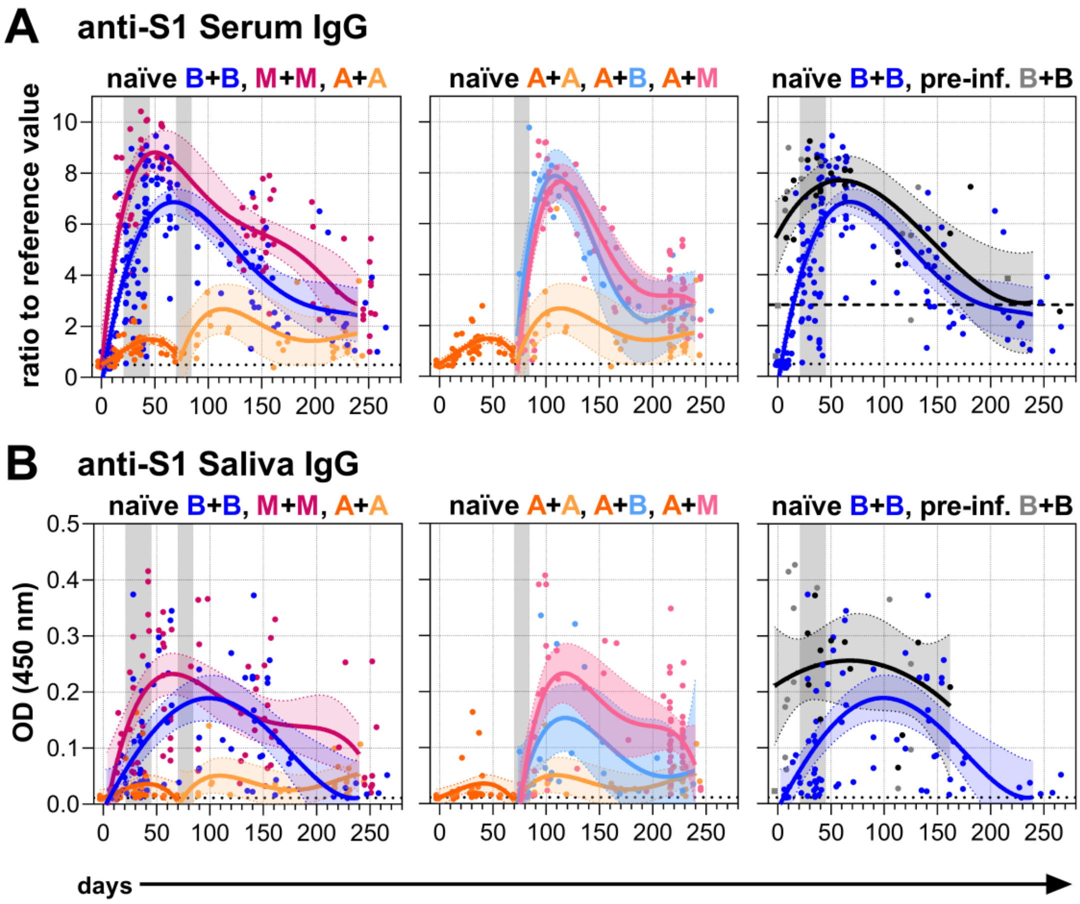

Figure 8: Longitudinal anti-S1 serum and salivary IgG levels after two vaccinations. **(A)** Anti-S1 serum IgG (HL-1 ELISA) levels (ratios to reference value) and **(B)** anti-S1 salivary IgG (HL-2 ELISA) levels (OD 450nm) of the indicated six vaccination groups as introduced in Figure 7: naïve **B/B** = BioNTech, **M/M** = Moderna, **A/A** = AstraZeneca, heterologous groups **A+B**, **A+M**; pre-infected **B/B** = BioNTech. The time windows of the second vaccinations are indicated by the grey bars: 21-45 days for mRNA and 70-84 days for adenovirus-based vaccines. The dotted lines indicate anti-S1 IgG levels of unvaccinated controls, the dashed line indicates levels of pre-infected subjects before vaccination. Statistics: polynomial regression.

Correlation analysis between anti-S1 serum and salivary IgG antibodies as seen in Figure 9 revealed significance for all groups. This positive correlation indicates a passive transfer of IgG antibodies from the blood into the lumen/mucosa of the respiratory tract.

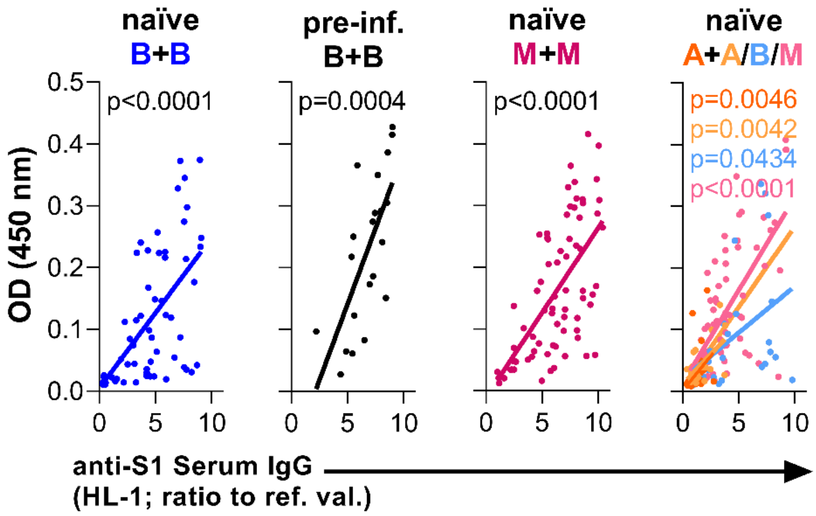

Figure 9: Correlations between serum and salivary IgG antibodies.

Pearson correlations between anti-S1 serum IgG levels (HL-1 ELISA) and anti-S1 salivary IgG levels (HL-2 ELISA). p-values of the indicated correlations are shown. Groups: naïve **B**/B = BioNTech, **M**/M = Moderna, **A**/A = AstraZeneca, heterologous groups **A**+B, **A**+M; pre-infected **B** = BioNTech.

3.1.1 Dominant IgG1 and IgG3 antibody responses after two vaccinations

Subsequently, anti-S1 serum IgG subclass antibody levels were examined. The mRNA vaccines (especially Moderna) induced strong anti-S1 IgG1 levels. Anti-S1 IgG1 levels were significantly lower after vaccination with AstraZeneca (Figure 10). Both the mRNA vaccines (especially Moderna) and AstraZeneca induced anti-S1 IgG3 responses. Interestingly, the differences between the mRNA vaccines and the AstraZeneca adenovirus vaccine were more pronounced at early anti-S1 IgG1 levels than at early IgG3 levels.

The pre-infected group showed an increase of the anti-S1 IgG1 response after vaccination but hardly any anti-S1 IgG3 response. This suggests that only a few IgG3^{+} memory B cells may have developed after infection and were re-activated by a vaccination.

Over time up to day 270, both anti-S1 IgG1 and IgG3 levels decreased to comparable levels in all groups.

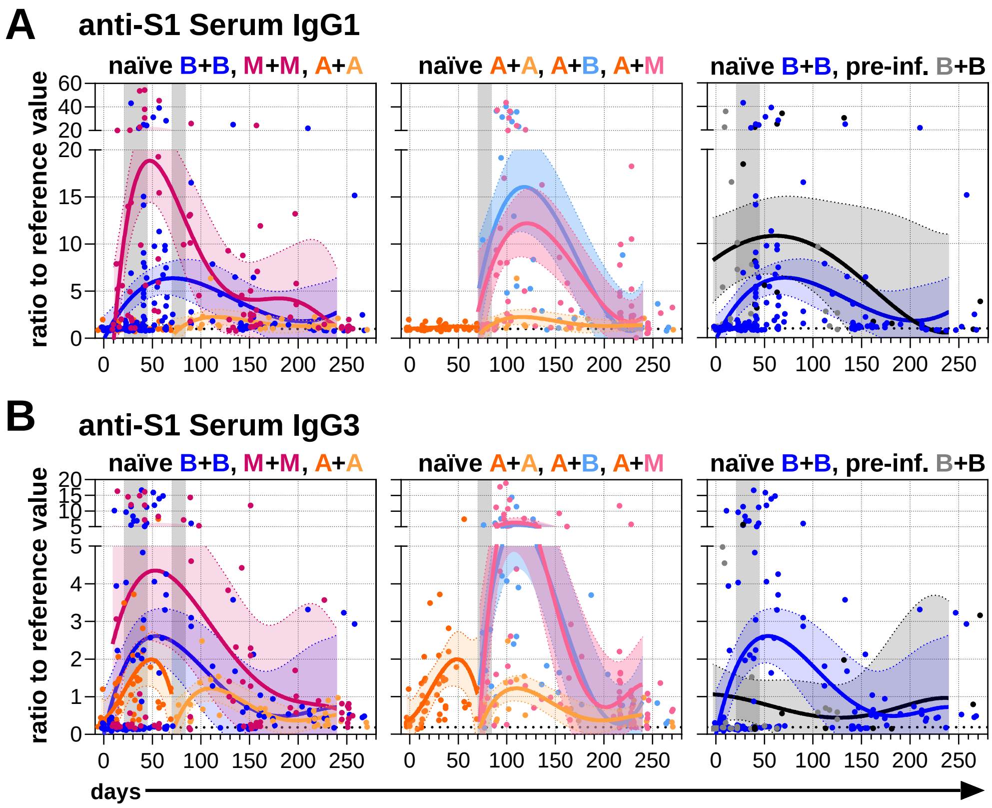

Figure 10: Longitudinal anti-S1 serum IgG1 and IgG3 subclass levels after two vaccinations.

Anti-S1 serum **(A)** IgG1 and **(B)** IgG3 levels (ratios to reference values) of the indicated six vaccination groups: naïve **B/B** = BioNTech, **M/M** = Moderna, **A/A** = AstraZeneca, heterologous groups **A+B**, **A+M**; pre-infected **B/B** = BioNTech. The time windows of the second vaccinations are indicated by the grey bars: 21-45 days for mRNA and 70-84 days for adenovirus-based vaccines. The dotted lines indicate anti-S1 IgG1 or IgG3 levels of unvaccinated controls. Statistics: polynomial regression.

3.1.2 Late-emerging IgG4 levels after two mRNA vaccinations

Next, anti-S1 IgG2 and IgG4 (HL-1) ELISA were performed (Figure 11). Interestingly, the dynamics observed for the other two subclasses were absent here.

Anti-S1 IgG2 levels were almost constant over time for the mRNA vaccines, while lower IgG2 antibody levels were detectable for two adenovirus-based vaccinations and in pre-infected individuals (Figure 11A). In contrast to the IgG1 and IgG3 antibody responses, there was no convergence of IgG2 levels over time.

Surprisingly, two mRNA as well as heterologous vaccinations induced late-emerging IgG4 levels in naïve individuals (Figure 11B). These responses were particularly strong with the Moderna mRNA vaccine. The adenovirus-based vaccination of naïve individuals and mRNA vaccination in pre-infected vaccinees did not show this late-emerging anti-S1 IgG4 response.

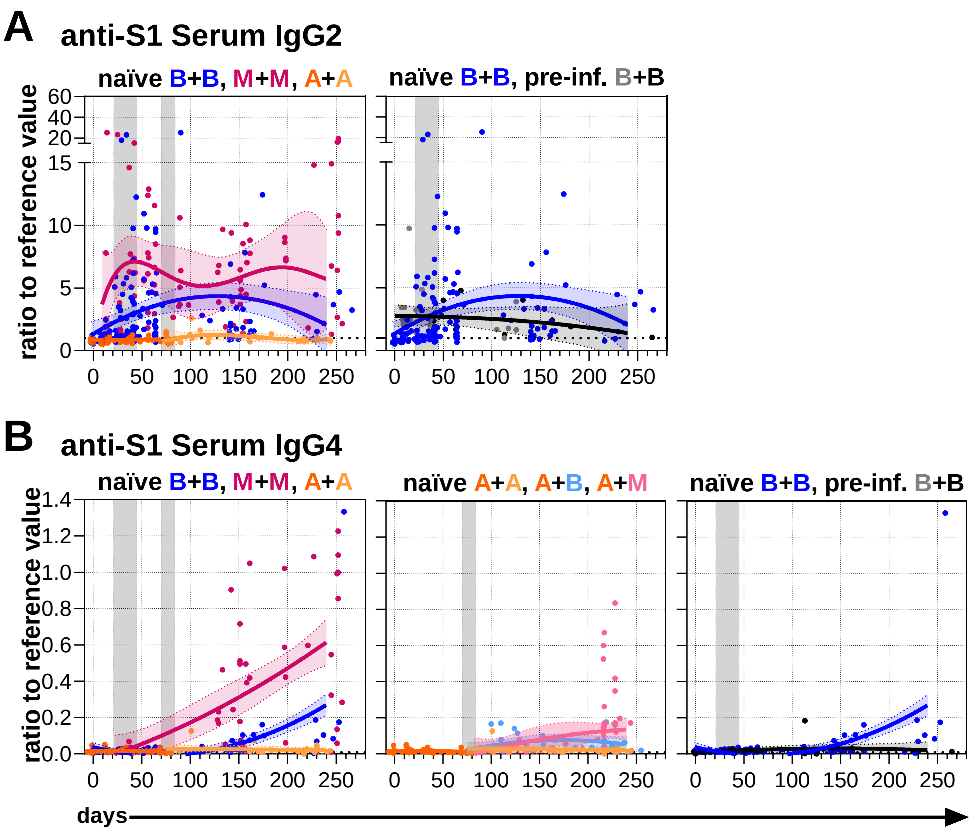

Figure 11: Longitudinal anti-S1 serum IgG2/4 subclass levels after two vaccinations. Anti-S1 serum **(A)** IgG2 and **(B)** IgG4 levels (ratios to reference values) of the indicated six vaccination groups. Groups: naïve **B/B** = BioNTech, **M/M** = Moderna, **A/A** = AstraZeneca, heterologous groups **A+B**, **A+M**; pre-infected B/B = BioNTech. The A+B and A+M groups were not analyzed for IgG2. The time windows of the second vaccinations are indicated by the grey bars: 21-45 days for mRNA and 70-84 days for adenovirus-based vaccines. The dotted lines indicate anti-S1 IgG2 or IgG4 levels of unvaccinated controls. Statistics: polynomial regression.

Taken together, the mRNA vaccines induced a strong initial anti-S1 IgG1 responses. The overall anti-S1 IgG response of the different vaccination groups was comparable over time up to day 270 after the first immunization. Surprisingly, the mRNA vaccines induced late-emerging anti-S1 IgG4 responses after two vaccinations.

3.1.3 IgG1 Fc glycosylation patterns are characterized by transient afucosylation and initially high and long-term low levels of galactosylation and sialylation

Next, IgG1 Fc glycosylation was investigated to assess the glycosylation profile of the different vaccination groups over time and up to 270 days after the first vaccination. Therefore, LC-MS analysis of antigen-specific IgG1 antibodies was performed and 12 major glycan traits were detected and the six glycans with the highest abundances are shown in Figure 12A. All detected glycopeptides can be seen in Table S1.

Of particular interest was i) the level of afucosylated (F0) IgG1 antibodies, as all vaccine formats encode a membrane-bound S; ii) whether our laboratory's previous findings in mice that antigen-specific IgG antibodies are generally high galactosylated initially and low galactosylated long-term after immunization could be confirmed; and iii) whether the different vaccines induce distinct levels of glycosylation due to their different formats and potentially different adjuvant effects.

Firstly, analysis of anti-S serum IgG1 fucosylation shortly after the first vaccination revealed an initial peak of F0 antibodies (up to 20%), which, however, rapidly decreased. After the second vaccination, almost all IgG1 antibodies were highly fucosylated (~98%, Figure 12B). The total IgG1 showed a constant level of fucosylation of about 94% over the entire period. In contrast, pre-infected vaccinees did not show the initial F0 IgG1 peak. Instead, they showed a constant level of ~4% anti-S1 F0 IgG1, which was higher than the long-term F0 level of naïve vaccinees. A previous infection appears to result in a higher and stable level of long-term anti-S IgG1 afucosylation, which was confirmed by another study with a larger cohort (Van Coillie et al., 2023). These findings indicate an altered immune response in previously infected individuals compared to naïve individuals.

Anti-S serum IgG1 bisection levels were lowest for naïve and pre-infected vaccines shortly after the second vaccination and then increased slightly in the long-term (Figure 12C). Vaccination with the AstraZeneca vaccine resulted in higher bisection levels compared to mRNA vaccination after the first vaccination, and two vaccinations with the AstraZeneca vaccine also showed slightly elevated levels of anti-S IgG1 bisection over time. Long-term anti-S1 bisection levels remained below their total counterpart. Interestingly, pre-infected vaccinees showed slightly higher anti-S IgG1 bisection levels over time.

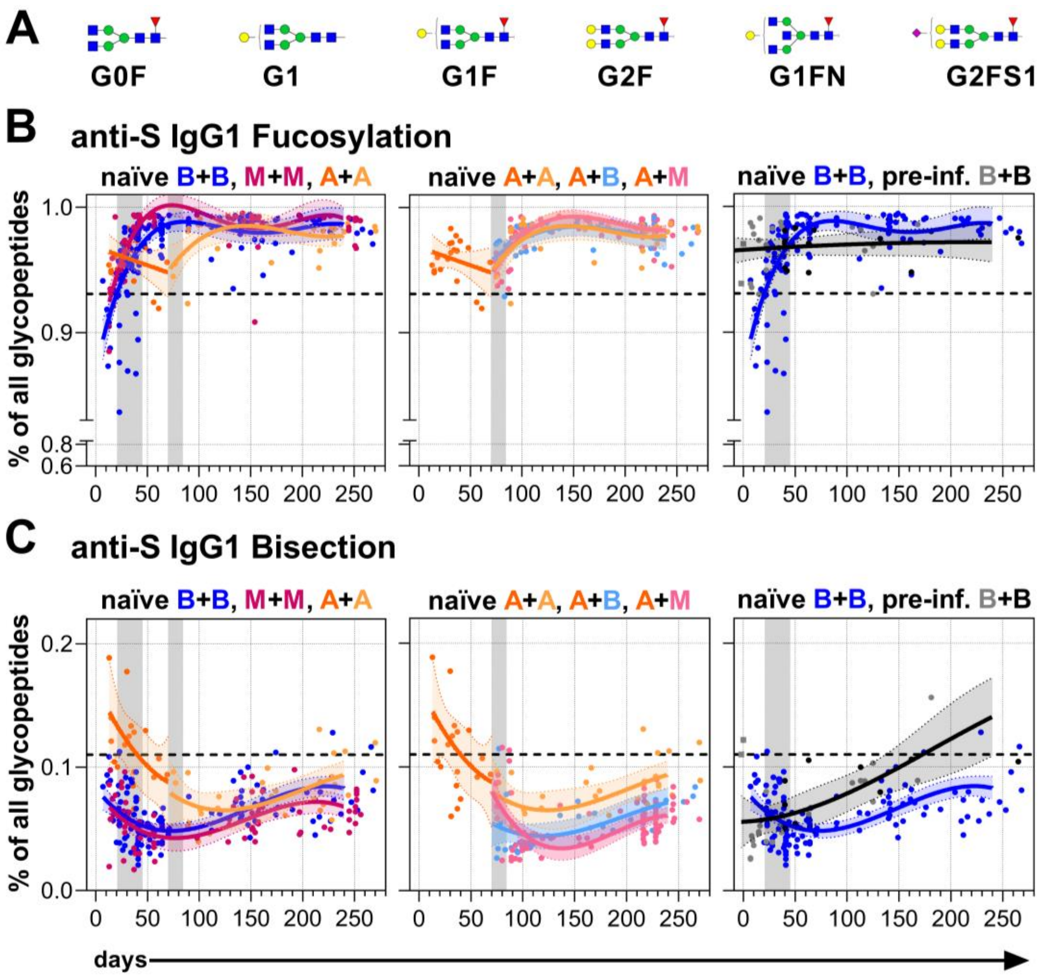

Figure 12: Longitudinal anti-S serum IgG1 fucosylation and bisection after two vaccinations.

(A) The six most frequently occurring IgG Fc-*N* glycans found with an average relative frequency of more than 3%. G Galactose (yellow circle), S sialic acid (purple diamond), F fucose (red triangle), mannose (green circle); N *N*-acetylglucosamine (blue square). **(B)** Anti-S serum IgG1 Fc *N*-fucosylation and **(C)** anti-S serum IgG1 Fc *N*-bisection of the indicated six vaccination groups: naïve **B/B** = BioNTech, **M/M** = Moderna, **A/A** = AstraZeneca, heterologous groups **A+B**, **A+M**; pre-infected **B/B** = BioNTech. The time windows of the second vaccinations are indicated by the grey bars: 21-45 days for mRNA and 70-84 days for adenovirus-based vaccines. The dashed lines indicate the total IgG1 fucosylation or bisection levels, respectively. Statistics: polynomial regression. The LC-MS analysis was performed in cooperation by the Center for Proteomics and Metabolomics (Director, Prof. Manfred Wuhrer), LUMC, Leiden, the Netherlands.

Next, anti-S serum IgG1 sialylation and galactosylation levels were assessed longitudinally (Figure 13). Both anti-S IgG1 glycosylation features showed a wave-like pattern, starting with high galactosylation and sialylation levels after both vaccinations and decreasing over time until total serum IgG1 levels were reached. The wave of anti-S IgG1 galactosylation and sialylation matches the dynamics of increasing anti-S1 IgG1 levels after the first and second vaccination and the subsequent decline over time (Figure 10).

The data, like previous mouse studies (Bartsch et al., 2020), suggest that initial extrafollicular plasma cells can generate high levels of anti-S IgG1 galactosylation and sialylation, while GC-derived long-lived plasma cells can generate lower levels of galactosylated and sialylated anti-S IgG1 antibodies. In the long-term, both glycosylation features were comparable in all investigated vaccination groups, suggesting a comparable T_H1-driven adjuvant effect.

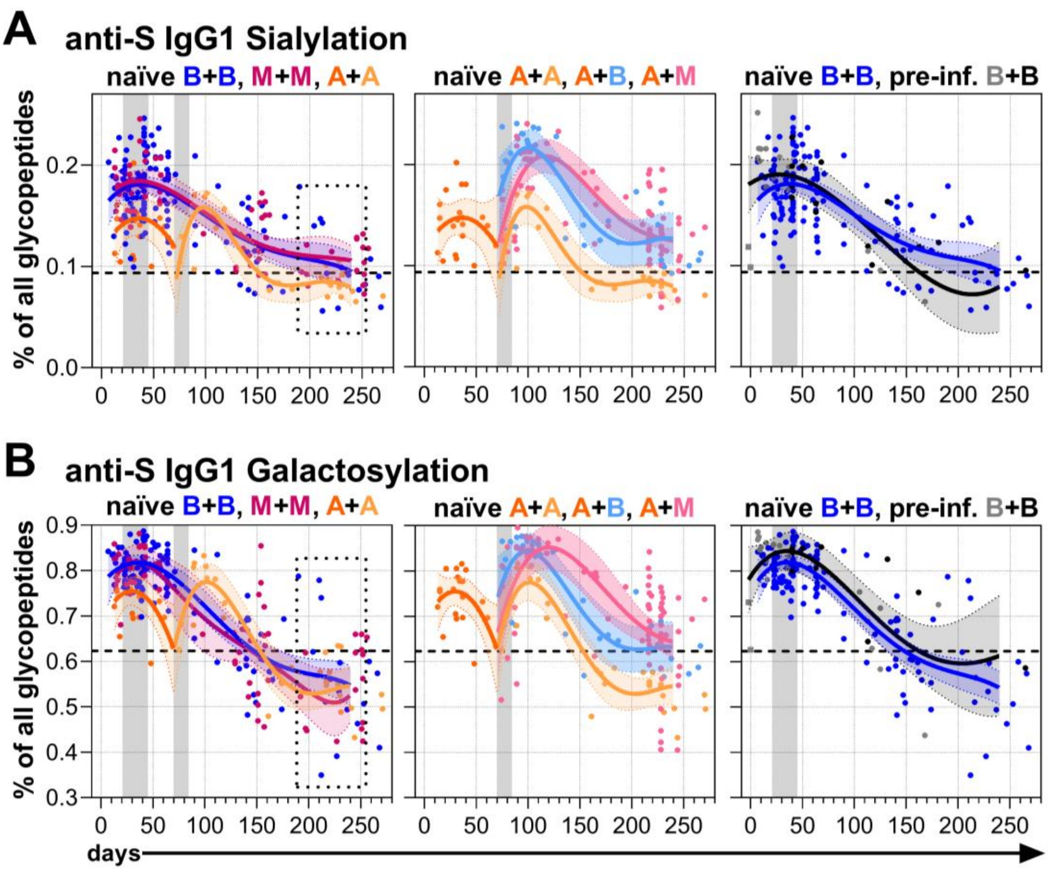

Figure 13: Longitudinal anti-S serum IgG1 sialylation and galactosylation after two vaccinations.

(A) Anti-S serum IgG1 Fc *N*-sialylation and **(B)** anti-S serum IgG1 Fc *N*-galactosylation of the indicated six vaccination groups: naïve **B/B** = BioNTech, **M/M** = Moderna, **A/A** = AstraZeneca, heterologous groups **A+B**, **A+M**; pre-infected **B/B** = BioNTech. The time windows of the second vaccinations are indicated by the grey bars: 21-45 days for mRNA and 70-84 days for adenovirus-based vaccines. The dashed lines indicate the total IgG1 sialylation or galactosylation levels, respectively. Dashed squares include samples, that were further analyzed in Figure 14. Statistics: polynomial regression. The LC-MS analysis was performed in cooperation by the Center for Proteomics and Metabolomics (Director, Prof. Manfred Wuhrer), LUMC, Leiden, the Netherlands.

To shed more light on the late IgG1 sialylation and galactosylation levels, samples from homologously vaccinated naïve vaccinees collected between days 190 and 256 were selected and further analyzed (Figure 13A, B dotted squares). As shown in Figure 14, these samples were then compared to the corresponding total IgG1 sialylation and galactosylation levels. Both two mRNA vaccinations and two adenovirus-based vaccinations induced late anti-S IgG1 galactosylation levels that were significantly lower than their total IgG1 galactosylation levels. Long-term anti-S IgG1 sialylation levels were approximately equal to their total IgG1 levels.

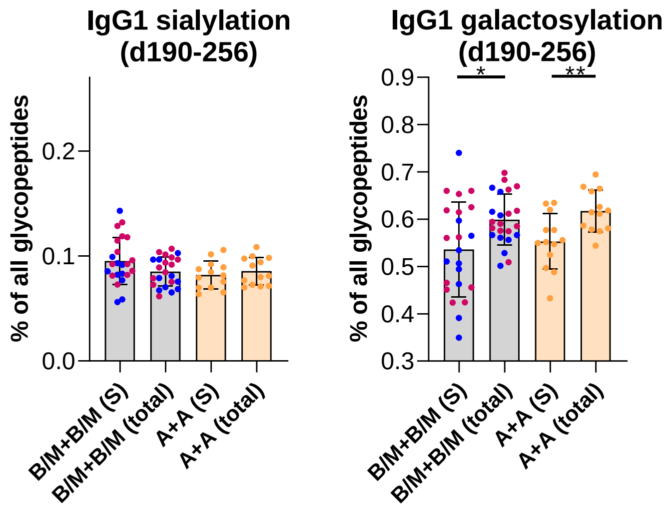

Figure 14: Long-term anti-S serum IgG1 sialylation and galactosylation after two vaccinations.

Comparison of anti-S and total IgG1 sialylation and galactosylation levels of samples from mRNA (B (BioNTech)/M (Moderna)+B/M; B: blue; M: pink; n=23) or adenovirus (A (AstraZeneca)+A; n=12) vaccinated individuals collected late between day 190 and 256 upon first immunization (as indicated by the dashed squares in Figure 13). Statistics: Kruskal-Wallis test, *p < 0.05, **p < 0.01. The LC-MS analysis was performed in cooperation by the Center for Proteomics and Metabolomics (Director, Prof. Manfred Wuhrer), LUMC, Leiden, the Netherlands.

Together, the LC-MS data showed only a transient afucosylated anti-S IgG1 response with all vaccine combinations in naïve subjects. In contrast, pre-infected subjects showed higher constant anti-S IgG1 afucosylation levels (4%) over time compared to 2% long-term anti-S IgG1 afucosylation levels in naïve subjects. Interestingly, a dynamic change in anti-S IgG1 galactosylation, sialylation and bisection was observed over time. The initial response after two vaccinations was characterized by high levels of galactosylation and sialylation and low levels of bisecting anti-S IgG1 in all groups, most likely generated by extrafollicular plasma cell responses. Over time, when probably mainly IgG responses from GC-derived long-lived plasma cells became dominant, a decrease of anti-S IgG1 galactosylation and sialylation and an increase of bisection was observed.

3.1.4 A discriminatory analysis of the different vaccination groups separates them according to their long-term anti-S IgG1 responses

Subsequently, a partial least squares-discriminant analysis (PLS-DA) was performed to further investigate the potential of the different vaccine formulations and combinations on long-term IgG subclass antibody responses. The underlying hypothesis was that the long-term anti-S IgG1 responses are most likely produced mainly by GC-derived long-lived plasma cells. All collected antibody data of the long-term responses should now be included to clarify evidence of different GC reactions of the various vaccine formulas and combinations.

In contrast to principal component analysis (PCA), PLS-DA analyses are a supervised model. It contains a categorical component that defines the groups that were compared. By calculating the area under the receiver operating characteristic curve (AUROC)-value, the statistical reliability of the separation between the evaluated groups was assessed. PLS-DA analyses were performed together with Dr. Franziska Schmelter from the same institute.

Firstly, the influence of pre-infection on late anti-S(1) IgG antibody responses was investigated (Figure 15). Samples collected between 100 and 170 days after the first vaccination from individuals who had been vaccinated twice with the BioNTech mRNA vaccine were used. Both groups showed differences in their antibody profiles. For example, the analysis revealed higher anti-S serum IgG1 bisection levels in the pre-infection group. In contrast, as mentioned above, the naïve group showed higher anti-S IgG1 fucosylation levels.

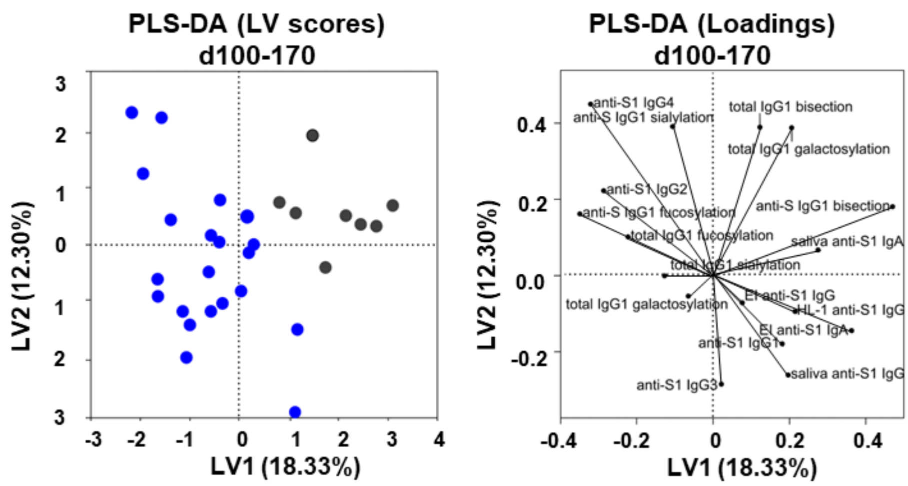

Figure 15: Partial least squares-discriminant analysis (PLS-DA) of long-term antibodies from naïve and pre-infected individuals after two mRNA vaccinations.

PLS-DA of data collected from the naïve and pre-infected B+(B) vaccination cohorts between day 100 and 170 upon first vaccination. Groups: naïve **B** = BioNTech; pre-infected **B** = BioNTech. Latent variable (LV) scores and loadings are shown. The area under the receiver operating characteristic curve (AUROC) for cross-validation is 0.8810 for both groups.

Next, late samples (collected between day 209-256 after the first vaccination) from naïve individuals vaccinated with different vaccine combinations were compared. As shown in Figure 16, a clear separation between the different vaccination groups was observed. For the mRNA vaccines, there was overlap, while the heterologous vaccination groups and those vaccinated with adenovirus-based only were separated from all other groups. For instance, the naïve vaccination group vaccinated twice with the adenovirus-based vaccine had higher anti-S IgG1 bisection levels.

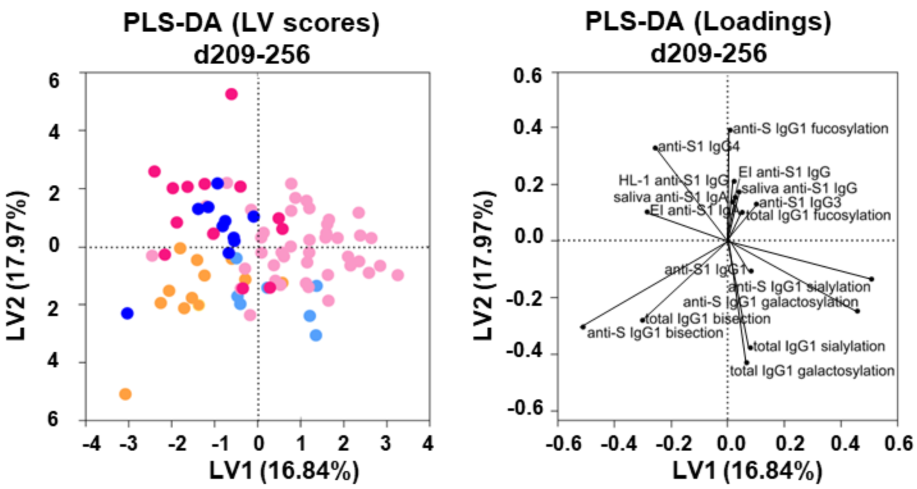

Figure 16: Partial least squares-discriminant analysis (PLS-DA) of long-term antibodies from naïve individuals vaccinated with different vaccine combinations.

PLS-DA of data collected from all naïve vaccination cohorts between day 209 and 256 upon first vaccination. Latent variable (LV) scores and loadings are shown. The AUROC values for cross-validation are B+B: 0.8304, M+M: 0.8449, A+A: 0.7416, A+B: 0.8773, and A+M: 0.9094. Groups: naïve **B**/B = BioNTech, **M**/M = Moderna, A = AstraZeneca, heterologous groups **A**+B, **A**+M.

3.1.5 Fut8-expression levels in an early plasma cell subset correlate with transiently afucosylated anti-S1 IgG1 antibodies

To characterize the occurrence of transient afucosylated anti-S IgG1 antibodies in naïve individuals, cell analyses of naïve and pre-infected vaccinees (7-14 days after the first and 5-8 days after the second vaccination) were performed. A subset of plasma cells was identified that may produce afucosylated anti-S IgG1 antibodies. The plasma cell subsets were assessed regarding their expression of Fut8 (Fucosyltransferase-8), the enzyme that facilitates the addition of core fucosylation of the IgG Fc glycan. PBMCs from either naïve or antigen-experienced individuals were isolated and analyzed by flow cytometry. All following results were gathered together with Anne-Sophie Lixenfeld, a former MD candidate in our laboratory.

After gating for lymphocytes, single cells and live events, S1-specific cells were gated. As shown in Figure 17, the staining was specific for the antigen (S1). Naïve individuals without prior infection and vaccination showed almost no S1-specific cell staining (Figure 17A), whereas vaccinated individuals showed a positive signal (Figure 17B). The staining of B cells with CD19 and plasma cells with CD38 revealed a separation of different subsets derived from B cells. As antibody producing and secreting plasma cells were targeted, further gating of CD38^{high}CD19^{int} plasma cells and subsequently IgG^{+} cells was performed. Two further plasma cell markers were used to divide the plasma cells into four different subsets depending on the following markers: CD27$^{high/intermediate}$ and CD138$^{+/-}$.

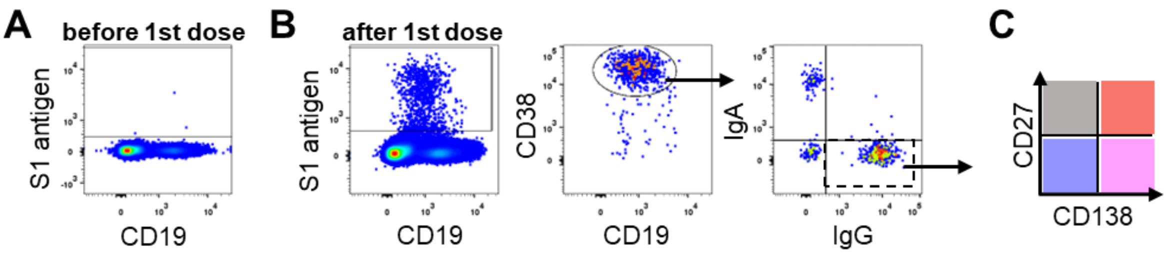

Figure 17: Gating strategy of antigen-specific plasma cell subpopulations by flow cytometry.

The flow cytometry blood cell gating strategy exemplified for a naïve individual **(A)** before the first vaccination and **(B)** 13 days after the first mRNA vaccination. S1-reactive, single, living B lymphocytes were gated and further gated for CD19^{int} CD38^{high} plasma cells to gate for IgG^{+} plasma cells. These cells were further subdivided in four subpopulations as defined by **(C)** CD27 and CD138: CD27^{high}/CD138^{-}, CD27^{high}/CD138^{+}, CD27^{int}/CD138^{-}, CD27^{int}/CD138^{+}.

As indicated in Figure 18, the IgG^{+} S1-specific plasma cells were further divided into four subpopulations. The subpopulations were examined for their expression of CD27 and CD138 and the following subpopulations were defined: CD27^{high}/CD138^{-}, CD27^{high}/CD138^{+}, CD27^{int}/CD138^{-}, CD27^{int}/CD138^{+}. The analysis showed that significantly more CD27^{int} plasma cells were present in naïve compared to pre-infected individuals (Figure 18A, C), especially after the first vaccination. Overall, pre-infected individuals had more CD27^{high} plasma cells than naïve vaccinees. Analysis of the percentages showed that the CD27^{high}CD138^{-} cells were the predominant subpopulation in the pre-infected individuals. Naïve individuals had mainly CD27^{int}CD138^{-} plasma cells but showed an almost even distribution pattern after the second vaccination (Figure 18B, D). This indicates that vaccination of pre-infected individuals resulted in a different composition of plasma cell populations than vaccination of naïve individuals. In particular, CD27^{high} plasma cells appear to occur after vaccination of pre-infected vaccinees.

Next, the relative expression level of the Fut8 was analyzed in all subsets. The dominant subclass in naïve individuals (CD27^{int}CD138^{-}) also had the lowest expression level of Fut8. With the second vaccination, both the dominance and the low expression of Fut8 disappeared in this population (Figure 18B, D). The low expression of Fut8 in the CD27^{int}CD138^{-} plasma cell subset reflects the initial anti-S1 afucosylated IgG1 response in naïve individuals (Figure 12B).

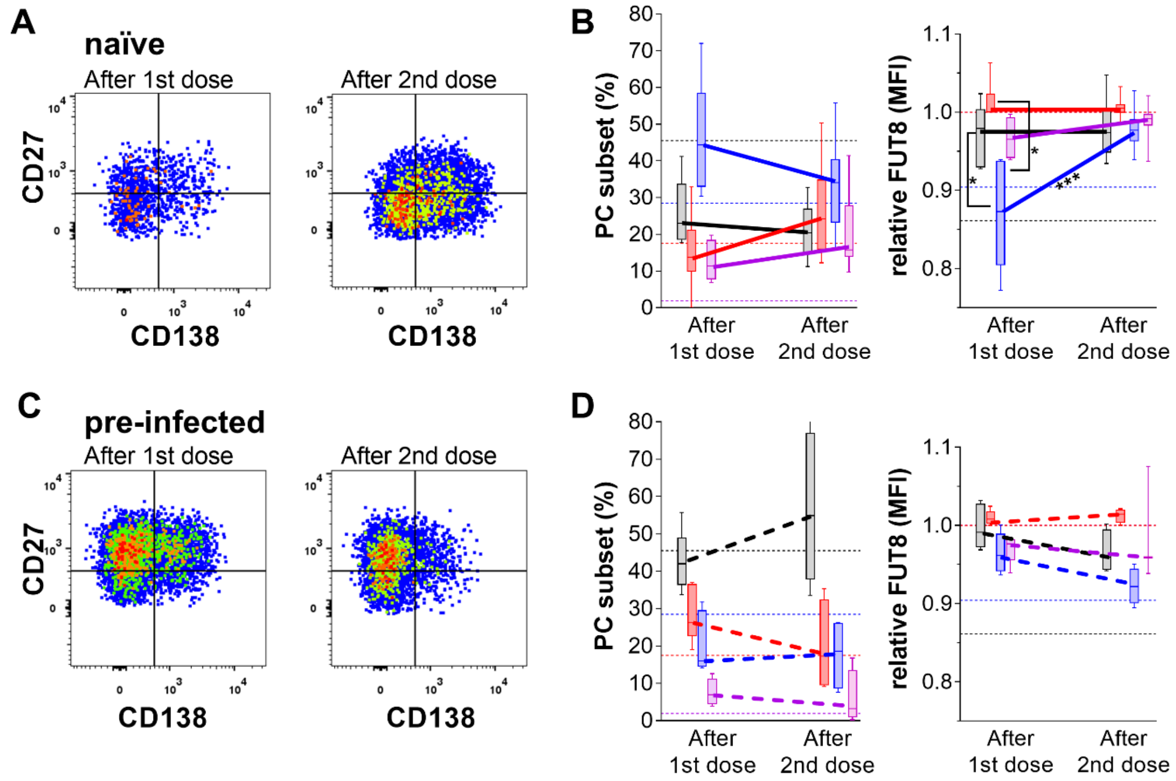

Figure 18: Different subpopulations of S1-specific plasma cells (PCs) express distinct levels of the fucosyltransferase-8.

Flow cytometry analyses of CD19^{int}CD38^{high} plasma cells to analyze IgG^{+} plasma cell subsets as defined by CD27 and CD138. **(A, B)** Naïve and **(C, D)** pre-infected vaccinees were analyzed 7-14 days (naïve n=15, pre-infected n=6) after the first or 5-8 days (naïve n=6, pre-infected n=4) after the second vaccination according to the gating strategy as shown in Figure 17. The individuals were investigated. The colour scheme in B and D is shown in Figure 17C. Statistics: Relative fucosyltransferase 8 (FUT8; median fluorescence intensity (MFI)) expression per IgG+ plasma cell subset compared by Mann–Whitney U test. $p < 0.05$, ***$p < 0.001$.

Taken together, the data in section 3.1 provide a holistic picture of the antigen-specific IgG responses after two vaccinations with the newly developed mRNA- and adenovirus-based vaccines. Particularly at the beginning, the mRNA vaccines were characterized by significantly higher IgG1 and, to a lesser extent, IgG3 levels. Over time, however, these levels became comparable to those of adenovirus-based vaccines (Figure 8, Figure 10, Figure 11, Figure S1). Therefore, the early antibody responses, presumably generated by extrafollicular plasma cells, differed significantly between the different vaccination strategies. However, the long-term responses, which are most likely produced by GC-derived long-lived plasma cells, were comparable. One exception was the late-emerging IgG4 levels after mRNA vaccination (Figure 11).

Furthermore, afucosylated IgG1 antibodies were only transiently found in naïve individuals, while pre-infected vaccinees maintained higher stable afucosylation levels over time (Figure 12). Flow cytometry analysis showed that the IgG^{+} S1-specific $CD38^{high}CD19^{int}$ plasma cells of naïve vaccines were predominantly $CD27^{int}$ after the first vaccination, whereas the plasma cells of pre-infected vaccinees were predominantly $CD27^{high}$. These analyses further showed that $CD27^{int}CD138^{-}$ IgG^{+} S1-specific plasma cells had the lowest levels of Fut8 after vaccination, suggesting that this subset may produce the early afucosylated IgG1 antibodies after one vaccination (Figure 18).

Sialylation and galactosylation showed comparatively high levels shortly after vaccination, although these levels decreased over time and became comparatively low in all groups. The long-term galactosylation level was even lower than the total counterpart (Figure 13, Figure 14). The short-term highly galactosylated and sialylated IgG antibodies are probably produced by extrafollicular plasma cells, whereas the long-term IgG response might be mainly generated by GC-derived plasma cells. PLS-DA analyses further showed that the different vaccination strategies (Figure 15) or the infection status before the first vaccination (Figure 16) induce unique antibody characteristics.

The experiments shown in the sections 3.1.1 – 3.1.4 were successfully published in:

Buhre JS*, Pongracz T*, Künsting I, Lixenfeld AS, Wang W, Nouta J, Lehrian S, Schmelter F, Lunding HB, Dühring L, Kern C, Petry J, Martin EL, Föh B, Steinhaus M, von Kopylow V, Sina C, Graf T, Rahmöller J, Wuhrer M, Ehlers M. mRNA vaccines against SARS-CoV-2 induce comparably low long-term IgG Fc galactosylation and sialylation levels but increasing long-term IgG4 responses compared to an adenovirus-based vaccine. Front Immunol. 2023; 13:1020844. doi: 10.3389/fimmu.2022.1020844. PMID: 36713457; PMCID: PMC9877300. (*these authors contributed equally)

The experiments shown in sections 3.1.5 were successfully published in:

van Coillie J, Pongracz T, Rahmöller J, Chen HJ, Geyer CE, van Vught LA, Buhre JS, Šuštić T, van Osch TLJ, Steenhuis M, Hoepel W, Wang W, Lixenfeld AS, Nouta J, Keijzer S, Linty F, Visser R, Larsen MD, Martin EL, Künsting I, Lehrian S, von Kopylow V, Kern C, Lunding HB, de Winther M, van Mourik N, Rispens T, Graf T, Slim MA, Minnaar RP, Bomers MK, Sikkens JJ, Vlaar APJ, van der Schoot CE, den Dunnen J, Wuhrer M, Ehlers M, Vidarsson G; Fatebenefratelli-Sacco Infectious Diseases Physicians group; UMC COVID-19 S3/HCW study group. The BNT162b2 mRNA SARS-CoV-2 vaccine induces transient afucosylated IgG1 in naive but not in antigen-experienced vaccinees. EBioMedicine. 2023 ;87:104408. doi: 10.1016/j.ebiom.2022.104408. PMID: 36529104; PMCID: PMC9756879.

3.2 The role of vaccination-induced IgG4 responses

The late-emerging levels of IgG4 in mRNA vaccinated individuals were one rather unexpected finding of the vaccination study described above and were of great interest (Buhre et al., 2023; Irrgang et al., 2023; Pillai, 2023). It was therefore of particular concern to shed more light on these antibodies.

An increase in IgG4 responses can be observed after repeated exposition to an antigen, as has been described in AIT (Gehlhar et al., 1999) and trials with a new HIV vaccine (Chung et al., 2014). In general, however, studies investigating IgG4 responses after vaccination are rare. IgG4 antibodies are a subclass that, in contrast to IgG1 and IgG3, have a low activation potential and are more likely to associated with tolerogenic or even inhibitory states (Bruhns et al., 2009; Buhre et al., 2022; Lilienthal et al., 2018; Nimmerjahn & Ravetch, 2008b; Y. Wang et al., 2022). Therefore, the vaccination study described above was extended to further characterize the development and function of these IgG4 antibodies as well as their Fc glycosylation pattern, which could further influence their functionality.

3.2.1 IgG4 antibodies show a similar Fc *N*-glycosylation pattern to IgG1

First, the LC-MS data of 23 of the 25 individuals in the Moderna-vaccination group (M+M) described above were a re-analyzed, as these showed the highest values of all IgG subclasses and, in particular, the late-emerging IgG4 (Figure 11). Beside the anti-S and total IgG1, the IgG2/3 and IgG4 glycopeptide intensities were now also analyzed. In contrast to the semi-quantitative anti-S1 IgG1-4 ELISA, the LC-MS analysis of summed glycopeptide intensity (sum-intensity) of each subclass allows a comparison of the relative abundances of each IgG subclass within a sample. The LC-MS analysis used cannot distinguish between IgG2 and IgG3, therefore these two subclasses are shown together as IgG2/3 (Figure 19B).

In accordance with the ELISA data, a strong peak of especially anti-S1 IgG1 was observed shortly after the second vaccination. The sum-intensities of anti-S IgG1 also reflected the longitudinal decrease of this subclass. Anti-S IgG2/3 sum-intensities were mostly visible at later time points, reflecting the observations from the ELISA. Furthermore, the late-emerging IgG4 antibodies were verified by LC-MS sum-intensity analysis. Evaluable anti-S IgG4 antibodies appeared on approximately day 130 after the second vaccination. It could be shown that anti-S IgG antibodies accounted for the majority of all anti-S IgGs during the entire study period (up to 270 days after the first vaccination). Notably, several months after the second vaccination, the proportion of IgG4 was higher than that of IgG2 and IgG3 combined (Figure 19). To validate the congruence of both methods used (ELISA and LC-MS) the data sets for anti-S(1) IgG1 and IgG4 were compared and showed a strong correlation (Figure S3).

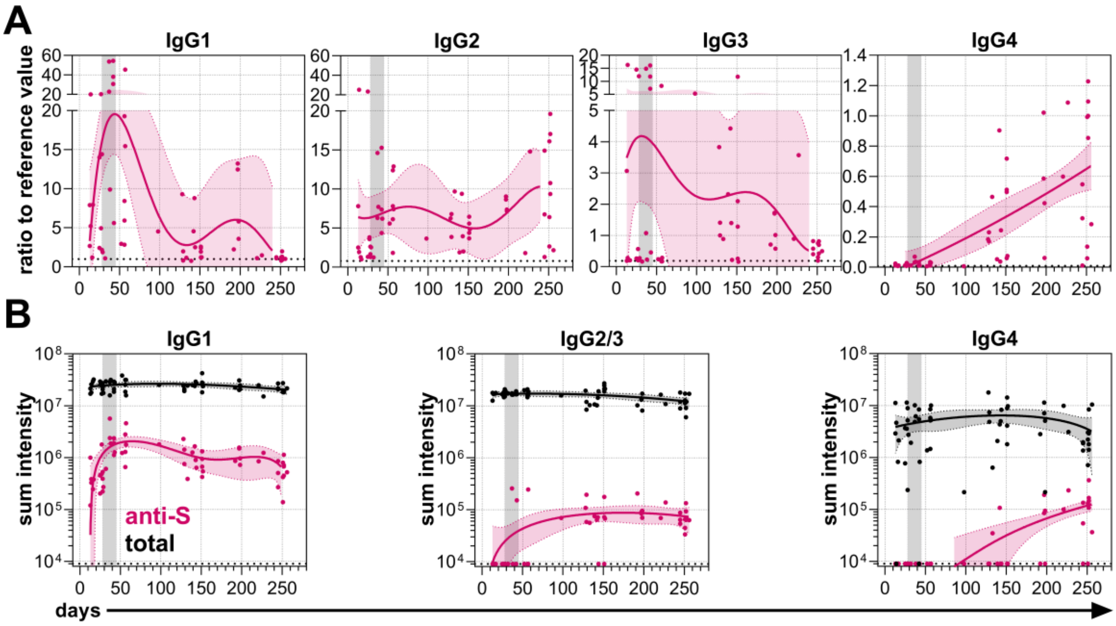

Figure 19: Anti-S(1) IgG subclass levels after two vaccinations with Moderna's mRNA vaccine.

(A) Longitudinal anti-S1 serum levels of all four IgG subclasses obtained by ELISA (ratios to reference values). **(B)** Longitudinal anti-S (pink) and respective total (black) serum summed glycopeptide intensities of the IgG subclasses as analyzed by LC-MS. The grey bar indicates the time frame of the second shot (day 28-45). The dotted horizontal line represents the cut-off threshold. Statistics: polynomial regression, n=61 samples of 23 individuals. The LC-MS analysis was performed in cooperation by the Center for Proteomics and Metabolomics (Director, Prof. Manfred Wuhrer), LUMC, Leiden, the Netherlands.

The sum-intensities of each total IgG subclasses were also re-analyzed using LC-MS. As can be seen in Figure 19B, the level of each subclass remained consistent during the entire study period. This shows that the anti-S IgG antibodies, although they rise sharply after the vaccinations, are still so low in mass that the total IgG subclass levels remain unaffected.

Next, the IgG Fc *N*-glycosylation patterns of all re-analyzed subclasses were compared. As shown above and in Figure 20, the Moderna mRNA vaccine induced a transient peak of afucosylated IgG1. However, no anti-S afucosylation responses were defined for IgG2/3 and IgG4. The glycopeptide peaks detected for the anti-S IgG1, IgG2/3, and IgG4 were also used for the analysis of total IgG1, IgG2/3 and IgG4. Therefore, no afucosylated total IgG2/3 and IgG4 peaks are described, although it cannot be excluded that there are other afucosylated IgG subclass glycopeptide peaks for the total IgG subclasses.

The re-analysis of the LC-MS data showed that IgG2/3 and IgG4, like IgG1, follow the same longitudinal time course of bisection. The lowest levels were found after the second vaccination, which increased slightly over time, but did not reach the level of the corresponding total IgG subclasses.

The re-analysis of the galactosylation and sialylation levels of anti-S and total IgG subclasses confirmed the initially high anti-S galactosylation and sialylation responses for IgG1, which eventually decreased over time. Accordingly, anti-S IgG2/3 and IgG4 showed a similar course of galactosylation and sialylation. The galactosylation levels of all anti-S IgG subclasses fell below the corresponding total level. Anti-S IgG subclass sialylation levels also decreased over time but did not fall below the corresponding total level.

The extent of late low galactosylated and comparatively low sialylated antigen-specific IgG antibodies became even more pronounced when the ratio of sialylation/galactosylation was analyzed (Figure 20).

Taken together, the re-analysis showed that the IgG subclasses, including IgG4, follow the same glycosylation dynamics with the initial high galactosylation and sialylation decreasing over time and the initial lowest bisection increasing.

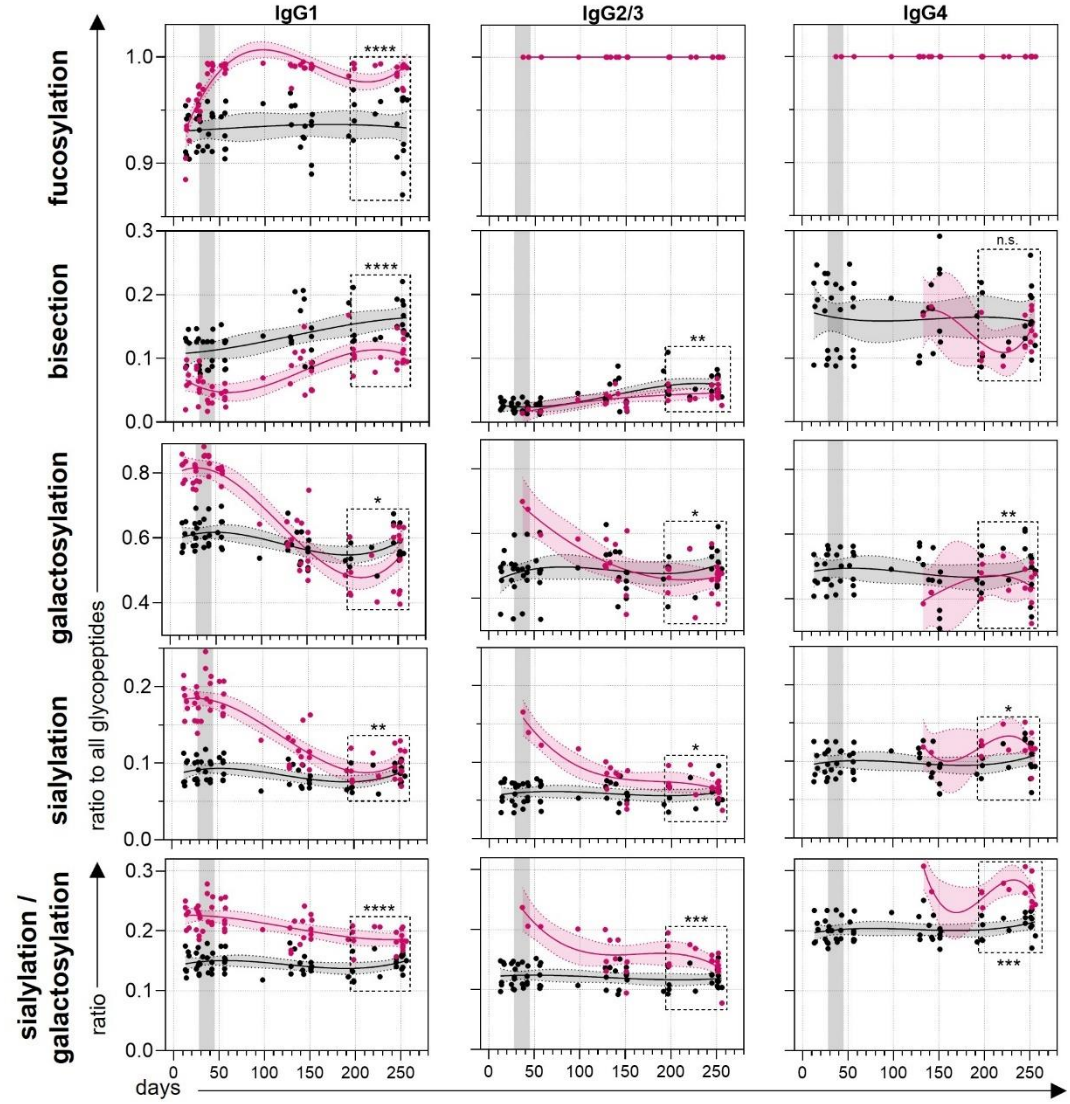

Figure 20: Anti-S IgG subclass glycosylation patterns after two vaccinations with Moderna's mRNA vaccine.

Longitudinal analysis of anti-S (pink) and total (black) serum IgG subclass glycosylation patterns and of the anti-S and total IgG subclass sialylation to galactosylation ratios. Grey bars: time windows of the second shot after the first shot with an mRNA (between day 21 and 45) vaccine. The dashed squares contain samples that were collected at least 197 days after the first vaccination and are further analyzed in Figure 21. Statistics: polynomial regression and Wilcoxon-test between anti-S and total IgG subclass glycosylation levels from the dashed squared and as shown in Figure 21, n=61 samples of 23 individuals. The LC-MS analysis was performed in cooperation by the Center for Proteomics and Metabolomics (Director, Prof. Manfred Wuhrer), LUMC, Leiden, the Netherlands.

Next, the LC-MS glycosylation data of the anti-S and total IgG subclasses of samples collected at least 197 days after the first vaccination (see Figure 20, dashed squares) were further analyzed. As shown in Figure 21, the differences between the glycosylation levels of anti-S and total IgG subclass can be seen in these late-collected samples.

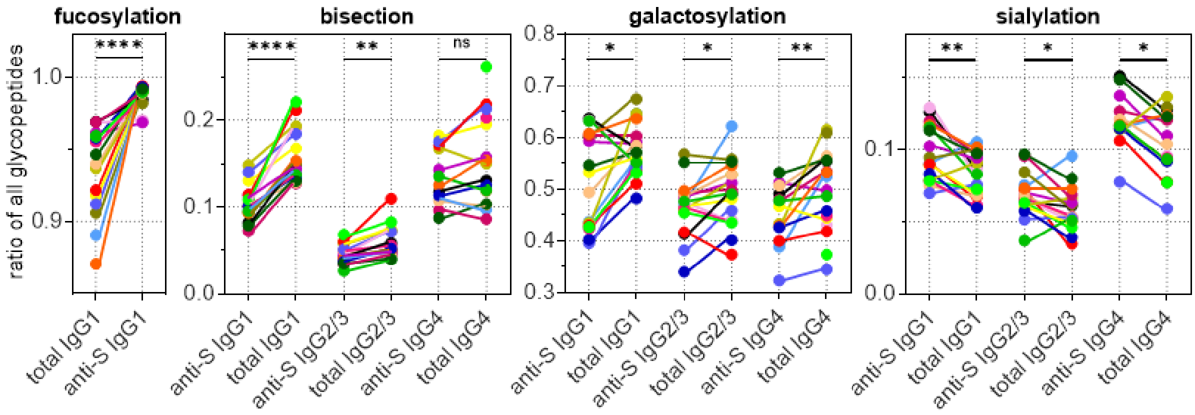

Figure 21: Comparison of anti-S and total IgG subclass Fc glycosylation levels from late (197+ days upon first vaccination) samples after two vaccinations with Moderna's mRNA vaccine.

Comparison of anti-S and total IgG subclass glycosylation levels. Each colour represents one individual (n=17). Statistics: Wilcoxon test. p < 0.05, **p < 0.01, ***p < 0.001, ****p < 0.0001.

Furthermore, a correlation analysis of the anti-S IgG and total subclasses with each glycosylation trait was performed (Figure 22). Strong correlations were observed between antigen-specific and total IgG glycosylation traits, but also between the subclasses.

Taken together, the data from the section 3.2.1 provide new information on IgG Fc *N*-glycosylation patterns in all subclasses. Interestingly, the detection of anti-S afucosylated antibodies was only possible for IgG1. The initial anti-S IgG antibodies showed high levels of galactosylation and sialylation, which were found in all subclasses. These high levels decreased over time. In contrast, anti-S IgG bisection was initially low in all subclasses but increased slightly over time (Figure 20, Figure 21). The data further suggest that these dynamics of galactosylation, sialylation and bisection may be reinitiated after each subsequent vaccination. This assumption is examined below (see section 3.4.1).

Moreover, individual anti-S IgG glycosylation patterns were strongly correlated between subclasses and between individual anti-S and total IgG subclass pairs (Figure 21). This suggests a strong dependence of the induced anti-S IgG subclass glycosylation level on total IgG subclass glycosylation, which may reflect the inflammatory status of individuals.

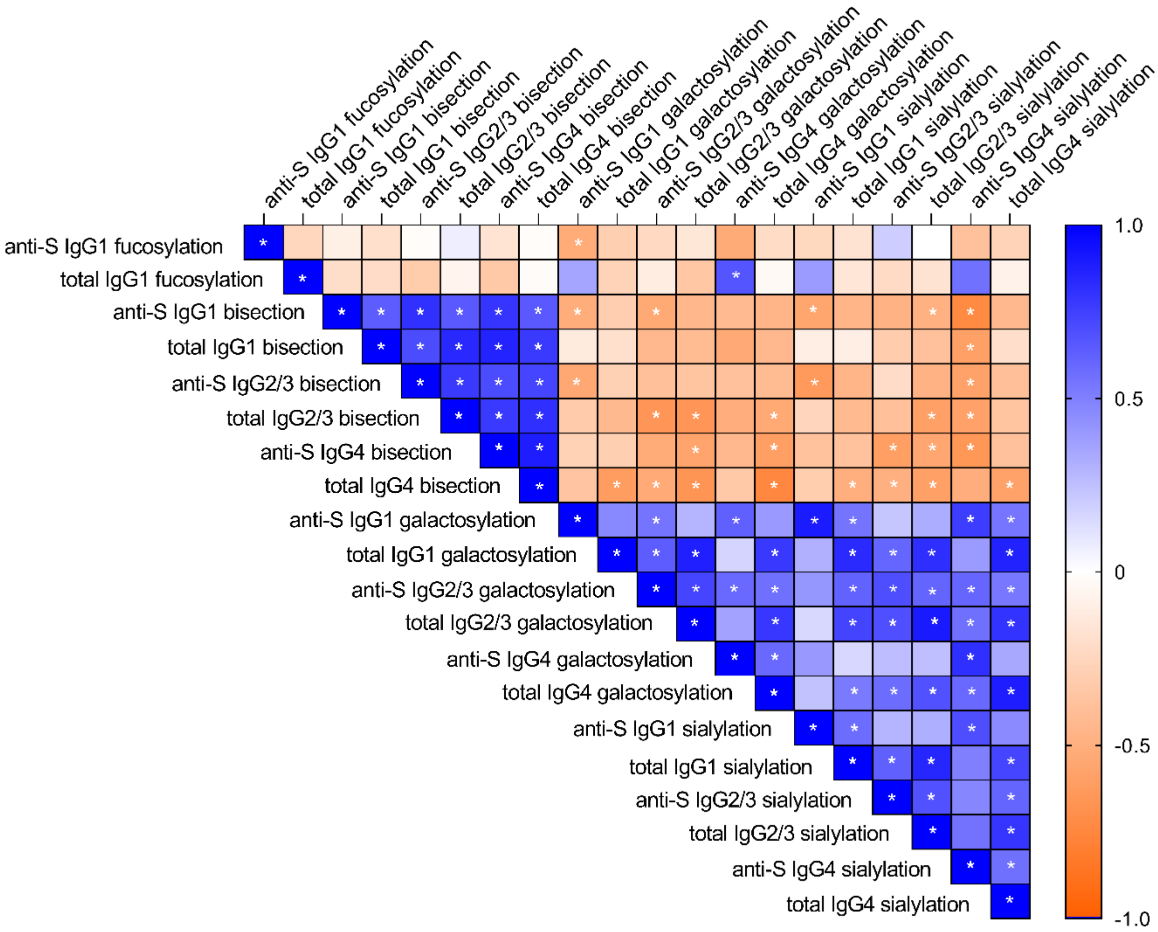

Figure 22: Spearman correlations of anti-S and total IgG subclass glycosylation patterns. A heat map displaying spearman correlations between the indicated anti-S and total IgG subclass Fc glycosylation patterns of late (197+ days upon first vaccination) samples after two vaccinations with Moderna's mRNA vaccine. The heat map legend (Spearman correlation coefficient) is displayed on the right side. Asterisks indicate statistically significant p-values ($p < 0.05$).

3.2.2 IgG4 antibody levels increase with a booster vaccination

The proportion of anti-S IgG4 after repeated mRNA vaccination was then examined further. For this purpose, samples from vaccinated individuals who received up to two vaccinations with the mRNA vaccine from Moderna were used, as well as other samples collected at the UzL and UKSH in Lübeck, Germany. In addition, samples from vaccinees who had been vaccinated up to four times with mRNA vaccines were analyzed (Table 2 and Table 14). These samples were provided by the University Medical Center Charité, Berlin, Germany, or the Semmelweis University, Budapest, Hungary. The samples from Budapest have been described previously (Kiszel et al., 2023). As shown in Figure 23, all these samples were divided into either short-term or long-term samples after each vaccination.

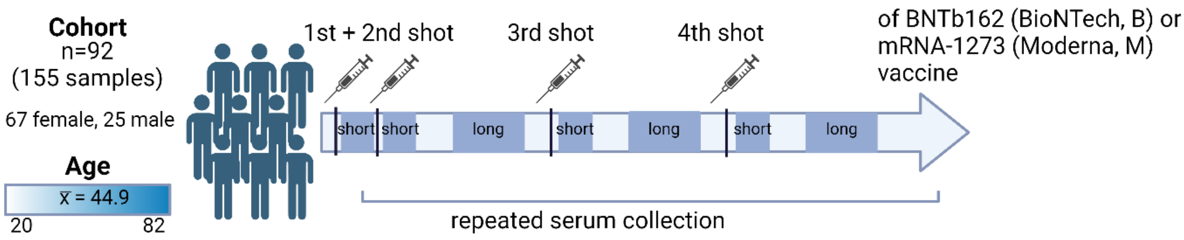

Figure 23: Schematic description of the samples used for investigation of vaccination-induced anti-S IgG4 proportions after repeated vaccinations.

This illustration was created with BioRender.com.

Anti-S1 IgG subclass ELISA and, for some samples, anti-S IgG subclass LC-MS sum-intensity analyses were performed. Subsequently, anti-S(1) IgG subclass standard curves were calculated from the ELISA values and LC-MS sum-intensities as described in section 2.2.3.2. These curves were then used to calculate anti-S IgG subclass sum-intensities for samples for which such data were not yet available. The proportions of anti-S(1) IgG subclass were then calculated.

Table 14: Summary of anti-S(1) IgG frequencies across four mRNA vaccinations.
Abbreviations: M = Moderna; B = BioNTech.

Group	Vaccine strategy	Days post vaccination (min-max)	Individuals (samples)	% anti-S IgG1	% anti-S IgG2/3	% anti-S IgG4
Shortly post 1st	M	22 (13-32)	9 (15)	99.7	0.3	0
Shortly post 2nd	M+M	19 (7-28)	8 (14)	98.5	1.5	0
Long post 2nd	M+M	158 (70-221)	22 (32)	85.6	8.5	5.9
Shortly post 3rd	B+B+B	29 (6-39)	36 (36)	72.9	4.8	22.6
Long post 3rd	B+B+B	169 (153-385)	28 (28)	73.0	5.1	21.8
Shortly post 4th	B+B+B+M	27 (24-30)	6 (6)	67.7	5.2	27.2
Long post 4th	B+B+B+M	221 (151-466)	17 (24)	71.1	4.9	24.0

As shown in Table 14 and Figure 24, the proportion of anti-S(1) IgG4 increased with each mRNA vaccination in the short-and long-term at the expense of IgG1 (however: IgG2 and IgG3 cannot be distinguished). Shortly after the first and second vaccination, IgG1 was the dominant subclass. IgG2/3 remained comparatively low over the entire period, reached a peak long-term after the second vaccination, and decreased again with the third and fourth vaccination.

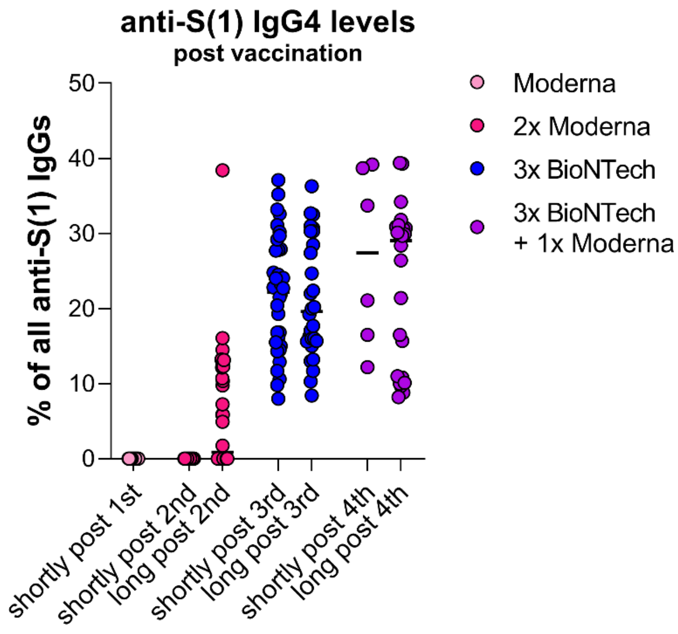

Figure 24: Anti-S(1) IgG4 proportions after repeated mRNA vaccination.
Calculated anti-S(1) IgG4 proportions after repeated mRNA vaccination (n=155, for details see Table 14). The proportions are based on anti-S1 IgG4 ELISA data of all values and a calibration curve (as described in as described in section 2.2.3.2).

Taken together, the data in Table 14 and Figure 24 confirm other findings (Irrgang et al., 2023; Kiszel et al., 2023) that the proportion of IgG4 increased with each mRNA vaccination. The data analyzed here also show that the anti-S IgG4 proportions increased both in the short-term and long-term after each vaccination.

3.2.3 Depletion of IgG4 decreases the activation of neutrophils and increases the activation of NK cells

Since IgG4 accounts for a significant proportion of all anti-S IgG antibodies after repeated mRNA vaccination, the significance and functionality of this subclass in various functional assays should be deciphered. Therefore, an IgG4 depletion and an IgG4 enrichment approach were used (Figure 25).

For this purpose, an anti-human IgG4 coupled to a sepharose column was used to deplete or purify IgG4 from selected samples collected either short-term or long-term after vaccination (section 2.2.6). The purified IgG4 was used in its native form or enzymatically galactosylated and sialylated (sial) or enzymatically desialylated and degalactosylated (degal) to enrich samples.

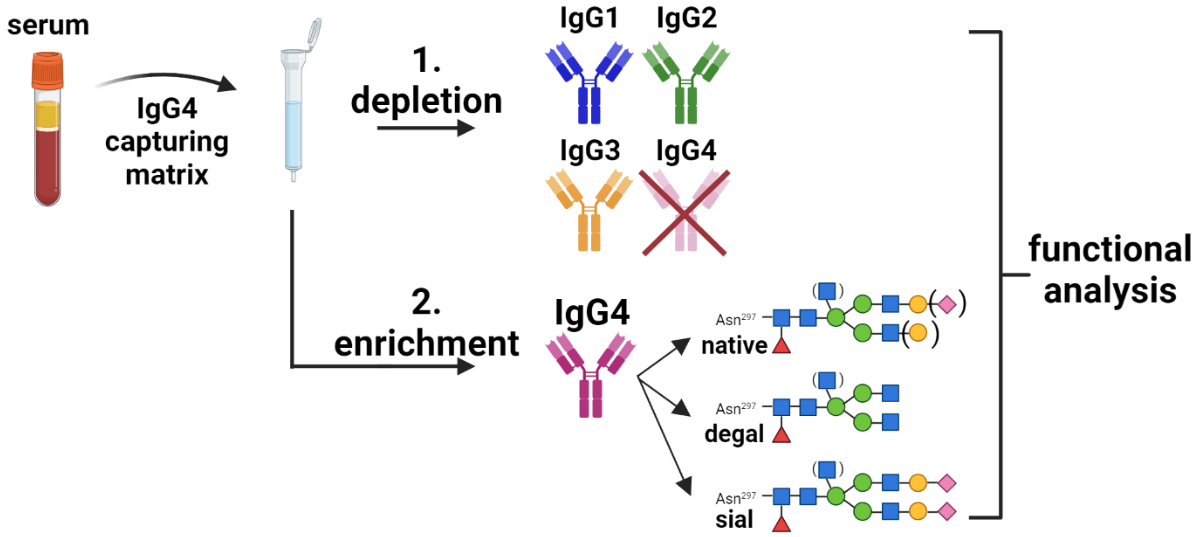

Figure 25: Schematic description of the IgG4 depletion and enrichment approach.
Serum samples collected either short- or long-term after vaccination were used to deplete or purify IgG4. The purified IgG4 was used in its native form or enzymatically galactosylated and sialylated (sial) or enzymatically desialylated and degalactosylated (degal) for subsequent enrichment or samples. This illustration was created with BioRender.com.

As the experiments in sections 3.2.1 have shown that the anti-S IgG4 galactosylation and sialylation levels decrease over time, the impact of these different glycosylation states on the functional activities of the sera should be analyzed by sample selection and glycoengineering.

The selected samples short- and long-term after vaccination for the IgG4 depletion approach are described in Table S2. The success of IgG4 depletion was verified by IgG subclass ELISA (Figure S4). In summary, IgG4 depletion was successful, although, depending on the initial IgG4 content, only a strong reduction rather than complete IgG4 depletion could be achieved. IgG1 was not cross-adsorbed, while partial cross-adsorption of IgG2 and IgG3 antibodies was observed. However, as the combined proportion of anti-S IgG2 and IgG3 was less than 5% of all anti-S IgGs in the selected samples, it can be assumed that their partial depletion makes only a small contribution to the functional analysis conducted (Supplementary Tables 1, 2).

Antibody-dependent neutrophil phagocytosis (ADNP), antibody-dependent cellular phagocytosis (ADCP), antibody-dependent complement deposition (ADCD) and antibody-dependent Natural-Killer-Cell activation (ADNKA) were analyzed. For functional analysis, the IgG4 depleted and non-depleted samples were sent to Mareike Schubert (Laboratory of Dr. Yannic C. Bartsch, Twincore, Hannover, Germany). Assay and experiment-specific results were normalized by calculated z-scores ((value-mean)/standard deviation) (Figure 26).

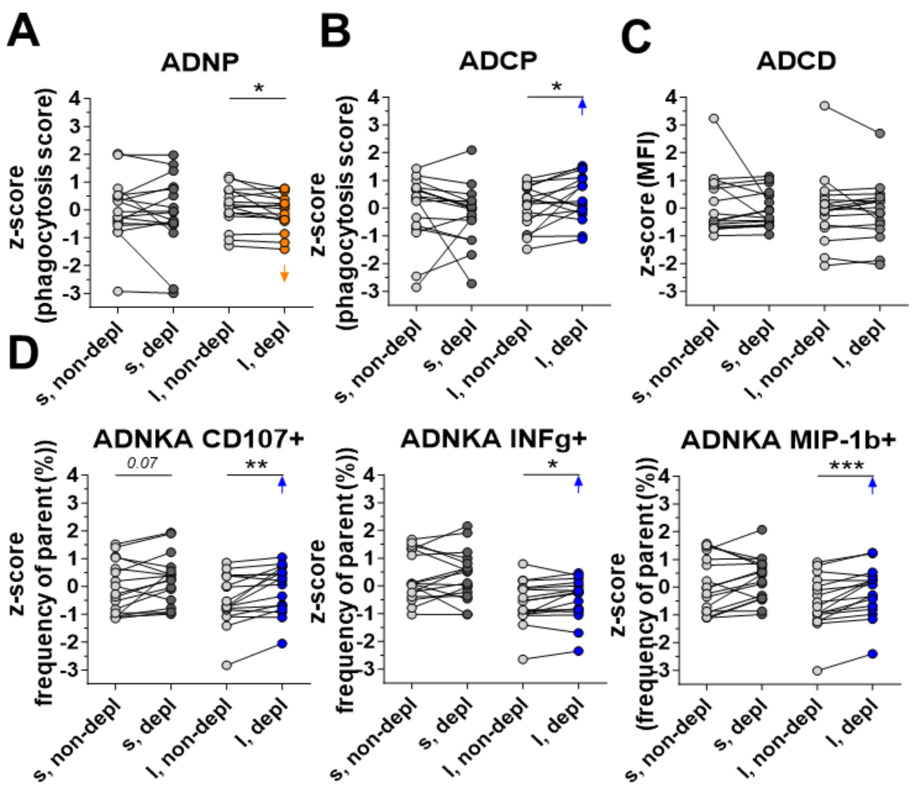

Figure 26: Functional analyses of IgG4 depleted and non-depleted short(s)- and long(l)-term samples after vaccination.

Short (s)- and long (l)-term samples that were either IgG4 non-depleted (non-depl, n=17) or depleted (depl, n=17) were analyzed regarding their potential to activate **(A)** antibody-dependent neutrophil phagocytosis (ADNP), **(B)** antibody-dependent cellular phagocytosis (ADCP), **(C)** antibody-dependent complement deposition (ADCD) and **(D)** antibody-dependent natural killer cell activation (ADNKA-IFNy/CD107a/MIP-1b) with three readouts. Assay and experiment-specific results were normalized by calculated z-scores ((value-mean)/standard deviation). Statistics: Wilcoxon-test, *p < 0.05, **p < 0.01, ***p < 0.001. The functional assays were conducted by Mareike Schubert (Twincore (Laboratory of Dr. Yannic C, Bartsch), Hannover, Germany).

As shown in Figure 26, depletion of IgG4 resulted in increasing or decreasing effects. A significant decrease in ADNP was observed in long-term samples (Figure 26A), indicating an activating effect of IgG4. Instead, IgG4 depletion resulted in increased ADCP in long-term samples (Figure 26B). In addition, IgG4 depletion significantly increased the potential to activate ADNKA in long-term samples and to a lesser extent in short-term samples (Figure 26D). This indicates an inhibitory effect of IgG4 on NK cells. Notably, the samples taken short-term after vaccination showed a higher potential for ADNKA than the long-term samples (Figure 26D). No effects were observed in the ADCD assay (Figure 26C).

Next, correlation analyses were performed with the IgG4-depleted and non-depleted samples used above to investigate whether the potential of a sample to activate effector cells or complement depends on a specific anti-S IgG subclass. Therefore, IgG1 and IgG4 ELISA values (ratio to reference value) or the calculated frequencies of IgG4 were correlated with the generated functional data. No correlation analysis was performed for IgG2 and IgG3 as their frequencies were very low (Table 14).

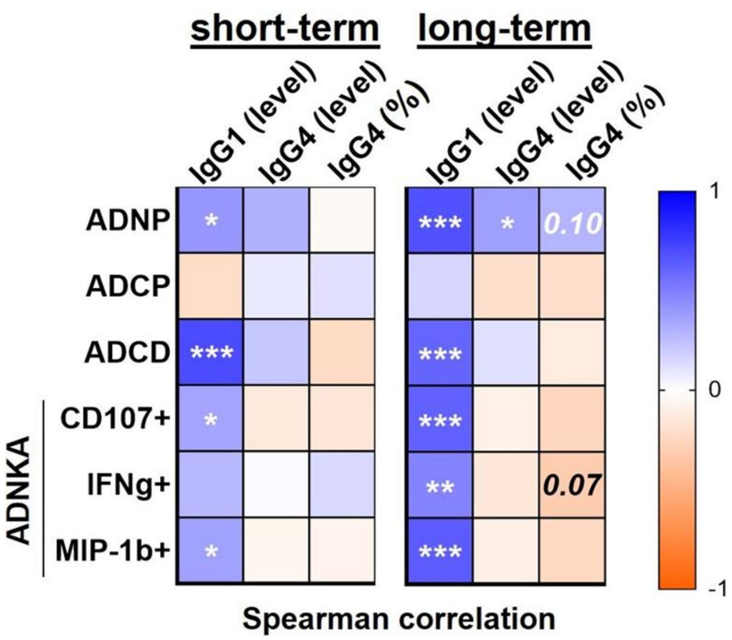

Figure 27: Correlation of anti-S1 IgG1 and IgG4 antibody levels, IgG4 frequencies (%) and functional assays.

The functional z-score data of the IgG4 depleted and non-depleted sera (Figure 26) were correlated with their anti-S1 IgG1 and IgG4 levels as well as their anti-S1 IgG4 proportions (%). Functional assays: antibody-dependent neutrophil phagocytosis (ADNP), antibody-dependent cellular phagocytosis (ADCP), antibody-dependent complement deposition (ADCD), and antibody-dependent NK cell activation (ADNKA) with three different readouts (CD107a+, IFNy+ and MIP-1b+). Statistics: Spearman-correlation coefficients (r, colour) and corresponding p-values are shown; $*p < 0.05$, $**p < 0.01$, $***p < 0.001$.

As shown in Figure 27, strong positive correlations were observed between the functional assay data (except ADCP) and anti-S(1) IgG1 levels for both short- and long-term samples. ADNP also correlated positively with long-term anti-S IgG4 levels. In contrast, negative correlations tended to be observed between the ADNKA data and anti-S1 IgG4 frequencies (and weaker for IgG4 levels), especially for the long-term samples. These correlation results emphasize the observed effects of reduced ANDP after IgG4 depletion in long-term samples and increased ADNKA after IgG4 depletion in both short-term and long-term samples (Figure 26).

3.2.4 Enriched degalactosylated IgG4 increases the activation of neutrophils

Next, the results described above were to be verified by IgG4 enrichment of short- and long-term samples after vaccination. For this purpose, IgG4 was purified and used in its native form (which also had different glycosylation levels as short- and long-term samples were used) or enzymatically glycoengineered (sialylated or de-galactosylated) to enrich untreated samples. These enriched samples were then tested in the functional assays mentioned above.

The anti-human IgG4 column was again used for IgG4 purification. As a certain amount of IgG4 was required, sera from different time points after vaccination were pooled and used for this depletion: i) long-term post second vaccination, ii) short-term post third vaccination, and iii) long-term post third vaccination (Table S4). By using the different time points, further effects caused by the different glycosylation of the antibodies should be elucidated. As already described, native IgG4 from short-term samples showed higher levels of galactosylation and sialylation as well as lower bisection than IgG4 purified from long-term samples. Part of these IgG4 antibodies were then enzymatically galactosylated and sialylated (sial) or desialylated and degalactosylated (degal) as described in 2.2.7.1 and 2.2.7.2. Eventually, three different states of the IgG4 antibodies of all three time points were achieved: native, sialylated (sial), and degalactosylated (degal). Both the IgG4 concentrations as well as the sialylation states were verified by ELISA (Figure 28).

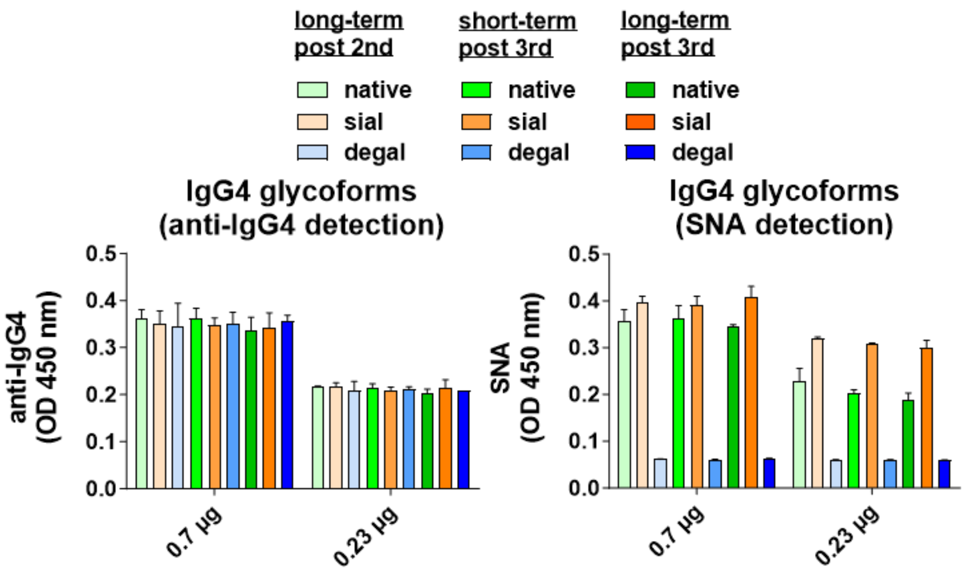

Figure 28: Anti-IgG4 and SNA-ELISA of isolated and differently glycosylated IgG4 antibodies.

All pooled, purified and enzymatically glycoengineered antibodies of the three indicated time points were coated in two concentrations and detected with either anti-IgG4-HRP or SNA-HRP. Abbreviations: sial sialylated, degal degalactosylated. Data are presented as mean +/- SD.

Next, the effect of IgG4 enrichment in short- and long-term sera after vaccination with purified and differently glycosylated IgG4 antibodies was tested in the functional assays. Purified native IgG4 antibodies from short- or long-term samples were only added to samples from the respective time points, while sial and degal IgG4 forms were given to samples from both time points (Table S5).

10 µg of native, sial, or degal IgG4 were added to 10 µL of serum. IgG4 accounts for approximately 1-3% of the IgG content in serum, with a general mean IgG concentration of 10-16 mg/mL (Jazayeri et al., 2013). Therefore, ~ 0.26 mg/mL IgG4 can be found in sera, which corresponds to 2.6 µg in 10 µL. When 10 µg of IgG4 was added to 10 µL of serum, a significant increase in total IgG4 and thus anti-S IgG4 was achieved.

In particular, the addition of IgG4 alone without serum showed a very low activation potential (Figure S5, dashed lines). Furthermore, no significant effects on the functional activation potential were observed after the addition of native or sial IgG4 (Figure 29, Figure S5). In contrast, the addition of degal IgG4 led to an increase in ADNP in both the short- and long-term samples. The addition of degal IgG4 also increased ADCP. Instead, additional degal IgG4 decreased ADCD. Interestingly, IgG4 could not strongly affect ADNKA in any glycosylation state, although a slight inhibitory effect of additional, mainly native IgG4 was observed.

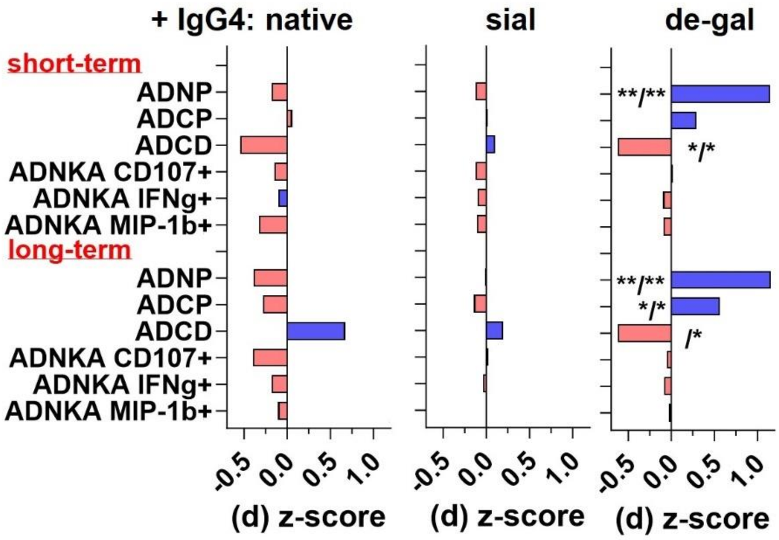

Figure 29: Functional analyses of short-term and long-term sera after vaccination enriched with purified native and glycoengineered IgG4.

IgG4 from short- or long-term sera was purified and enzymatically glycoengineered. Native, galactosylated+sialylated (sial), or desialylated+degalactosylated (de-gal) IgG4 was added to short- or long-term sera and the effects on the functional activities were analyzed with the following assays: antibody-dependent neutrophil phagocytosis (ADNP), antibody-dependent cellular phagocytosis (ADCP), antibody-dependent complement deposition (ADCD), antibody-dependent NK cell activation (ADNKA; three different readouts (CD107a, IFNy and MIP-1b)). Z-scores were calculated and delta (d) z-scores (z-scores of IgG4 enriched sera minus z-scores of non-enriched sera) were calculated (Figure S5). The Friedman test was used to compare the different groups. Asterisks indicate statistically significant p values (*$p < 0.05$, **$p < 0.01$), the first asterisks compare the degal and no-enriched groups and the second asterisks compare the degal and sial groups.

Taken together, the experiments shown in sections 3.2.2- 3.2.4 reveal increasing proportions of anti-S IgG4 with each mRNA vaccination (Table 14, Figure 24). Depletion of IgG4, especially in long-term samples, decreased ADNP and increased ADNKA, suggesting an activating potential of IgG4 on neutrophils and an inhibitory potential of IgG4 on NK cells (Figure 26). The correlation analyses

(Figure 27) showed that IgG1 in particular seems to be the key driver of antibody-dependent cellular activation and complement, while IgG4 showed weaker positive but also negative correlations with functional assays.

An approximately fourfold enrichment of short- and long-term samples with corresponding purified native total IgG4 and accordingly anti-S IgG4 showed only minor functional effects for reasons that are yet unclear. Enrichment with glycoengineered sial IgG4 showed hardly any effects (Figure 29, Figure S5). In contrast, enrichment with degal IgG4 led to increased activation of neutrophils and monocytes activation, while complement activation was decreased. The activating potential of degal IgG4 on ADNP is consistent with the observation that IgG4 depletion of long-term samples leads to reduced ADNP. Notably, the addition of the three IgG4 glycosylation states without any serum showed only very little functional effects (Figure S5, dashed lines).

3.3 The involvement of Tumor-necrosis factor (TNF) in vaccination-induced antibody responses

TNF, and in particular TNFα, is a pro-inflammatory cytokine that is involved in inflammatory responses and is also required for the proper development of humoral immune responses (Pasparakis et al., 1996). It could be shown that TNFα-knockout mice fail to form proper GCs and also show significantly lower antibody responses. Since vaccination leads to long-term immunity by mainly GC-derived long-lived plasma cells and memory B cells, it is reasonable to assume that patients undergoing TNF-blockade for the treatment of inflammatory (auto-) immune diseases also show significantly reduced vaccination-induced B cell and subsequently antibody responses. Accordingly, several publications deal with TNF treated patients and their immune responses after vaccination (Andrisani et al., 2013; Elkayam, 2004). In these studies, suboptimal vaccination success was always assumed, while the read-out was primarily decreased antibody levels – regardless of their IgG subclass and glycosylation pattern.

Therefore, a vaccination study that investigated anti-TNF treatment during COVID-19 vaccinations was of particular interest. This study showed that the vaccination-induced anti-S1 IgG and IgA antibodies were significantly reduced six months after the second vaccination (Geisen, Sümbül, et al., 2021). This finding supports the assumption, that TNF-blockade inhibits GC-derived antibody responses. Therefore, a collaborative project was started with Prof. Bimba Hoyer and Dr. Ulf Geisen from the UKSH Kiel (Clinic for Rheumatology (director, Prof. Bimba Hoyer), UKSH, Kiel, Germany), who collected samples from anti-TNF treated patients. By analyzing the abundancies of vaccination-induced IgG subclasses, their Fc glycosylation patterns and their functional effects, the importance of the GC response for the vaccination-induced IgG antibody response should be deciphered.

3.3.1 TNF is critically involved in both short- and long-term IgG antibody responses after vaccination

As shown in Figure 30, the cohort consisted of patients suffering from chronic inflammatory diseases who were treated with either anti-TNF (n=11) or other disease-modifying anti-rheumatic drugs (DMARDs; n=12). A control group of healthy individuals (n=23) was also included. All recruited individuals received two to three vaccinations with the mRNA vaccine from BioNTech. Four time points were analyzed: i) shortly after the first vaccination, ii) shortly after the second vaccination, iii) six months after the second vaccination, and iv) shortly after the third vaccination.

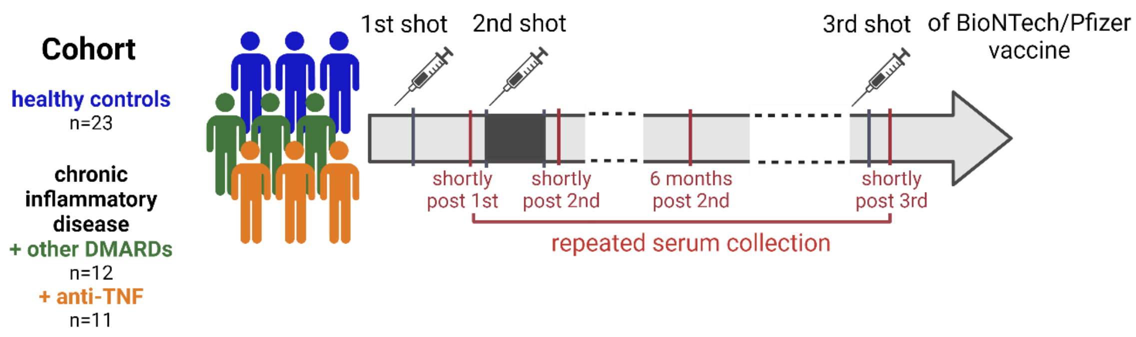

Figure 30: Description of the cohort with anti-TNF treated patients and two control groups. This illustration was created with BioRender.com.

To investigate anti-S1 IgG subclass levels over time using (HL-1) ELISA, all four different time points were analyzed. Shortly after the first vaccination (that is just before the second vaccination), no differences were observed. Thereafter, anti-S1 IgG subclass levels in the anti-TNF treated group decreased progressively with each vaccination. For IgG1, this reduction was already visible shortly after the second vaccination (Figure 31A). At the last two time points, significant reductions in IgG1 and IgG4 levels and trending reductions in IgG2 and IgG3 levels were observed between the healthy control group and the anti-TNF treated patients. The patients, that were treated with anti-TNF, showed very low responses for all IgG subclasses after the third vaccination.

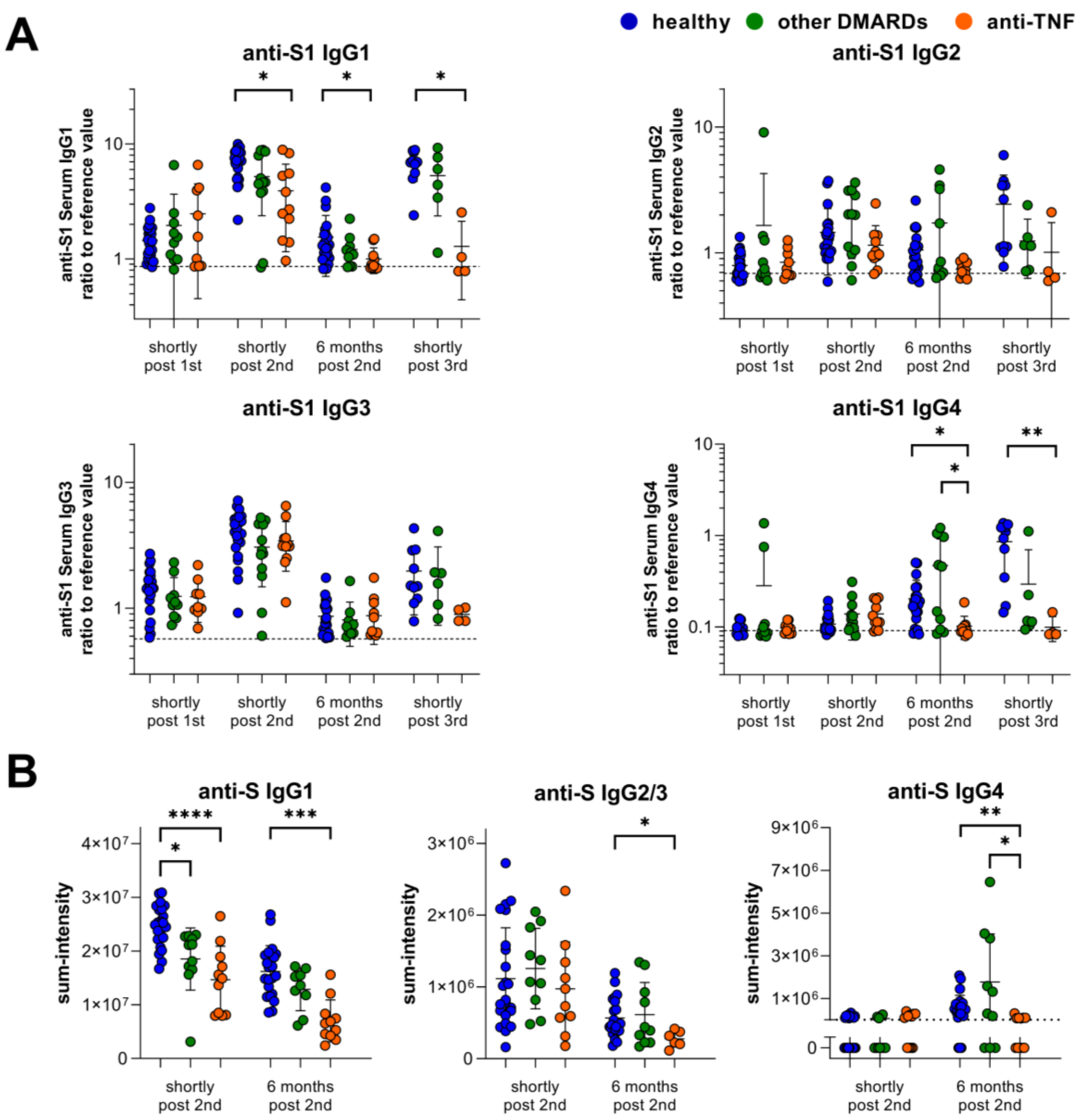

Figure 31: Anti-S(1) serum IgG subclass levels in anti-TNF treated patients.

(A) Anti-S1 serum IgG1-4 (HL-1 ELISA) levels (ratio to the reference value) of the three groups indicated. Four different time points were analyzed: i) shortly after the first and just before the second vaccination, ii) one week, iii) six months after the second, and iv) shortly after the third vaccination. The dashed lines indicate corresponding average anti-S1 IgG subclass levels of the non-vaccinated healthy controls. **(B)** IgG subclass sum-intensities as detected by LC-MS. The dotted line in the IgG4 graph represents the cut-off threshold, meaning that samples below this line did not have sufficient anti-S IgG4 glycopeptide peaks for analysis. Statistics: Kruskal-Wallis test, *$p < 0.05$, **$p < 0.01$, ***$p < 0.001$, ****$p < 0.0001$, n= 23 healthy controls, n=12 other DMARDs and n=11 anti-TNF treated patients were repeatedly sampled, but not all time points were available from each subject.. Abbreviations: n.d. not determined.

In addition, the levels of anti-S IgG subclasses were analyzed at two time points, one week (shortly) and six months after two vaccinations by LC-MS analysis in collaboration with the Center for Proteomics and Metabolomics (director: Prof. Manfred Wuhrer), LUMC, Leiden, the Netherlands. The ELISA results were confirmed and even more conclusive (Figure 31B).

3.3.2 Anti-TNF treatment is critical for low galactosylated and sialylated long-term IgG responses after vaccination

The glycosylation analysis of the anti-S IgG subclasses in the samples one week and six months after two mRNA vaccinations showed higher levels of galactosylation and sialylation of the IgG subclasses long post the second vaccination in anti-TNF treated patients than in healthy controls. Accordingly, the bisection was lower (Figure 32). Interestingly, increased galactosylation and reduced bisection of IgG4 were observed already shortly after the second vaccination (Figure 32B, C).

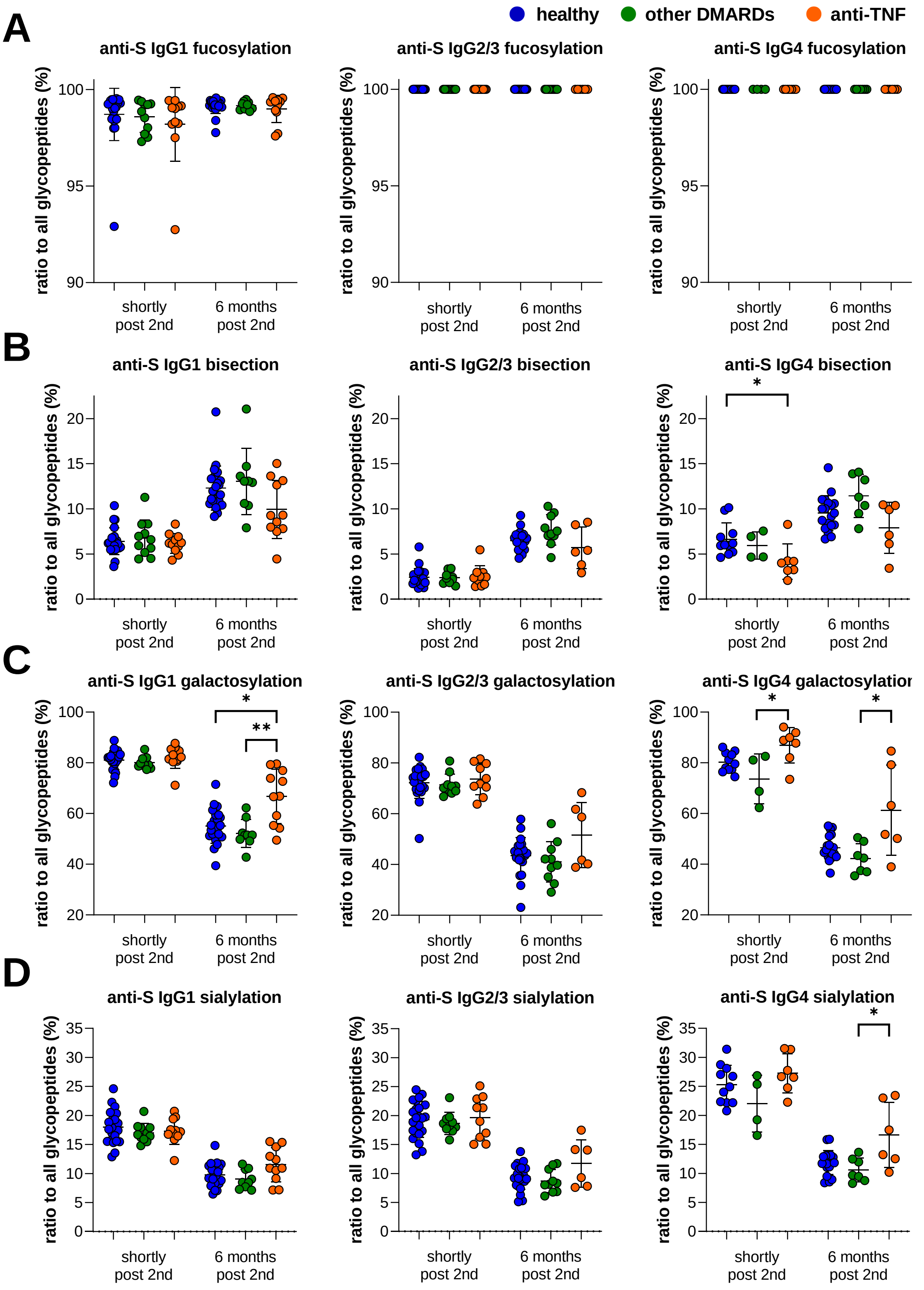

Figure 32: Anti-S IgG subclass glycosylation patterns in anti-TNF treated patients.
Anti-S serum IgG1-4 Fc glycosylation: **(A)** fucosylation, **(B)** bisection, **(C)** galactosylation, and **(D)** sialylation of the three groups indicated. Two different time points were analyzed: shortly (one week) and six months post second vaccination. Statistics: Kruskal-Wallis test, *$p < 0.05$, **$p < 0.01$, ***$p < 0.001$, ****$p < 0.0001$, n= 23 healthy controls, n=12 other DMARDs and n=11 anti-TNF treated patients were repeatedly sampled, but not all time points were available from each subject. The LC-

MS analysis was performed in cooperation by the Center for Proteomics and Metabolomics (Director, Prof. Manfred Wuhrer), LUMC, Leiden, the Netherlands.

3.3.3 Anti-TNF treatment during vaccination impairs anti-S antibody-mediated functional activities

The functional potential of the short- and long-term samples after the second vaccination was then analyzed using the functional assays described above: ADNP, ADCP, ADCD and ADNKA (with three readouts). All functional analyses shown were performed in collaboration by Mareike Schubert (Twincore (Laboratory of Dr. Yannic C, Bartsch), Hannover, Germany).

As shown in Figure 33, anti-TNF treatment significantly reduced the functional activity of the short- and long-term samples in all assays.

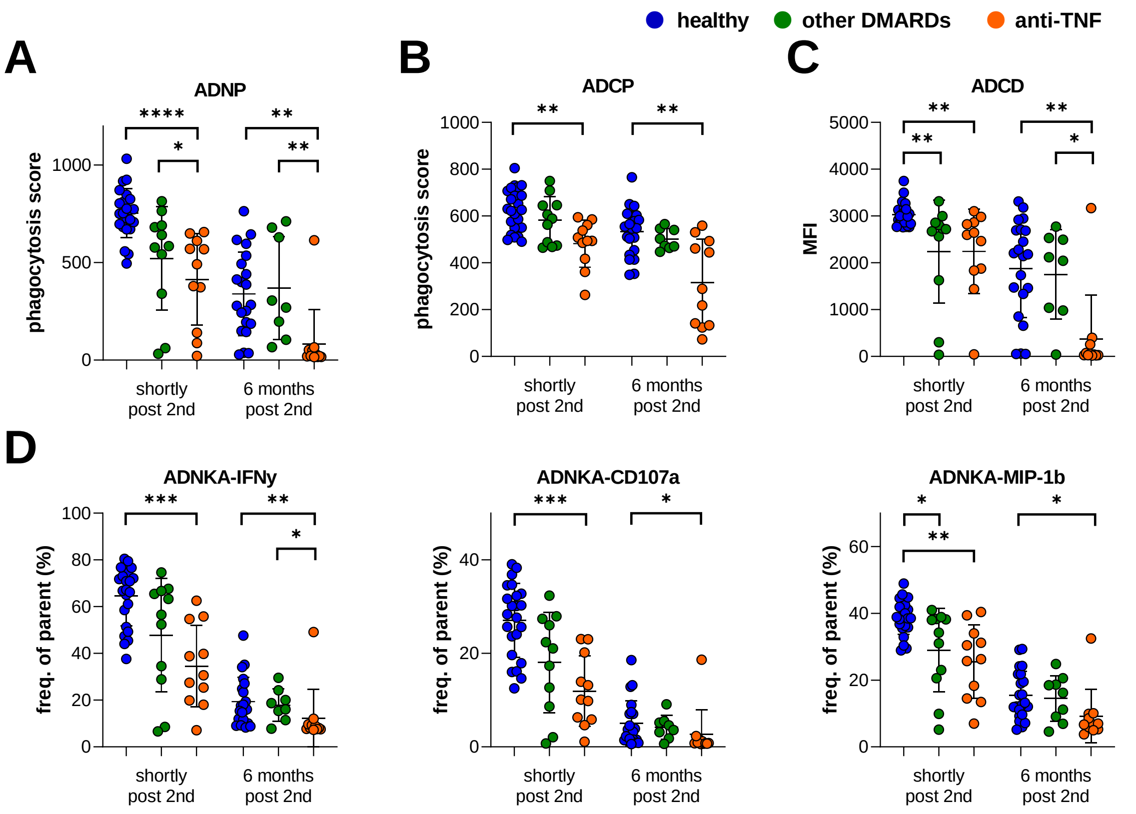

Figure 33: Functional activity of anti-S antibody responses from anti-TNF treated patients. Sera from two different time points (shortly (one week) and six months post second vaccination) were analyzed for their potential to activate **(A)** antibody-dependent neutrophil phagocytosis (ADNP), **(B)** antibody-dependent cellular phagocytosis (ADCP), **(C)** antibody-dependent complement deposition (ADCD) and **(D)** antibody-dependent natural killer cell activation with three readouts (ADNKA-IFNy/CD107a/MIP-1b). Statistics: Kruskal-Wallis test, *p < 0.05, **p < 0.01, ***p

< 0.001, ****p < 0.0001, n= 23 healthy controls, n=12 other DMARDs and n=11 anti-TNF treated patients were repeatedly sampled, but not all time points were available from each subject. The functional assays were conducted by Mareike Schubert (Twincore (Laboratory of Dr. Yannic C, Bartsch), Hannover, Germany).

Correlation analyses were performed to clarify the cause for the reduced anti-S antibody activities of the samples from the anti-TNF treated patients (Figure S6). These analyses revealed that the strongest correlations for both time points studied were those comparing each functional activity with anti-S IgG1 levels in all three groups (Figure 34).

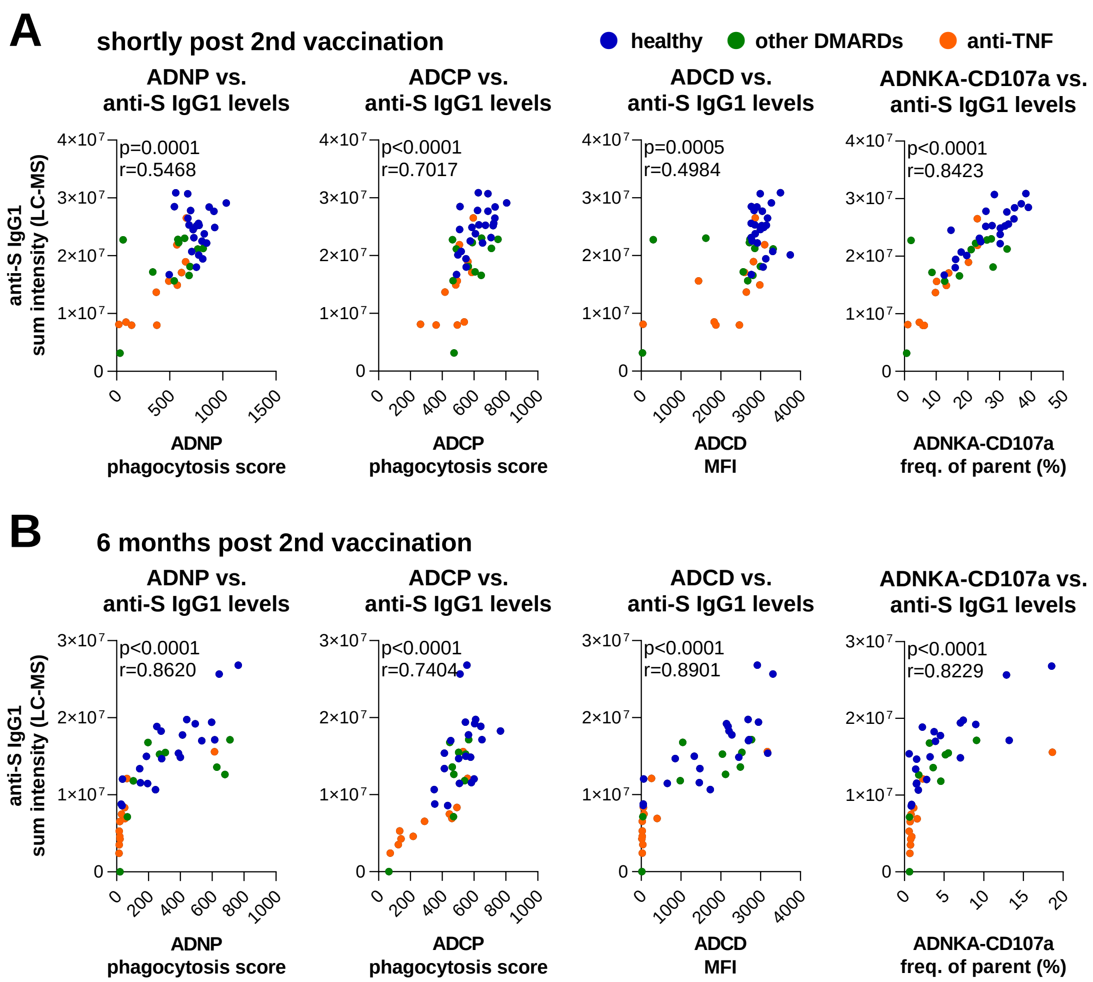

Figure 34: Correlation of functional data with anti-S1 IgG1 levels from the cohort with anti-TNF treated patients.

Functional activities were correlated with anti-S IgG1 levels (sum of intensities identified by LC-MS) **(A)** shortly (one week) and **(B)** six months post-second vaccination. Statistics: Spearman-Correlation, respective p-values, and r of each correlation are shown.

3.3.4 Anti-TNF treatment inhibits memory B cell development

The reduced anti-S1 IgG subclass antibody levels shortly after the second and third vaccination suggest that TNF inhibition not only inhibits GC-derived long-lived plasma cell responses but may also play a role in the generation of GC-derived memory B cells that generate plasma cells after re-activation.

Accordingly, Ulf Geisen from the UKSH (Clinic for Rheumatology (director, Prof. Bimba Hoyer), UKSH, Kiel, Germany) in collaboration re-analyzed existing data (Geisen et al., 2022) for anti-S1 memory B cells shortly after the second vaccination. Memory B cells were defined by flow cytometry as anti-$S1^+$, $CD19^+$, $CD27^+$ and $CD20^+$ cells.

Analysis of anti-S1 memory B cell revealed that significantly lower number of such cells were found in anti-TNF treated patients shortly after the second vaccination (Figure 35A). Next, a correlation analysis of the memory B cell numbers with the anti-S1 IgG subclass levels at the same time point was performed. Significant correlations were identified for all subclasses, in particular for IgG1 and IgG3, assuming, that memory B cells could actively contribute to the short-term IgG levels, likely by a re-activation into antibody-producing plasma cells (Figure 35B).

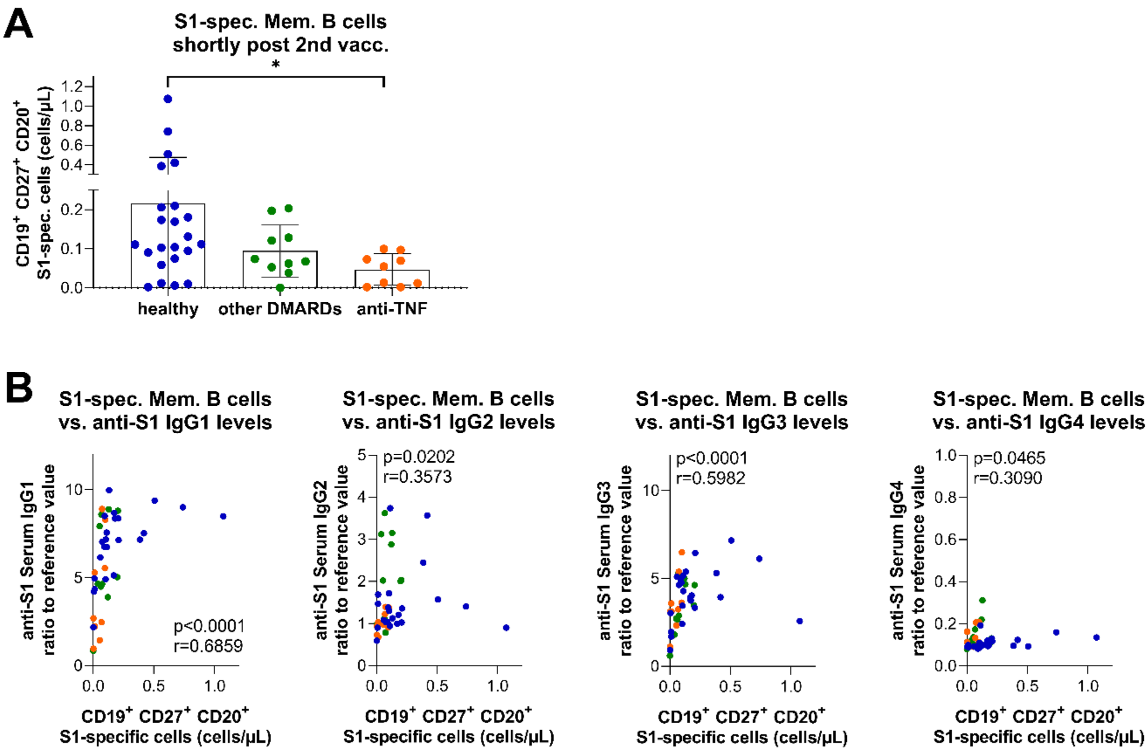

Figure 35: Antigen-specific memory B cells in the cohort with anti-TNF treated patients. **(A)** Antigen-specific memory B cells, which were identified by flow cytometry as S1-specific CD19+ CD27+ CD20+ cells/ µL blood, shortly (one week) post-second vaccination. Statistics: Kruskal-Wallis-test, *p < 0.05. **(B)** Antigen-specific memory B cells shortly post-second vaccination were correlated with anti-S1 IgG1-4 levels shortly post-second vaccination. Statistics: Spearman correlation (r) and corresponding p values are shown, n= 23 healthy controls, n=12 other DMARDs and n=11 anti-TNF treated patients were repeatedly sampled, but not all time points were available from each subject. The flow cytometry analysis was performed in cooperation by Dr. Ulf Geisen (Rheumatology (director, Prof. Bimba Hoyer), UKSH in Kiel, Germany).

Together, the data presented in the sections 3.3.1 – 3.3.4 showed that anti-TNF treatment reduced both the short- and long-term IgG subclass antibody responses after repeated vaccinations (Figure 31, Figure 32). The data suggest that TNF is important for the generation of both GC-derived long-lived plasma cells and GC-derived memory B cells (Figure 35).

3.3.5 Anti-TNF treatment increases the risk of developing COVID-19

As the short- and long-term IgG antibody responses were reduced in anti-TNF treated patients, the next step was to analyze whether these patients have a higher risk of becoming infected with SARS-CoV-2. The following investigation was performed in collaboration by Prof. Ralf Ludwig, Director of the Lübecker Institute of Experimental Dermatology, University of Lübeck and University Medical Center Schleswig-Holstein, Lübeck, Germany.

Patient data were evaluated in August 2023 by using TriNetX, a federal global healthcare database, to determine the risk of COVID-19 breakthrough infection rates. As described in 2.2.9, breakthrough infections analyzed by PCR over an 18-month period following two mRNA vaccinations in patients with chronic inflammatory diseases, treated with i) anti-TNF, or ii) anti-α4β7-integrin or MTX were investigated.

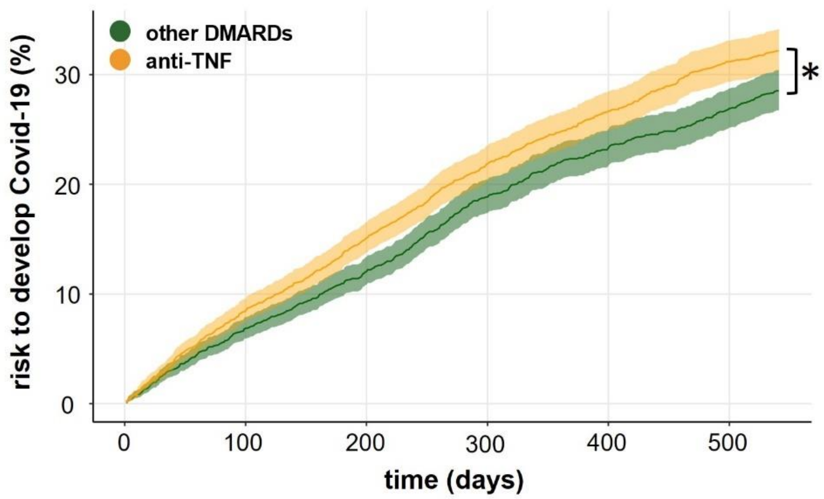

Figure 36: Real-world data-analysis of COVID-19 breakthrough infections in patients with chronic inflammatory diseases.

Increased risk of COVID-19 breakthrough infection observed in patients with chronic inflammatory (auto-) immune diseases treated with TNF inhibitors versus those receiving α4β7 integrin inhibitors or MTX (other DMARDs) after two mRNA vaccinations over a period of 18 months. The shaded areas represent the 95% confidence intervals. Kaplan-Meier curves were compared using the log-rank test; p=0.0027, n= 2742 anti-TNF treated patients and n=2783 other DMARDs treated patients.

The analysis revealed a significantly increased risk of SARS-CoV-2 infection in patients treated with anti-TNF compared to the other treatments. Specifically, 771 out of 2742 (28.1%) anti-TNF treated patients developed a breakthrough infection after the second mRNA vaccination, while only 683 out of 2783 (24.5%) control patients developed a detected breakthrough infection during the same period (Figure 36).

Taken together, anti-TNF treatment increased the risk of SARS-CoV-2 breakthrough infection after two mRNA vaccinations compared to treatment with anti-α4β7 integrin or MTX (other DMARDs) in patients with inflammatory diseases (Figure 36).

3.3.6 TNFα-blocking in mice increases immunization-induced anti-Ova IgG1 Fc galactosylation and sialylation

To further validate TNF-blocking and the consequences on GC-dependent changes in IgG Fc glycosylation patterns, a mouse experiment was conducted. This experiment was performed together with Janna Quack, a former Bachelor candidate, and Dr. Hanna Lunding, a former PhD candidate of our laboratory.

C57BL/6 mice were immunized with 100 µg of ovalbumin (Ova) in enriched complete Freunds`adjuvant (eCFA). The immunization induces a strong Ova-specific GC reaction and a strong anti-Ova IgG response (Bartsch et al., 2020). In addition, half of the mice were regularly treated with an anti-TNF blocking antibody as indicated in Figure 37A. Therefore, the effects of anti-TNF blocking on the GC-dependent antibody response were analyzed. After sacrificing the mice on day 12, their blood was collected by heart puncture and the samples were analyzed for anti-Ova IgG1 Fc glycosylation in collaboration by the Center for Proteomics and Metabolomics (director, Prof. Manfred Wuhrer), LUMC, Leiden, The Netherlands.

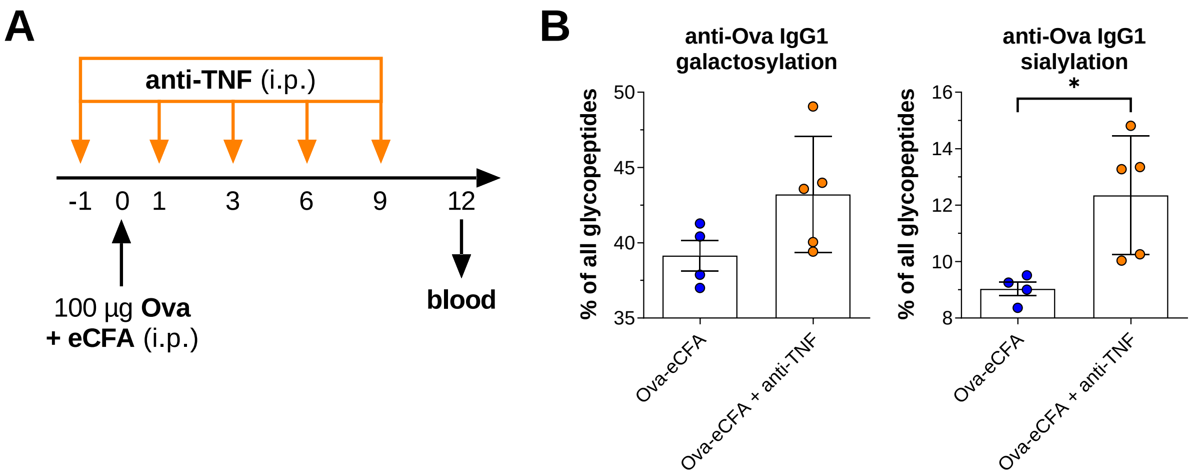

Figure 37: TNF-blocking in mice in the Ova-immunization model.

(A) Experimental setup of the Ova-immunization model. Mice were immunized i.p. at day 0 with 100 µg Ova in eCFA. 100 µg of a monoclonal blocking antibody against TNF**α** was injected on the indicated days: -1, 1, 3, 6, and 9. Blood serum was sampled on day 12 after immunization. **(B)** Percentages of serum anti-Ova IgG1 Fc galactosylation and sialylation levels. Shown are the mean values ± SD. Statistics: Unpaired t-test, *p<0.05, n = 4-5. The LC-MS analysis was performed in cooperation by the Center for Proteomics and Metabolomics (director, Prof. Manfred Wuhrer), LUMC, Leiden, the Netherlands.

As shown in Figure 37B, anti-TNF treatment 12 days after immunization led to a reduction in galactosylation and sialylation levels of anti-Ova IgG1. The data suggest that a reduced GC response by TNF-blockade results in a dominance of extrafollicular higher galactosylated and sialylated anti-Ova IgG1 antibodies (Bartsch et al., 2020).

3.4 B cell differentiation during repeated vaccination

IgG4 antibodies only appeared late after mRNA vaccination. In addition, inhibition of TNF and thus GC disruption diminished IgG4 levels (Figure 31). Therefore, the late-emerging IgG4 antibodies seemed to be GC-dependent (Figure 31) (Hartley et al., 2023; Irrgang et al., 2023). Furthermore, the increase in anti-S IgG4 proportions not only in the long-term, but also in the short-term after repeated vaccination indicates the possible existence of IgG4^{+} memory B cells that are re-activated and differentiate into IgG4-producing plasma cells. Accordingly, a strong correlation between vaccination-induced memory B cells and respective short-term IgG subclass antibody responses was observed (Figure 35).

Mouse vaccination studies (Bartsch et al, 2020) and the human vaccination studies described above (section 3.1, 3.2.1) (Bartsch et al., 2020; Buhre et al., 2023; Van Coillie et al., 2023) characterized early antigen-specific plasma cell responses by high galactosylation, and sialylation and low bisection. Late antigen-specific plasma cell responses were characterized by lower galactosylation and sialylation as well as higher bisection levels. The studies further suggest that the early antibodies after immunization are generated by extrafollicular plasma cells, whereas the late antibodies are mainly generated by GC-derived long-lived plasma cells.

Therefore, it was of interest whether a re-activation of anti-S memory B cells produces anti-S IgG antibodies with the same characteristics as extrafollicular plasma cells (high galactosylation/sialylation) or whether the anti-S IgG glycosylation pattern remains comparatively low after re-activation. To address this question, the IgG antibody responses after a third vaccination were characterized in detail.

3.4.1 A third vaccination induces highly galactosylated and sialylated anti-S IgG subclass antibodies

Samples from healthy individuals recruited during the vaccination study from section 3.1 and from whom samples were available shortly before and after the third vaccination were further analyzed by anti-S1 IgG subclass (HL-1) ELISA and LC-MS IgG subclass glycopeptide analyses.

LC-MS IgG subclass glycopeptide analysis of the anti-S IgG subclass was performed in collaboration by the Center for Proteomics and Metabolomics (director, Prof. Manfred Wuhrer), LUMC, Leiden, The Netherlands.

As expected, the increase in anti-S(1) IgG subclass antibody responses after the third vaccination was reconfirmed after the third vaccination. These increased antibody levels were significant for all subclasses, as confirmed by both ELISA (Figure 38A) and LC-MS sum-intensity analysis of IgG subclasses (Figure 38B).

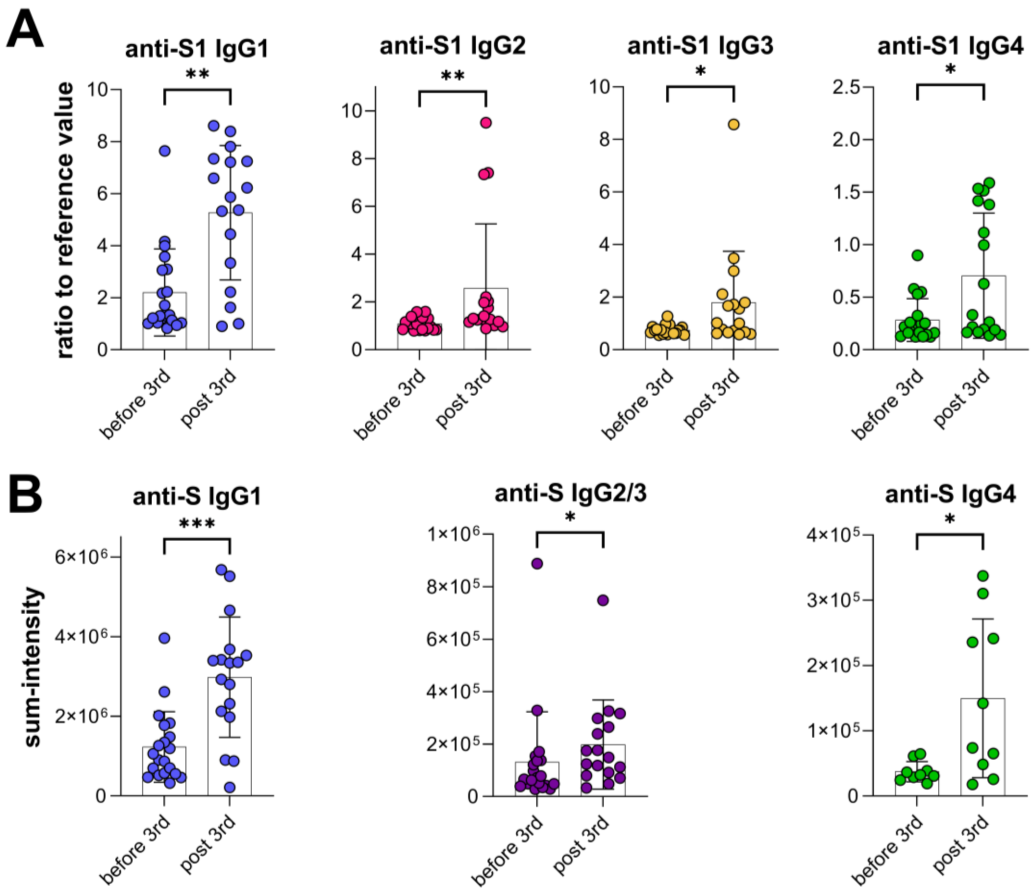

Figure 38: Vaccination-induced IgG responses shortly before/after a third vaccination. **(A)** Anti-S1 IgG subclass titers identified by (HL-1) ELISA and **(B)** anti-S summed glycopeptide intensities of the IgG subclasses as detected by LC-MS anti-S IgG subclass glycopeptide analysis. Samples before (n=20) and after (n=17) a third vaccination were used. Shown are the mean values ± SD. Statistics: Mann-Whitney test, *p<0.05, **p<0.01. The LC-MS analysis was performed in cooperation by the Center for Proteomics and Metabolomics (Director, Prof. Manfred Wuhrer), LUMC, Leiden, the Netherlands.

As shown in Figure 39, the anti-S IgG subclass glycosylation analyses revealed that all subclasses, including IgG4 antibodies, had unaltered fucosylation after the third vaccination, but higher levels of galactosylation and sialylation and less bisection than before.

The data suggest that re-activated memory B cells apparently also produce IgG antibodies with similar galactosylation, sialylation and bisection found very early after the first and second vaccination.

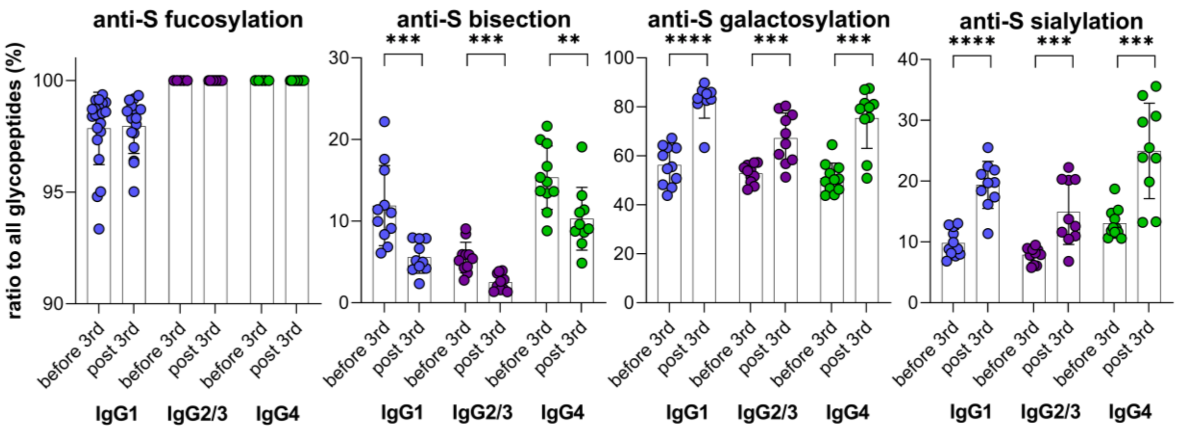

Figure 39: Anti-S IgG subclass glycosylation patterns after re-activation of potential GC-derived IgG(4)+ memory B cells shortly post third vaccination.

Anti-S IgG subclass glycosylation levels before (n=11) and shortly post (n=10) a third vaccination. Shown are the mean values ± SD. Statistics: Mann-Whitney test, **p<0.01, ***p < 0.001, ****p < 0.0001. The LC-MS analysis was performed in cooperation by the Center for Proteomics and Metabolomics (Director, Prof. Manfred Wuhrer), LUMC, Leiden, the Netherlands.

Taken together, the data in section 3.4.1 describe that after the third vaccination, IgG Fc *N*-glycosylation patterns exhibit the same characteristics as shortly after the first and second vaccination (Figure 38, Figure 39). Since vaccination-induced IgG4 antibodies probably originate from (GC-derived) memory B cells, the glycosylation pattern of the IgG4 antibodies after the third vaccination was used to infer their origin. Consequently, a holistic picture of the vaccination-induced B cell responses (including TNF-dependence) was proposed (Figure 40).

These new findings, together with the data described above and others, suggest a model that is illustrated in Figure 40. First, with each vaccination, a part of naïve B cells class switch to IgG and develop into IgG^+ extrafollicular short-lived plasma cells that generate rapidly emerging IgG antibodies characterized by high galactosylation and sialylation as well as low levels of bisection. Secondly, activated naïve B cells migrate into TNF-dependently formed GCs and undergo IgG class switching and affinity maturation. IgG^+ GC B cells either develop into long-lived plasma cells that generate IgG antibodies characterized by lower galactosylation and sialylation and higher bisection levels, or they differentiate into GC-derived memory B cells. After a booster vaccination, these GC-derived memory B cells are re-activated upon antigen stimulation and partly develop into IgG^+ extrafollicular short-lived plasma cells, which form highly galactosylated and sialylated as well as low bisected IgG antibodies. Another part of these memory B cells re-enters the GC reaction.

The formation of GCs and thus GC-dependent B cell differentiation is TNF dependent, which explains why patients treated with anti-TNF have significantly reduced long-term IgG responses, but interestingly also impaired responses shortly after the second and third vaccination (3.3). This implies again that TNF and thus the GC reaction is critically involved in not only long-lived plasma cells, but also in the re-activation and differentiation of presumably memory B cells into short-lived (extrafollicular) plasma cells.

The data described here further suggest that IgG antibodies generated by short-lived extrafollicular plasma cells (coming from re-activated memory B cells), which are characterized by high galactosylation and sialylation and low bisection, may play a different role than IgG antibodies generated by GC-derived long-lived plasma cells, which are characterized by lower galactosylation and sialylation and higher bisection levels. Accordingly, low galactosylated IgG responses generated by GC-derived long-lived plasma cells of all IgG subclasses, can for instance activate neutrophils. Short-term highly galactosylated and sialylated antibodies may instead contribute to cytotoxicity and NK cell activation.

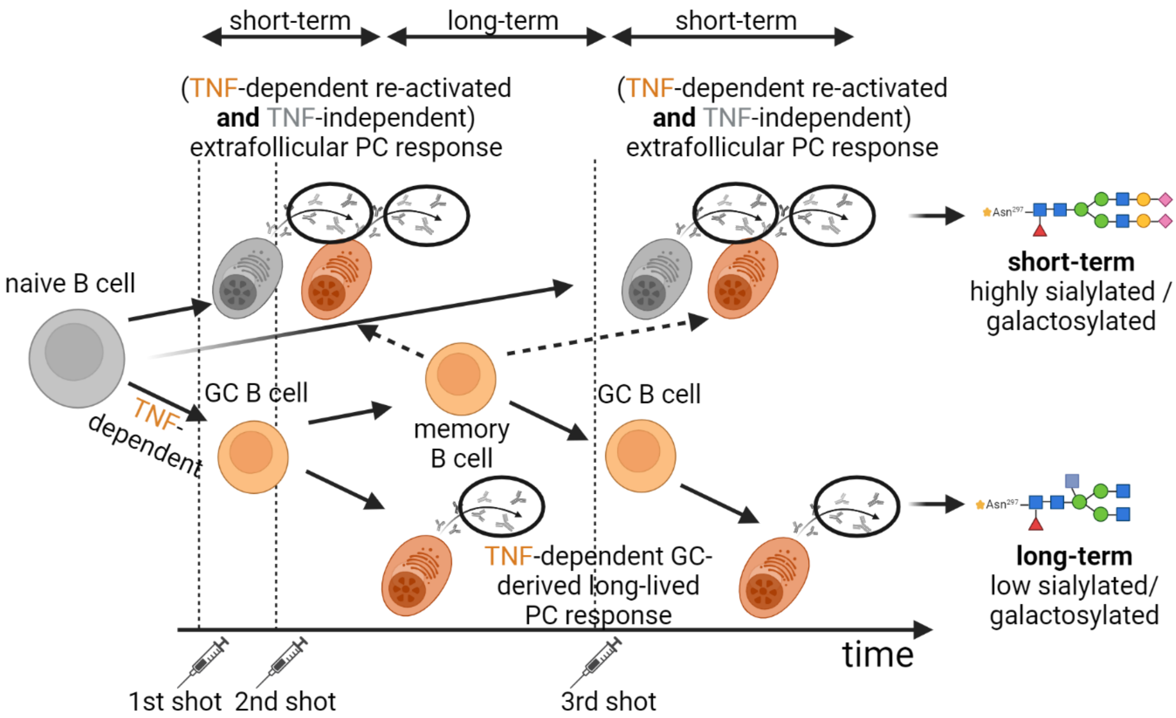

Figure 40: Proposed model of B-cell differentiation and re-activation after booster vaccination.

Briefly, and as mentioned in the text, upon antigen-stimulation naïve B cells can differentiate into IgG^+ extrafollicular plasma cells (PCs) or migrate into the GC, where they develop into either IgG^+ memory B cells or IgG^+ long-lived plasma cells. All GC responses are TNF-dependent (orange cells). Memory B cells can be re-activated and differentiate into extrafollicular plasma cells or migrate into GCs. Short-term antibody responses are characterized by high sialylation and galactosylation and low bisection, while long-term antibody responses show low sialylation and galactosylation and high bisection. This illustration was created with BioRender.com.

4. Discussion

First of all, it should be noted that the newly developed vaccines against COVID-19 have made a significant contribution to reducing infection and hospitalization rates and have successfully counteracted the pandemic during the acute phase (Firouzabadi et al., 2023; Mohammed et al., 2022). Nevertheless, there have been numerous breakthrough infections, and the induced immune response of the new vaccines still needs to be studied in more detail in order to further optimize them.

Immune responses induced by the newly developed vaccine formats

In preclinical studies on the newly developed mRNA- and adenovirus-based vaccines, a strong T_H1-response was described for all three vaccines investigated, while only a weak T_H2-response was found (Buhre et al., 2023; Laczkó et al., 2020; Lixenfeld et al., 2021; Sahin et al., 2020; Swanson et al., 2021). T_H1-responses in humans are characterized by the production of IgG1 and IgG3 antibodies (Kawasaki et al., 2004), which also fits the data shown: Initially, the dominant subclasses were IgG1 and IgG3 for all three vaccines (Figure 10, Figure 11). In addition to that, $T_{FH}1$ responses were described after vaccination, indicating the involvement of T follicular helper cells (T_{FH} cells). Surrogate biomarkers such as circulating T_{FH} cells can be used to predict and monitor the induced GC responses (Havenar-Daughton et al., 2016; Vella et al., 2019).

Furthermore, a recent study in mice comparing the potential of different adjuvants to induce T_{FH}-cell responses concluded that a certain antigen-specific IgG Fc glycosylation pattern can be expected depending on the kind of T_{FH} response (Bartsch et al., 2020). It has been shown that $T_{FH}1$ responses after immunization with oil-in-water adjuvants such as incomplete Freund's adjuvant (IFA) initially induce high levels of IgG Fc galactosylation and sialylation and later low galactosylation and sialylation levels. This $T_{FH}1$-response was characterized by IFNγ. Stronger adjuvants that induce even stronger inflammatory immune responses, such as enriched complete Freund's adjuvant (eCFA), additionally led to IL-17-producing T_{FH}17-cells, resulting in even lower galactosylation levels (Bartsch et al., 2020).

Consistent with these observations, the long-term anti-S antibody responses induced by both mRNA and adenovirus-based vaccines resulted in low galactosylation and sialylation patterns (Figure 13), while galactosylation levels were even lower than the corresponding total IgG galactosylation levels (Figure 14). Elevated IL-6 and IL-17 levels were detected in COVID-19 patients who had to be hospitalized, indicating both a T_{FH}1 and T_{FH}17-response (Golovkin et al., 2021; Martonik et al., 2021; Sharif-Askari et al., 2022). Subsequently, the IgG Fc glycosylation pattern of these patients showed even lower galactosylation and sialylation patterns compared to healthy vaccinees (Buhre et al., 2023; Pongracz et al., 2022). Because of that, the upcoming T_{FH}17-repsonse resulting in very low IgG galactosylation and sialylation levels in hospitalized patients appears to be an indicator of a severe inflammatory disease outbreak (Pongracz et al., 2022).

In contrast, a T_{FH}1 response has been described in non-hospitalized COVID-19 patients (Golovkin et al., 2021). Consequently, the galactosylation and sialylation pattern of COVID-19 patients who did not require hospitalization is similar to that of naïvely vaccinated individuals (Buhre et al., 2023). Vaccination studies in mice also confirmed that mRNA vaccines induce a T_{FH}1-response (Lederer et al., 2020). In addition, T_H1- and very few T_H2-polarized T_{FH} cells were found in the lymph nodes of vaccinated individuals, but no T_H cells resembling a T_{FH}17-phenotype (Lederer et al., 2022).

Taken together, the identified anti-S IgG subclasses and Fc glycosylation patterns emphasize the described T_{FH}1-response for all three different vaccination formulations.

Comparison of the newly developed vaccine formats

The comparative vaccination study showed that the mRNA vaccines from BioNTech and Moderna had significantly higher initial antibody titers than the adenovirus-based vaccine from AstraZeneca (Figure 8) (Buhre et al., 2023). This observation may also reflect the different levels of efficacy obtained during the clinical trials of the three vaccines: While BioNTech and Moderna reported efficacy of up to 95% three weeks after the second vaccination (Baden et al., 2021; Polack et al., 2020), the AstraZeneca vaccine (as well as another adenovirus-based vaccine from Janssen-Cilag, which was not studied in this project) was reported to have an efficacy of around 70% several weeks after the second vaccination (Shay et al., 2021; Voysey et al., 2021). However, the efficacy was only determined a few weeks after the administration of two doses and literature on long-term data remains rare.

However, it was reported that the tolerability of the three vaccines is different. While all three vaccines studied had comparable levels of moderate side effects, some degree of severe side effects were stated for the vaccines from Moderna and AstraZeneca (Adjobimey et al., 2022). In particular, fatal cases of thrombocytopenia were reported after injection of the AstraZeneca vaccine, which is why this vaccine was later forbidden in Germany (Greinacher et al., 2021). This is also the reason why the here used vaccination cohort includes a significant number of individuals who were vaccinated with a heterologous vaccination scheme (AstraZeneca followed by an mRNA vaccine) (Table 2).

Although it was found that there were considerable differences in antibody levels between the vaccines, these differences decreased over time and equalized in the long term after the second vaccination (Figure 8). The mRNA vaccines appear to elicit a very strong initial antibody response, probably generated by extrafollicular short-lived plasma cells. This early extrafollicular antibody response was weaker after vaccination with the AstraZeneca adenovirus-based formula (Buhre et al., 2023). Long-term antibody responses are mainly facilitated by GC-derived long-lived plasma cells (Buhre et al., 2023; Irrgang et al., 2023; Manz et al., 1997, 2005; Turner et al., 2021) and were similar in contrast to the early responses. The mRNA vaccines therefore appear to have a stronger potential to induce a strong extrafollicular (mainly IgG1) response, while the potential in terms of a GC-dependent long-term response is comparable. Furthermore, IgG4 antibodies occurred after homologous mRNA vaccination or heterologous vaccination, but neither after homologous adenovirus-based vaccination nor in the investigated pre-infected individuals (Figure 11) (Buhre et al., 2023; Irrgang et al., 2023; Kiszel et al., 2023).

The observed differences in the early results between mRNA and adenovirus-based vaccines suggest that the mRNA in LNP-delivery format may either trigger a stronger initial antibody response, potentially through PRRs recognition, or lead to a higher amount of expressed spike protein compared to the dsDNA from the viral vector. Although the latter is difficult to investigate, the fact that Moderna's vaccine induces higher titers compared to BioNTech's vaccine would indicate a dose dependency (Figure 8) (Adjobimey et al., 2022; Buhre et al., 2023). The vaccine from Moderna contains 100 µg mRNA per injection and BioNTech's vaccine contains 30 µg mRNA per injection (Baden et al., 2021; Polack et al., 2020). However, it has been reported that both the RNA sequences and the LNP formulations of the two vaccines differ slightly, which might contribute to different initial antibody levels (Heinz & Stiasny, 2021). Notably, another difference between the two different vaccine strategies is their capability to stimulate the innate immune response: while the mRNA is mainly recognized by TLR7 and TLR3, the adenovirus-delivered dsDNA binds to TLR9. Although it is assumed that both stimulations lead to the secretion of type I interferons, differences cannot be ruled out (Figure 1) (Teijaro & Farber, 2021).

Examination of the heterologous vaccination groups (starting with AstraZeneca's vaccine and an mRNA-formula as the second vaccine) revealed that the second vaccination led to IgG antibodies comparable to those of homologous mRNA vaccination (Figure 8). Interestingly, it was later discussed that this hybrid vaccination regimen might be even more effective than a homologous strategy. Pozzetto and colleagues found that heterologous vaccination (AstraZeneca's + BioNTech's vaccines) had a higher neutralizing capacity of the antibodies compared to homologous vaccination (BioNTech's + BioNTech's vaccines) (Pozzetto et al., 2021). This was particularly striking as the antibody levels were comparable, suggesting that there must be differences in the quality of these antibodies. It was also found that while mRNA vaccines induce significantly higher titers, adenovirus-based vaccines induce a stronger T-cell response, so that a heterologous vaccination might have a complementary effect (Pozzetto et al., 2021).

Consistent with these observations, the PLS-DA analysis led to a clear separation of three different vaccination groups: homologous mRNA, homologous adenovirus-based, and heterologous adenovirus + mRNA. In addition to antibody levels, IgG Fc glycosylation patterns were also included in the model (Figure 16), supporting the idea that a hybrid vaccination scheme may lead to unique antibody properties. Nevertheless, this needs to be further investigated.

IgG Fc glycosylation patterns are an important modulator of Fc-mediated effector functions in addition to the subclass of an IgG antibody (Anthony et al., 2011; Arnold et al., 2007; Buhre et al., 2022; De Jong et al., 2016; Epp et al., 2018; Hess et al., 2013; Kaneko et al., 2006; Lilienthal et al., 2018; Nimmerjahn & Ravetch, 2008b; Oefner et al., 2012; Ohmi et al., 2016; Petry et al., 2021; Pincetic et al., 2014). Especially at the beginning, the mRNA vaccines induced slightly higher galactosylated and sialylated and less bisected IgG1 antibodies, suggesting a stronger initial extrafollicular plasma cell response (Figure 12, Figure 13). Over time, these differences vanished, and after several months, the IgG1 antibodies induced by the various vaccine combinations exhibited a comparable glycosylation pattern, characterized by the following features: comparably low galactosylation and sialylation, high bisection and almost no afucosylation. Later, the same long-term IgG Fc glycosylation pattern was also observed for the other IgG subclasses (Figure 20). However, different glycosylated antibodies during the early and late vaccination response might not only reflect different origins but could also reflect functionally divergent roles.

A previous study suggested that membrane-associated antigens induce the generation of afucosylated IgG antibodies. Since the encoded spike (S) protein of the different vaccines investigated is expressed as such a membrane associated protein, an afucosylated IgG1 response was expected for all groups (Larsen et al., 2021). Afucosylation is a glycosylation feature that is strongly associated with a high potential to bind to activating FcγRIII (Dekkers et al., 2017; Ferrara et al., 2011; Shields et al., 2002). In line with increased binding to activating FcγRs, afucosylated antibodies may be associated with alloimmunity (Kapur et al., 2014) as well as disease severity in cases of dengue fever (Bournazos et al., 2021). With regard to COVID-19, afucosylated IgG antibodies correlate with disease severity and have been repeatedly found (Chakraborty et al., 2021, 2022; Hoepel et al., 2021; Larsen et al., 2021). However, the strong potential to activate effector cells could also be the reason why a certain proportion of afucosylated antibodies appears to have a protective effect in both HIV infections and malaria (Ackerman et al., 2013; Larsen et al., 2021). Thus, the induction of afucosylated IgG1 antibodies seems to be an aim for vaccine development. Nonetheless, although membrane-associated, the vaccine-induced S proteins in the three vaccine formats investigated induced only a transient peak of afucosylated IgG1 antibodies after the first vaccination (at least in naïve individuals, the pre-infected group will be discussed later) (Figure 12) (Buhre et al., 2023; Van Coillie et al., 2023). Already after the second vaccination, about 98% of the IgG1 antibodies were fucosylated. Later, the absence of long-term afucosylation was also confirmed for the other IgG subclasses (Figure 20).

Recently, it has been discussed that early highly galactosylated and sialylated IgG antibodies facilitate antigen delivery to GCs to further enhance affinity maturation and the production of antibodies with strong neutralizing capabilities (Lofano et al., 2018; T. T. Wang et al., 2015). Interestingly, higher neutralizing capacities of IgG antibodies were observed with dual mRNA vaccination compared to dual AstraZeneca vaccination (Adjobimey et al., 2022). Furthermore, it has been suggested that highly galactosylated IgGs are potent activators of NK cells (Jennewein et al., 2019) and may interact better with C1q than agalactosylated IgG antibodies (Dekkers et al., 2017; Quast et al., 2015; van Osch et al., 2021). This suggests that early vaccination-induced antibody responses have a higher cytotoxic potential as compared to later, less galactosylated and sialylated responses.

In contrast to the initially highly galactosylated and sialylated IgG antibodies, the long-term antibodies were lower sialylated and galactosylated. Interestingly, very low IgG Fc galactosylation and sialylation states are associated with increased inflammation in (auto-) immune diseases. This is likely due to an increased interaction with activating FcγRs and thereby activation of for instance neutrophils (Anthony et al., 2011; Arnold et al., 2007; Bartsch et al., 2018; Buhre et al., 2022; Clauder et al., 2021; De Jong et al., 2016; Epp et al., 2018; Hess et al., 2013; Kaneko et al., 2006; Lilienthal et al., 2018; Nimmerjahn & Ravetch, 2008b; Oefner et al., 2012; Ohmi et al., 2016; Petry et al., 2021; Pincetic et al., 2014). Vaccination-induced long-term IgG antibodies with low galactosylation and sialylation levels might therefore mediate neutrophil phagocytosis or pathogen exposure, to re-start an immune response after repeated vaccination or infection. However, further research is needed to elucidate different roles of differently glycosylated short- and long-term antibody responses.

Nevertheless, little is known about the exact role of glycosylation of IgG antibodies, particularly in the context of protection against pathogens. In addition, different glycosylation states might have different effector functions on distinct cell types or complement (Nimmerjahn et al., 2023). Next to glycosylation patterns, other glycan binding receptors could also play a role and further skew the immune response (Anthony et al., 2011; Arnold et al., 2007; Banda et al., 2008; Dühring et al., 2023; Karsten et al., 2012; Petry et al., 2021; Pincetic et al., 2014; T. T. Wang et al., 2015). The functional tasks of the differently glycosylated IgG antibodies are therefore still very complex and require further investigation.

Vaccination in previously infected individuals

Interesting differences were found when comparing the vaccination reactions of pre-infected and naïve individuals. The pre-infected group showed particularly strong IgG1 responses after vaccination, while the IgG3 responses were weaker compared to the naïve individuals (Figure 10). The initially higher IgG1 responses in the pre-infected individuals after the first vaccination were probably due to reactivation of pre-existing memory B and T cells that were formed during the infection. In contrast to IgG1, IgG3 responses were significantly reduced in pre-infected individuals. IgG3 is the subclass that is triggered earliest after infection, which may also be due to the positioning of the genetic locus. In humans, IgG3 is the first gene locus, sequentially followed by IgG1 (Damelang et al., 2019; Horns et al., 2016; Kitaura et al., 2017). Interestingly, the IgG3 response of naïve individuals also decreases in the long term, so that the IgG3 responses are hardly present after the third and fourth vaccination (Table 14). Taken together, this suggests that IgG3 is mainly present due to an initial infection or a first vaccination, but that the B cells switch to the other subclasses during the ongoing GC response. Furthermore, the weak IgG3 responses after a second vaccination in pre-infected individuals or after a third/fourth vaccination in naïve individuals suggest that only a few memory B cells are $IgG3^{+}$.

It has also been reported that IgA levels in serum and especially in saliva were higher in pre-infected than in naïve individuals (Buhre et al., 2023). Several studies suggest that vaccination of previously infected individuals leads to better protection than in naïve individuals (Abu-Raddad et al., 2021; Petráš et al., 2021). One explanation for this better protection could be these mucosal IgA antibodies, as COVID-19 is a disease that infects the respiratory tract. Therefore, mucosal antibodies (and presumably tissue-resident T and B cells) are likely early responders during viral entry, making them critical for adequate protection (Iwasaki, 2016; Tang et al., 2022). In line with these observations, intranasal immunizations in mice resulted in better vaccination outcomes than systemic immunizations (Tang et al., 2022). The strategy of intranasal vaccination against diseases that require a certain degree of mucosal protection is increasingly being discussed (Dhama et al., 2022; Tang et al., 2022).

Another interesting difference between pre-infected and naïve individuals after vaccination is afucosylation, which is only transient in naïve individuals but stable in pre-infected vaccinees (Figure 12) (Buhre et al., 2023; Van Coillie et al., 2023). In contrast, initial and long-term anti-S IgG1 galactosylation and sialylation levels were similar between naïve and pre-infected vaccinees. As mentioned above, afucosylated IgG antibodies have an increased potential to activate effector cells through increased affinities to activating FcγRs. This increased potential to activate further immune responses could also contribute to the elevated protection of pre-infected individuals.

Cellular analyses revealed that an initial IgG-producing plasma cell subpopulation in naïve individuals may be associated with transient afucosylation (Figure 18). Precisely, in naïve individuals, $CD138^{-}CD27^{-}$ was the dominant subpopulation of all antigen-specific IgG^{+} $CD38^{+}CD19^{int}$ plasma cells shortly after the first vaccination. This population showed the lowest expression level of Fut8, which may explain the increased appearance of afucosylated IgG1 antibodies. After the second vaccination, this population decreased and was almost as present as the other subpopulations, while Fut8 levels became similar in all subpopulations.

In pre-infected individuals, instead, $CD27^{high}CD138^{-}$ IgG^{+} plasma cells were the dominant population after both vaccinations, which may represent a population of reactivated memory B cells. CD27 is a known memory B cell marker (Agematsu et al., 2000; Tangye et al., 1998), but is also present in $CD38^+$ plasma cells (Jung et al., 2000). However, it must be clarified whether the persistent 6% afucosylated IgG1 antibodies derive from this specific plasma cell subpopulation.

The observation of only transiently afucosylated antibodies allows the following conclusions to be drawn: the newly developed vaccine formats cannot induce a robust pool of long-lived plasma cells, that continuously produce afucosylated IgG antibodies. Moreover, this feature of afucosylation is absent in memory B cells, as the afucosylation only occurs after the first vaccination and appears to be restricted to extrafollicular plasma cells.

These observations suggest that the vaccine formats investigated may lack certain stimuli to induce a long-lived plasma cell subset that produces afucosylated IgG1 antibodies. In contrast, studies in patients with severe COVID-19 disease showed that these patients had even higher levels of afucosylated antibodies than individuals with mild disease outbreaks. In addition, the strong inflammatory responses in hospitalized patients were associated with an additional T_{FH}17-response (Golovkin et al., 2021; Martonik et al., 2021; Sharif-Askari et al., 2022). It would therefore be interesting to investigate whether afucosylated antibodies are associated with T_{FH}17 responses.

Furthermore, PLS-DA analyses of the long-term antibody responses of both pre-infected and naïve individuals demonstrated a clear separation between the two groups (Figure 15). This emphasizes that the immune reactions induced by natural infections differ from those of vaccination in terms of adjuvant potential and lead to unique antibody signatures.

Overall, the comparison between naïve and pre-infected patients showed that an earlier infection can influence the subsequent vaccination response. The following differences were found: i) enhanced and more robust mucosal antibody responses (especially IgA), ii) robust afucosylation levels in IgG1 antibodies, iii) different IgG-producing plasma cell subsets, and iv) significantly reduced IgG4 levels in pre-infected individuals over time. All these differences could contribute to better protection against breakthrough/re-infection in pre-infected individuals.

Vaccination-induced IgG4 responses

The investigated mRNA vaccines showed late-emerging IgG4 antibodies that were not present after adenovirus-based vaccinations or in pre-infected individuals (Figure 11B) (Buhre et al., 2023; Irrgang et al., 2023; Kiszel et al., 2023). Sequencing of memory B cells revealed that the GC reaction persisted up to six months after vaccination (Muecksch et al., 2022; Röltgen et al., 2022), hence it is likely that the class switch may also last for several months. As already mentioned, IgG3 is the first subclass of the gene locus, followed by IgG1 and IgG2. In contrast, IgG4 is the most downstream subclass (Damelang et al., 2019; Horns et al., 2016; Kitaura et al., 2017).

A recent study suggests that the IgG4 antibodies develop in a GC-dependent manner (Irrgang et al., 2023). This assumption can be strengthened by the TNF study presented in section 3.3. Here, anti-TNF treated individuals who have a greatly reduced GC-reaction due to TNF-inhibition showed almost no IgG4 antibodies (Figure 31).

Looking at the IgG4 proportions over several vaccinations, it is noticeable that the proportion increases over time (Figure 24). Nonetheless, one limitation of the analysis is an inconsistent vaccination strategy, as almost all samples received Moderna's vaccine as a fourth vaccination. Therefore, it cannot be ruled out that the increase from the third to the fourth vaccination is due to the choice of vaccine.

Interestingly, the individuals who had been vaccinated with the mRNA vaccine from Moderna showed the highest IgG4 levels, but a comparison of IgG4 levels with all IgG antibodies showed that there was a strong positive correlation. This suggests that vaccination with Moderna's vaccine generally induced higher IgG levels, including IgG4 (Buhre et al., 2023). One explanation for the increasing IgG4 levels could be the amount of the antigen. As mentioned above, Moderna's vaccine has a higher mRNA content than BioNTech's vaccine. Consequently, the vaccine from BioNTech leads to lower IgG4 development. However, not only the amount of antigen seems to be decisive, but also the antigen-specific immune status, as significantly less IgG4 could be detected in pre-infected individuals vaccinated with the BioNTech vaccine (Figure 11B) (Buhre et al., 2023; Kiszel et al., 2023).

The development of high levels of IgG4 antibodies has been described in the context of allergen-specific immunotherapy (AIT), in which IgG4 presumably blocks IgE-mediated effects thorugh allergen masking and crosslinking of an IgE-receptor with the inhibitory receptor FcγRIIb (Akdis & Blaser, 2000; Epp et al., 2018). Furthermore, increasing IgG4 levels have been measured in beekeepers, assuming that IgG4 becomes stronger with repeated antigen encounters (Aalberse et al., 1983).

In the context of vaccination or infection, a potential inhibitory the role of IgG4 has only been investigated in a few studies. Two different vaccine regimens against HIV were compared, both of which were administered repetitively. The RV144 vaccine regimen, which is a heterologous vaccination with a vector-based vaccine followed by a protein vaccine, resulted in IgG1 and IgG3 responses and protection. Instead, vaccination with VAX003, a protein vaccine, resulted in significant amounts of IgG4 responses and less protection (Chung et al., 2014). Depletion of IgG3 in the tested samples led to a significant reduction in further effector functions such as antibody-dependent cellular cytotoxicity (ADCC) and antibody-dependent cellular phagocytosis (ADCP), while depletion of IgG4 antibodies led to increased activation potential (Chung et al., 2014).

Interestingly, COVID-19 infections led to rare IgG4 responses (Lixenfeld et al., 2021; Moura et al., 2021). However, severe disease courses correlated with elevated antigen-specific IgG4 antibodies (Moura et al., 2021). In another study, IgG subclass responses after measles infection were compared with those after vaccination. It was shown that IgG4 appeared in the early phase after infection and remained stable over time. In contrast, vaccine-induced IgG4 responses were lower and declined over time (Isa et al., 2002).

A recent study in nonhuman primates found that after vaccination with Moderna's vaccine, IgG4 responses were comparable to those in humans. In this study, a third vaccination with either an mRNA vaccine or protein vaccine was analyzed, and the frequency of IgG4 antibodies was even higher with the latter than with a homologous mRNA vaccine regimen (58% versus 77%) (Routhu et al., 2023). Despite the large amount of IgG4 antibodies, the researchers reported an even better protection when they challenged the heterologous vaccinated animals (Routhu et al., 2023).

In summary, however, the development, role and protective or inhibitory potential of IgG4 remains controversial and needs further clarification.

For this reason, functional antibody-dependent assays with IgG4-depleted or enriched samples should help to decipher the relevance of emerging IgG4 levels. A first interesting observation was that IgG1, but not IgG4, correlated most strongly with the activation potential in the functional assays (Figure 27). This is consistent with the literature, according to which IgG1 and IgG3 are the subclasses with strong activation activities (Bruhns et al., 2009; Buhre et al., 2022; Lilienthal et al., 2018; Y. Wang et al., 2022). The generally low contribution of IgG4 to the activation potential of serum samples is supported by the observation that only low activation was measured when performing the functional assays with purified IgG4 alone. Further enrichment of the complete sera with purified IgG4 also showed little effects (Figure S5). However, the depletion of IgG4 led to an enhanced activation of NK cells and reduced the activation of neutrophils (Figure 26).

Therefore, IgG1 appears to be the key activator associated with mRNA-induced vaccination. While IgG2 and IgG3 are almost absent over time, the main antibodies that play a role seem to be IgG1 antibodies, which in turn seem to be modulated by IgG4 antibodies in an activating or inhibitory manner.

The inhibitory effect of IgG4 on NK cells appears to be independent of the respective glycosylation profile (Figure 29, Figure S5). IgG4 could inhibit NK cells via FcγRIIb binding, the only classical inhibitory FcγR. However, since only a small subset of NK cells express this receptor (Dutertre et al., 2008), an inhibitory mechanism of IgG4 through FcγRIIb binding is unlikely. In contrast, NK cells express the activating FcγRIIIa (Vivier et al., 2008), and IgG1 and IgG3 in particular have high affinities for these activating receptors (Warncke et al., 2012). Therefore, the inhibitory mechanism of action of IgG4 on NK cells could be via Fc-Fc interactions (Lighaam & Rispens, 2016; Rispens et al., 2009). Alternatively, IgG4 might compete with IgG1 for antigen binding.

Further, inhibitory effects of enzymatically degalactosylated IgG4 on antibody-dependent complement deposition (ADCD) were found (Figure 29, Figure S5), although depletion of IgG4 did not show this effect (Figure 26C). This suggests that the observed inhibitory effects were strongly dependent on the glycosylation form of the IgG4 antibodies. One suspected mechanism by which IgG4 can suppress further immune responses is by interrupting hexamer formation of the activating IgG subclasses. These hexamers are crucial for C1q-binding and thus activation of the classical complement pathway (Cook et al., 2016; De Jong et al., 2016; Diebolder et al., 2014; Lilienthal et al., 2018; Melis et al., 2015; G. Wang et al., 2016). The data suggest that particularly low or agalactosylated IgG4 is a potent inhibitor of ADCD, but this needs to be further investigated.

In contrast to the inhibitory potentials of IgG4, increased antibody-dependent neutrophil phagocytosis (ADNP) was observed. It could be shown that IgG4 depletion reduced ADNP in most long-term samples (Figure 26A). Consistent with this, the addition of enzymatically degalactosylated IgG4 increased ADNP (Figure 29, Figure S5). These observations led assume, that especially low or degalactosylated IgG4 has an activating potential on neutrophils. Neutrophils mainly express the activating FcγRIIa (Y. Wang & Jönsson, 2019), which can also be activated by IgG4 (Bruhns et al., 2009). Low galactosylated antibodies in particular play a role in the context of inflammatory (auto-) immune conditions. In recent literature, IgG4 has been proposed as a contributory cause of IgG4-related inflammatory diseases (Stone et al., 2012). These low galactosylated IgG4 antibodies could therefore be involved in pathogenesis via neutrophil activation.

Taken together, the presented data and the current state of research indicate that IgG4 has a rather complex potential to influence immune reactions, which needs further investigation. IgG4 can exert both inhibitory and activating immunomodulatory functions, which appear to be strongly dependent on cell type and other IgG subclasses. These different modes of action may reflect different phases of the immune response.

The impact of anti-TNF therapy on vaccination responses

Recent studies have shown that TNF inhibition during vaccination leads to a significant reduction in long-term IgG and IgA responses (Geisen, Sümbül, et al., 2021). Furthermore, serum samples from anti-TNF treated patients were found to have reduced virus-neutralizing capacities, and additional flow cytometry analyses revealed that the subjects had a less specific plasma cell response (Geisen et al., 2022). These observations emphasize the involvement of TNF (especially TNFα) in the GC response. By generating TNFα-deficient mice, it could be shown that TNFα does not seem to be crucial for the development of the animals. However, when the mice were confronted with an infection, it was found that their GC and antibody responses were significantly impaired (Pasparakis et al., 1996).

The observations that the long-term antibody responses are significantly reduced under TNF-blockade were replicated, but now the individual IgG subclasses were also examined (Figure 31). When the antibody levels were analyzed over time, several things became clear. Shortly after the second vaccination, IgG1 antibody levels were already reduced, but not IgG3. This indicates that there may be a re-activation of pre-existing IgG1$^+$, but not IgG3$^+$ memory B cells that have developed in a GC-dependent manner. Since IgG3 is the first IgG subclass on the IgG gene locus (Damelang et al., 2019; Horns et al., 2016; Kitaura et al., 2017), these “TNF-independent” IgG3 antibodies may be produced by activation of naïve B cells and newly generated extrafollicular plasma cells. IgG3 antibodies decreased over time in both healthy controls and anti-TNF treated patients, while only healthy controls had a significant increase in IgG3 levels after the third vaccination (Figure 31). This indicates that there is still a certain amount of IgG3$^+$ memory B cells in healthy individuals. Interestingly, almost no IgG4 responses were detectable in the TNF-inhibited group. This once again strengthens the idea that the late-emerging IgG4 antibodies develop in a GC-dependent manner (Irrgang et al., 2023).

The analysis of antigen-specific memory B cells shortly after the second vaccination confirmed the assumption that these cells are re-activated and could contribute significantly to the secreted IgG antibodies. These memory B cells were reduced in TNF-inhibited patients. Moreover, their numbers correlated significantly with IgG antibody levels (Figure 35). It is therefore likely that a significant amount of IgG antibodies is produced by such re-activated memory B cells after the second and third vaccination. This assumption is also supported by the fact that the IgG4 antibodies only appear late after the second vaccination. They increase particularly strongly after the third vaccination, which indicates that both IgG4^{+} long-lived plasma cells and memory B cells develop over time (Figure 31).

There is increasing evidence that early, extrafollicular responses can be characterized by highly galactosylated and sialylated IgG antibodies, which change to lower galactosylated and sialylated levels in the long-term (Bartsch et al., 2020; Buhre et al., 2023). In the vaccinations studied here, IgG Fc galactosylation and sialylation decreased significantly over time, while antigen-specific IgG galactosylation even fell below the respective total IgG levels (Figure 14, Figure 20, Figure 21). In line with these observations, TNF-inhibited patients showed significantly elevated anti-S galactosylation levels in the long-term (Figure 32C). This again suggests that the programming of the low IgG Fc galactosylation and sialylation pattern is facilitated in GC-derived long-lived plasma cells (Bartsch et al., 2020). Subsequently, the IgG glycosylation pattern could serve as a marker of a proper GC-dependent response. Furthermore, TNF blocking in a mouse immunization model showed that already 12 days after vaccination, TNF inhibition alters the antigen-specific IgG1 glycosylation pattern towards higher IgG sialylation and galactosylation levels (Figure 37B). This underlines the idea that TNF-dependent GC reactions already occur after the first immunization.

The consequences of improper short- and long-term antibody responses became even clearer when the samples were analyzed for their potential to activate further effector cells/complement. A lower activation potential of the samples from the TNF-inhibited group was observed for all analyzed time points (Figure 33). Correlation analyses revealed that the main reason for these lower levels was the significantly reduced IgG1 levels in anti-TNF treated patients (Figure 34, Figure S6). This observation supports the previously discussed assumption that the major activator of long-term IgG antibody responses is IgG1. The reduced and altered immune responses showed clear effects on vaccine protection, as confirmed by a real-world data-analysis using TriNetX (Figure 36).

Further characterization of IgG antibody responses shortly before and after a third vaccination revealed that re-activated memory B cells also produce IgG antibodies with similar glycosylation patterns as extrafollicular responses (Figure 39). Finally, a holistic picture of the B cell differentiation and re-activation was obtained, in which the GC dependence was integrated (Figure 40).

Taken together, the TNF-dependent GC reaction seems to be involved in the development of long-lived plasma cell responses, but also in short-term plasma cell responses. These short-term responses presumably dependent on the re-activated TNF-dependent GC-derived memory B cells, which generate short-term IgG antibodies that are highly galactosylated and sialylated.

Conclusion and Outlook

The data presented in this thesis provide a holistic picture of antibody responses after vaccination with the newly developed vaccines against COVID-19. The antibody responses were described by their IgG subclass and Fc glycosylation pattern, both of which have a significant impact on Fc-mediated effector functions. With each vaccination, glycosylation and sialylation levels develop in a wave-like pattern.

Two vaccinations have successfully reduced severe courses after infection and at least short-term antibody responses have protected effectively (Mohammed et al., 2022). Nonetheless, breakthrough infections are common, with individuals who were already infected before vaccination showing better protection (Abu-Raddad et al., 2021; Petráš et al., 2021). The antibody and cell studies presented describe certain differences that could indicate what needs to be considered in future vaccine development.

An interesting finding was the late appearance of IgG4 antibodies after immunization with mRNA vaccines. IgG4 is generally considered an inhibitory subclass and is therefore unexpected in the context of an immunization response against pathogens. However, the data presented do not imply that IgG4 has a strong inhibitory rather than an immunomodulatory effect. Nevertheless, the role of increasing proportion of IgG4 after each booster vaccination needs to be further investigated.

Furthermore, the results presented show that TNF inhibition during vaccination significantly impairs the vaccination outcome and emphasize that adequate GC responses are essential not only for long-term antibody responses, but also for re-activation of GC-derived memory B cells. The data propose that patients treated with anti-TNF may have little benefit from booster vaccinations.

B. References

Aalberse, R. C., van der Gaag, R., & van Leeuwen, J. (1983). Serologic aspects of IgG4 antibodies. I. Prolonged immunization results in an IgG4-restricted response. *Journal of Immunology (Baltimore, Md.: 1950)*, *130*(2), 722–726.

Abu-Raddad, L. J., Chemaitelly, H., Ayoub, H. H., Yassine, H. M., Benslimane, F. M., Al Khatib, H. A., Tang, P., Hasan, M. R., Coyle, P., Al Kanaani, Z., Al Kuwari, E., Jeremijenko, A., Kaleeckal, A. H., Latif, A. N., Shaik, R. M., Abdul Rahim, H. F., Nasrallah, G. K., Al Kuwari, M. G., Butt, A. A., … Bertollini, R. (2021). Association of Prior SARS-CoV-2 Infection With Risk of Breakthrough Infection Following mRNA Vaccination in Qatar. *JAMA*, *326*(19), Article 19. https://doi.org/10.1001/jama.2021.19623

Ackerman, M. E., Crispin, M., Yu, X., Baruah, K., Boesch, A. W., Harvey, D. J., Dugast, A.-S., Heizen, E. L., Ercan, A., Choi, I., Streeck, H., Nigrovic, P. A., Bailey-Kellogg, C., Scanlan, C., & Alter, G. (2013). Natural variation in Fc glycosylation of HIV-specific antibodies impacts antiviral activity. *Journal of Clinical Investigation*, *123*(5), Article 5. https://doi.org/10.1172/JCI65708

Ada, G. (2005). Overview of Vaccines and Vaccination. *Molecular Biotechnology*, *29*(3), 255–272. https://doi.org/10.1385/MB:29:3:255

Adjobimey, T., Meyer, J., Sollberg, L., Bawolt, M., Berens, C., Kovačević, P., Trudić, A., Parcina, M., & Hoerauf, A. (2022). Comparison of IgA, IgG, and Neutralizing Antibody Responses Following Immunization With Moderna, BioNTech, AstraZeneca, Sputnik-V, Johnson and Johnson, and Sinopharm's COVID-19 Vaccines. *Frontiers in Immunology*, *13*, 917905. https://doi.org/10.3389/fimmu.2022.917905

Agematsu, K., Hokibara, S., Nagumo, H., & Komiyama, A. (2000). CD27: A memory B-cell marker. *Immunology Today*, *21*(5), 204–206. https://doi.org/10.1016/S0167-5699(00)01605-4

Ahmed, R., & Gray, D. (1996). Immunological Memory and Protective Immunity: Understanding Their Relation. *Science*, *272*(5258), 54–60. https://doi.org/10.1126/science.272.5258.54

Akdis, C. A., & Blaser, K. (2000). Mechanisms of allergen-specific immunotherapy. *Allergy*, *55*(6), 522–530. https://doi.org/10.1034/j.1398-9995.2000.00120.x

Alter, G., Ottenhoff, T. H. M., & Joosten, S. A. (2018). Antibody glycosylation in inflammation, disease and vaccination. *Seminars in Immunology*, *39*, 102–110. https://doi.org/10.1016/j.smim.2018.05.003

Anderson, R. P., & Jabri, B. (2013). Vaccine against autoimmune disease: Antigen-specific immunotherapy. *Current Opinion in Immunology*, *25*(3), 410–417. https://doi.org/10.1016/j.coi.2013.02.004

Andrisani, G., Frasca, D., Romero, M., Armuzzi, A., Felice, C., Marzo, M., Pugliese, D., Papa, A., Mocci, G., De Vitis, I., Rapaccini, G. L., Blomberg, B. B., & Guidi, L. (2013). Immune response to influenza A/H1N1 vaccine in inflammatory bowel disease patients treated with anti TNF-α agents: Effects of combined therapy with immunosuppressants. *Journal of Crohn's and Colitis*, *7*(4), Article 4. https://doi.org/10.1016/j.crohns.2012.05.011

Anthony, R. M., Kobayashi, T., Wermeling, F., & Ravetch, J. V. (2011). Intravenous gammaglobulin suppresses inflammation through a novel TH2 pathway. *Nature*, *475*(7354), 110–113. https://doi.org/10.1038/nature10134

Arnold, J. N., Wormald, M. R., Sim, R. B., Rudd, P. M., & Dwek, R. A. (2007). The Impact of Glycosylation on the Biological Function and Structure of Human Immunoglobulins. *Annual Review of Immunology*, *25*(1), Article 1. https://doi.org/10.1146/annurev.immunol.25.022106.141702

Baden, L. R., El Sahly, H. M., Essink, B., Kotloff, K., Frey, S., Novak, R., Diemert, D., Spector, S. A., Rouphael, N., Creech, C. B., McGettigan, J., Khetan, S., Segall, N., Solis, J., Brosz, A., Fierro, C., Schwartz, H., Neuzil, K., Corey, L., … Zaks, T. (2021). Efficacy and Safety of the mRNA-1273 SARS-CoV-2 Vaccine. *New England Journal of Medicine*, *384*(5), 403–416. https://doi.org/10.1056/NEJMoa2035389

Banda, N. K., Wood, A. K., Takahashi, K., Levitt, B., Rudd, P. M., Royle, L., Abrahams, J. L., Stahl, G. L., Holers, V. M., & Arend, W. P. (2008). Initiation of the alternative pathway of murine complement by immune complexes is dependent on *N* -glycans in IgG antibodies. *Arthritis & Rheumatism*, *58*(10), 3081–3089. https://doi.org/10.1002/art.23865

Banerjee, S., Phelan, C. P., Reese, B. B., Conroy, M. E., & Anthony, R. M. (2024). Sialylation of IgE does not impact its interaction with FcεRI. *Allergy*, *79*(3), 761–764. https://doi.org/10.1111/all.16014

Bartsch, Y. C., Cizmeci, D., Kang, J., Gao, H., Shi, W., Chandrashekar, A., Collier, A. Y., Chen, B., Barouch, D. H., & Alter, G. (2023). Selective SARS-CoV2 BA.2 escape of antibody Fc/Fc-receptor interactions. *iScience*, *26*(5), Article 5. https://doi.org/10.1016/j.isci.2023.106582

Bartsch, Y. C., Eschweiler, S., Leliavski, A., Lunding, H. B., Wagt, S., Petry, J., Lilienthal, G.-M., Rahmöller, J., de Haan, N., Hölscher, A., Erapaneedi, R., Giannou, A. D., Aly, L., Sato, R., de Neef, L. A., Winkler, A., Braumann, D., Hobusch, J., Kuhnigk, K., … Ehlers, M. (2020). IgG Fc sialylation is regulated during the germinal center reaction following immunization with different adjuvants. *Journal of Allergy and Clinical Immunology*, *146*(3), Article 3. https://doi.org/10.1016/j.jaci.2020.04.059

Bartsch, Y. C., Rahmöller, J., Mertes, M. M. M., Eiglmeier, S., Lorenz, F. K. M., Stoehr, A. D., Braumann, D., Lorenz, A. K., Winkler, A., Lilienthal, G.-M., Petry, J., Hobusch, J., Steinhaus, M., Hess, C., Holecska, V., Schoen, C. T., Oefner, C. M., Leliavski, A., Blanchard, V., & Ehlers, M. (2018). Sialylated Autoantigen-Reactive IgG Antibodies Attenuate Disease Development in Autoimmune Mouse Models of Lupus Nephritis and Rheumatoid Arthritis. *Frontiers in Immunology*, *9*, 1183. https://doi.org/10.3389/fimmu.2018.01183

Bentebibel, S.-E., Lopez, S., Obermoser, G., Schmitt, N., Mueller, C., Harrod, C., Flano, E., Mejias, A., Albrecht, R. A., Blankenship, D., Xu, H., Pascual, V., Banchereau, J., Garcia-Sastre, A., Palucka, A. K., Ramilo, O., & Ueno, H. (2013). Induction of ICOS + CXCR3 + CXCR5 + T H Cells Correlates with Antibody Responses to Influenza Vaccination. *Science Translational Medicine*, *5*(176). https://doi.org/10.1126/scitranslmed.3005191

Boruah, B. M., Kadirvelraj, R., Liu, L., Ramiah, A., Li, C., Zong, G., Bosman, G. P., Yang, J.-Y., Wang, L.-X., Boons, G.-J., Wood, Z. A., & Moremen, K. W. (2020). Characterizing human α-1,6-fucosyltransferase (FUT8) substrate specificity and structural similarities with related fucosyltransferases. *Journal of Biological Chemistry*, *295*(50), Article 50. https://doi.org/10.1074/jbc.RA120.014625

Boudreau, C. M., Burke, J. S., Shuey, K. D., Wolf, C., Katz, J., Tielsch, J., Khatry, S., LeClerq, S. C., Englund, J. A., Chu, H. Y., & Alter, G. (2022). Dissecting Fc signatures of protection in neonates following maternal influenza vaccination in a placebo-controlled trial. *Cell Reports*, *38*(6), Article 6. https://doi.org/10.1016/j.celrep.2022.110337

Boudreau, C. M., Burke, J. S., Yousif, A. S., Sangesland, M., Jastrzebski, S., Verschoor, C., Kuchel, G., Lingwood, D., Kleanthous, H., De Bruijn, I., Landolfi, V., Sridhar, S., & Alter, G. (2023). Antibody-mediated NK cell activation as a correlate of immunity against influenza infection. *Nature Communications*, *14*(1), Article 1. https://doi.org/10.1038/s41467-023-40699-8

Bournazos, S., Vo, H. T. M., Duong, V., Auerswald, H., Ly, S., Sakuntabhai, A., Dussart, P., Cantaert, T., & Ravetch, J. V. (2021). Antibody fucosylation predicts disease severity in secondary dengue infection. *Science*, *372*(6546), Article 6546. https://doi.org/10.1126/science.abc7303

Broder, K., Cortese, M., Iskander, J., Kretsinger, K., Slade, B., Brown, K., Mijalski, C., Tiwari, T., Weston, E., Cohn, A., Srivastava, P., Moran, J., Schwartz, B., & Murphy, T. (2006). *Preventing tetanus, diphtheria, and pertussis among adolescents: Use of tetanus toxoid, reduced diphtheria toxoid and acellular pertussis vaccines recommendations of the Advisory Committee on Immunization Practices (ACIP)*. *55*, 1–34.

Bröker, M., Berti, F., Schneider, J., & Vojtek, I. (2017). Polysaccharide conjugate vaccine protein carriers as a “neglected valency” – Potential and limitations. *Vaccine*, *35*(25), Article 25. https://doi.org/10.1016/j.vaccine.2017.04.078

Bruhns, P., Iannascoli, B., England, P., Mancardi, D. A., Fernandez, N., Jorieux, S., & Daëron, M. (2009). Specificity and affinity of human Fcγ receptors and their polymorphic variants for human IgG subclasses. *Blood*, *113*(16), Article 16. https://doi.org/10.1182/blood-2008-09-179754

Buhre, J. S., Becker, M., & Ehlers, M. (2022). IgG subclass and Fc glycosylation shifts are linked to the transition from pre- to inflammatory autoimmune conditions. *Frontiers in Immunology*, *13*, 1006939. https://doi.org/10.3389/fimmu.2022.1006939

Buhre, J. S., Pongracz, T., Künsting, I., Lixenfeld, A. S., Wang, W., Nouta, J., Lehrian, S., Schmelter, F., Lunding, H. B., Dühring, L., Kern, C., Petry, J., Martin, E. L., Föh, B., Steinhaus, M., von Kopylow, V., Sina, C., Graf, T., Rahmöller, J., … Ehlers, M. (2023). mRNA vaccines against SARS-CoV-2 induce comparably low long-term IgG Fc galactosylation and sialylation levels but increasing long-term IgG4 responses compared to an adenovirus-based vaccine. *Frontiers in Immunology*, *13*, 1020844. https://doi.org/10.3389/fimmu.2022.1020844

Castrodeza-Sanz, J., Sanz-Muñoz, I., & Eiros, J. M. (2023). Adjuvants for COVID-19 Vaccines. *Vaccines*, *11*(5), 902. https://doi.org/10.3390/vaccines11050902

Chakraborty, S., Gonzalez, J. C., Sievers, B. L., Mallajosyula, V., Chakraborty, S., Dubey, M., Ashraf, U., Cheng, B. Y.-L., Kathale, N., Tran, K. Q. T., Scallan, C., Sinnott, A., Cassidy, A., Chen, S. T., Gelbart, T., Gao, F., Golan, Y., Ji, X., Kim-Schulze, S., … Wang, T. T. (2022). Early non-neutralizing, afucosylated antibody responses are associated with COVID-19 severity. *Science Translational Medicine*, *14*(635), eabm7853. https://doi.org/10.1126/scitranslmed.abm7853

Chakraborty, S., Gonzalez, J., Edwards, K., Mallajosyula, V., Buzzanco, A. S., Sherwood, R., Buffone, C., Kathale, N., Providenza, S., Xie, M. M., Andrews, J. R., Blish, C. A., Singh, U., Dugan, H., Wilson, P. C., Pham, T. D., Boyd, S. D., Nadeau, K. C., Pinsky, B. A., … Wang, T. T. (2021). Proinflammatory IgG Fc structures in patients with severe COVID-19. *Nature Immunology*, *22*(1), Article 1. https://doi.org/10.1038/s41590-020-00828-7

Chung, A. W., Ghebremichael, M., Robinson, H., Brown, E., Choi, I., Lane, S., Dugast, A.-S., Schoen, M. K., Rolland, M., Suscovich, T. J., Mahan, A. E., Liao, L., Streeck, H., Andrews, C., Rerks-Ngarm, S., Nitayaphan, S., de Souza, M. S., Kaewkungwal, J., Pitisuttithum, P., … Alter, G. (2014). Polyfunctional Fc-Effector Profiles Mediated by IgG Subclass Selection Distinguish RV144 and VAX003 Vaccines. *Science Translational Medicine*, *6*(228), Article 228. https://doi.org/10.1126/scitranslmed.3007736

Ciotti, M., Ciccozzi, M., Terrinoni, A., Jiang, W.-C., Wang, C.-B., & Bernardini, S. (2020). The COVID-19 pandemic. *Critical Reviews in Clinical Laboratory Sciences*, *57*(6), 365–388. https://doi.org/10.1080/10408363.2020.1783198

Clauder, A.-K., Kordowski, A., Bartsch, Y. C., Köhl, G., Lilienthal, G.-M., Almeida, L. N., Lindemann, T., Petry, J., Rau, C. N., Gramalla-Schmitz, A., Dühring, L., Elbracht, C., Kenno, S., Tillmann, J., Wuhrer, M., Ludwig, R. J., Ibrahim, S. M., Bieber, K., Köhl, J., … Manz, R. A. (2021). IgG Fc N-Glycosylation Translates MHCII Haplotype into Autoimmune Skin Disease. *Journal of Investigative Dermatology*, *141*(2), 285–294. https://doi.org/10.1016/j.jid.2020.06.022

Coffman, R. L., Sher, A., & Seder, R. A. (2010). Vaccine Adjuvants: Putting Innate Immunity to Work. *Immunity*, *33*(4), 492–503. https://doi.org/10.1016/j.immuni.2010.10.002

Collins, E. S., Galligan, M. C., Saldova, R., Adamczyk, B., Abrahams, J. L., Campbell, M. P., Ng, C.-T., Veale, D. J., Murphy, T. B., Rudd, P. M., & FitzGerald, O. (2013). Glycosylation status of serum in inflammatory arthritis in response to anti-TNF treatment. *Rheumatology*, *52*(9), Article 9. https://doi.org/10.1093/rheumatology/ket189

Colucci, M., Stöckmann, H., Butera, A., Masotti, A., Baldassarre, A., Giorda, E., Petrini, S., Rudd, P. M., Sitia, R., Emma, F., & Vivarelli, M. (2015). Sialylation of N-Linked Glycans Influences the Immunomodulatory Effects of IgM on T Cells. *The Journal of Immunology*, *194*(1), 151–157. https://doi.org/10.4049/jimmunol.1402025

Cook, E. M., Lindorfer, M. A., Van Der Horst, H., Oostindie, S., Beurskens, F. J., Schuurman, J., Zent, C. S., Burack, R., Parren, P. W. H. I., & Taylor, R. P. (2016). Antibodies That Efficiently Form Hexamers upon Antigen Binding Can Induce Complement-Dependent Cytotoxicity under Complement-Limiting Conditions. *The Journal of Immunology*, *197*(5), 1762–1775. https://doi.org/10.4049/jimmunol.1600648

Damelang, T., Rogerson, S. J., Kent, S. J., & Chung, A. W. (2019). Role of IgG3 in Infectious Diseases. *Trends in Immunology*, *40*(3), 197–211. https://doi.org/10.1016/j.it.2019.01.005

De Haan, N., Reiding, K. R., Krištić, J., Hipgrave Ederveen, A. L., Lauc, G., & Wuhrer, M. (2017). The N-Glycosylation of Mouse Immunoglobulin G (IgG)-Fragment Crystallizable Differs Between IgG Subclasses and Strains. *Frontiers in Immunology*, *8*, 608. https://doi.org/10.3389/fimmu.2017.00608

De Jong, R. N., Beurskens, F. J., Verploegen, S., Strumane, K., Van Kampen, M. D., Voorhorst, M., Horstman, W., Engelberts, P. J., Oostindie, S. C., Wang, G., Heck, A. J. R., Schuurman, J., & Parren, P. W. H. I. (2016). A Novel Platform for the Potentiation of Therapeutic Antibodies Based on Antigen-Dependent Formation of IgG Hexamers at the Cell Surface. *PLOS Biology*, *14*(1), e1002344. https://doi.org/10.1371/journal.pbio.1002344

de Jong, S. E., Selman, M. H. J., Adegnika, A. A., Amoah, A. S., van Riet, E., Kruize, Y. C. M., Raynes, J. G., Rodriguez, A., Boakye, D., von Mutius, E., Knulst, A. C., Genuneit, J., Cooper, P. J., Hokke, C. H., Wuhrer, M., & Yazdanbakhsh, M. (2016). IgG1 Fc N-glycan galactosylation as a biomarker for immune activation. *Scientific Reports*, *6*(1), 28207. https://doi.org/10.1038/srep28207

Dekkers, G., Rispens, T., & Vidarsson, G. (2018). Novel Concepts of Altered Immunoglobulin G Galactosylation in Autoimmune Diseases. *Frontiers in Immunology*, *9*, 553. https://doi.org/10.3389/fimmu.2018.00553

Dekkers, G., Treffers, L., Plomp, R., Bentlage, A. E. H., De Boer, M., Koeleman, C. A. M., Lissenberg-Thunnissen, S. N., Visser, R., Brouwer, M., Mok, J. Y., Matlung, H., Van Den Berg, T. K., Van Esch, W. J. E., Kuijpers, T. W., Wouters, D., Rispens, T., Wuhrer, M., & Vidarsson, G. (2017). Decoding the Human Immunoglobulin G-Glycan Repertoire Reveals a Spectrum of Fc-

Receptor- and Complement-Mediated-Effector Activities. *Frontiers in Immunology*, *8*, 877. https://doi.org/10.3389/fimmu.2017.00877

Dhama, K., Dhawan, M., Tiwari, R., Emran, T. B., Mitra, S., Rabaan, A. A., Alhumaid, S., Alawi, Z. A., & Al Mutair, A. (2022). COVID-19 intranasal vaccines: Current progress, advantages, prospects, and challenges. *Human Vaccines & Immunotherapeutics*, *18*(5), 2045853. https://doi.org/10.1080/21645515.2022.2045853

Diebolder, C. A., Beurskens, F. J., De Jong, R. N., Koning, R. I., Strumane, K., Lindorfer, M. A., Voorhorst, M., Ugurlar, D., Rosati, S., Heck, A. J. R., Van De Winkel, J. G. J., Wilson, I. A., Koster, A. J., Taylor, R. P., Ollmann Saphire, E., Burton, D. R., Schuurman, J., Gros, P., & Parren, P. W. H. I. (2014). Complement Is Activated by IgG Hexamers Assembled at the Cell Surface. *Science*, *343*(6176), 1260–1263. https://doi.org/10.1126/science.1248943

Doolan, D. L., Dobaño, C., & Baird, J. K. (2009). Acquired Immunity to Malaria. *Clinical Microbiology Reviews*, *22*(1), 13–36. https://doi.org/10.1128/CMR.00025-08

Du, N., Song, L., Li, Y., Wang, T., Fang, Q., Ou, J., & Nandakumar, K. S. (2020). Phytoestrogens protect joints in collagen induced arthritis by increasing IgG glycosylation and reducing osteoclast activation. *International Immunopharmacology*, *83*, 106387. https://doi.org/10.1016/j.intimp.2020.106387

Dühring, L., Petry, J., Lilienthal, G., Bartsch, Y. C., Kubiak, M., Pfeufer, C., Lehrian, S., Buhre, J. S., Lunding, H. B., Kern, C., Behrends, J., Walsemann, T., Gädert, L., Sommer, C., Krüger, L., Blanchard, V., Dehmel, S., Jappe, U., Rahmöller, J., & Ehlers, M. (2023). Sialylation of IGE reduces FCERIA interaction and mast cell and basophil activation in vitro and increases IGE half-life in vivo. *Allergy*, *78*(8), 2301–2305. https://doi.org/10.1111/all.15665

Dutertre, C.-A., Bonnin-Gélizé, E., Pulford, K., Bourel, D., Fridman, W.-H., & Teillaud, J.-L. (2008). A novel subset of NK cells expressing high levels of inhibitory FcγRIIB modulating antibody-dependent function. *Journal of Leukocyte Biology*, *84*(6), 1511–1520. https://doi.org/10.1189/jlb.0608343

Elkayam, O. (2004). The Effect of tumor necrosis factor blockade on the response to pneumococcal vaccination in patients with rheumatoid arthritis and ankylosing spondylitis. *Seminars in Arthritis and Rheumatism*, *33*(4), Article 4. https://doi.org/10.1053/j.semarthrit.2003.10.003

Engdahl, C., Bondt, A., Harre, U., Raufer, J., Pfeifle, R., Camponeschi, A., Wuhrer, M., Seeling, M., Mårtensson, I.-L., Nimmerjahn, F., Krönke, G., Scherer, H. U., Forsblad-d'Elia, H., & Schett, G. (2018). Estrogen induces St6gal1 expression and increases IgG sialylation in mice and patients with rheumatoid arthritis: A potential explanation for the increased risk of rheumatoid arthritis in postmenopausal women. *Arthritis Research & Therapy*, *20*(1), Article 1. https://doi.org/10.1186/s13075-018-1586-z

Epp, A., Hobusch, J., Bartsch, Y. C., Petry, J., Lilienthal, G.-M., Koeleman, C. A. M., Eschweiler, S., Möbs, C., Hall, A., Morris, S. C., Braumann, D., Engellenner, C., Bitterling, J., Rahmöller, J., Leliavski, A., Thurmann, R., Collin, M., Moremen, K. W., Strait, R. T., … Ehlers, M. (2018). Sialylation of IgG antibodies inhibits IgG-mediated allergic reactions. *Journal of Allergy and Clinical Immunology*, *141*(1), Article 1. https://doi.org/10.1016/j.jaci.2017.06.021

Ercan, A., Cui, J., Chatterton, D. E. W., Deane, K. D., Hazen, M. M., Brintnell, W., O'Donnell, C. I., Derber, L. A., Weinblatt, M. E., Shadick, N. A., Bell, D. A., Cairns, E., Solomon, D. H., Holers, V. M., Rudd, P. M., & Lee, D. M. (2010). Aberrant IgG galactosylation precedes disease onset, correlates with disease activity, and is prevalent in autoantibodies in rheumatoid arthritis. *Arthritis & Rheumatism*, *62*(8), 2239–2248. https://doi.org/10.1002/art.27533

Ercan, A., Kohrt, W. M., Cui, J., Deane, K. D., Pezer, M., Yu, E. W., Hausmann, J. S., Campbell, H., Kaiser, U. B., Rudd, P. M., Lauc, G., Wilson, J. F., Finkelstein, J. S., & Nigrovic, P. A. (2017). Estrogens regulate glycosylation of IgG in women and men. *JCI Insight*, *2*(4), Article 4. https://doi.org/10.1172/jci.insight.89703

Fang, E., Liu, X., Li, M., Zhang, Z., Song, L., Zhu, B., Wu, X., Liu, J., Zhao, D., & Li, Y. (2022). Advances in COVID-19 mRNA vaccine development. *Signal Transduction and Targeted Therapy*, *7*(1), 94. https://doi.org/10.1038/s41392-022-00950-y

Ferrara, C., Grau, S., Jäger, C., Sondermann, P., Brünker, P., Waldhauer, I., Hennig, M., Ruf, A., Rufer, A. C., Stihle, M., Umaña, P., & Benz, J. (2011). Unique carbohydrate–carbohydrate interactions are required for high affinity binding between FcγRIII and antibodies lacking core fucose. *Proceedings of the National Academy of Sciences*, *108*(31), Article 31. https://doi.org/10.1073/pnas.1108455108

Firouzabadi, N., Ghasemiyeh, P., Moradishooli, F., & Mohammadi-Samani, S. (2023). Update on the effectiveness of COVID-19 vaccines on different variants of SARS-CoV-2. *International Immunopharmacology*, *117*, 109968. https://doi.org/10.1016/j.intimp.2023.109968

Firth, M. A., Shewen, P. E., & Hodgins, D. C. (2005). Passive and active components of neonatal innate immune defenses. *Animal Health Research Reviews*, *6*(2), 143–158. https://doi.org/10.1079/AHR2005107

Flemming, A. (2018). Uncovering the mystery of secreted IgD. *Nature Reviews Immunology*, *18*(11), 668–669. https://doi.org/10.1038/s41577-018-0080-9

Flevaris, K., & Kontoravdi, C. (2022). Immunoglobulin G N-glycan Biomarkers for Autoimmune Diseases: Current State and a Glycoinformatics Perspective. *International Journal of Molecular Sciences*, *23*(9), Article 9. https://doi.org/10.3390/ijms23095180

Fokkink, W.-J. R., Selman, M. H. J., Dortland, J. R., Durmuş, B., Kuitwaard, K., Huizinga, R., van Rijs, W., Tio-Gillen, A. P., van Doorn, P. A., Deelder, A.

M., Wuhrer, M., & Jacobs, B. C. (2014). IgG Fc N-Glycosylation in Guillain–Barré Syndrome Treated with Immunoglobulins. *Journal of Proteome Research*, *13*(3), Article 3. https://doi.org/10.1021/pr401213z

Freund, J., Casals, J., & Hosmer, E. P. (1937). Sensitization and Antibody Formation after Injection of Tubercle Bacilli and Paraffin Oil. *Experimental Biology and Medicine*, *37*(3), 509–513. https://doi.org/10.3181/00379727-37-9625

Gehlhar, Schlaak, Becker, & Bufe. (1999). Monitoring allergen immunotherapy of pollen-allergic patients: The ratio of allergen-specific IgG4 to IgG1 correlates with clinical outcome. *Clinical & Experimental Allergy*, *29*(4), Article 4. https://doi.org/10.1046/j.1365-2222.1999.00525.x

Geisen, U. M., Berner, D. K., Tran, F., Sümbül, M., Vullriede, L., Ciripoi, M., Reid, H. M., Schaffarzyk, A., Longardt, A. C., Franzenburg, J., Hoff, P., Schirmer, J. H., Zeuner, R., Friedrichs, A., Steinbach, A., Knies, C., Markewitz, R. D., Morrison, P. J., Gerdes, S., … Hoyer, B. F. (2021). Immunogenicity and safety of anti-SARS-CoV-2 mRNA vaccines in patients with chronic inflammatory conditions and immunosuppressive therapy in a monocentric cohort. *Annals of the Rheumatic Diseases*, *80*(10), Article 10. https://doi.org/10.1136/annrheumdis-2021-220272

Geisen, U. M., Rose, R., Neumann, F., Ciripoi, M., Vullriede, L., Reid, H. M., Berner, D. K., Bertoglio, F., Hoff, P., Hust, M., Longardt, A. C., Lorentz, T., Martini, G. R., Saggau, C., Schirmer, J. H., Schubert, M., Sümbül, M., Tran, F., Voß, M., … Hoyer, B. F. (2022). The long term vaccine-induced anti-SARS-CoV-2 immune response is impaired in quantity and quality under TNFα blockade. *Journal of Medical Virology*, *94*(12), 5780–5789. https://doi.org/10.1002/jmv.28063

Geisen, U. M., Sümbül, M., Tran, F., Berner, D. K., Reid, H. M., Vullriede, L., Ciripoi, M., Longardt, A. C., Hoff, P., Morrison, P. J., Schneider, V. E., Zeuner, R., Schirmer, J. H., Steinbach, A., Nikolaus, S., Gerdes, S., Schreiber, S., Bacher, P., & Hoyer, B. F. (2021). Humoral protection to SARS-CoV2 declines faster in patients on TNF alpha blocking therapies. *RMD Open*, *7*(3), e002008. https://doi.org/10.1136/rmdopen-2021-002008

Glenny, A. T., Pope, C. G., Waddington, H., & Wallace, U. (1926). Immunological notes. Xvii–xxiv. *J Pathol Bacteriol*, *29.1*, 31–40.

Golovkin, A., Kalinina, O., Bezrukikh, V., Aquino, A., Zaikova, E., Karonova, T., Melnik, O., Vasilieva, E., & Kudryavtsev, I. (2021). Imbalanced Immune Response of T-Cell and B-Cell Subsets in Patients with Moderate and Severe COVID-19. *Viruses*, *13*(10), 1966. https://doi.org/10.3390/v13101966

Greinacher, A., Thiele, T., Warkentin, T. E., Weisser, K., Kyrle, P. A., & Eichinger, S. (2021). Thrombotic Thrombocytopenia after ChAdOx1 nCov-19 Vaccination. *New England Journal of Medicine*, *384*(22), 2092–2101. https://doi.org/10.1056/NEJMoa2104840

Greto, V. L., Cvetko, A., Štambuk, T., Dempster, N. J., Kifer, D., Deriš, H., Cindrić, A., Vučković, F., Falchi, M., Gillies, R. S., Tomlinson, J. W., Gornik, O., Sgromo, B., Spector, T. D., Menni, C., Geremia, A., Arancibia-Cárcamo, C. V., & Lauc, G. (2021). Extensive weight loss reduces glycan age by altering IgG N-glycosylation. *International Journal of Obesity*, *45*(7), Article 7. https://doi.org/10.1038/s41366-021-00816-3

Haddad, G., Lorenzen, J. M., Ma, H., de Haan, N., Seeger, H., Zaghrini, C., Brandt, S., Kölling, M., Wegmann, U., Kiss, B., Pál, G., Gál, P., Wüthrich, R. P., Wuhrer, M., Beck, L. H., Salant, D. J., Lambeau, G., & Kistler, A. D. (2021). Altered glycosylation of IgG4 promotes lectin complement pathway activation in anti-PLA2R1–associated membranous nephropathy. *Journal of Clinical Investigation*, *131*(5), e140453. https://doi.org/10.1172/JCI140453

Hammers, C. M., Bieber, K., Kalies, K., Banczyk, D., Ellebrecht, C. T., Ibrahim, S. M., Zillikens, D., Ludwig, R. J., & Westermann, J. (2011). Complement-Fixing Anti-Type VII Collagen Antibodies Are Induced in Th1-Polarized Lymph Nodes of Epidermolysis Bullosa Acquisita-Susceptible Mice. *The Journal of Immunology*, *187*(10), 5043–5050. https://doi.org/10.4049/jimmunol.1100796

Hartley, G. E., Fryer, H. A., Gill, P. A., Boo, I., Bornheimer, S. J., Hogarth, P. M., Drummer, H. E., O'Hehir, R. E., Edwards, E. S. J., & Van Zelm, M. C. (2023). *Third dose COVID-19 mRNA vaccine enhances IgG4 isotype switching and recognition of Omicron subvariants by memory B cells after mRNA but not adenovirus priming* [Preprint]. Immunology. https://doi.org/10.1101/2023.09.15.557929

Havenar-Daughton, C., Lindqvist, M., Heit, A., Wu, J. E., Reiss, S. M., Kendric, K., Bélanger, S., Kasturi, S. P., Landais, E., Akondy, R. S., McGuire, H. M., Bothwell, M., Vagefi, P. A., Scully, E., IAVI Protocol C Principal Investigators, Tomaras, G. D., Davis, M. M., Poignard, P., Ahmed, R., … Inambao, M. (2016). CXCL13 is a plasma biomarker of germinal center activity. *Proceedings of the National Academy of Sciences*, *113*(10), 2702–2707. https://doi.org/10.1073/pnas.1520112113

Heinz, F. X., & Stiasny, K. (2021). Distinguishing features of current COVID-19 vaccines: Knowns and unknowns of antigen presentation and modes of action. *Npj Vaccines*, *6*(1), 104. https://doi.org/10.1038/s41541-021-00369-6

Hess, C., Winkler, A., Lorenz, A. K., Holecska, V., Blanchard, V., Eiglmeier, S., Schoen, A.-L., Bitterling, J., Stoehr, A. D., Petzold, D., Schommartz, T., Mertes, M. M. M., Schoen, C. T., Tiburzy, B., Herrmann, A., Köhl, J., Manz, R. A., Madaio, M. P., Berger, M., … Ehlers, M. (2013). T cell–independent B cell activation induces immunosuppressive sialylated IgG antibodies. *Journal of Clinical Investigation*, *123*(9), Article 9. https://doi.org/10.1172/JCI65938

Hoepel, W., Chen, H.-J., Geyer, C. E., Allahverdiyeva, S., Manz, X. D., de Taeye, S. W., Aman, J., Mes, L., Steenhuis, M., Griffith, G. R., Bonta, P. I., Brouwer,

P. J. M., Caniels, T. G., van der Straten, K., Golebski, K., Jonkers, R. E., Larsen, M. D., Linty, F., Nouta, J., … den Dunnen, J. (2021). High titers and low fucosylation of early human anti–SARS-CoV-2 IgG promote inflammation by alveolar macrophages. *Science Translational Medicine*, *13*(596), Article 596. https://doi.org/10.1126/scitranslmed.abf8654

Horns, F., Vollmers, C., Croote, D., Mackey, S. F., Swan, G. E., Dekker, C. L., Davis, M. M., & Quake, S. R. (2016). Lineage tracing of human B cells reveals the in vivo landscape of human antibody class switching. *eLife*, *5*, e16578. https://doi.org/10.7554/eLife.16578

Irrgang, P., Gerling, J., Kocher, K., Lapuente, D., Steininger, P., Habenicht, K., Wytopil, M., Beileke, S., Schäfer, S., Zhong, J., Ssebyatika, G., Krey, T., Falcone, V., Schülein, C., Peter, A. S., Nganou-Makamdop, K., Hengel, H., Held, J., Bogdan, C., … Tenbusch, M. (2023). Class switch toward noninflammatory, spike-specific IgG4 antibodies after repeated SARS-CoV-2 mRNA vaccination. *Science Immunology*, *8*(79), Article 79. https://doi.org/10.1126/sciimmunol.ade2798

Isa, M. B., Martínez, L., Giordano, M., Passeggi, C., De Wolff, M. C., & Nates, S. (2002). Comparison of Immunoglobulin G Subclass Profiles Induced by Measles Virus in Vaccinated and Naturally Infected Individuals. *Clinical and Vaccine Immunology*, *9*(3), 693–697. https://doi.org/10.1128/CDLI.9.3.693-697.2002

Ito, K., Furukawa, J., Yamada, K., Tran, N. L., Shinohara, Y., & Izui, S. (2014). Lack of Galactosylation Enhances the Pathogenic Activity of IgG1 but Not IgG2a Anti-Erythrocyte Autoantibodies. *The Journal of Immunology*, *192*(2), Article 2. https://doi.org/10.4049/jimmunol.1302488

Iwasaki, A. (2016). Exploiting Mucosal Immunity for Antiviral Vaccines. *Annual Review of Immunology*, *34*(1), 575–608. https://doi.org/10.1146/annurev-immunol-032414-112315

Iwasaki, A., & Medzhitov, R. (2010). Regulation of Adaptive Immunity by the Innate Immune System. *Science*, *327*(5963), 291–295. https://doi.org/10.1126/science.1183021

Jackson, L. A. (1999). Safety of Revaccination With Pneumococcal Polysaccharide Vaccine. *JAMA*, *281*(3), 243. https://doi.org/10.1001/jama.281.3.243

Jazayeri, M. H., Pourfathollah, A. A., Rasaee, M. J., Porpak, Z., & Jafari, M. E. (2013). The concentration of total serum IgG and IgM in sera of healthy individuals varies at different age intervals. *Biomedicine & Aging Pathology*, *3*(4), Article 4. https://doi.org/10.1016/j.biomag.2013.09.002

Jennewein, M. F., Goldfarb, I., Dolatshahi, S., Cosgrove, C., Noelette, F. J., Krykbaeva, M., Das, J., Sarkar, A., Gorman, M. J., Fischinger, S., Boudreau, C. M., Brown, J., Cooperrider, J. H., Aneja, J., Suscovich, T. J., Graham, B. S., Lauer, G. M., Goetghebuer, T., Marchant, A., … Alter, G. (2019). Fc Glycan-Mediated Regulation of Placental Antibody Transfer. *Cell*, *178*(1), Article 1. https://doi.org/10.1016/j.cell.2019.05.044

Jensen-Jarolim, E., Roth-Walter, F., Jordakieva, G., & Pali-Schöll, I. (2021). Allergens and Adjuvants in Allergen Immunotherapy for Immune Activation, Tolerance, and Resilience. *The Journal of Allergy and Clinical Immunology: In Practice*, *9*(5), Article 5. https://doi.org/10.1016/j.jaip.2020.12.008

Jung, J., Choe, J., Li, L., & Choi, Y. S. (2000). Regulation of CD27 expression in the course of germinal center B cell differentiation: The pivotal role of IL-10. *European Journal of Immunology*, *30*(8), 2437–2443. https://doi.org/10.1002/1521-4141(2000)30:8<2437::AID-IMMU2437>3.0.CO;2-M

Kaneko, Y., Nimmerjahn, F., & Ravetch, J. V. (2006). Anti-Inflammatory Activity of Immunoglobulin G Resulting from Fc Sialylation. *Science*, *313*(5787), Article 5787. https://doi.org/10.1126/science.1129594

Kapur, R., Della Valle, L., Sonneveld, M., Hipgrave Ederveen, A., Visser, R., Ligthart, P., De Haas, M., Wuhrer, M., Van Der Schoot, C. E., & Vidarsson, G. (2014). Low anti- R h D I g G - F c-fucosylation in pregnancy: A new variable predicting severity in haemolytic disease of the fetus and newborn. *British Journal of Haematology*, *166*(6), 936–945. https://doi.org/10.1111/bjh.12965

Karsten, C. M., Pandey, M. K., Figge, J., Kilchenstein, R., Taylor, P. R., Rosas, M., McDonald, J. U., Orr, S. J., Berger, M., Petzold, D., Blanchard, V., Winkler, A., Hess, C., Reid, D. M., Majoul, I. V., Strait, R. T., Harris, N. L., Köhl, G., Wex, E., … Köhl, J. (2012). Anti-inflammatory activity of IgG1 mediated by Fc galactosylation and association of FcγRIIB and dectin-1. *Nature Medicine*, *18*(9), Article 9. https://doi.org/10.1038/nm.2862

Kasperkiewicz, M., Vorobyev, A., Bieber, K., Kridin, K., & Ludwig, R. J. (2023). Risk of comorbid autoimmune diseases in patients with immunobullous disorders: A global large-scale cohort study. *Journal of the American Academy of Dermatology*, *89*(6), 1269–1271. https://doi.org/10.1016/j.jaad.2023.07.1030

Katz, S. L., Enders, J. F., & Holloway, A. (1962). The Development and Evaluation of an Attenuated Measles Virus Vaccine. *American Journal of Public Health and the Nations Health*, *52*(Suppl_2), 5–10. https://doi.org/10.2105/AJPH.52.Suppl_2.5

Katz-Agranov, N., Khattri, S., & Zandman-Goddard, G. (2015). The role of intravenous immunoglobulins in the treatment of rheumatoid arthritis. *Autoimmunity Reviews*, *14*(8), Article 8. https://doi.org/10.1016/j.autrev.2015.04.003

Kaur, S. P., & Gupta, V. (2020). COVID-19 Vaccine: A comprehensive status report. *Virus Research*, *288*, 198114. https://doi.org/10.1016/j.virusres.2020.198114

Kavran, J. M., & Leahy, D. J. (2014). Coupling Antibody to Cyanogen Bromide-Activated Sepharose. In *Methods in Enzymology* (Vol. 541, pp. 27–34). Elsevier. https://doi.org/10.1016/B978-0-12-420119-4.00003-3

Kawasaki, Y., Suzuki, J., Sakai, N., Isome, M., Nozawa, R., Tanji, M., & Suzuki, H. (2004). Evaluation of T helper-1/-2 balance on the basis of IgG subclasses and serum cytokines in children with glomerulonephritis. *American Journal of Kidney Diseases*, *44*(1), 42–49. https://doi.org/10.1053/j.ajkd.2004.03.029

Keyt, B. A., Baliga, R., Sinclair, A. M., Carroll, S. F., & Peterson, M. S. (2020). Structure, Function, and Therapeutic Use of IgM Antibodies. *Antibodies*, *9*(4), 53. https://doi.org/10.3390/antib9040053

Kiszel, P., Sík, P., Miklós, J., Kajdácsi, E., Sinkovits, G., Cervenak, L., & Prohászka, Z. (2023). Class switch towards spike protein-specific IgG4 antibodies after SARS-CoV-2 mRNA vaccination depends on prior infection history. *Scientific Reports*, *13*(1), Article 1. https://doi.org/10.1038/s41598-023-40103-x

Kitaura, K., Yamashita, H., Ayabe, H., Shini, T., Matsutani, T., & Suzuki, R. (2017). Different Somatic Hypermutation Levels among Antibody Subclasses Disclosed by a New Next-Generation Sequencing-Based Antibody Repertoire Analysis. *Frontiers in Immunology*, *8*, 389. https://doi.org/10.3389/fimmu.2017.00389

Kleiveland, C. R. (2015). Peripheral Blood Mononuclear Cells. In K. Verhoeckx, P. Cotter, I. López-Expósito, C. Kleiveland, T. Lea, A. Mackie, T. Requena, D. Swiatecka, & H. Wichers (Eds.), *The Impact of Food Bioactives on Health* (pp. 161–167). Springer International Publishing. https://doi.org/10.1007/978-3-319-16104-4_15

Kool, M., Fierens, K., & Lambrecht, B. N. (2012). Alum adjuvant: Some of the tricks of the oldest adjuvant. *Journal of Medical Microbiology*, *61*(7), 927–934. https://doi.org/10.1099/jmm.0.038943-0

Kräutler, N. J., Suan, D., Butt, D., Bourne, K., Hermes, J. R., Chan, T. D., Sundling, C., Kaplan, W., Schofield, P., Jackson, J., Basten, A., Christ, D., & Brink, R. (2017). Differentiation of germinal center B cells into plasma cells is initiated by high-affinity antigen and completed by Tfh cells. *Journal of Experimental Medicine*, *214*(5), 1259–1267. https://doi.org/10.1084/jem.20161533

Kreiter, S., Diken, M., Selmi, A., Türeci, Ö., & Sahin, U. (2011). Tumor vaccination using messenger RNA: Prospects of a future therapy. *Current Opinion in Immunology*, *23*(3), 399–406. https://doi.org/10.1016/j.coi.2011.03.007

Kridin, K., & Ludwig, R. J. (2023). Isotretinoin and the risk of psychiatric disturbances: A global study shedding new light on a debatable story. *Journal of the American Academy of Dermatology*, *88*(2), 388–394. https://doi.org/10.1016/j.jaad.2022.10.031

Kurosaki, T., Kometani, K., & Ise, W. (2015). Memory B cells. *Nature Reviews Immunology*, *15*(3), 149–159. https://doi.org/10.1038/nri3802

Labrijn, A. F., Buijsse, A. O., Van Den Bremer, E. T. J., Verwilligen, A. Y. W., Bleeker, W. K., Thorpe, S. J., Killestein, J., Polman, C. H., Aalberse, R. C., Schuurman, J., Van De Winkel, J. G. J., & Parren, P. W. H. I. (2009). Therapeutic IgG4 antibodies engage in Fab-arm exchange with endogenous human IgG4 in vivo. *Nature Biotechnology*, *27*(8), 767–771. https://doi.org/10.1038/nbt.1553

Laczkó, D., Hogan, M. J., Toulmin, S. A., Hicks, P., Lederer, K., Gaudette, B. T., Castaño, D., Amanat, F., Muramatsu, H., Oguin, T. H., Ojha, A., Zhang, L., Mu, Z., Parks, R., Manzoni, T. B., Roper, B., Strohmeier, S., Tombácz, I., Arwood, L., … Pardi, N. (2020). A Single Immunization with Nucleoside-Modified mRNA Vaccines Elicits Strong Cellular and Humoral Immune Responses against SARS-CoV-2 in Mice. *Immunity*, *53*(4), 724-732.e7. https://doi.org/10.1016/j.immuni.2020.07.019

Larché, M., Akdis, C. A., & Valenta, R. (2006). Immunological mechanisms of allergen-specific immunotherapy. *Nature Reviews Immunology*, *6*(10), 761–771. https://doi.org/10.1038/nri1934

Larsen, M. D., Lopez-Perez, M., Dickson, E. K., Ampomah, P., Tuikue Ndam, N., Nouta, J., Koeleman, C. A. M., Ederveen, A. L. H., Mordmüller, B., Salanti, A., Nielsen, M. A., Massougbodji, A., van der Schoot, C. E., Ofori, M. F., Wuhrer, M., Hviid, L., & Vidarsson, G. (2021). Afucosylated Plasmodium falciparum-specific IgG is induced by infection but not by subunit vaccination. *Nature Communications*, *12*(1), Article 1. https://doi.org/10.1038/s41467-021-26118-w

Lauc, G., Huffman, J. E., Pučić, M., Zgaga, L., Adamczyk, B., Mužinić, A., Novokmet, M., Polašek, O., Gornik, O., Krištić, J., Keser, T., Vitart, V., Scheijen, B., Uh, H.-W., Molokhia, M., Patrick, A. L., McKeigue, P., Kolčić, I., Lukić, I. K., … Rudan, I. (2013). Loci Associated with N-Glycosylation of Human Immunoglobulin G Show Pleiotropy with Autoimmune Diseases and Haematological Cancers. *PLoS Genetics*, *9*(1), Article 1. https://doi.org/10.1371/journal.pgen.1003225

Lederer, K., Bettini, E., Parvathaneni, K., Painter, M. M., Agarwal, D., Lundgreen, K. A., Weirick, M., Muralidharan, K., Castaño, D., Goel, R. R., Xu, X., Drapeau, E. M., Gouma, S., Ort, J. T., Awofolaju, M., Greenplate, A. R., Le Coz, C., Romberg, N., Trofe-Clark, J., … Locci, M. (2022). Germinal center responses to SARS-CoV-2 mRNA vaccines in healthy and immunocompromised individuals. *Cell*, *185*(6), Article 6. https://doi.org/10.1016/j.cell.2022.01.027

Lederer, K., Castaño, D., Gómez Atria, D., Oguin, T. H., Wang, S., Manzoni, T. B., Muramatsu, H., Hogan, M. J., Amanat, F., Cherubin, P., Lundgreen, K. A., Tam, Y. K., Fan, S. H. Y., Eisenlohr, L. C., Maillard, I., Weissman, D., Bates, P., Krammer, F., Sempowski, G. D., … Locci, M. (2020). SARS-CoV-2 mRNA Vaccines Foster Potent Antigen-Specific Germinal Center Responses Associated with Neutralizing Antibody Generation. *Immunity*, *53*(6), Article 6. https://doi.org/10.1016/j.immuni.2020.11.009

Levast, B., Awate, S., Babiuk, L., Mutwiri, G., Gerdts, V., & Van Drunen Littel-van Den Hurk, S. (2014). Vaccine Potentiation by Combination Adjuvants. *Vaccines*, *2*(2), 297–322. https://doi.org/10.3390/vaccines2020297

Lighaam, L., & Rispens, T. (2016). The Immunobiology of Immunoglobulin G4. *Seminars in Liver Disease*, *36*(03), Article 03. https://doi.org/10.1055/s-0036-1584322

Lilienthal, G.-M., Rahmöller, J., Petry, J., Bartsch, Y. C., Leliavski, A., & Ehlers, M. (2018). Potential of Murine IgG1 and Human IgG4 to Inhibit the Classical Complement and Fcγ Receptor Activation Pathways. *Frontiers in Immunology*, *9*, 958. https://doi.org/10.3389/fimmu.2018.00958

Linares-Fernández, S., Lacroix, C., Exposito, J.-Y., & Verrier, B. (2020). Tailoring mRNA Vaccine to Balance Innate/Adaptive Immune Response. *Trends in Molecular Medicine*, *26*(3), Article 3. https://doi.org/10.1016/j.molmed.2019.10.002

Liu, D., Chu, X., Wang, H., Dong, J., Ge, S.-Q., Zhao, Z.-Y., Peng, H.-L., Sun, M., Wu, L.-J., Song, M.-S., Guo, X.-H., Meng, Q., Wang, Y.-X., Lauc, G., & Wang, W. (2018). The changes of immunoglobulin G N-glycosylation in blood lipids and dyslipidaemia. *Journal of Translational Medicine*, *16*(1), Article 1. https://doi.org/10.1186/s12967-018-1616-2

Lixenfeld, A. S., Künsting, I., Martin, E. L., Kopylow, V. von, Lehrian, S., Lunding, H. B., Buhre, J. S., Quack, J., Steinhaus, M., Graf, T., Ehlers, M., & Rahmöller, J. (2021). *The BioNTech / Pfizer vaccine BNT162b2 induces class-switched SARS-CoV-2-specific plasma cells and potential memory B cells as well as IgG and IgA serum and IgG saliva antibodies upon the first immunization* [Preprint]. Infectious Diseases (except HIV/AIDS). https://doi.org/10.1101/2021.03.10.21252001

Lofano, G., Gorman, M. J., Yousif, A. S., Yu, W.-H., Fox, J. M., Dugast, A.-S., Ackerman, M. E., Suscovich, T. J., Weiner, J., Barouch, D., Streeck, H., Little, S., Smith, D., Richman, D., Lauffenburger, D., Walker, B. D., Diamond, M. S., & Alter, G. (2018). Antigen-specific antibody Fc glycosylation enhances humoral immunity via the recruitment of complement. *Science Immunology*, *3*(26), Article 26. https://doi.org/10.1126/sciimmunol.aat7796

Lu, L. L., Chung, A. W., Rosebrock, T. R., Ghebremichael, M., Yu, W. H., Grace, P. S., Schoen, M. K., Tafesse, F., Martin, C., Leung, V., Mahan, A. E., Sips, M., Kumar, M. P., Tedesco, J., Robinson, H., Tkachenko, E., Draghi, M., Freedberg, K. J., Streeck, H., … Alter, G. (2016). A Functional Role for Antibodies in Tuberculosis. *Cell*, *167*(2), 433-443.e14. https://doi.org/10.1016/j.cell.2016.08.072

Malhotra, R., Wormald, M. R., Rudd, P. M., Fischer, P. B., Dwek, R. A., & Sim, R. B. (1995). Glycosylation changes of IgG associated with rheumatooid arthritis can activate complement via the mannose-binding protein. *Nature Medicine*, *1*(3), 237–243. https://doi.org/10.1038/nm0395-237

Manz, R. A., Hauser, A. E., Hiepe, F., & Radbruch, A. (2005). MAINTENANCE OF SERUM ANTIBODY LEVELS. *Annual Review of Immunology*, *23*(1), 367–386. https://doi.org/10.1146/annurev.immunol.23.021704.115723

Manz, R. A., Thiel, A., & Radbruch, A. (1997). Lifetime of plasma cells in the bone marrow. *Nature*, *388*(6638), Article 6638. https://doi.org/10.1038/40540

Martonik, D., Parfieniuk-Kowerda, A., Rogalska, M., & Flisiak, R. (2021). The Role of Th17 Response in COVID-19. *Cells*, *10*(6), 1550. https://doi.org/10.3390/cells10061550

McMichael, A. J. (2006). HIV VACCINES. *Annual Review of Immunology*, *24*(1), 227–255. https://doi.org/10.1146/annurev.immunol.24.021605.090605

Melchers, F. (2015). Checkpoints that control B cell development. *Journal of Clinical Investigation*, *125*(6), 2203–2210. https://doi.org/10.1172/JCI78083

Melis, J. P. M., Strumane, K., Ruuls, S. R., Beurskens, F. J., Schuurman, J., & Parren, P. W. H. I. (2015). Complement in therapy and disease. *Molecular Immunology*, *67*(2), 117–130. https://doi.org/10.1016/j.molimm.2015.01.028

Meng, L., Forouhar, F., Thieker, D., Gao, Z., Ramiah, A., Moniz, H., Xiang, Y., Seetharaman, J., Milaninia, S., Su, M., Bridger, R., Veillon, L., Azadi, P., Kornhaber, G., Wells, L., Montelione, G. T., Woods, R. J., Tong, L., & Moremen, K. W. (2013). Enzymatic Basis for N-Glycan Sialylation. *Journal of Biological Chemistry*, *288*(48), 34680–34698. https://doi.org/10.1074/jbc.M113.519041

Mesin, L., Ersching, J., & Victora, G. D. (2016). Germinal Center B Cell Dynamics. *Immunity*, *45*(3), 471–482. https://doi.org/10.1016/j.immuni.2016.09.001

Modlin, J. F., Jabbour, J. T., Witte, J. J., & Halsey, N. A. (1977). Epidemiologic Studies of Measles, Measles Vaccine, and Subacute Sclerosing Panencephalitis. *Pediatrics*, *59*(4), 505–512. https://doi.org/10.1542/peds.59.4.505

Mohammed, I., Nauman, A., Paul, P., Ganesan, S., Chen, K.-H., Jalil, S. M. S., Jaouni, S. H., Kawas, H., Khan, W. A., Vattoth, A. L., Al-Hashimi, Y. A., Fares, A., Zeghlache, R., & Zakaria, D. (2022). The efficacy and effectiveness of the COVID-19 vaccines in reducing infection, severity, hospitalization, and mortality: A systematic review. *Human Vaccines & Immunotherapeutics*, *18*(1), 2027160. https://doi.org/10.1080/21645515.2022.2027160

Mond, J. J., Lees, A., & Snapper, C. M. (1995). T Cell-Independent Antigens Type 2. *Annual Review of Immunology*, *13*(1), 655–692. https://doi.org/10.1146/annurev.iy.13.040195.003255

Moremen, K. W., Tiemeyer, M., & Nairn, A. V. (2012). Vertebrate protein glycosylation: Diversity, synthesis and function. *Nature Reviews Molecular Cell Biology*, *13*(7), 448–462. https://doi.org/10.1038/nrm3383

Moura, A. D., Da Costa, H. H. M., Correa, V. A., De S. Lima, A. K., Lindoso, J. A. L., De Gaspari, E., Hong, M. A., Cunha-Junior, J. P., & Prudencio, C. R. (2021). Assessment of avidity related to IgG subclasses in SARS-CoV-2 Brazilian infected patients. *Scientific Reports*, *11*(1), 17642. https://doi.org/10.1038/s41598-021-95045-z

Muecksch, F., Wang, Z., Cho, A., Gaebler, C., Ben Tanfous, T., DaSilva, J., Bednarski, E., Ramos, V., Zong, S., Johnson, B., Raspe, R., Schaefer-Babajew, D., Shimeliovich, I., Daga, M., Yao, K.-H., Schmidt, F., Millard, K. G., Turroja, M., Jankovic, M., … Nussenzweig, M. C. (2022). Increased memory B cell potency and breadth after a SARS-CoV-2 mRNA boost. *Nature*, *607*(7917), 128–134. https://doi.org/10.1038/s41586-022-04778-y

Mufson, E. J., Presley, L. N., & Kordower, J. H. (1991). Nerve growth factor receptor immunoreactivity within the nucleus basalis (Ch4) in Parkinson's disease: Reduced cell numbers and co-localization with cholinergic neurons. *Brain Research*, *539*(1), 19–30. https://doi.org/10.1016/0006-8993(91)90682-L

Murphy, K. P., Janeway, C., Travers, P., Walport, M., Mowat, A., & Weaver, C. P. (2012). *Janeway's immunobiology.* (8th ed.). Garland Science.

Nikolac Perkovic, M., Pucic Bakovic, M., Kristic, J., Novokmet, M., Huffman, J. E., Vitart, V., Hayward, C., Rudan, I., Wilson, J. F., Campbell, H., Polasek, O., Lauc, G., & Pivac, N. (2014). The association between galactosylation of immunoglobulin G and body mass index. *Progress in Neuro-Psychopharmacology and Biological Psychiatry*, *48*, 20–25. https://doi.org/10.1016/j.pnpbp.2013.08.014

Nimmerjahn, F., & Ravetch, J. V. (2005). Divergent Immunoglobulin G Subclass Activity Through Selective Fc Receptor Binding. *Science*, *310*(5753), Article 5753. https://doi.org/10.1126/science.1118948

Nimmerjahn, F., & Ravetch, J. V. (2008a). Anti-Inflammatory Actions of Intravenous Immunoglobulin. *Annual Review of Immunology*, *26*(1), 513–533. https://doi.org/10.1146/annurev.immunol.26.021607.090232

Nimmerjahn, F., & Ravetch, J. V. (2008b). Fcγ receptors as regulators of immune responses. *Nature Reviews Immunology*, *8*(1), 34–47. https://doi.org/10.1038/nri2206

Nimmerjahn, F., Vidarsson, G., & Cragg, M. S. (2023). Effect of posttranslational modifications and subclass on IgG activity: From immunity to immunotherapy. *Nature Immunology*, *24*(8), 1244–1255. https://doi.org/10.1038/s41590-023-01544-8

Oefner, C. M., Winkler, A., Hess, C., Lorenz, A. K., Holecska, V., Huxdorf, M., Schommartz, T., Petzold, D., Bitterling, J., Schoen, A.-L., Stoehr, A. D., Vu Van, D., Darcan-Nikolaisen, Y., Blanchard, V., Schmudde, I., Laumonnier, Y., Ströver, H. A., Hegazy, A. N., Eiglmeier, S., … Ehlers, M. (2012). Tolerance induction with T cell–dependent protein antigens induces regulatory sialylated IgGs. *Journal of Allergy and Clinical Immunology*, *129*(6), Article 6. https://doi.org/10.1016/j.jaci.2012.02.037

Ogata, S., Shimizu, C., Franco, A., Touma, R., Kanegaye, J. T., Choudhury, B. P., Naidu, N. N., Kanda, Y., Hoang, L. T., Hibberd, M. L., Tremoulet, A. H., Varki, A., & Burns, J. C. (2013). Treatment Response in Kawasaki Disease Is Associated with Sialylation Levels of Endogenous but Not Therapeutic

Intravenous Immunoglobulin G. *PLoS ONE*, *8*(12), Article 12. https://doi.org/10.1371/journal.pone.0081448

Ohmi, Y., Ise, W., Harazono, A., Takakura, D., Fukuyama, H., Baba, Y., Narazaki, M., Shoda, H., Takahashi, N., Ohkawa, Y., Ji, S., Sugiyama, F., Fujio, K., Kumanogoh, A., Yamamoto, K., Kawasaki, N., Kurosaki, T., Takahashi, Y., & Furukawa, K. (2016). Sialylation converts arthritogenic IgG into inhibitors of collagen-induced arthritis. *Nature Communications*, *7*(1), 11205. https://doi.org/10.1038/ncomms11205

Oliver, S. E., Gargano, J. W., Marin, M., Wallace, M., Curran, K. G., Chamberland, M., McClung, N., Campos-Outcalt, D., Morgan, R. L., Mbaeyi, S., Romero, J. R., Talbot, H. K., Lee, G. M., Bell, B. P., & Dooling, K. (2020). The Advisory Committee on Immunization Practices' Interim Recommendation for Use of Pfizer-BioNTech COVID-19 Vaccine—United States, December 2020. *MMWR. Morbidity and Mortality Weekly Report*, *69*(50), 1922–1924. https://doi.org/10.15585/mmwr.mm6950e2

Oskam, N., Damelang, T., Streutker, M., Ooijevaar-de Heer, P., Nouta, J., Koeleman, C., Van Coillie, J., Wuhrer, M., Vidarsson, G., & Rispens, T. (2023). Factors affecting IgG4-mediated complement activation. *Frontiers in Immunology*, *14*, 1087532. https://doi.org/10.3389/fimmu.2023.1087532

Pallikkuth, S., Parmigiani, A., Silva, S. Y., George, V. K., Fischl, M., Pahwa, R., & Pahwa, S. (2012). Impaired peripheral blood T-follicular helper cell function in HIV-infected nonresponders to the 2009 H1N1/09 vaccine. *Blood*, *120*(5), 985–993. https://doi.org/10.1182/blood-2011-12-396648

Pantaleo, G., & Fauci, A. S. (1996). IMMUNOPATHOGENESIS OF HIV INFECTION. *Annual Review of Microbiology*, *50*(1), Article 1. https://doi.org/10.1146/annurev.micro.50.1.825

Parekh, R. B., Dwek, R. A., Sutton, B. J., Fernandes, D. L., Leung, A., Stanworth, D., Rademacher, T. W., Mizuochi, T., Taniguchi, T., Matsuta, K., Takeuchi, F., Nagano, Y., Miyamoto, T., & Kobata, A. (1985). Association of rheumatoid arthritis and primary osteoarthritis with changes in the glycosylation pattern of total serum IgG. *Nature*, *316*(6027), 452–457. https://doi.org/10.1038/316452a0

Pasparakis, M., Alexopoulou, L., Episkopou, V., & Kollias, G. (1996). Immune and inflammatory responses in TNF alpha-deficient mice: A critical requirement for TNF alpha in the formation of primary B cell follicles, follicular dendritic cell networks and germinal centers, and in the maturation of the humoral immune response. *Journal of Experimental Medicine*, *184*(4), Article 4. https://doi.org/10.1084/jem.184.4.1397

Pasquale, A., Preiss, S., Silva, F., & Garçon, N. (2015). Vaccine Adjuvants: From 1920 to 2015 and Beyond. *Vaccines*, *3*(2), 320–343. https://doi.org/10.3390/vaccines3020320

Paus, D., Phan, T. G., Chan, T. D., Gardam, S., Basten, A., & Brink, R. (2006). Antigen recognition strength regulates the choice between extrafollicular plasma cell and germinal center B cell differentiation. *The Journal of*

Experimental Medicine, *203*(4), 1081–1091. https://doi.org/10.1084/jem.20060087

Petráš, M., Lesná, I. K., Večeřová, L., Nyčová, E., Malinová, J., Klézl, P., Nezvedová, M., White, R. E., Máčalík, R., Dáňová, J., Čelko, A. M., & Adámková, V. (2021). The Effectiveness of Post-Vaccination and Post-Infection Protection in the Hospital Staff of Three Prague Hospitals: A Cohort Study of 8-Month Follow-Up from the Start of the COVID-19 Vaccination Campaign (COVANESS). *Vaccines*, *10*(1), Article 1. https://doi.org/10.3390/vaccines10010009

Petrovsky, N., & Aguilar, J. C. (2004). Vaccine adjuvants: Current state and future trends. *Immunology & Cell Biology*, *82*(5), 488–496. https://doi.org/10.1111/j.0818-9641.2004.01272.x

Petry, J., Rahmöller, J., Dühring, L., Lilienthal, G.-M., Lehrian, S., Buhre, J. S., Bartsch, Y. C., Epp, A., Lunding, H. B., Moremen, K. W., Leliavski, A., & Ehlers, M. (2021). Enriched blood IgG sialylation attenuates IgG-mediated and IgG-controlled-IgE-mediated allergic reactions. *Journal of Allergy and Clinical Immunology*, *147*(2), Article 2. https://doi.org/10.1016/j.jaci.2020.05.056

Pfeifle, R., Rothe, T., Ipseiz, N., Scherer, H. U., Culemann, S., Harre, U., Ackermann, J. A., Seefried, M., Kleyer, A., Uderhardt, S., Haugg, B., Hueber, A. J., Daum, P., Heidkamp, G. F., Ge, C., Böhm, S., Lux, A., Schuh, W., Magorivska, I., … Krönke, G. (2017). Regulation of autoantibody activity by the IL-23–TH17 axis determines the onset of autoimmune disease. *Nature Immunology*, *18*(1), Article 1. https://doi.org/10.1038/ni.3579

Pieper, K., Grimbacher, B., & Eibel, H. (2013). B-cell biology and development. *Journal of Allergy and Clinical Immunology*, *131*(4), 959–971. https://doi.org/10.1016/j.jaci.2013.01.046

Pietrzak, B., Tomela, K., Olejnik-Schmidt, A., Mackiewicz, A., & Schmidt, M. (2020). Secretory IgA in Intestinal Mucosal Secretions as an Adaptive Barrier against Microbial Cells. *International Journal of Molecular Sciences*, *21*(23), 9254. https://doi.org/10.3390/ijms21239254

Pilkington, C., Yeung, E., Isenberg, D., Lefvert, A. K., & Rook, G. A. W. (1995). Agalactosyl IgG and Antibody Specificity in Rheumatoid Arthritis, Tuberculosis, Systemic Lupus Erythematosus and Myasthenia Gravis. *Autoimmunity*, *22*(2), Article 2. https://doi.org/10.3109/08916939508995306

Pillai, S. (2023). Is it bad, is it good, or is IgG4 just misunderstood? *Science Immunology*, eadg7327. https://doi.org/10.1126/sciimmunol.adg7327

Pilzecker, B., & Jacobs, H. (2019). Mutating for Good: DNA Damage Responses During Somatic Hypermutation. *Frontiers in Immunology*, *10*, 438. https://doi.org/10.3389/fimmu.2019.00438

Pincetic, A., Bournazos, S., DiLillo, D. J., Maamary, J., Wang, T. T., Dahan, R., Fiebiger, B.-M., & Ravetch, J. V. (2014). Type I and type II Fc receptors regulate innate and adaptive immunity. *Nature Immunology*, *15*(8), 707–716. https://doi.org/10.1038/ni.2939

Plotkin, S. A. (2005). Vaccines: Past, present and future. *Nature Medicine*, *11*(S4), S5–S11. https://doi.org/10.1038/nm1209

Plotkin, S. A. (2010). Correlates of Protection Induced by Vaccination. *Clinical and Vaccine Immunology*, *17*(7), 1055–1065. https://doi.org/10.1128/CVI.00131-10

Polack, F. P., Thomas, S. J., Kitchin, N., Absalon, J., Gurtman, A., Lockhart, S., Perez, J. L., Pérez Marc, G., Moreira, E. D., Zerbini, C., Bailey, R., Swanson, K. A., Roychoudhury, S., Koury, K., Li, P., Kalina, W. V., Cooper, D., Frenck, R. W., Hammitt, L. L., … Gruber, W. C. (2020). Safety and Efficacy of the BNT162b2 mRNA Covid-19 Vaccine. *New England Journal of Medicine*, *383*(27), Article 27. https://doi.org/10.1056/NEJMoa2034577

Pongracz, T., Nouta, J., Wang, W., van Meijgaarden, K. E., Linty, F., Vidarsson, G., Joosten, S. A., Ottenhoff, T. H. M., Hokke, C. H., de Vries, J. J. C., Arbous, S. M., Roukens, A. H. E., & Wuhrer, M. (2022). Immunoglobulin G1 Fc glycosylation as an early hallmark of severe COVID-19. *eBioMedicine*, *78*, 103957. https://doi.org/10.1016/j.ebiom.2022.103957

Porter, R. R. (1973). Structural Studies of Immunoglobulins. *Science*, *180*(4087), 713–716. https://doi.org/10.1126/science.180.4087.713

Pozzetto, B., Legros, V., Djebali, S., Barateau, V., Guibert, N., Villard, M., Peyrot, L., Allatif, O., Fassier, J.-B., Massardier-Pilonchéry, A., Brengel-Pesce, K., Yaugel-Novoa, M., Denolly, S., Boson, B., Bourlet, T., Bal, A., Valette, M., Andrieu, T., Lina, B., … Trouillet-Assant, S. (2021). Immunogenicity and efficacy of heterologous ChAdOx1–BNT162b2 vaccination. *Nature*, *600*(7890), 701–706. https://doi.org/10.1038/s41586-021-04120-y

Pulendran, B., S. Arunachalam, P., & O'Hagan, D. T. (2021). Emerging concepts in the science of vaccine adjuvants. *Nature Reviews Drug Discovery*, *20*(6), Article 6. https://doi.org/10.1038/s41573-021-00163-y

Quast, I., Keller, C. W., Maurer, M. A., Giddens, J. P., Tackenberg, B., Wang, L.-X., Münz, C., Nimmerjahn, F., Dalakas, M. C., & Lünemann, J. D. (2015). Sialylation of IgG Fc domain impairs complement-dependent cytotoxicity. *Journal of Clinical Investigation*, *125*(11), 4160–4170. https://doi.org/10.1172/JCI82695

Rashid, A., Rasheed, K., Asim, M., & Hussain, A. (2009). Risks of vaccination: A review. *Journal of Venomous Animals and Toxins Including Tropical Diseases*, *15*(1). https://doi.org/10.1590/S1678-91992009000100003

Rashid, H., Khandaker, G., & Booy, R. (2012). Vaccination and herd immunity: What more do we know? *Current Opinion in Infectious Diseases*, *25*(3), 243–249. https://doi.org/10.1097/QCO.0b013e328352f727

Ray, S. K., Putterman, C., & Diamond, B. (1996). Pathogenic autoantibodies are routinely generated during the response to foreign antigen: A paradigm for autoimmune disease. *Proceedings of the National Academy of Sciences*, *93*(5), 2019–2024. https://doi.org/10.1073/pnas.93.5.2019

Riedel, S. (2005). Edward Jenner and the History of Smallpox and Vaccination. *Baylor University Medical Center Proceedings*, *18*(1), 21–25. https://doi.org/10.1080/08998280.2005.11928028

Rispens, T., & Huijbers, M. G. (2023). The unique properties of IgG4 and its roles in health and disease. *Nature Reviews Immunology*, *23*(11), 763–778. https://doi.org/10.1038/s41577-023-00871-z

Rispens, T., Ooievaar-De Heer, P., Vermeulen, E., Schuurman, J., Van Der Neut Kolfschoten, M., & Aalberse, R. C. (2009). Human IgG4 Binds to IgG4 and Conformationally Altered IgG1 via Fc-Fc Interactions. *The Journal of Immunology*, *182*(7), 4275–4281. https://doi.org/10.4049/jimmunol.0804338

Roco, J. A., Mesin, L., Binder, S. C., Nefzger, C., Gonzalez-Figueroa, P., Canete, P. F., Ellyard, J., Shen, Q., Robert, P. A., Cappello, J., Vohra, H., Zhang, Y., Nowosad, C. R., Schiepers, A., Corcoran, L. M., Toellner, K.-M., Polo, J. M., Meyer-Hermann, M., Victora, G. D., & Vinuesa, C. G. (2019). Class-Switch Recombination Occurs Infrequently in Germinal Centers. *Immunity*, *51*(2), 337-350.e7. https://doi.org/10.1016/j.immuni.2019.07.001

Röltgen, K., Nielsen, S. C. A., Silva, O., Younes, S. F., Zaslavsky, M., Costales, C., Yang, F., Wirz, O. F., Solis, D., Hoh, R. A., Wang, A., Arunachalam, P. S., Colburg, D., Zhao, S., Haraguchi, E., Lee, A. S., Shah, M. M., Manohar, M., Chang, I., … Boyd, S. D. (2022). Immune imprinting, breadth of variant recognition, and germinal center response in human SARS-CoV-2 infection and vaccination. *Cell*, *185*(6), 1025-1040.e14. https://doi.org/10.1016/j.cell.2022.01.018

Rook, G. A. W., Steele, J., Brealey, R., Whyte, A., Isenberg, D., Sumar, N., Nelson, J. L., Bodman, K. B., Young, A., Roitt, I. M., Williams, P., Scragg, I., Edge, C. J., Arkwright, P. D., Ashford, D., Wormald, M., Rudd, P., Redman, C. W. G., Dwek, R. A., & Rademacher, T. W. (1991). Changes in IgG glycoform levels are associated with remission of arthritis during pregnancy. *Journal of Autoimmunity*, *4*(5), Article 5. https://doi.org/10.1016/0896-8411(91)90173-A

Routhu, N. K., Stampfer, S. D., Lai, L., Akhtar, A., Tong, X., Yuan, D., Chicz, T. M., McNamara, R. P., Jakkala, K., Davis-Gardner, M. E., St Pierre, E. L., Smith, B., Green, K. M., Golden, N., Picou, B., Jean, S. M., Wood, J., Cohen, J., Moore, I. N., … Amara, R. R. (2023). Efficacy of mRNA-1273 and Novavax ancestral or BA.1 spike booster vaccines against SARS-CoV-2 BA.5 infection in nonhuman primates. *Science Immunology*, *8*(88), eadg7015. https://doi.org/10.1126/sciimmunol.adg7015

Saenz-Badillos, J., Amin, S. P., & Granstein, R. D. (2001). RNA as a tumor vaccine: A review of the literature. *Experimental Dermatology*, *10*(3), 143–154. https://doi.org/10.1034/j.1600-0625.2001.010003143.x

Sahin, U., Muik, A., Derhovanessian, E., Vogler, I., Kranz, L. M., Vormehr, M., Baum, A., Pascal, K., Quandt, J., Maurus, D., Brachtendorf, S., Lörks, V., Sikorski, J., Hilker, R., Becker, D., Eller, A.-K., Grützner, J., Boesler, C., Rosenbaum, C., … Türeci, Ö. (2020). COVID-19 vaccine BNT162b1 elicits human antibody and TH1 T cell responses. *Nature*, *586*(7830), 594–599. https://doi.org/10.1038/s41586-020-2814-7

Scherer, H. U., Van Der Woude, D., Ioan-Facsinay, A., El Bannoudi, H., Trouw, L. A., Wang, J., Häupl, T., Burmester, G., Deelder, A. M., Huizinga, T. W. J., Wuhrer, M., & Toes, R. E. M. (2010). Glycan profiling of anti–citrullinated protein antibodies isolated from human serum and synovial fluid. *Arthritis & Rheumatism*, *62*(6), 1620–1629. https://doi.org/10.1002/art.27414

Schroeder, H. W., & Cavacini, L. (2010). Structure and function of immunoglobulins. *Journal of Allergy and Clinical Immunology*, *125*(2), S41–S52. https://doi.org/10.1016/j.jaci.2009.09.046

Selman, M. H. J., Derks, R. J. E., Bondt, A., Palmblad, M., Schoenmaker, B., Koeleman, C. A. M., Van De Geijn, F. E., Dolhain, R. J. E. M., Deelder, A. M., & Wuhrer, M. (2012). Fc specific IgG glycosylation profiling by robust nano-reverse phase HPLC-MS using a sheath-flow ESI sprayer interface. *Journal of Proteomics*, *75*(4), 1318–1329. https://doi.org/10.1016/j.jprot.2011.11.003

Shade, K.-T., & Anthony, R. (2013). Antibody Glycosylation and Inflammation. *Antibodies*, *2*(4), Article 4. https://doi.org/10.3390/antib2030392

Shade, K.-T. C., Conroy, M. E., Washburn, N., Kitaoka, M., Huynh, D. J., Laprise, E., Patil, S. U., Shreffler, W. G., & Anthony, R. M. (2020). Sialylation of immunoglobulin E is a determinant of allergic pathogenicity. *Nature*, *582*(7811), 265–270. https://doi.org/10.1038/s41586-020-2311-z

Sharif-Askari, F. S., Sharif-Askari, N. S., Hafezi, S., Mdkhana, B., Alsayed, H. A. H., Ansari, A. W., Mahboub, B., Zakeri, A. M., Temsah, M.-H., Zahir, W., Hamid, Q., & Halwani, R. (2022). Interleukin-17, a salivary biomarker for COVID-19 severity. *PLOS ONE*, *17*(9), e0274841. https://doi.org/10.1371/journal.pone.0274841

Shay, D. K., Gee, J., Su, J. R., Myers, T. R., Marquez, P., Liu, R., Zhang, B., Licata, C., Clark, T. A., & Shimabukuro, T. T. (2021). Safety Monitoring of the Janssen (Johnson & Johnson) COVID-19 Vaccine—United States, March–April 2021. *MMWR. Morbidity and Mortality Weekly Report*, *70*(18), 680–684. https://doi.org/10.15585/mmwr.mm7018e2

Shields, R. L., Lai, J., Keck, R., O'Connell, L. Y., Hong, K., Meng, Y. G., Weikert, S. H. A., & Presta, L. G. (2002). Lack of Fucose on Human IgG1 N-Linked Oligosaccharide Improves Binding to Human FcγRIII and Antibody-dependent Cellular Toxicity. *Journal of Biological Chemistry*, *277*(30), Article 30. https://doi.org/10.1074/jbc.M202069200

Shlomchik, M. J., Luo, W., & Weisel, F. (2019). Linking signaling and selection in the germinal center. *Immunological Reviews*, *288*(1), 49–63. https://doi.org/10.1111/imr.12744

Snapper, C. M., Finkelman, F. D., & Paul, W. E. (1988). Regulation of IgG1 and IgE Production by Interleukin 4. *Immunological Reviews*, *102*(1), Article 1. https://doi.org/10.1111/j.1600-065X.1988.tb00741.x

Snapper, C. M., McIntyre, T. M., Mandler, R., Pecanha, L. M., Finkelman, F. D., Lees, A., & Mond, J. J. (1992). Induction of IgG3 secretion by interferon gamma: A model for T cell-independent class switching in response to T cell-independent type 2 antigens. *The Journal of Experimental Medicine*, *175*(5), Article 5. https://doi.org/10.1084/jem.175.5.1367

Soni, D., Van Haren, S. D., Idoko, O. T., Evans, J. T., Diray-Arce, J., Dowling, D. J., & Levy, O. (2020). Towards Precision Vaccines: Lessons From the Second International Precision Vaccines Conference. *Frontiers in Immunology*, *11*, 590373. https://doi.org/10.3389/fimmu.2020.590373

Stebegg, M., Kumar, S. D., Silva-Cayetano, A., Fonseca, V. R., Linterman, M. A., & Graca, L. (2018). Regulation of the Germinal Center Response. *Frontiers in Immunology*, *9*, 2469. https://doi.org/10.3389/fimmu.2018.02469

Steffen, U., Koeleman, C. A., Sokolova, M. V., Bang, H., Kleyer, A., Rech, J., Unterweger, H., Schicht, M., Garreis, F., Hahn, J., Andes, F. T., Hartmann, F., Hahn, M., Mahajan, A., Paulsen, F., Hoffmann, M., Lochnit, G., Muñoz, L. E., Wuhrer, M., … Schett, G. (2020). IgA subclasses have different effector functions associated with distinct glycosylation profiles. *Nature Communications*, *11*(1), 120. https://doi.org/10.1038/s41467-019-13992-8

Stoliaroff-Pepin, A., Peine, C., Herath, T., Lachmann, J., Hellenbrand, W., Perriat, D., Dörre, A., Nitsche, A., Michel, J., Grossegesse, M., Hofmann, N., Rinner, T., Kohl, C., Brinkmann, A., Meyer, T., Stern, D., Treindl, F., Dorner, B. G., Hein, S., … Harder, T. (2023). Vaccine effectiveness against severe COVID-19 during the Omicron wave in Germany: Results from the COViK study. *Infection*, *51*(4), 1093–1102. https://doi.org/10.1007/s15010-023-02012-z

Stone, J. H., Zen, Y., & Deshpande, V. (2012). IgG4-Related Disease. *New England Journal of Medicine*, *366*(6), Article 6. https://doi.org/10.1056/NEJMra1104650

Strait, R. T., Posgai, M. T., Mahler, A., Barasa, N., Jacob, C. O., Köhl, J., Ehlers, M., Stringer, K., Shanmukhappa, S. K., Witte, D., Hossain, M. M., Khodoun, M., Herr, A. B., & Finkelman, F. D. (2015). IgG1 protects against renal disease in a mouse model of cryoglobulinaemia. *Nature*, *517*(7535), 501–504. https://doi.org/10.1038/nature13868

Swanson, P. A., Padilla, M., Hoyland, W., McGlinchey, K., Fields, P. A., Bibi, S., Faust, S. N., McDermott, A. B., Lambe, T., Pollard, A. J., Durham, N. M., Kelly, E. J., & AstraZeneca/Oxford/VRC Study Group. (2021). AZD1222/ChAdOx1 nCoV-19 vaccination induces a polyfunctional spike protein–specific T $_H$ 1 response with a diverse TCR repertoire. *Science Translational Medicine*, *13*(620), Article 620. https://doi.org/10.1126/scitranslmed.abj7211

Tan, M. (2021). Norovirus Vaccines: Current Clinical Development and Challenges. *Pathogens*, *10*(12), 1641. https://doi.org/10.3390/pathogens10121641

Tang, J., Zeng, C., Cox, T. M., Li, C., Son, Y. M., Cheon, I. S., Wu, Y., Behl, S., Taylor, J. J., Chakaraborty, R., Johnson, A. J., Shiavo, D. N., Utz, J. P., Reisenauer, J. S., Midthun, D. E., Mullon, J. J., Edell, E. S., Alameh, M. G., Borish, L., … Sun, J. (2022). Respiratory mucosal immunity against SARS-CoV-2 after mRNA vaccination. *Science Immunology*, *7*(76), eadd4853. https://doi.org/10.1126/sciimmunol.add4853

Tangye, S. G., Liu, Y.-J., Aversa, G., Phillips, J. H., & De Vries, J. E. (1998). Identification of Functional Human Splenic Memory B Cells by Expression of CD148 and CD27. *The Journal of Experimental Medicine*, *188*(9), 1691–1703. https://doi.org/10.1084/jem.188.9.1691

Tao, M. H., & Morrison, S. L. (1989). Studies of aglycosylated chimeric mouse-human IgG. Role of carbohydrate in the structure and effector functions mediated by the human IgG constant region. *The Journal of Immunology*, *143*(8), 2595–2601. https://doi.org/10.4049/jimmunol.143.8.2595

Teijaro, J. R., & Farber, D. L. (2021). COVID-19 vaccines: Modes of immune activation and future challenges. *Nature Reviews Immunology*, *21*(4), 195–197. https://doi.org/10.1038/s41577-021-00526-x

Toellner, K.-M., Luther, S. A., Sze, D. M.-Y., Choy, R. K.-W., Taylor, D. R., MacLennan, I. C. M., & Acha-Orbea, H. (1998). T Helper 1 (Th1) and Th2 Characteristics Start to Develop During T Cell Priming and Are Associated with an Immediate Ability to Induce Immunoglobulin Class Switching. *The Journal of Experimental Medicine*, *187*(8), 1193–1204. https://doi.org/10.1084/jem.187.8.1193

Turner, J. S., Kim, W., Kalaidina, E., Goss, C. W., Rauseo, A. M., Schmitz, A. J., Hansen, L., Haile, A., Klebert, M. K., Pusic, I., O'Halloran, J. A., Presti, R. M., & Ellebedy, A. H. (2021). SARS-CoV-2 infection induces long-lived bone marrow plasma cells in humans. *Nature*, *595*(7867), 421–425. https://doi.org/10.1038/s41586-021-03647-4

Vaccari, M., Gordon, S. N., Fourati, S., Schifanella, L., Liyanage, N. P. M., Cameron, M., Keele, B. F., Shen, X., Tomaras, G. D., Billings, E., Rao, M., Chung, A. W., Dowell, K. G., Bailey-Kellogg, C., Brown, E. P., Ackerman, M. E., Vargas-Inchaustegui, D. A., Whitney, S., Doster, M. N., … Franchini, G. (2016). Erratum: Corrigendum: Adjuvant-dependent innate and adaptive immune signatures of risk of SIVmac251 acquisition. *Nature Medicine*, *22*(10), Article 10. https://doi.org/10.1038/nm1016-1192a

van Behring, E., & Kitasato, S. (1890). The mechanism of immunity in animals to diphtheria and tetanus. *Deutsche Medizinsche Wochenschrift*, *16:1113–4*.

Van Coillie, J., Pongracz, T., Rahmöller, J., Chen, H.-J., Geyer, C. E., van Vught, L. A., Buhre, J. S., Šuštić, T., van Osch, T. L. J., Steenhuis, M., Hoepel, W., Wang, W., Lixenfeld, A. S., Nouta, J., Keijzer, S., Linty, F., Visser, R., Larsen, M. D., Martin, E. L., … Wiersinga, J. W. (2023). The BNT162b2 mRNA SARS-CoV-2 vaccine induces transient afucosylated IgG1 in naive but not in antigen-experienced vaccinees. *eBioMedicine*, *87*, 104408. https://doi.org/10.1016/j.ebiom.2022.104408 van de Geijn, F. E., Wuhrer, M., Selman, M. H., Willemsen, S. P., de Man, Y. A., Deelder, A. M., Hazes, J. M., & Dolhain, R. J. (2009). Immunoglobulin G galactosylation and sialylation are associated with pregnancy-induced improvement of rheumatoid arthritis and the postpartum flare: Results from a large prospective cohort study. *Arthritis Research & Therapy*, *11*(6), Article 6. https://doi.org/10.1186/ar2892

van der Neut Kolfschoten, M., Schuurman, J., Losen, M., Bleeker, W. K., Martínez-Martínez, P., Vermeulen, E., den Bleker, T. H., Wiegman, L., Vink, T., Aarden, L. A., De Baets, M. H., van de Winkel, J. G. J., Aalberse, R. C., & Parren, P. W. H. I. (2007). Anti-Inflammatory Activity of Human IgG4 Antibodies by Dynamic Fab Arm Exchange. *Science*, *317*(5844), Article 5844. https://doi.org/10.1126/science.1144603

van Osch, T. L. J., Nouta, J., Derksen, N. I. L., van Mierlo, G., van der Schoot, C. E., Wuhrer, M., Rispens, T., & Vidarsson, G. (2021). Fc Galactosylation Promotes Hexamerization of Human IgG1, Leading to Enhanced Classical Complement Activation. *The Journal of Immunology*, *207*(6), 1545–1554. https://doi.org/10.4049/jimmunol.2100399

Vella, L. A., Buggert, M., Manne, S., Herati, R. S., Sayin, I., Kuri-Cervantes, L., Bukh Brody, I., O'Boyle, K. C., Kaprielian, H., Giles, J. R., Nguyen, S., Muselman, A., Antel, J. P., Bar-Or, A., Johnson, M. E., Canaday, D. H., Naji, A., Ganusov, V. V., Laufer, T. M., … Wherry, E. J. (2019). T follicular helper cells in human efferent lymph retain lymphoid characteristics. *Journal of Clinical Investigation*, *129*(8), 3185–3200. https://doi.org/10.1172/JCI125628

Victora, G. D., & Nussenzweig, M. C. (2022). Germinal Centers. *Annual Review of Immunology*, *40*(1), 413–442. https://doi.org/10.1146/annurev-immunol-120419-022408

Victora, G. D., Schwickert, T. A., Fooksman, D. R., Kamphorst, A. O., Meyer-Hermann, M., Dustin, M. L., & Nussenzweig, M. C. (2010). Germinal Center Dynamics Revealed by Multiphoton Microscopy with a Photoactivatable Fluorescent Reporter. *Cell*, *143*(4), 592–605. https://doi.org/10.1016/j.cell.2010.10.032

Vidarsson, G., Dekkers, G., & Rispens, T. (2014). IgG Subclasses and Allotypes: From Structure to Effector Functions. *Frontiers in Immunology*, *5*. https://doi.org/10.3389/fimmu.2014.00520

Vivier, E., Tomasello, E., Baratin, M., Walzer, T., & Ugolini, S. (2008). Functions of natural killer cells. *Nature Immunology*, *9*(5), 503–510. https://doi.org/10.1038/ni1582

Voysey, M., Clemens, S. A. C., Madhi, S. A., Weckx, L. Y., Folegatti, P. M., Aley, P. K., Angus, B., Baillie, V. L., Barnabas, S. L., Bhorat, Q. E., Bibi, S., Briner, C., Cicconi, P., Collins, A. M., Colin-Jones, R., Cutland, C. L., Darton, T. C., Dheda, K., Duncan, C. J. A., … Zuidewind, P. (2021). Safety and efficacy of the ChAdOx1 nCoV-19 vaccine (AZD1222) against SARS-CoV-2: An interim analysis of four randomised controlled trials in Brazil, South Africa, and the UK. *The Lancet*, *397*(10269), 99–111. https://doi.org/10.1016/S0140-6736(20)32661-1

Wahl, A., Van Den Akker, E., Klaric, L., Štambuk, J., Benedetti, E., Plomp, R., Razdorov, G., Trbojević-Akmačić, I., Deelen, J., Van Heemst, D., Slagboom, P. E., Vučković, F., Grallert, H., Krumsiek, J., Strauch, K., Peters, A., Meitinger, T., Hayward, C., Wuhrer, M., … Gieger, C. (2018). Genome-Wide Association Study on Immunoglobulin G Glycosylation Patterns. *Frontiers in Immunology*, *9*, 277. https://doi.org/10.3389/fimmu.2018.00277

Wang, G., de Jong, R. N., van den Bremer, E. T. J., Beurskens, F. J., Labrijn, A. F., Ugurlar, D., Gros, P., Schuurman, J., Parren, P. W. H. I., & Heck, A. J. R. (2016). Molecular Basis of Assembly and Activation of Complement Component C1 in Complex with Immunoglobulin G1 and Antigen. *Molecular Cell*, *63*(1), 135–145. https://doi.org/10.1016/j.molcel.2016.05.016

Wang, T. T., Maamary, J., Tan, G. S., Bournazos, S., Davis, C. W., Krammer, F., Schlesinger, S. J., Palese, P., Ahmed, R., & Ravetch, J. V. (2015). Anti-HA Glycoforms Drive B Cell Affinity Selection and Determine Influenza Vaccine Efficacy. *Cell*, *162*(1), 160–169. https://doi.org/10.1016/j.cell.2015.06.026

Wang, Y., & Jönsson, F. (2019). Expression, Role, and Regulation of Neutrophil Fcγ Receptors. *Frontiers in Immunology*, *10*, 1958. https://doi.org/10.3389/fimmu.2019.01958

Wang, Y., Krémer, V., Iannascoli, B., Goff, O. R., Mancardi, D. A., Ramke, L., De Chaisemartin, L., Bruhns, P., & Jönsson, F. (2022). Specificity of mouse and human Fcgamma receptors and their polymorphic variants for IgG subclasses of different species. *European Journal of Immunology*, *52*(5), 753–759. https://doi.org/10.1002/eji.202149766

Wang, Z.-B., & Xu, J. (2020). Better Adjuvants for Better Vaccines: Progress in Adjuvant Delivery Systems, Modifications, and Adjuvant–Antigen Codelivery. *Vaccines*, *8*(1), 128. https://doi.org/10.3390/vaccines8010128

Warncke, M., Calzascia, T., Coulot, M., Balke, N., Touil, R., Kolbinger, F., & Heusser, C. (2012). Different Adaptations of IgG Effector Function in Human and Nonhuman Primates and Implications for Therapeutic Antibody Treatment. *The Journal of Immunology*, *188*(9), 4405–4411. https://doi.org/10.4049/jimmunol.1200090

Wei, B., Gao, X., Cadang, L., Izadi, S., Liu, P., Zhang, H.-M., Hecht, E., Shim, J., Magill, G., Pabon, J. R., Dai, L., Phung, W., Lin, E., Wang, C., Whang, K., Sanchez, S., Oropeza Jr, J., Camperi, J., Zhang, J., … Jiang, G. (2021). Fc galactosylation follows consecutive reaction kinetics and enhances immunoglobulin G hexamerization for complement activation. *mAbs*, *13*(1), Article 1. https://doi.org/10.1080/19420862.2021.1893427

Weisel, F. J., Zuccarino-Catania, G. V., Chikina, M., & Shlomchik, M. J. (2016). A Temporal Switch in the Germinal Center Determines Differential Output of Memory B and Plasma Cells. *Immunity*, *44*(1), 116–130. https://doi.org/10.1016/j.immuni.2015.12.004

World Health Organization (Ed.). (1980). *International classification of impairments, disabilities, and handicaps: A manual of classification relating to the consequences of disease*. World Health Organization ; sold by WHO Publications Centre USA].

Yu, X., Wang, Y., Kristic, J., Dong, J., Chu, X., Ge, S., Wang, H., Fang, H., Gao, Q., Liu, D., Zhao, Z., Peng, H., Pucic Bakovic, M., Wu, L., Song, M., Rudan, I., Campbell, H., Lauc, G., & Wang, W. (2016). Profiling IgG N-glycans as potential biomarker of chronological and biological ages: A community-based study in a Han Chinese population. *Medicine*, *95*(28), e4112. https://doi.org/10.1097/MD.0000000000004112

Zuo, Y., Evangelista, F., Culton, D., Guilabert, A., Lin, L., Li, N., Diaz, L., & Liu, Z. (2016). IgG4 autoantibodies are inhibitory in the autoimmune disease bullous pemphigoid. *Journal of Autoimmunity*, *73*, 111–119. https://doi.org/10.1016/j.jaut.2016.06.019

C. Supplements

Table S1: Anti-S IgG subclass glycoforms.

Abbreviation and structure of the identified IgG subclass glycoforms. ✓ identified; - not identified; n.d. not determined.

Glycoform	Structure	IgG1		IgG2/3		IgG4	
		anti-S	total	anti-S	total	anti-S	total
G0F	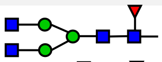	✓	✓	✓	✓	✓	✓
G0FN	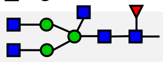	✓	✓	✓	✓	✓	✓
G1	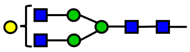	✓	✓	-	-	-	-
G2	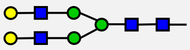	✓	✓	-	-	-	-
G1F	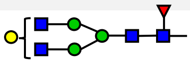	✓	✓	✓	✓	✓	✓
G2F	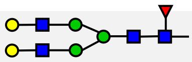	✓	✓	✓	✓	✓	✓
G1FN	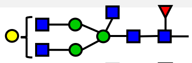	✓	✓	✓	✓	✓	✓
G2FN	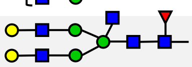	✓	✓	-	-	-	-
G1FNS1	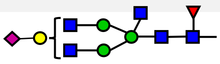	✓	✓	-	-	-	-
G2S1	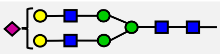	✓	✓	-	-	-	-
G1FS1	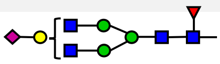	✓	✓	✓	✓	✓	✓
G2FS1	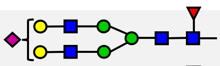	✓	✓	✓	✓	✓	✓
G2FNS1	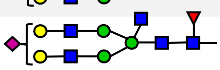	✓	✓	-	n.d.	-	n.d.
G2FS2	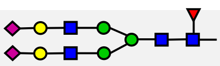	✓	✓	-	n.d.	-	n.d.

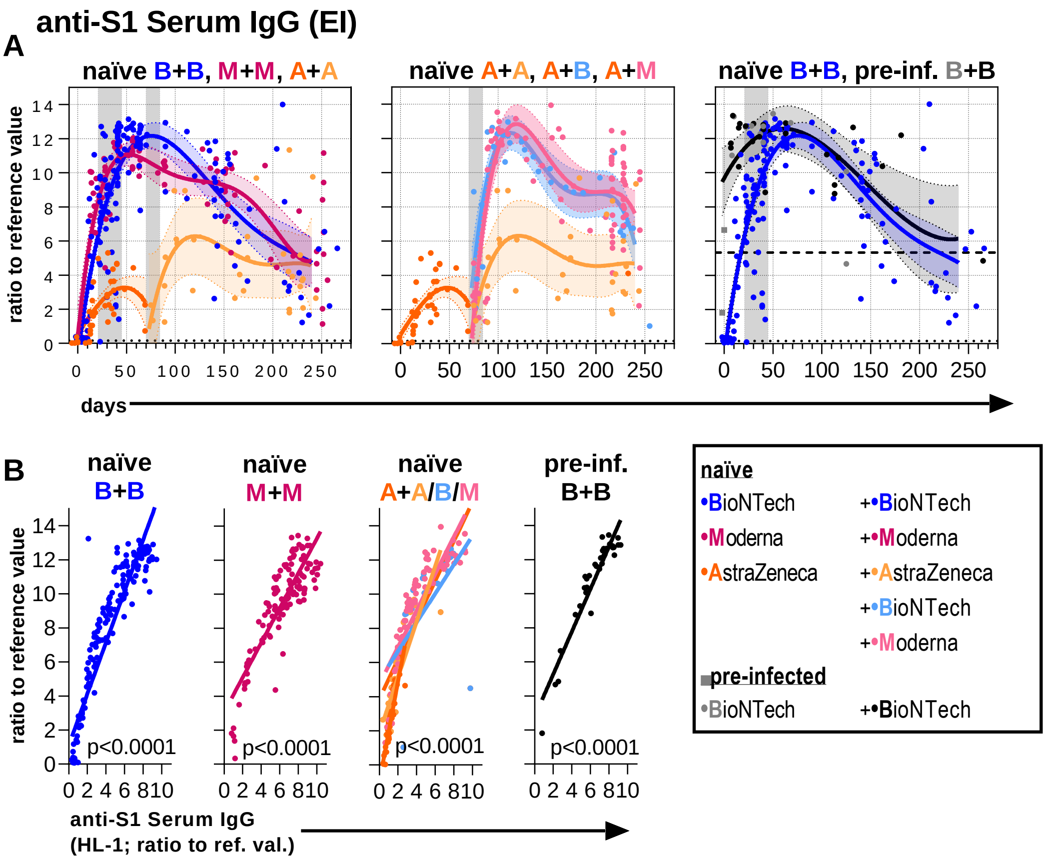

Figure S1: Longitudinal anti-S1 serum IgG levels after two vaccinations.
(A) Anti-S1 serum IgG (EUROIMMUN (EI) ELISA) levels (ratio to reference values) of the indicated six vaccination groups. The time windows of the second vaccinations are indicated by the grey bars: 21-45 days for mRNA and 70-84 days for adenovirus-based vaccines. The dotted lines indicate the anti-S1 IgG levels of unvaccinated controls, the dashed line indicates the level of anti-S1 IgG of pre-infected individuals before a vaccination. **(B)** Pearson correlations between anti-S1 serum IgG (HL-1 ELISA) levels (data points from Figure 8) and anti-S1 serum IgG (EI ELISA) levels. p-values of the indicated correlations are shown (the p-values for the naïve A+A/B/M groups are the same). Statistics: polynomial regression.

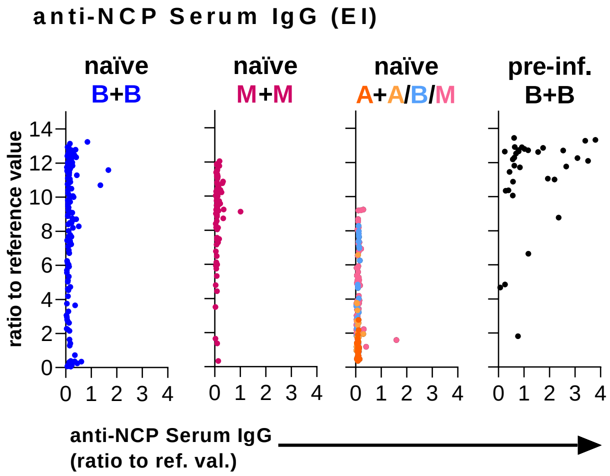

Figure S2: Validation of the antigen-experienced status via anti-NCP serum IgG ELISA. Correlations between anti-NCP (nucleocapsid-protein) serum IgG levels (ratio to reference value) and anti-S1 serum IgG (EI ELISA) levels (the same axis as in Figure S1) of the indicated groups.

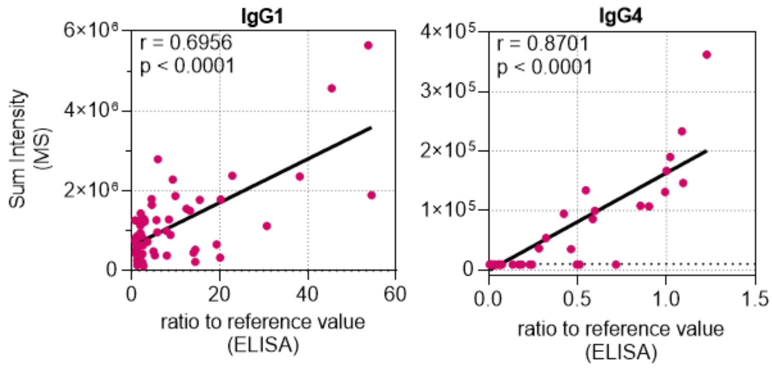

Figure S3: Correlation of anti-S(1) serum IgG subclass levels gathered by two different techniques.

Correlation of IgG1- and IgG4-levels measured by both methods (ELISA (ratio to reference value) and MS (Sum-intensity). The dotted horizontal line represents the cut-off threshold. Statistics: Pearson-correlation, the respective p-value and r are shown.

Table S2: Summary of the samples used for the first depletion approach.
Indicated are respective time frame (short- or long-term), origin, vaccination strategy as well as the calculated anti-S IgG frequencies for IgG1, IgG2/3, and IgG4. Further, the IgG4 frequencies after IgG4 depletion are indicated. Abbreviations: HL Lübeck, Germany; AstraZeneca; M Moderna; B BioNTech.

Time frame	Individual	Origin	Vaccination	% IgG1	% IgG2/3	% IgG4	% IgG4 after depletion
Shortly post 3rd	AM1	HL	A+M+B	90.4	2.9	6.7	1.8
	B49	HL	B+B+B	82.6	7.2	10.3	4.1
	B52	HL	B+B+B	86.8	3.9	9.3	2.5
	B50	HL	B+B+B	79.9	5.3	14.9	3
	B53	HL	B+B+B	82.6	7.8	9.7	3.7
	B51	HL	B+B+B	80.7	6.5	12.8	3.2
	B16	HL	B+B+B	84.0	5.9	10.1	1.7
Long post 3rd	AM1	HL	A+M+B	74.3	7.2	18.6	3.9
	A2	HL	A+A+B	79.7	6.1	14.2	10.1
	AM2	HL	A+M+B	84.4	3.8	11.8	4.9
	AM4	HL	A+M+B	86.9	4.0	9.1	2
	AM32	HL	A+M+B	70.6	9.3	20.1	4.8
	M26	HL	M+M+B	75.2	8.8	16	3.2
	A3	HL	A+A+B	87.1	5.5	7.3	3.8
	AM3	HL	A+M+B	75.9	6.7	17.4	4.8

Table S3: Summary of the samples used for the second depletion approach.
Indicated are respective time frame (short- or long-term), origin, vaccination strategy as well as the calculated anti-S IgG frequencies for IgG1, IgG2/3, and IgG4. Further, the IgG4 frequencies after IgG4 depletion are indicated. Abbreviations: BE Universitätsmedizin Berlin Charité, Germany; BU Semmelweis University in Budapest, Hungary; B BioNTech; M Moderna.

Time frame	Individual	Origin	Vaccination	% IgG1	% IgG2/3	% IgG4	% IgG4 after depletion
Shortly post 3rd/4th	BE11	BE	B+B+B	61.1	5.7	33.2	5.6
	BE33	BE	B+B+B+M	61.5	4.8	33.7	18.5
	BU7	BU	B+B+B	61.0	6.4	32.7	6.8
	BU9	BU	B+B+B	65.5	3.4	31.2	8.0
	BE22	BE	B+B+B	64.0	6.0	30.0	8.8
	BE18	BE	B+B+B	71.7	4.1	24.2	11.6
	BE13	BE	B+B+B	70.7	4.6	24.7	11.5
	BE21	BE	B+B+B	66.0	4.6	29.4	10.8
	BU3	BU	B+B+B	67.8	4.2	28.1	11.6
	BE17	BE	B+B+B	58.3	6.4	35.2	6.6
Long post 3rd/4th	BE34	BE	B+B+B+M	62.6	6.5	31.0	8.4
	BE40	BE	B+B+B+M	64.3	5.1	30.7	8.5
	BE41	BE	B+B+B+M	63.1	5.0	31.9	6.8
	BE33	BE	B+B+B+M	60.6	5.3	34.2	9.1
	BE43	BE	B+B+B+M	64.8	4.1	31.1	5.2
	BU3	BU	B+B+B	62.6	4.9	32.5	11.1
	BU4	BU	B+B+B	59.9	7.3	32.8	8.0
	BU15	BU	B+B+B	63.3	5.5	31.2	10.4
	BU20	BU	B+B+B	64.9	4.7	30.4	6.0

Table S4: Summary of the samples used for the IgG4 purification.

Indicated are respective time frame (short- or long-term), origin, vaccination strategy, age, sex as well as the calculated IgG frequencies for IgG1, IgG2/3, and IgG4. Abbreviations: A AstraZeneca, B BioNTech, M Moderna; f female; m male.

	Individual	Vaccine strategy	days post last vaccination	Age	Sex f / m	% anti-S IgG1	% anti-S IgG2/3	% anti-S IgG4
Long post 2nd "lp2"	M5	M+M	192	53	f	76.9	8.6	14.5
	M6	M+M	217	30	f	73.8	10.1	16.1
	M16	M+M	217	43	f	47.5	14.1	38.4
	M7	M+M	216	48	f	80.3	6.5	13.2
	M11	M+M	167	56	f	84.5	4.7	10.7
	M20	M+M	217	60	f	80.4	7.4	12.2
Shortly post 3rd "sp3"	B51	B+B+B	21	22	f	80.7	6.5	12.8
	B49	B+B+B	28	31	f	82.6	7.2	10.3
	B16	B+B+B	14	26	f	84.0	5.9	10.1
	B52	B+B+B	15	31	f	86.8	3.9	9.3
	B50	B+B+B	6	47	f	79.9	5.3	14.9
Long post 3rd "lp3"	AM1	A+M+B	250+	26	f	74.3	7.2	18.6
	AM3	A+M+B	250+	54	m	75.9	6.7	17.4
	AM4	A+M+B	250+	26	f	86.9	4.0	9.1
	AM2	A+M+B	250+	26	f	84.4	3.8	11.8
	AM32	A+M+B	250+	26	f	70.6	9.3	20.1
	M26	M+M+B	250+	26	f	75.2	8.8	16.0

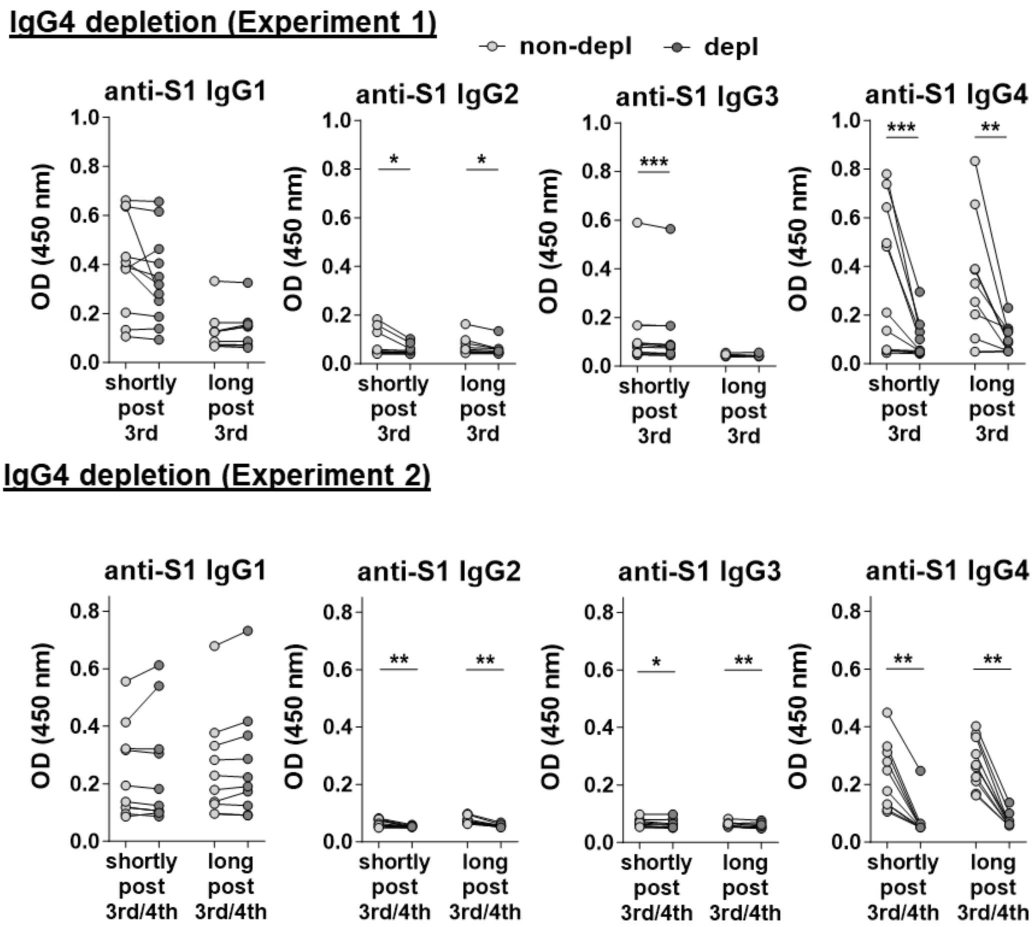

Figure S4: IgG4 depletion verification by anti-S1 IgG subclass ELISA.

Samples of both depletion experiments were analyzed regarding their anti-S1 IgG subclass levels (OD 450 nm). The samples were IgG4 non-depleted or IgG4 depleted. For ELISA, the serum samples were diluted 1:120 in ELISA-buffer. Statistics: Wilcoxon test. Asterisks indicate statistically significant p values *p<0.05, **p<0.01, ***p < 0.001.

Table S5: Summary of the samples used for the IgG4 enrichment.

Purified naive, sial and degal IgG4 from long-term post 2nd (lp2), short-term post 3rd (sp3), and long-term post 3rd (lp3) vaccination sera as described in Table S4 were added to 10 short-term and 10 long-term post 3rd/4th vaccination sera (native IgG4 from short-term or long-term sera were only added to short-term or long-term sera, respectively).

							native			sial			degal		
	Indivi-dual	**Vacc. strategy**	**days post last vacc.**	**% anti-S IgG1**	**% anti-S IgG2/3**	**% anti-S IgG4**	lp 2	sp 3	lp 3	lp 2	sp 3	lp 3	lp 2	sp 3	lp 3
shortly post 3rd "sp3"	BE11	B+B+B	28	61.1	5.7	33.2		x		x	x	x	x	x	x
	BE33	B+B+B+M	29	61.5	4.8	33.7		x		x	x	x	x	x	x
	BU7	B+B+B	37	61.0	6.4	32.7				x			x		
	BU9	B+B+B	37	65.5	3.4	31.2				x	x		x	x	
	BE22	B+B+B	29	64.0	6.0	30.0		x		x	x	x	x	x	x
	BE18	B+B+B	22	71.7	4.1	24.2				x			x	x	x
	BE13	B+B+B	28	70.7	4.6	24.7				x			x	x	x
	BE21	B+B+B	30	66.0	4.6	29.4				x			x	x	x
	BU3	B+B+B	37	67.8	4.2	28.1				x			x	x	x
	BE17	B+B+B	29	58.3	6.4	35.2				x			x	x	x
long post 3rd "lp3"	BE34	B+B+B+M	188	62.6	6.5	31.0	x			x	x	x	x	x	x
	BE40	B+B+B+M	183	64.3	5.1	30.7	x			x	x	x	x	x	x
	BE41	B+B+B+M	192	63.1	5.0	31.9	x			x	x	x	x	x	x
	BE33	B+B+B+M	180	60.6	5.3	34.2	x			x	x	x	x	x	x
	BE43	B+B+B+M	250	64.8	4.1	31.1	x			x	x	x	x	x	x
	BU3	B+B+B	160	62.6	4.9	32.5				x			x	x	x
	BU4	B+B+B	160	59.9	7.3	32.8				x			x	x	x
	B15	B+B+B	160	63.3	5.5	31.2				x			x	x	x
	BU20	B+B+B	160	64.9	4.7	30.4				x			x	x	x
	BE41	B+B+B+M	270	65.2	4.9	29.9				x			x	x	x

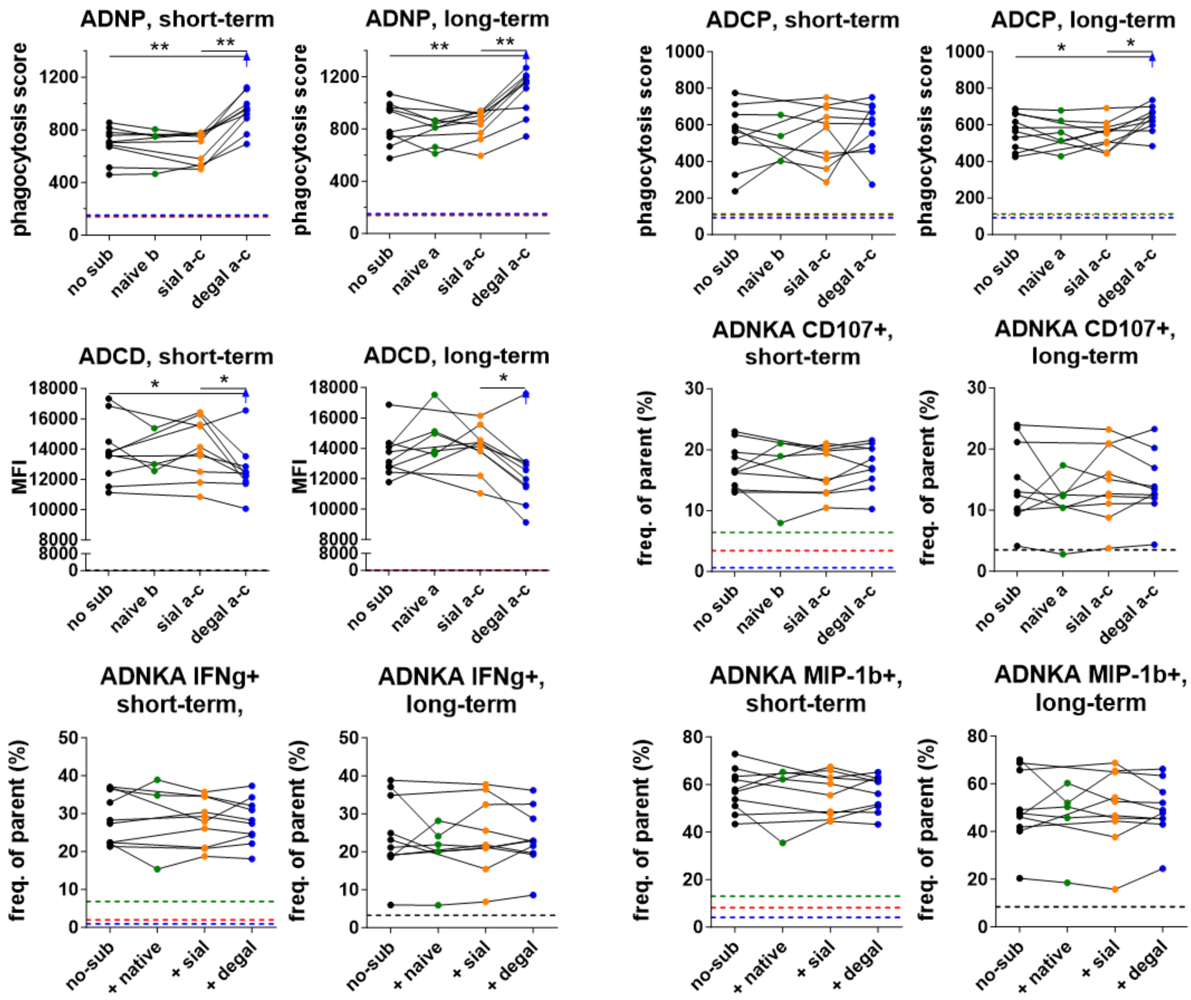

Figure S5: Role of anti-S IgG4 enrichment in different functional assays.

Purified native, sial, and degal IgG4 from long-term post 2nd, short-term post 3rd, and long-term post 3rd vaccination sera were added to short-term (n=10) and long-term (n=10) post 3rd/4th vaccination sera. Native IgG4 from short-term or long-term sera was added to only part of the 10 short-term or 10 long-term sera, respectively. After enrichment, various functional assays were perfomed: ADNP, ADCP, ADCD, and ADNKA (with 3 different readouts (CD107+, IFNg+, and MIP-1b+)). No-sub: no substituted serum. Statistics: Ordinary one-way ANOVA was used to compare no-sub, sial, and degal samples. Asterisks indicate statistically significant p-values (*p<0.05, **p<0.01). Dashed horizontal lines in the corresponding colours indicate the functional potential of the corresponding IgG4 amounts (n=3) without serum. The functional assays were conducted by Mareike Schubert (Twincore (Laboratory of Dr. Yannic C, Bartsch), Hannover, Germany).

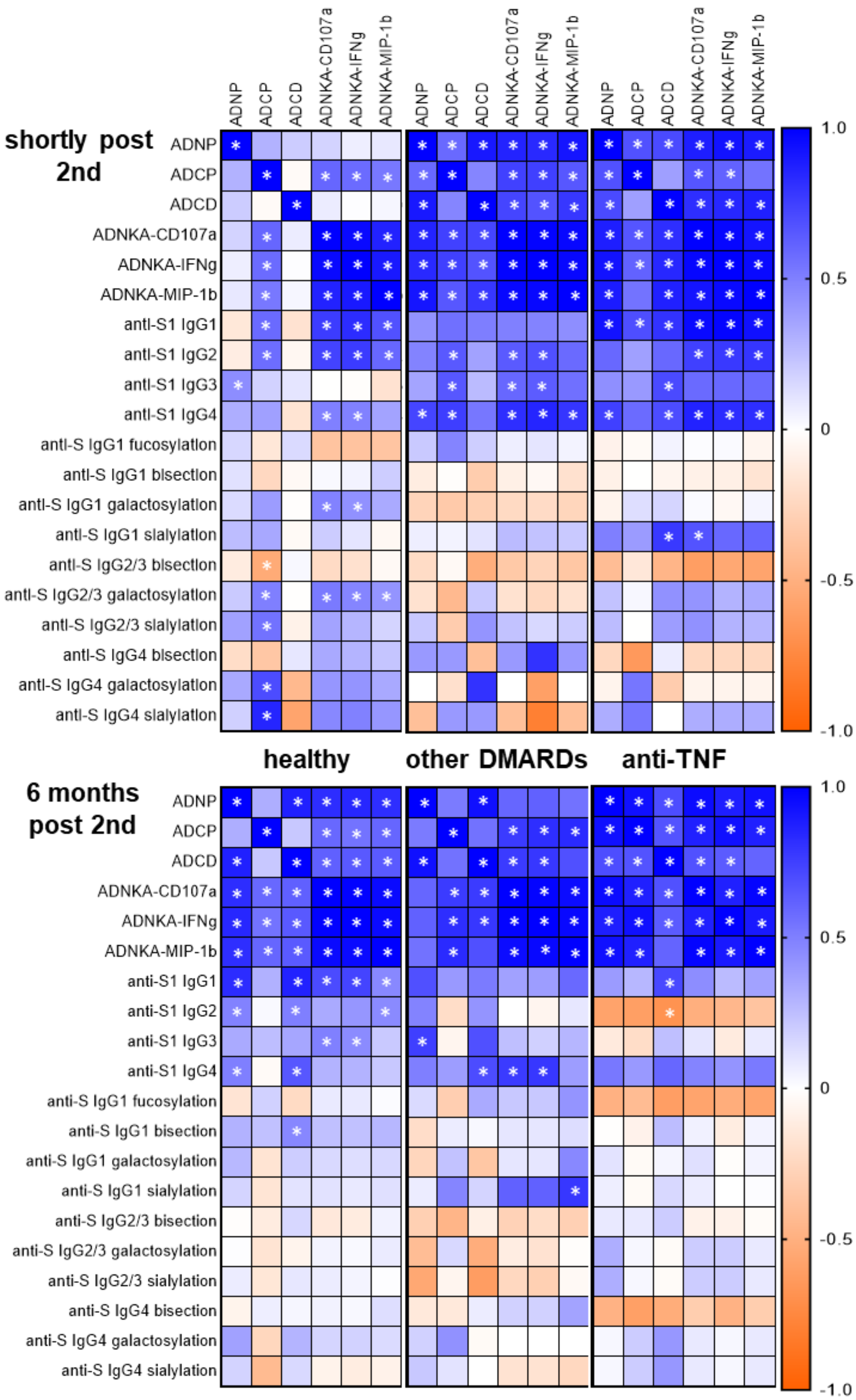

Figure S6: Correlations of functional data, anti-S1 IgG antibody levels as well as glycosylation patterns.

Two time points (shortly after the second vaccination and 6 months after the second vaccination) for all assessed groups (healthy, anti-TNF, and other DMARDs) were analyzed. Spearman correlation, asterisks indicate statistically significant p-values (*p<0.05).

D. List of Abbreviations

µg *microgram*

µL *microliter*

ADCC *antibody-dependent cellular cytotoxicity*

ADCD *antibody-dependent-complement-deposition*

ADCP *antibody-dependent-cell-phagocytosis*

ADNKA *antibody-dependent-NK cell-activation*

ADNP *antibody-dependent-neutrophil-phagocytosis*

AID *activation-induced cytidine deaminase*

AIT *antigen-specific immune therapies*

anti-NCP *anti-viral nucleocapsid protein*

APC *Antigen-presenting cell*

ARDS *acute respiratory distress syndrome*

AUROC *area under the receiver operating characteristic curve*

B4galt1 β*1,4-galactosyltransferase*

BCR *B cell receptor*

BE *Universitätsmedizin Berlin Charité*

BMI *body mass index*

BU *Semmelweis University in Budapest*

CD *Crohn's disease*

CFA *complete Freund's adjuvant*

CMP *cytidine monophosphate*

CNBr *cyanogen bromide*

COVID-19 *coronavirus disease 2019*

CSR *class switch recombination*

DAMPs *danger-associated molecular patterns*

DC *dendritic cell*

DMARD *disease-modifying anti-rheumatic drug*

DNA *Deoxyribonucleic acid*

ds *double stranded*

DZ *dark zone*

eCFA *enriched complete Freund's adjuvant*

EDTA *Ethylenediamine tetraacetic acid*

EMR *electronic medical record*

ER endoplasmic reticulum

F *fucose, fucosylated residue*

F0 *afucosylated residue*

Fab *Fragment-antigen-binding*

Fc *Fragment-crystallizable*

FcγR *IgG Fc receptors*

Fut8 *alpha1,6-fucosyltransferase 8*

G *galactose, galactosylated residue*

G0 *agalactosylated residue*

GC *germinal center*

GlcNAc *N-acetylglucosamine*
HIV *human immunodeficiency virus*
HK *Kiel*
HL *Lübeck*
HRP *Horse radish peroxidase*
hu *human*
i.p. *intraperitoneal*
IFA *incomplete Freund's adjuvant*
IFNy *Interferon gamma*
Ig *immunoglobulin*
IL-4 *Interleukin-4*
kDa *kilodalton*
LC-MS *Liquid Chromatography-Mass Spectrometry*
LNPs *lipid nanoparticles*
LUMC *Leiden University Medical Center*
LV *latent variable*
LZ *light zone*
M molar
MFI *median fluorescence intensity*
mg *milligram*
MHC *major histocompatibility complex*
mRNA *messenger RNA*
Mtb *Mycobacterium tuberculosis*
MTX *methotrexate*
mu *murine*
N *Asparagine 297*
NK cell *Natural Killer cell*
nm *nanometer*
OD *optical density*
PAMPs *pathogen-associated molecular patterns*
PBMC *peripheric mononuclear blood cell*
PBS *Phosphate buffered saline*
PCA *Principal component analyses*
PLS-DA *partial least square-discriminant analyses*
PRRs *pattern-recognition receptors*
Pso *psoriasis*
RA *rheumatoid arthritis*
rpm *rounds per minute*
RT *room temperature*
S *Spike*, *sialic acid, sialylated resiude*
S1 *Subunit 1 of the spike protein*
SARS-CoV-2 *severe acute respiratory syndrome coronavirus type 2*
SD *Standard Deviation*
SHM *somatic hypermutation*
SNA *Sambucus nigra*
St6gal1 α*2,6-sialyltransferase*
sum-intensity *summed glycopeptide intensity*
TCR *T cell receptor*
TD *T cell-dependent*
T_{FH} *T follicular helper*
T_{FR} *regulatory follicular T cells*
TGFβ *Transforming growth factor beta*
T_H *T helper*
TI *T cell-independent*
TLR *Toll-like receptor*
TNFα *tumor necrosis factor alpha*
U *unit*

UKSH *University Medical Center Schleswig-Holstein*

UzL *University of Lübeck*

w/v *weight per volume*

WHO *World Health Organization*

xg *acceleration of gravity*

E. List of Figures

F. List of Tables

G. Acknowledgement

I would like to take this opportunity to thank everyone who has supported me along the way.

My special thanks go to my supervisor Marc Ehlers, who gave me the opportunity to do my work in his laboratories. Dear Marc, thank you for your valuable thoughts and ideas, for your constant challenges and for your support. I am also very grateful for my participation in the RTG-2633 under the direction of Ralf Ludwig and Jenny Hundt as well as for my mentors, Rudolf Manz, Mareike Becker, and Anja Stähle, and their support.

I would also like to thank the entire Ehlers group: first and foremost, Selina, Lara and Hanna, who have always supported me and with whom I was able to share many valuable moments. Further, I would like to thank Inga, Bandik, Janina, Johann and Anne. It was always a pleasure to work with them and they supported me significantly in my project.

I would like to thank all the cooperation partners involved who contributed significantly to my projects and made them possible, especially Tamas Pongracz and Manfred Wuhrer, Mareike Schubert and Yannic Bartsch, Ulf Geisen and Bimba Hoyer as well as Ralf Ludwig and Franziska Schmelter. Furthermore, I am very grateful that the two groups from Berlin and Budapest kindly provided us with samples.

My project was largely dependent on the fact that many people donated blood and I would like to express my sincere thanks for this willingness. Without this spirit, a work like mine would be impossible.

A big thank you goes to my friends and family.
My friends, whose company I always enjoy and appreciate. Your time was an important counterbalance to my time in the lab and in the data jungle.
Rasmus, you are my rock. Thank you for always picking me up and for being my haven of peace.
Finally, I would like to thank my parents and my brother. You are my safety net and have made all of this possible.